On Reducing Piping Uncertainties

A Bayesian Decision Approach

Propositions

accompanying the dissertation

ON REDUCING PIPING UNCERTAINTIES
A BAYESIAN DECISION APPROACH

by

Timo SCHWECKENDIEK

1. Ensuring the non-existence of weak spots (true negative) is more relevant for levee reliability than finding them (true positive).
2. Killing black swans with site investigation is pure luck.
3. For geotechnical structures in natural deposits, uncertainties in stratification are more important than spatial variability within strata.
4. The limit state based on the Sellmeijer model cannot be observed in the field.
5. Using data scarcity as an an argument against probabilistic approaches is confusing statistics with probability theory.
6. Model validation is an outdated concept and should be replaced by model uncertainty analysis.
7. The Achilles heel of the Dutch safety assessments of flood defences is the lack of technical reviews.
8. R&D projects for decision support systems should start from the decisions to be taken, not with improving prediction capacity.
9. The most important virtues to successfully finish a dissertation are the serenity to accept that it will not solve all problems, the perseverance to pursue tractable solutions and the wisdom to identify the latter.
10. Innovation in the public sector is like teenage sex: a lot of talking, few results.

These propositions are regarded as opposable and defendable, and have been approved as such by the supervisors prof. drs. ir. J.K. Vrijling and prof. ir. A.C.W.M. Vrouwenvelder.

Stellingen

behorende bij het proefschrift

ON REDUCING PIPING UNCERTAINTIES
A BAYESIAN DECISION APPROACH

door

Timo SCHWECKENDIEK

1. Voor de betrouwbaarheid van een dijk is belangrijker zwakke punten uit te kunnen sluiten (true negative) dan ze te vinden (true positive).
2. Als grondonderzoek een black swan ontdekt is dat puur geluk.
3. Voor constructies in natuurlijk afgezette grond zijn onzekerheden in de laagopbouw belangrijker dan ruimtelijke variabiliteit binnen lagen.
4. De door de pipingregel van Sellmeijer beschreven grenstoestand kan niet in het veld worden geobserveerd.
5. Gebrek aan data aanvoeren als argument om geen probabilistische aanpak toe te passen is statistiek en kansrekening met elkaar verwarren.
6. Validatie van modellen is een absurd concept dat onzekerheden vermijdt. Dat geldt in het bijzonder voor "validatie"van rekenmodellen met experimenten.
7. De achilleshiel van de Nederlandse Toetsing van waterkeringen is het ontbreken van een externe technische review.
8. R&D projecten met belisondersteunende systemen als doel zouden moeten worden opgetuigd vanuit de te maken beslissing en niet door meteen te beginnen met het verbeteren van de voorspelcapaciteit.
9. De belangrijkste deugden voor het afronden van een dissertatie zijn de gemoedsrust te accepteren dat het proefschrift niet alle problemen op zal lossen, de vasthoudendheid om haalbare doelen na te streven en de wijsheid haalbaarheid in te schatten.
10. Innovatie in de publieke sector is als sex voor tieners: er wordt vooral over gesproken.

Deze stellingen worden opponeerbaar en verdedigbaar geacht en zijn als zodanig goedgekeurd door de promotoren prof. drs. ir. J.K. Vrijling en prof. ir. A.C.W.M. Vrouwenvelder.

ON REDUCING PIPING UNCERTAINTIES

A BAYESIAN DECISION APPROACH

Proefschrift

ter verkrijging van de graad van doctor
aan de Technische Universiteit Delft,
op gezag van de Rector Magnificus prof. ir. K. C. A. M. Luyben,
voorzitter van het College voor Promoties,
in het openbaar te verdedigen op vrijdag 4 juli 2014 om 10:00 uur

door

Timo SCHWECKENDIEK

civiel ingenieur
geboren te Cuxhaven, Duitsland.

Dit proefschrift is goedgekeurd door de promotoren:

Prof. drs. ir. J.K. Vrijling
Prof. ir. A.C.W.M. Vrouwenvelder

Samenstelling promotiecommissie:

Rector Magnificus	voorzitter
Prof. drs. ir. J.K. Vrijling	Technische Universiteit Delft, promotor
Prof. ir. A.C.W.M. Vrouwenvelder	Technische Universiteit Delft, promotor
Prof. dr. M.H. Faber	Technical University of Denmark
Prof. dr. G.A. Fenton	Dalhousie University
Prof. dr. M.A. Hicks	Technische Universiteit Delft
Prof. dr. ir. P.H.A.J.M. van Gelder	Technische Universiteit Delft
Prof. dr. ir. S.N. Jonkman	Technische Universiteit Delft
Prof. dr. ir. M. Kok	Technische Universiteit Delft, reservelid

Ir. E.O.F. Calle heeft als begeleider in belangrijke mate aan de totstandkoming van het proefschrift bijgedragen.

Keywords: levee reliability, internal erosion, uplift, piping, risk-based decision support, Bayesian updating, inequality information, equality information, field observations, pore pressure monitoring, soundings, cone penetration testing, Kriging, conditional simulation, random fields

Printed by: Ridderprint B.V.

Front & Back: Mercedes García Ballester

ISBN 978-90-5335-880-1

An electronic version of this dissertation is available at
http://repository.tudelft.nl/.

To Merche, Raúl and Arne.

ABSTRACT

DIKES and levees play a crucial role in flood protection in deltaic areas such as the Netherlands. Internal erosion piping or under-seepage is a major cause of levee failures and a main contributor to the probability of failure of river levees due to the large (mostly geotechnical) uncertainties. The present thesis investigates how geotechnical uncertainties can be reduced and how we can provide input for rational investment decisions for uncertainty reduction measures such as monitoring or site investigation. The general trade-off is between investing in uncertain reduction realizing cost reductions of retrofitting measures necessary to achieve the required reliability target.

The key ingredients of the approach are Bayesian posterior and decision analysis. Posterior analysis allows us to update the piping reliability with new information; Bayesian decision analysis enables us to for estimate the the consequences and costs of the considered decision options. The goal of the decision analysis is to identify the strategy with the least expected cost which meets the reliability target as set by the safety standard. The essential strategy options are (a) investing in uncertainty reduction and (b) retrofitting (i.e., taking physical measures to increase the structural reliability). Within each strategy we optimize the "design parameters" such as the site investigation density or the width of piping berms.

Several sources of information are investigated in this thesis, the first being field performance observations made during substantial loading conditions such as seepage or sand boils. Whereas earlier studies only considered survival information (in Dutch: "bewezen sterkte"), the proposed approach allows to incorporate much more detailed performance observations indicating good or poor performance of the levee. The case study results suggest that the probability of piping failure can decrease or increase roughly one order of magnitude depending on the prior uncertainties and the observation made.

Another source of information is monitoring the response of the hydraulic head in the aquifer, which can have a considerable effect on the piping reliability, because it provides information on the geo-hydrological properties in the foundation of the levee. The same holds for site investigation such as soundings, which allow us to "map" the stratification including the thickness of the blanket layer, which is very important for the sub-mechanisms uplift and heave. Pre-posterior decision analysis enables us to determine the optimal monitoring configuration or site investigation density such that the sum of investigation cost and expected retrofitting cost is minimized.

The application examples elaborated in this thesis suggest that investments in back-analysis of historical observations, monitoring and site investigation can be very cost-effective. The results also show that a framework which does not consider the benefits of risk reduction beyond meeting the reliability target is sub-optimal in an overall risk sense.

ACKNOWLEDGEMENTS

THE work on this dissertation started in 2008, when my former employer GeoDelft merged with WL | Delft Hydraulics and parts of Rijkswaterstaat and TNO to become Deltares. One may say I was Deltares' first PhD candidate - the first to begin, not the first to finish though. The greatest challenge in finishing this dissertation proved to be keeping focus, while working on Deltares projects at the same time. Projects have short term deadlines and a more intensive rhythm. The clients and and team mates ask for results and advice. Anyhow, the work being finished now there is quite a few people I'd like to thank for the many ways they have played a role in this.

First I would like to acknowledge my supervisors. Han Vrijling was there from the beginning with invaluable suggestions and making sure I would never lose track of the implications of the work for practice. Han also made it possible for me to join a post-flood field investigation in Thailand after the country had been hit by severe floods in the autumn of 2011. Seeing the disastrous consequences large-scale floodings is an enormous motivation to work on flood risk management and flood defenses, which I am very grateful for. Ton Vrouwenvelder joined a little later, but his impact on my work was tremendous. With Ton's sharp and critical attitude as well as inestimable comments, the work on this dissertation actually began to get shape and become much more productive and gratifying. I am very thankful for the opportunity to learn from these two founding fathers of today's Dutch flood risk management.

Ed Calle has been my mentor, since I joined GeoDelft. He has taught me many technical things I have been using to accomplish this dissertation, but above all critical attitude, a slowly vanishing virtue. Pieter van Gelder was always there, when I had doubts about mathematical issues, and he frequently came up with provoking ideas. Many thanks also go to the rest of my committee for their very valued comments and challenging discussions, which have led to a considerable improvement of the thesis.

I would also like to express my appreciation for my colleagues who kept me motivated and made me feel comfortable, both at TU Delft as well as at Deltares. It is impossible to name them all, but I would like to point out a few. Kees den Heijer helped me out with many things most PhD students struggle with (e.g., Latex or Matlab). My special thanks go to Wim Kanning for all the stimulating technical, political and football-related discussions we had. There is no good boxer without a good sparring partner. My colleagues and good friends Patrick Arnold and Richard de Jager were willing to stand by my side during the defense and to be my paranymphs, I could not be more fortunate.

Both, TU Delft and Deltares supported my project over the years. On the TU Delft side, Han Vrijling was willing to take his chances with me and accept me as his PhD student. Bas Jonkman continued to support me as Han's successor at the chair of Hydraulic Engineering. The post-flood field investigation to Germany in 2013 together with Bas was particularly enriching and the starting point of a very promising collaboration in the field of flood defenses. Also on the Deltares side, I experienced full support. Be-

sides thanking the company for the financial support, I would especially like to thank Peter van den Berg, Harm Aantjes, Jos Maccabiani, Jan-Aart van Twillert and Maya Sule for putting trust in me and for the opportunity to engage and accomplish this endeavor. Also my closest colleagues and room mates, Wim Kanning, Ana Teixeira and Maximilian Huber deserve mention for their patience and support in the finishing phases of the work.

Last but not least, I want to thank my family. Merche for her unconditional support, tenderness and patience over the years and my sons, Raúl and Arne, for their innocent sacrifice.

Timo Schweckendiek
Delft, July 2014

CONTENTS

1

INTRODUCTION

Do not be afraid to challenge even the most established concepts.

Arvid Landva

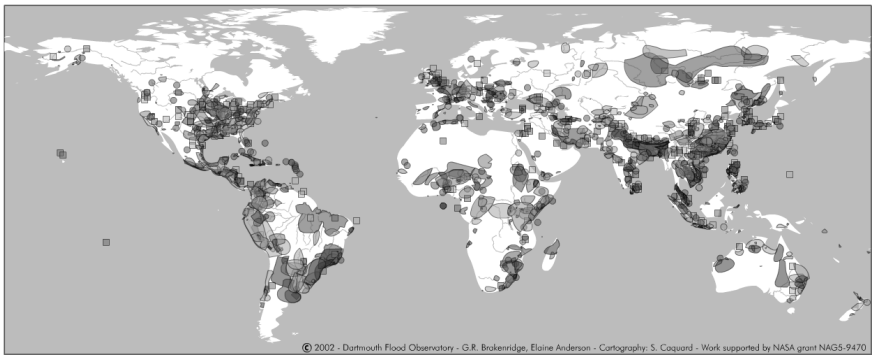

Figure 1.1: Global archive map of extreme floods 1985-2002 (source: Dartmouth Flood Observatory)

Floods are a major natural hazards and flood defenses play a pivotal role in safeguarding the welfare of people living in flood-prone areas. Internal erosion mechanisms are among the most frequent causes of levee failures. The ground conditions governing these mechanisms are highly uncertain. This introductory chapter provides an overview of the general background, the research questions and an outline of this thesis.

1.1. MOTIVATION AND SOCIETAL RELEVANCE

FLOODS are the most common and widespread of all natural disasters, besides fire. World-wide, flood disasters account for about a third of all natural disasters (by number and economic losses) (UNESCO, 2008). The average death toll per year is approximately 7,000 people; the annual average number of people suffering flood damage is about 66 million.

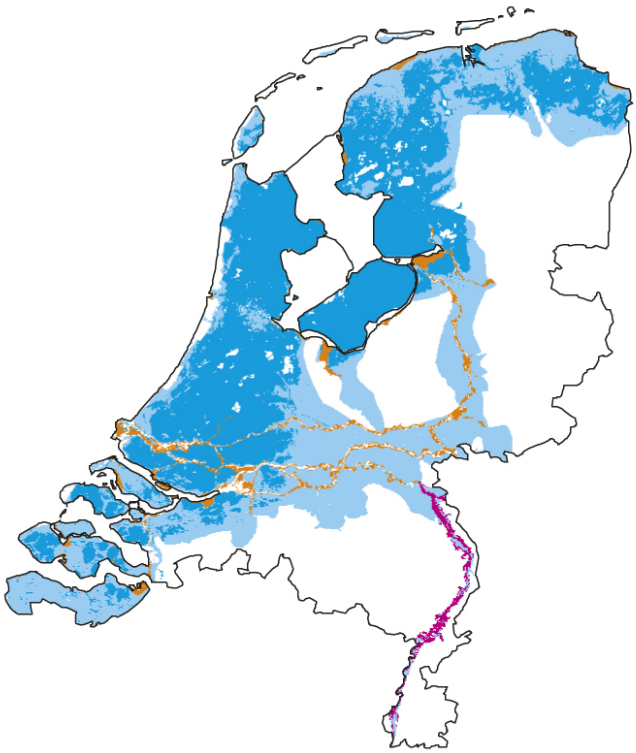

Figure 1.2: Flood-prone areas in the Netherlands, source: PBL (2009)

Dikes and levees play a pivotal role in flood protection. In the Netherlands, approximately 6 million people live in flood-prone areas (Figure 1.2) and roughly one third of the GDP is generated there (CBS, 2009). Dike-rings are flood-prone areas surrounded by dikes or other types of hydraulic structures and/or high grounds, designed to prevent flooding from the sea, rivers and lakes. Breaches in these protection systems can be devastating depending on their location and the intensity of the event. Therefore, Dutch safety assessments of flood defenses require a relatively high target reliability.

The dominant failure mechanism in terms of contribution to the probability of failure of (river) dikes in the Netherlands is piping (Rijkswaterstaat (2005), also called *underseepage* or *backward erosion*), mainly due to the large uncertainty in ground conditions.

Figure 1.3: Sand boils in 1993 in the Netherlands covered by geotextiles and surrounded by sand bags (source: Beeldbank Rijkswaterstaat)

The fact that internal erosion and piping are not only a theoretical problem is underpinned by the numerous observations of sand boils during floods. Sand boils actually exhibit already eroded material at the landside of a levee (Figure 1.3). During the floods in 1993 and 1995 in the Netherlands alone, more than 300 such sand boils were observed and registered along the rivers Rhine, IJssel and Meuse.

Piping develops in the foundation of a dike where the forces of groundwater flow erode sand particles (Figure 1.4). A levee's foundation is generally naturally deposited material. As opposed to other materials involved in engineering structures, there is no quality control during production (except for ground improvement). Our knowledge of the materials at a site mainly originates from local geological expertise and geotechnical site investigation with limited spatial coverage and accuracy.

There are several ways to reduce piping uncertainties. A poorly exploited source of information are field observations of the structural performance during extreme events, which can actually be considered as involuntary load tests. Other, more obvious ways to obtain information on ground conditions influencing piping reliability are monitoring of the geo-hydrological response to loading or site investigation. However, monitoring

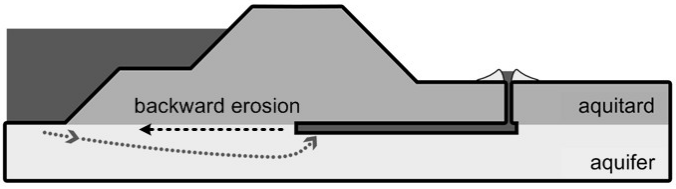

Figure 1.4: Conceptual illustration of the piping mechanism (illustration courtesy of Deltares)

and site investigation planning rely heavily on subjective engineering judgment. The problem with this kind of judgment is that there is no real feedback in terms of the adequacy of the amount or setup of site investigation, except for structural failure revealing previously unidentified weak spots. There is a clear need for systematic risk-based approaches to inform decisions regarding investments in uncertainty reduction.

On the one hand, investing too little in uncertainty reduction can lead to suboptimal designs. Levees can then be either unnecessarily costly or unsafe in a sense that society may be bearing unacceptably high levels of risk due to flooding. The excessive cost in terms of over-design may well be in the order of millions of Euros per retrofitting project, the excessive cost of risk-bearing even in the order of tens of millions of Euros per year for a country like the Netherlands. On the other hand, there is a trade off between investments in uncertainty reduction and the actual benefits in terms of design optimization and risk reduction. At some stage, there is a break-even point where investing more does not pay back.

Risk-informed and rational investment decisions help to avoid such inefficiencies. This thesis demonstrates how the reliability of levees can be increased to an acceptable level by reducing piping-related uncertainties and how monitoring, site investigation and retrofitting measures can be planned cost-effectively and in a consistent framework, while focusing on the Dutch safety assessment with risk-informed target reliability levels.

1.2. RESEARCH QUESTION AND METHODOLOGY

WHILE codes of practice such as Eurocode 7 (EN1997-2, 2007) provide qualitative requirements and recommendations for site investigation and monitoring planning, there is a lack of quantitative guidance. A few scholars have applied Bayesian probability theory (Bayes, 1763) to reducing uncertainties for geotechnical problems involving dikes and levees (Wolff, 1994; Vrijling and Gelder, 1998; Calle, 2005; Zhang et al., 2011), but never specifically to piping or under-seepage problems. The link with cost and utility as introduced by Von Neumann and Morgenstern (1947) has not been established so far.

The essential question this thesis strives to answer is:

> "How can piping-related uncertainty be reduced cost-effectively?"

This thesis contributes to closing this gap by developing a rational, systematic approach that treats uncertainties in a consistent and explicit manner. Bayesian Decision Analysis provides the theoretical basis for the envisaged type of engineering decision problems (e.g., Benjamin and Cornell, 1970). A core element in applying the theory to piping uncertainty reduction is to establish probabilistic failure models and observation models that are compatible with Bayesian Inference. Reduced uncertainty translates into an updated probability of failure, which can be compared to the target from the safety standard to be met. In order to find the optimal strategy to reduce uncertainties, the costs involved with data acquisition need to be compared to the difference in cost of retrofitting the levee caused by reducing uncertainties. The optimal strategy will be defined as the one with the least expected total cost (uncertainty reduction plus retrofitting).

1.3. LIMITATIONS

SINCE the main goal of this thesis is to show how piping-related uncertainty can be reduced and to find cost-effective strategies, the following assumptions and limitations have been imposed to the scope deliberately for the sake of tractability and clarity:

(a) A target reliability is supposed to be known as safety assessment criterion, which is common in civil engineering. In this sense, the approach is not fully risk-based, as it does not account for the potential consequences of piping failure explicitly. However, a target reliability will most probably be available for safety assessments in the Netherlands. Therefore, this limitation will actually increase the practical applicability of the developed approach.

(b) The reliability updating and optimization are limited to the failure mode piping (in combination with uplift and heave). Other failure modes like slope instability are neglected though the information obtained by site investigation typically affects the reliability of other mechanisms, too, and hence the retrofitting designs.

(c) Prior probability distributions of basic random variables are assumed to be known. The thesis does not discuss how priors can be established, only how these can be updated. Most of the values for prior distributions used in the application examples originate from the FLORIS/VNK2 project (Rijkswaterstaat, 2005) in the Netherlands, which already has established a considerable database of probability distributions for, amongst others, geotechnical parameters.

(d) The optimization of strategies is limited to one source of information (e.g., monitoring technique) at a time. In principle, the theoretical framework would allow an integral analysis of several sources of information simultaneously, however, for sake of practicability this was not considered.

Other limitations and assumptions concerning more detailed aspects are discussed in the respective chapters.

1.4. ORIGINALITY

THE main contribution of this thesis is the novel application of Bayesian inference and decision theory to updating piping reliability based on different sources of information (chapter 4). While only the survival of a levee was considered previously, chapter 5 provides more profound insights in how detailed visual observations of the performance can be incorporated. Reliability updating and decision analysis for head monitoring (chapter 6) and soundings (chapter 7) has not been presented earlier in the literature in the consistent and systematic fashion as in this thesis. Furthermore, though not to be generalized for the entire range of conditions, the application examples provide valuable insights into (finding) optimal site investigation strategies for typical Dutch river dikes.

1.5. OUTLINE

FIGURE 1.5 provides an overview of the chapters and their mutual relations. Working in a safety assessment framework poses requirements and limitations to the approach, which are discussed in chapter 2. Chapter 3 provides the conceptual and computational models for both the physics and the reliability with respect to uplift, heave and piping as well as the relevant uncertainties involved. Chapter 4 elaborates the proposed approach, starting with general decision theory and Bayesian inference followed by considering the safety assessment framework and the strategy options as well as their evaluation based on minimizing the expected cost.

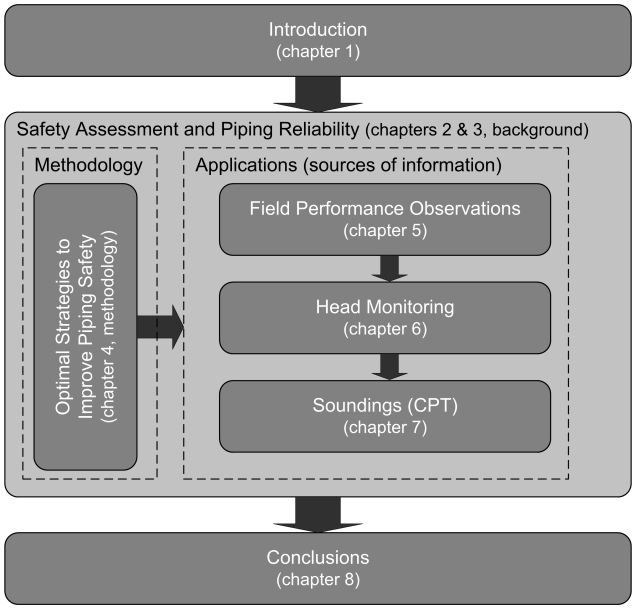

Figure 1.5: Visual thesis outline

Subsequently, three specific sources of information are discussed in detail followed by examples serving as proof of concept and by case studies. Chapter 5 shows how field performance observations during extreme floods such as the occurrence of sand boils can be used for uncertainty and reliability updating. Chapters 6 and 7 investigate hydraulic head measurements (in aquifers) and site investigation by means of soundings. Each application-related chapter (5-7) addresses the following key questions:

1. What relevant information is provided?
2. How can piping reliability be updated by incorporating the information?
3. How does this influence the data acquisition and retrofitting strategies?

While each chapter reports detailed observations and conclusions, chapter 8 synthesizes the main findings.

2

SAFETY ASSESSMENT FRAMEWORK

The best we can do is size up the chances, calculate the risks involved, estimate our ability to deal with them, and then make our plans with confidence.

Henry Ford

Figure 2.1: Signpost in Bitterfeld, Germany, indicating a levee breach location after the floods in June 2013

The main goal of this thesis is to show how piping-related uncertainties can be reduced cost-effectively in safety assessments for flood defenses. Before going into piping uncertainties and reliability updating, we need to be aware of the requirements and limitations a safety assessment situation imposes on the approach. Since this thesis focuses on the situation in the Netherlands, this chapter will provide the necessary background on the Dutch approach, starting with the historical context and ending with the target reliability to be met.

Some of the material in this chapter has been published in Schweckendiek, T., Vrouwenvelder, A.C.W.M., Calle, E.O.F., Kanning, W. and Jongejan, R.B. (2012). *Target Reliabilities and Partial Factors for Flood Defenses in the Netherlands.* In Arnold et al. (Eds.), Modern Geotechnical Codes of Practice - Code Development and Calibration (pp. 311 - 328). Taylor and Francis.

Contents

Figure 2.2: Flooded village in the Province of Zeeland in 1953 (source: Kennislink.nl)

2.1. HISTORICAL CONTEXT

To understand the current safety philosophy in the Netherlands, it is beneficial to know how it has developed historically, starting with the 1953 flood disaster, which had a major impact on Dutch society.

2.1.1. THE 1953 FLOOD DISASTER

The Dutch have protected their land from flooding for centuries. Flood protection is historically a collective effort organized by the water boards, some of which were founded in the 13^{th} century. Until the first half of the 20^{th} century the flood defense system used to be repaired and upgraded only after disasters had struck, before the major coastal flood disaster in 1953 initiated change. After large parts of the south-western delta of the Netherlands had been flooded (Figure 2.3) and more than 1800 persons had lost their lives, the attitude towards design and maintenance of flood defenses underwent a major transformation as explained in the next section.

Figure 2.3: Flooded areas in the South-west of the Netherlands during the North Sea flood of 1953 (source: Lencer, 2011)

2.1.2. THE FIRST DELTA-COMMITTEE

The Deltacommissie (1960), a group of experts assembled to develop a strategy to prevent disasters like 1953 in the future, advised the Dutch government to shorten the coast line by constructing the Delta Works (closures of estuaries by dams). Furthermore, and more importantly in this context, they proposed to bring all primary flood defenses to the "delta-level".

Interestingly, this delta-level was possibly the first time that risk-based economic optimization was applied to determine flood protection standards. Van Dantzig (1953) had provided the theoretical foundation in form of an economic model comparing the cost of dike reinforcement to its effect in terms of flood risk reduction, risk being defined as probability of flooding times consequences. The principle of such economically opti-

mal safety standards is illustrated in Figure 2.4, the core idea being to determine the investment strategy leading to the minimum total cost consisting of the investment costs themselves and the cost of risk-bearing (i.e., expected cost of failure). Even though the protection standards recommended by the Delta Committee were not implemented exactly as proposed, they represent, to a large extent, the basis for the safety standards for primary flood defenses in force at the time of writing.

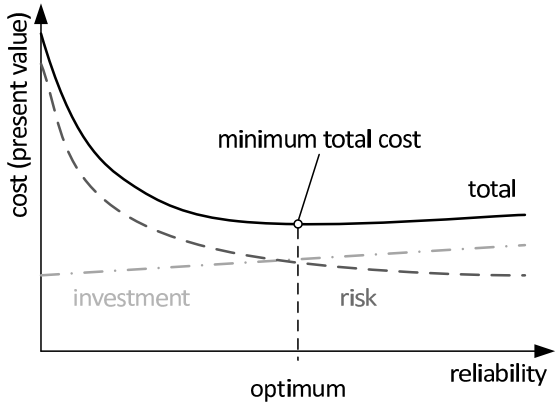

Figure 2.4: The principle of economically optimal levels of protection or safety

2.1.3. THE 1995 FLOOD DEFENSE ACT

Nowadays, the safety standards for primary flood defenses have a legal status in the Netherlands, which was defined in the 1995 Flood Defense Act (in Dutch: *Wet op de waterkering*). These safety standards, as presented in Figure 2.5, are expressed in terms of the expected exceedance frequencies of so-called normative load events. For example, for dike rings 13 and 14 along the central coast of the Netherlands, this means that the combination of the storm surge level and wave conditions used in safety assessments and designs of flood defenses has a return period of 10,000 years. Other areas have lower protection standards; the background of the differentiation are considerations of potential consequences, which are highest in Central Holland.

The compliance of the defenses to the safety standards needs to be verified by the waterboards through periodic safety assessments, currently every 6 years[1]. Non-complying defenses are to be reinforced.

For the sake of practicability, the definition of the legally defined safety standards is extended here from only a definition of the return period of the "design" load event to an acceptable probability of flooding or system failure for a so-called dike ring. As further discussed in 2.2, this extension is necessary to arrive at consistent design and assessment rules.

[1] The frequency of safety assessments was subject to political discussion at the time of writing; the expectation is that the frequency will be once every 12 years in the future.

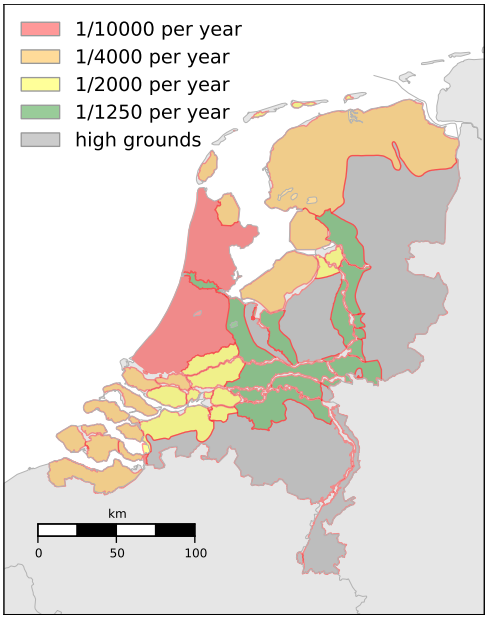

Figure 2.5: Safety standards of primary flood defenses in the Netherlands in terms of return periods of the design load events (according to the Dutch Flood Defense Act, 2009; illustration courtesy of Kees Den Heijer)

2.1.4. SAFETY ASSESSMENT

The common situation when starting a detailed safety assessment as investigated in this work is that the structure in question is considered unsafe based on the information at hand, i.e., the prior probability of failure exceeds the acceptable value. In the Netherlands, there are different stages or levels in the compulsory safety assessments:

Simple Simple assessment rules use very simple characteristics or parameters in a very conservative fashion. For example, the slope of a levee may be considered safe regarding slope stability just based on geometrical considerations (e.g., slope angle less than 1:4).

Detailed The detailed assessment rules use more sophisticated (usually physics-based) models requiring more input parameters as well. The models and the parameter determination are prescribed in a safety assessment manual (VTV, in Dutch: *Voorschift Toetsen op Veiligheid*).

Advanced Advanced assessments are usually carried out if state-of-the-art modeling techniques enable by-passing some of the conservative assumptions inherent to the detailed assessment rules. There are no explicit rules other than one needs to show that the target reliability is fulfilled.

The present work is based on safety assessments in the detailed or advanced category using a target (acceptable) probability of failure.

2.1.5. RECENT DEVELOPMENTS

Recently, the Second Delta Committee (Deltacommissie, 2008) formulated recommendations for preparing the Netherlands for the challenges in water management and flood protection in the 21^{st} century. Amongst others, the safety against flooding should be increased by a factor 10. Though not specified, a common interpretation was to lower the probability of flooding by a factor 10.

The project WV21[2] investigated updating the safety standards by acceptable risk criteria based on individual risk, group risk and (societal) cost-benefit analysis (see 2.2.1). The information is supposed to serve as input for a political decision on new safety standards[3]. It is expected that the safety standards for primary flood defenses in the Netherlands will be specified in terms of acceptable probabilities of flooding per dike ring. For this reason a probabilistic framework is adopted in this thesis and acceptable probabilities of failure are used as acceptance criteria.

The project WTI-2017[4] is currently developing safety assessment methods for levees, dunes and hydraulic structures in flood defense systems with semi-probabilistic as well as fully probabilistic methods and criteria. The proposed approach in this thesis will be appropriate for application to probabilistic assessments as envisaged in the WTI-2017 project for all safety assessments from 2017.

2.2. SAFETY REQUIREMENT AND TARGET RELIABILITY

THIS section briefly describes how target reliabilities at the system level are "down-scaled" by distributing them over failure modes and, finally, deriving local target reliabilities for independent dike sections. For details refer to Schweckendiek et al. (2012b), where also the derivation of partial safety factors is explained.

2.2.1. RISK ACCEPTANCE CRITERIA

Target reliabilities for engineered systems are ideally risk-informed. The higher the potential consequences of failure, the higher the target reliability. Three widely used types of risk acceptance criteria for floods and other natural and industrial hazards are discussed below.

INDIVIDUAL RISK CRITERIA

Individual risk criteria evaluate individual exposures, often defined as a maximum aacceptable annual probability of death. The stringency of individual risk criteria is often related to considerations regarding the voluntariness of exposure, and the degree to which an exposed person benefits from the hazardous activity (Vrijling et al., 1998). For Western countries a typical value for activities without direct benefit would be 10^{-6} (annual probability) as frequently used in industrial safety (e.g., chemical installations). Currently, for flooding an annual acceptable probability of 10^{-5} is considered.

[2] Reports on the essential results of the WV21-project can be downloaded from http://www.rijksoverheid.nl.
[3] For a description of an acceptable risk framework for flood defenses refer to Vrijling et al. (2011)
[4] Information on the WTI-2017 project is provided on http://www.helpdeskwater.nl.

SOCIETAL RISK CRITERIA

The FN-criterion is commonly used in the assessment of multi-fatality disasters (Jonkman et al., 2003). An FN-curve shows the exceedance probabilities (F) of different numbers of fatalities (N), plotted on double logarithmic scale (Figure 2.6). The FN-curve should not cross the criterion line, for definition and motivation of which reference is made to Jongejan (2008), Ball and Floyd (1998) or Stallen et al. (1996).

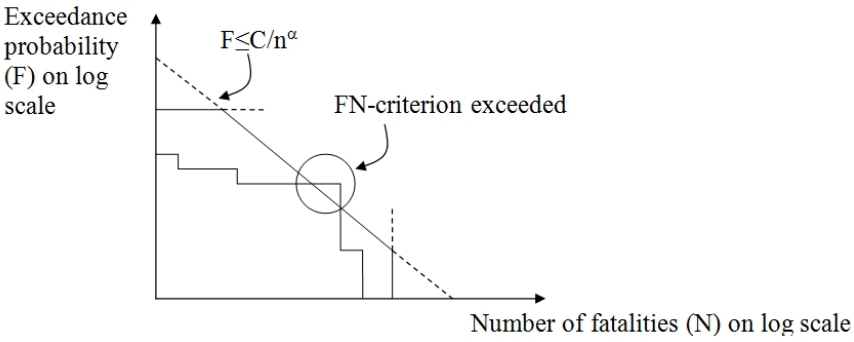

Figure 2.6: Schematic overview of FN-criteria comparing the number of fatalities per event with its annual exceeedance probability (source: Schweckendiek et al., 2012b)

ECONOMIC CRITERIA

As already shown by Van Dantzig (1953), the economically optimal reliability of an engineered system can be found by equating marginal costs with marginal benefits (i.e., cost-benefit analysis), or by minimizing the sum of the present value of the cost of strengthening flood defenses and the present value of the economic risk (i.e., expected cost of failure; see Figure 2.4).

2.2.2. SYSTEM TARGET RELIABILITY

Acceptable risk-criteria can serve as input to a political decision on protection standards. In the Netherlands, this would be an acceptable annual probability of failure[5] ($p_{T,sys}$) or annual target reliability $\beta_{T,sys}$ for a (sub-)system (e.g., a levee section). For practical reasons, these high level protection standards need to be translated into more specific requirements per levee reach and failure mode, unless fully probabilistic assessment of the entire system is feasible.

Practically workable safety requirements are usually expressed per failure mechanism and per element (e.g., homogeneous dike reach), either in terms of a target reliability (p_T or β_T) or in terms of semi-probabilistic criteria (e.g., safety factors). To arrive at such a local target reliability we contemplate the system reliability problem in an inverse fashion. Herein, we need to account for the different failure mechanisms involved

[5] At the time of writing, the actual legally defined high level requirements are not in terms probabilities of flooding or system failure but refer to exceedance probabilities of design load events. However, target system reliability levels are expected in the near future.

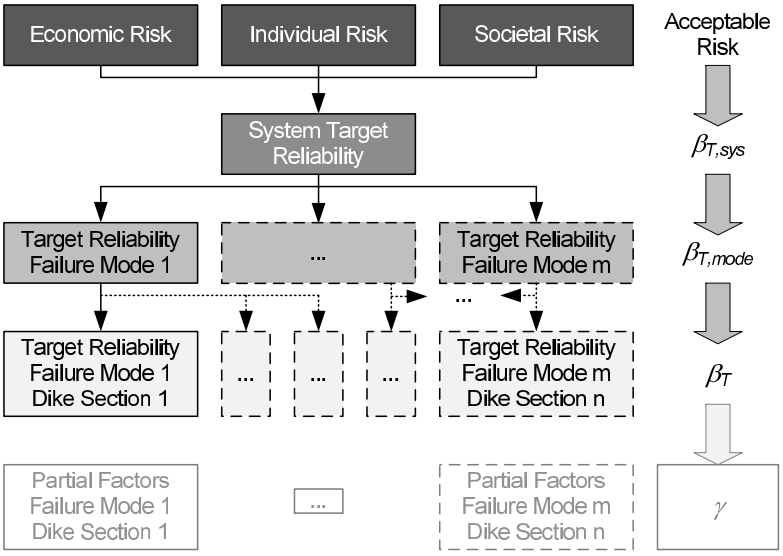

Figure 2.7: Steps in deriving target reliabilities from acceptable risk criteria (Schweckendiek et al., 2012b)

and for the system reliability and the length-effect (see e.g. Kanning, 2012) arising from the fact that all dike or levee reaches in the protection system contribute to the probability of (system) failure and that the probability of failure increases with the length of an element.

2.2.3. FAILURE MODE TARGET RELIABILITY

The first step in deriving low-level target reliabilities is assigning target reliability values for each failure mode $\beta_{T,mode}$ for the whole protection system[6]. Target reliabilities over all failure modes are ideally based on the relative cost of improvement measures for a failure mode (Voortman, 2003) and, hence, subject to economic optimization. A common requirement in practice is that the sum of the target probabilities per failure mode should not exceed the target system probability of failure ($\sum p_{T,mode} < p_{T,sys}$), which is a conservative criterion because the implicit assumption is that the failure modes are mutually exclusive.

[6] Note that the order is arbitrary, one can first account for the different failure modes or for the elements in the system. The description merely illustrates the Dutch approach.

2.2.4. LOCAL TARGET RELIABILITY

The second step is to take the so-called length effect (see e.g. Kanning 2012) into account. For a mechanism like piping, this can be simplified to deriving the equivalent correlation length l_{eq} and deriving the "local" target reliability (i.e., for an independent reach) from

$$p_T = \frac{p_{T,mode}}{1 + L_{mode}/l_{eq}} \tag{2.1}$$

where L_{mode} is the total length of dike reaches in the considered system contributing to the probability of piping failure. For details reference is made to Kanning (2012) and Schweckendiek et al. (2012b).

2.3. SUMMARY

THE work in this thesis aims to demonstrate how piping reliability can be increased to an acceptable level cost-effectively considering the effects of additional information by different types of observations (e.g., monitoring). The Dutch safety assessment framework is very suitable for approaching this challenge using probabilistic techniques, because it provides explicit reliability constraints. Similar to the Eurocode philosophy, the Dutch framework facilitates semi-probabilistic safety assessment and design of flood defenses for standard or simple cases, while the use of probabilistic techniques is possible where the simplifications of the semi-probabilistic approach pose significant limitations.

The work in this thesis is such a case, because incorporation of observations and monitoring data in semi-probabilistic assessments is not straightforward. Being able to work with reliability constraints (acceptable probabilities of failure) enables us to stay in the "doctrine of chances" (Bayes, 1763) and choose a probabilistic approach to the problem, not only in the academic work presented here but also for actual safety assessment of levees in the Netherlands. The basic safety requirement used in this thesis is the target reliability for piping per dike reach β_T or, equivalently, the target probability of failure $p_T = \Phi(-\beta_T)$.

3

PIPING RELIABILITY

I would disabuse myself of the idea of reporting a probability of failure to three significant figures, especially as the exponent might even be in question.

Dr. Ralph Peck[1]

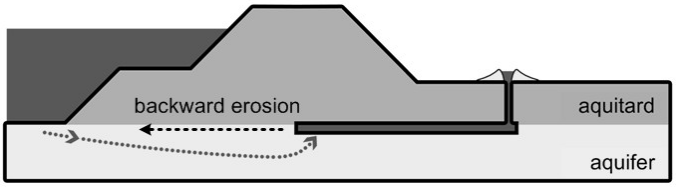

Figure 3.1: Schematic illustration of the backward erosion / piping process (illustration courtesy of Deltares)

This thesis focuses on the safety assessment for the failure mode piping, the general framework of which has been discussed in chapter 2. Piping (also called under-seepage or backward erosion) is an internal erosion mechanism that can undermine levees and lead to their collapse. This chapter commences with a description of the conceptual models of the physical process and the computational models used in safety assessments and reliability analysis, including the relevant uncertainties involved. It concludes with an example of (prior) reliability analysis in the Netherlands, which is revisited in the remaining chapters, where the focus is on reducing the dominant uncertainties in an economically efficient way where possible.

[1] Dr Ralph Peck at a Corps of Engineers workshop on Risk Analysis (2000) responded this to the question: "What approach would you recommend to obtain the final results (i.e. probability of failure = 4.65 x 10^{-4})?"

Contents

3.1. UPLIFT, HEAVE AND PIPING

ACCORDING to our current state of knowledge, uplift, heave and piping evolve in the phases illustrated in Fig. 3.2:

a) Uplift The pore pressures in the aquifer increase due to the large hydraulic head on the river side. If the upward pressure on the landside of the dike exceeds the weight of the blanket layer (aquitard), the latter is lifted up and ruptures.

b) Seepage Groundwater starts flowing upward through the ruptured blanket layer. The phenomenon observed at the surface is sometimes called *water boils*.

c) Start of Erosion (Heave) If the gradient at the exit point (also called *exit gradient*) exceeds a critical (heave) gradient, sand particles can start eroding.

d) Backward Erosion The erosion progresses upstream forming so-called "pipes", networks of erosion channels[2]. The eroded material around the exit point starts forming sand boils (Figure 3.3). The erosion may stop even under a constant head difference depending on the ground conditions and flow pattern (see 3.2.4).

e) Continuous Pipe If the erosion does not stop and the pipes reach the river, the flow velocity increases drastically due to the loss of hydraulic resistance.

f) Collapse The structure is undermined and collapses.

The process might stop at several points in time. For example, the blanket layer may be thin and ruptured, but the exit gradient insufficient to erode any particles. The limit states and assessment models are based on this conceptual model of the piping process.

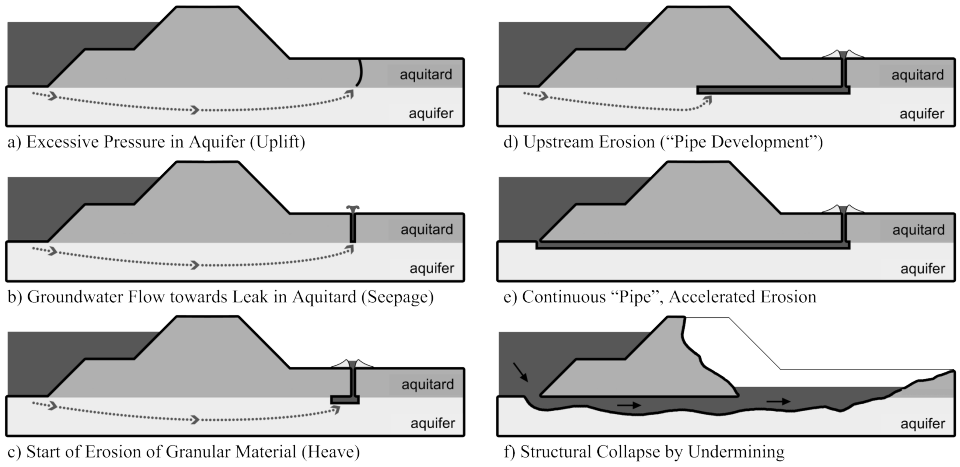

Figure 3.2: Phases of the piping process

Figure 3.3: Sand boils: in action (left) and after flood event (right), courtesy of Rijkswaterstaat

3.2. LIMIT STATES

THIS section gives a brief overview of the limit state functions for uplift, heave and piping used in this thesis. Notice that world-wide there are different approaches to assessing piping safety. For example, in the United States a heave criterion is applied to check whether erosion could start at a potential exit point (USACE, 2005). On the other hand, in the Netherlands, piping is assessed by an average gradient-based criterion based on Sellmeijer (1988) and piping, heave and uplift are considered as a parallel system. The presented load and resistance models play a role not only in (prior) reliability analysis, but they will also be used in reliability updating where observations need to be related to the failure-relevant physical processes.

3.2.1. GROUNDWATER FLOW

Before providing the actual performance or limit state functions, we introduce the groundwater flow model used for evaluating uplift and heave in this study. For both mechanisms, we need to estimate the potential ϕ_{exit} [m] at the landside exit point. Notice that in the following all surface and phreatic levels are denoted as h (with a subscript), whereas the ϕ stand for hydraulic heads in the aquifer.

The most common situation in the Netherlands, which will also be the standard situation in all analyses in this thesis, is an aquifer underlying a (semi-pervious) blanket layer (i.e., aquitard). A blanket may be present in the hinterland as well as in the foreshore. Figure 3.4 contains a schematic representation of that situation and the associated groundwater flow model used in this thesis. The potential at the exit point may be described by the damping factor λ defined as :

$$\phi_{exit} = h_p + \lambda(h - h_p) \tag{3.1}$$

where h [m] is the (river) water level and h_p [m] is the hinterland phreatic level (both with respect to mean sea level), the latter being assumed equal to the piezometric head in the far hinterland for the sake of simplicity. In general, λ can be estimated using groundwater flow models, calibration based on monitoring data or expert judgment. Notice that

[2] Notice that this type of internal erosion requires a cohesive blanket in for the so-called "roofing" effect, meaning that channels can form without soil from the top (roof) filling up the channels immediately.

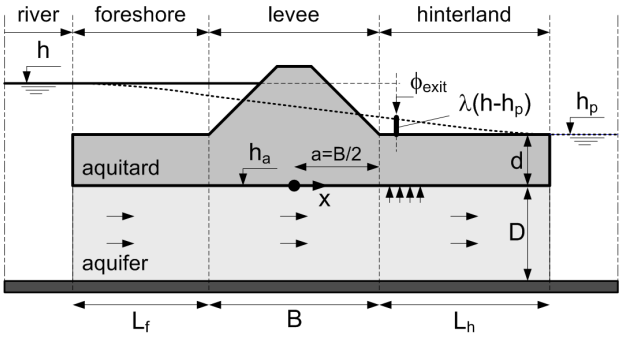

Figure 3.4: Groundwater flow model for an aquifer under an impermeable dike with leakage through the blankets (adopted from TAW (2004))

the so-called exit gradient i (i.e., the gradient in the blanket at the exit point) in this case is defined as

$$i = (\phi_{exit} - h_p)/d = \lambda(h - h_p)/d \tag{3.2}$$

where d [m] is the thickness of the hinterland blanket.

In most examples and cases studies in this thesis, we apply an analytical groundwater flow model based on Dupuit flow (i.e., predominantly horizontal flow with vertical leakage), which is described in appendix A. Making a few assumptions about the extent and permeability of the levee and the blankets, the damping factor can be approximated by:

$$\lambda = \frac{\lambda_h}{L_f + B + \lambda_h} \exp^{(B/2 - x_{exit})/\lambda_h}, \quad x_{exit} > B/2 \tag{3.3}$$

where x_{exit} [m] is the distance of the exit point from the center of the levee footprint, B [m] is the width of the levee, L_f [m] is the length of the (effective) foreshore, k [m/s] is the hydraulic conductivity of the aquifer, D [m] is the aquifer thickness, and λ_h [m] is the so-called "leakage factor" for the hinterland section given by

$$\lambda_h = \sqrt{kDd/k_h} \tag{3.4}$$

where k_h [m/s] its hydraulic conductivity. For details on the assumptions and the derivation it is referred to appendix A, where the approach is also compared with to the so-called "blanket equations" frequently applied in North America for safety assessment and design (see e.g., USACE, 2000).

3.2.2. UPLIFT

The uplift model used in this thesis is the same as the one used in safety assessments and design in the Netherlands (TAW, 1999) and elsewhere. It is based on a comparison of pore pressures at the upper boundary of the aquifer with the weight of the blanket

layer. This leads to the following limit state function in terms of gradients:

$$Z_u = g_u(\mathbf{x}) = m_u i_{c,u} - m_\phi i \tag{3.5}$$

$$i_{c,u} = \Delta\phi_{c,u}/d \tag{3.6}$$

$$\Delta\phi_{c,u} = d\frac{\gamma_{sat}-\gamma_w}{\gamma_w} \tag{3.7}$$

where m_u and m_ϕ are model factors addressing the uncertainty in the critical and actual gradients respectively (i.e., $i_{c,u}$ and i), $\Delta\phi_{c,u}$ [m] is the critical head difference, d the blanket thickness at the exit point, γ_{sat} [kN/m^3] the saturated volumetric weight of the blanket and γ_w [kN/m^3] the volumetric weight of water. The corresponding critical (river) water level (e.g., "failure water level") is

$$h_{c,u} = h_p + \frac{m_u \Delta\phi_{c,u}}{m_\phi \lambda} \tag{3.8}$$

which can be considered the cumulative resistance against the main loading on river levees - the water level h. This implies that an equivalent limit state function would be $g_u(\mathbf{X}) = h_{c,u} - h$ and that the CDF of $h_{c,u}$ is the uplift fragility curve (see 3.4.3).

3.2.3. HEAVE

While uplift is concerned with the rupturing of the low-permeability, cohesive blanket, heave considers the start of erosion of sand (i.e. aquifer material). The exceedance of a critical heave gradient $i_{c,h}$ is considered a necessary (but not sufficient) condition for the occurrence of heave:

$$Z_h = g_h(\mathbf{X}) = i_{c,h} - \min\{i, i_g\} \tag{3.9}$$

where i is the same exit gradient as in the uplift performance function (Eq. 3.5) and i_g is the so-called limit gradient. The background of the limit gradient i_g is the gradient corresponding to the pressure at the bottom of the blanket which equals the pressure exerted by the weight of the overlying blanket. Hence, for heads or gradients obtained by groundwater flow analysis which do not implicitly consider the limit gradient, taking the minimum of the two takes care of this aspect. The corresponding critical (river) water level is given by

$$h_{c,h} = \begin{cases} h_p + \frac{i_{c,h} d}{m_\phi \lambda} & \text{if } i_{c,h} \le i_g \\ \infty & \text{if } i_{c,h} > i_g \end{cases} \tag{3.10}$$

where the later case ($i_{c,h} > i_g$) reflects the fact that heave becomes impossible, if the limit gradient is less than the critical heave gradient. For blankets of homogeneous thickness, the limit gradient is the critical uplift gradient ($i_g = i_{c,u}$), whereas for situations with discontinuities in the blanket (e.g., ditches) the limit gradient may be greater ($i_g \ge i_{c,u}$). A word of caution seems appropriate regarding the applied heave model, the main limitation of which is that the heave limit state only depends on the (average) gradient over the blanket - an assumption which may not be universally applicable.

There are numerous approaches for the critical heave (exit) gradient in the literature such as the one by Terzaghi (1929):

$$i_{c,h} = \frac{(1-n)(\gamma_s - \gamma_w)}{\gamma_w} \approx 1.65(1-n) \tag{3.11}$$

where n is the porosity and γ_s [kN/m^3] is the volumetric weight of sand grains (=26.5 kN/m^3). Notice that various scholars after Terzaghi have developed variations of his approach (e.g., Harza, 1935; Bazant, 1953; Davidenkoff, 1956), which tend to result in lower critical gradients.

As the goal of this thesis is to show the relative effects of incorporating additional information, we do not enter the discussion on the critical heave gradient nor do we make a choice for a model in literature but we apply an even simpler approach which does not involve any sand parameters. The applied probability distribution is an educated guess based on experimental and field observations such as shown in Figure 3.5. The critical heave gradient will a-priori be assumed lognormal distributed with the following mean and standard deviation: $i_{c,h} \sim LN(0.7, 0.1)$ (which corresponds with the sand boils category in Figure 3.5).

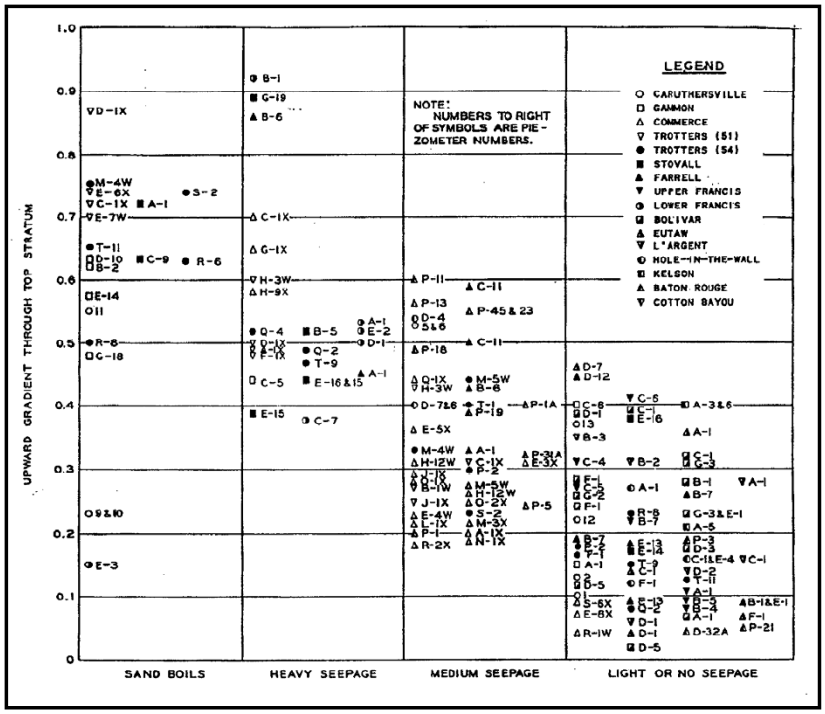

Figure 3.5: Severity of seepage as related to upward gradient through top stratum (source: USACE (1956))

With respect to Figure 3.5 it should be noted that from experience in the U.S. sand boils were also observed for rather low gradients around 0.2. However, later reviews (e.g. Wolff, 1994) express doubts about the measured gradients with those observations for the pressure release effect in the vicinity of the exit point. That means that the actual gradients at the observations were probably higher. Thus, the assumed distribution is deemed to be reasonable.

3.2.4. PIPING

The general form of the performance function for piping (i.e., backward erosion), which suits most computational assessment models, is:

$$Z_p = g_p(\mathbf{X}) = H_c - H \tag{3.12}$$

which is the difference between the critical head difference H_c [m] and the actual head difference $H = h - h_p$ [m]. Hence, the piping resistance is expressed in terms of a critical head difference or sometimes a critical piping gradient $i_{c,p} = H_c / L$ (where L is the seepage length [m]). Models formulated this way refer to average gradients addressing the piping process (phases d-e in Fig. 3.2) as opposed to another class of models addressing local gradients dominating the start of erosion like uplift and heave (phase b-c Fig. 3.2).

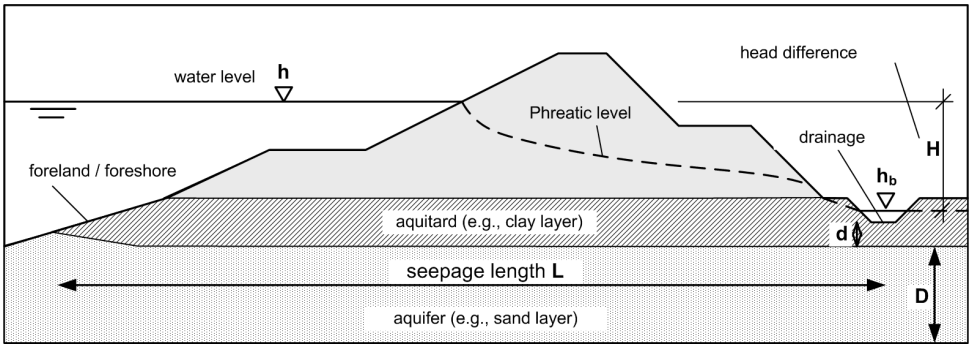

Figure 3.6: Definitions for piping assessment models

BLIGH AND LANE

Bligh (1910) was the first to treat the issue of piping for dams and levees scientifically. After having stated that the stability of a weir on a porous foundation depended on the weight of the structure in the first edition of "Practical Design of Irrigation Works" (Bligh, 1907), he revised his opinion and stated that the stability depends on the length of the percolation path or seepage length. He also realized that piping-resistance decreased with decreasing grain size. After analyzing a large number of dams, mostly for irrigation, in India, both failed and intact, he established empirical coefficients relating the required seepage length L_d [m] (design value of the resistance) to the head difference H_d [m] (design value of the load) by: $L_d = c H_d$. These percolation factor c depended on the grain size of the erodible material in the aquifer. Intuitively, that makes sense, since H/L is the average hydraulic gradient, the driving force for flow velocity and thereby erosion.

In safety assessments the seepage length L [m] is given and the performance function (Eq. 3.12) can be rewritten as:

$$Z_p = g_p(\mathbf{X}) = L/c - H \quad \Leftrightarrow \quad Z_p = L - c \cdot H \tag{3.13}$$

Bligh chose the coefficient c as a relatively safe value for design purposes. Designing a foundation with a seepage length of c times the head difference should give "perfect confidence in its stability" (Bligh, 1915). This conservatism needs to be kept in mind when using Bligh's percolation coefficients c in a probabilistic analysis, as addressed by Kanning (2012) who assessed the bias included in the percolation factor.

The next major insight was reported by Lane (1935) along with a corresponding proposed design rule. In his analysis of a large number of dams he distinguished between horizontal and vertical percolation paths. He found that vertical paths offered a 3 times higher resistance than horizontal ones. Since the focus in this thesis is on river dikes, vertical seepage paths are of minor relevance and will not be considered.

Table 3.1: Design percolation factors c based on (Bligh, 1915) as applied by TAW (1999)

Soil Type	median grain diameter d_{50} [μm]	Percolation Factor c
very fine sand	< 150	18
medium-fine sand	150 - 300	15
coarse sand	300 - 2000	12
gravel	> 2000	< 12

SELLMEIJER

Sellmeijer (1988) developed a theory on piping stability based on the flow pattern generated by the head difference between the waterside and the landside water level - the driving force of internal erosion - and the erosion resistance of the sand grains in a partially developed piping channel (Figure 3.7).

Using local stability criteria for sand grains, stability criteria were derived for levee safety assessment and design purposes in the Netherlands TAW (1999).

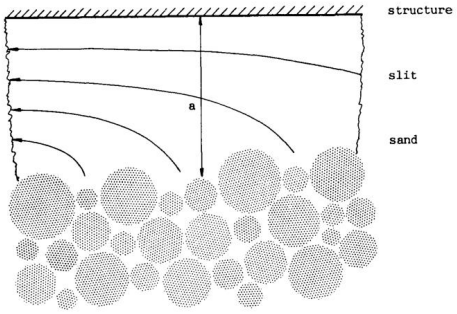

Figure 3.7: Erosion of sand grains in a piping slit (Sellmeijer, 1988). For a river levee, the high water level would be on the right-hand side and the structure on top of the figure would be the blanket layer.

Recently, a major effort in the Netherlands involving physical model tests up to prototype scale (Van Beek et al., 2011b) has led to a revision of the Sellmeijer formula (see also Sellmeijer et al., 2011). The performance function (related to Figure 3.6) reads:

$$Z_p = g_p(\mathbf{X}) = m_p H_c - H = m_p H_c - (h - h_p - 0.3d) \tag{3.14}$$

where

m_p	model (uncertainty) factor
$H_{c,p}$	critical head difference [m]
H	head difference [m]
h	water level at the entry point (water side) [m]
h_p	phreatic level at the exit point (land side) [m]
d	thickness of the blanket layer [m]

and the corresponding critical water level for piping $h_{c,p}$ is given by

$$h_{c,p} = m_p H_c + h_p + 0.3d \tag{3.15}$$

The critical head difference in the revised Sellmeijer formula is given by:

$$\begin{aligned} H_{c,p} &= F_1 F_2 F_3 L \\ F_1 &= \eta \left(\frac{\gamma_s}{\gamma_w} - 1 \right) \tan\theta \\ F_2 &= \frac{d_{70m}}{\sqrt[3]{\frac{\nu k L}{g}}} \left(\frac{d_{70}}{d_{70m}} \right)^{0.4} \\ F_3 &= 0.91 \, (D/L)^{\frac{0.28}{(D/L)^{2.8}-1} + 0.04} \end{aligned} \tag{3.16}$$

where

L	seepage length [m]
γ_s	volumetric weight of sand grains (=26.5 kN/m^3)
γ_w	volumetric weight of water (=10 kN/m^3)
θ	bedding angle [deg]
D	thickness of the aquifer [m]
η	drag factor coefficient
d_{70}	70%-fractile of the grain size distribution [m]
d_{70m}	reference value for d_{70} [m]
g	gravitational constant (=9.81 m^2/s)
k	permeability of the aquifer [m/s]

Note that the d_{70} refers to the the piping-sensitive layer, often fine sand underlying a blanket layer. This limit state (Eqs. 3.14-3.16) is supposed to be used for safety assessments in the Netherlands in the near future and will be employed in the remainder of this thesis.

3.2.5. UPLIFT, HEAVE AND PIPING - A PARALLEL SYSTEM

Backward internal erosion failure as considered in the conceptual model presented in section 3.1 can only occur if the uplift, heave and piping limit states are all exceeded. In system reliability terms, this can be described by a parallel system, for which the failure set of the failure mode is the intersection of the separate failure mechanisms:

$$F = F_u \cap F_h \cap F_p = \{\{g_u(\mathbf{x}) < 0\} \cap \{g_h(\mathbf{x}) < 0\} \cap \{g_p(\mathbf{x}) < 0\}\} \tag{3.17}$$

In a fault tree representation (Figure 3.8) the events are connect by and *AND*-gate.

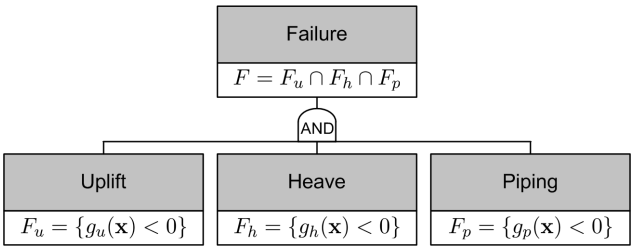

Figure 3.8: Fault tree for uplift, heave and piping

This notion is important not only for safety assessments but also for design considerations, as increased reliability of either sub-mechanism leads to an increase of the overall reliability.

3.3. UNCERTAINTIES

Mathematical models are necessarily abstractions of real world behavior. Model predictions are uncertain due to basically three reasons:

Input Variable Models have input variables such as material properties or load characteristics, which are rarely known deterministically. Their values have to be inferred from (indirect) measurements or need to be predicted themselves (e.g., future water levels) by other models. An important part of the uncertainty in model inputs is statistical uncertainty, which stems from the limited number of observations usually available.

Model Error Even under fully controlled conditions in a laboratory (i.e., the input values are known with certainty) models do not give perfect predictions. There is scatter around the results, because models do not include all aspects that affect the real world behavior in question. Furthermore, under non-controlled conditions there may be additional factors that influence the real-world behavior which are absent in the lab. Both these aspects together result in model error.

Site Characterization Models require their input in a certain format. Generating model input from real world observations usually requires (engineering) judgment in order to "squeeze" reality into the right format. The choices made in this process lead to uncertainty, which we call "characterization uncertainty".

The remainder of this section describes how the (prior) uncertainties related to uplift, heave and piping are modeled and which idealizations and assumptions were made.

3.3.1. INPUT VARIABLES

The sources of uncertainty in input variables are imperfect information or transformation errors (e.g., indirect measurements), statistical uncertainty due to limited numbers of observations, spatial variability and the random character of natural phenomena in time. Below we describe the idealizations and assumptions the have been made with respect to statistical uncertainty and spatial variability for the model input-related random variables

SPATIAL VARIABILITY

The random variables characterizing geotechnical and geo-hydrological properties in this thesis refer to *representative values* for the investigated levee sections in a spatial and mechanical sense[3]. That means that the treatment of spatial variability is implicit rather than explicit[4] (e.g., by means of random fields). Consequently, the length-effect (Kanning, 2012) is also taken into account in an implicit, not explicitly.

The classical geotechnical example for a representative value would be the shear strength assigned to a sliding plane in a slope stability analysis. If the sliding plane goes through a deposit with spatially variable shear strength, the representative value would be the average shear strength along the sliding plane. In general, the representative value is the value which used in modeling quasi-homogeneous deposits leads to the same result as modeling the spatial variability of the deposit explicitly. In principle, a representative value can be obtained for all ground properties, but we need to take care that its definition or interpretation suits the computational model or performance function in question. While for shear strength and many other geotechnical problems representative values are often spatial averages (Rackwitz, 2000), for groundwater flow we usually need to deal with upscaling of permeability (Bierkens and Van der Gaast, 1998) and for erodibility in internal erosion problems we need to consider a weakest path problem (Kanning, 2012).

Since idealization in terms of quasi-homogeneous representative properties is common practice and this thesis focusses on reliability updating and decision analysis, the input parameters for the illustrations and examples in the remainder are assumed as a given starting point. For discussions on prior estimates of uncertainties it is referred to the literature with the JCSS Probabilistic Model Code (Part 3.07: Soil Properties) probably being the most comprehensive source of information (Vrouwenvelder, 1997).

[3] Notice that the term *representative value* is frequently used with the meaning of a cautious estimate, sometimes with a statistical definition, in the context of codes of practice such as Eurocode or ISO-standards, which is different to the definition here.

[4] The only exception of the implicit treatment of spatial variability in this thesis is the 2D-random field modeling of the blanket layer in sections 7.3 to 7.5.

STATISTICAL UNCERTAINTY

As described above, the geotechnical and geo-hydrological random variables are assumed to model representative or effective values in a spatial as well mechanical sense. These properties are also assumed to not change in time, which implies that, in principle, they could be known exactly with sufficient measurement efforts. Hence, their nature is epistemic; the uncertainty reflects our lack of knowledge rather than actual heterogeneity. This notion is particularly relevant important for reliability updating as discussed in sections 4.2 and 4.3, because epistemic uncertainty is reducible. With these assumptions, in fact, all uncertainty modeled by the geotechnical and geo-hydrological random variables can be classified as statistical uncertainty. In other words, statistical uncertainty is included in the probability distributions of the input variables.

DEFAULT VALUES

Table 3.2 contains the default values as used for the considered failure mechanismsin the FLORIS project (Vrouwenvelder and Steenbergen, 2003) . These values are used if expected values can be estimated (e.g., by expert judgment) but at the same time there are insufficient data for determining the other moment(s) of the probability distribution functions. These values are applied throughout this thesis unless stated otherwise.

Table 3.2: Default values for probability distributions of uplift, heave and piping input parameters (based on Vrouwenvelder and Steenbergen (2003))

Symbol X	Unit	Distribution Type	Mean μ_X	CoV V_X	SD σ_X
h_p	[m]	Normal	nom[1]		0.10
d	[m]	Lognormal	nom[1]	0.30	
L	[m]	Lognormal	nom[1]	0.05	
D	[m]	Lognormal	nom[1]	0.10	
d_{70}	[m]	Lognormal	nom[1]	0.15	
k	[m/s]	Lognormal	nom[1]	1.00	
L_f	[m]	Lognormal	nom[1]	0.10	
B	[m]	Deterministic[2]	nom[1]		
x_{exit}	[m]	Lognormal	nom[1]		0.50
L_h	[m]	Lognormal	nom[1]	0.10	
k_h	[m/s]	Lognormal	nom[1]	1.00	
γ_{sat}	[kN/m^3]	Normal	nom[1]	0.05	
i_c		Lognormal	0.70		0.10

[1] nom = nominal value based on expert knowledge or local data

[2] The dike width is treated as a deterministic variable, related uncertainties are accounted for in the lengths of the foreshore and hinterland blankets L_f and L_h.

3.3.2. MODEL UNCERTAINTY

Model uncertainty deals with the part of the prediction error that originates from the imperfection of the model itself, not from the input variables (see 4.3.3). This section describes how model uncertainty is accounted for in the different models related to piping safety as applied in this study.

UPLIFT

Model uncertainties in the limit state function for uplift are covered by the model factors m_u and m_ϕ for the resistance and the load terms respectively. The models are assumed to give unbiased predictions (mean value equal to one) and that the uncertainty in both is about 10%.

Table 3.3: Probability distributions of uplift- and heave-related model factors

Symbol X	Unit	Distribution Type	Mean μ_X	CoV V_X	SD σ_X
m_u	[m]	Lognormal	1.0	0.10	0.10
m_ϕ	[m]	Lognormal	1.0	0.10	0.10

HEAVE

For heave, the model uncertainty is assumed to be included in the probability distribution of the critical heave gradient as specified in section 3.3.1.

BLIGH

Recently, Kanning (2012) re-assessed data from Bligh (1915) and Lane (1935) plus additional levee data from the United States and the Netherlands by means of Bayesian analysis. The percolation factors in Table 3.1 are meant to be design values, that means they are conservative and the real value will be lower with high confidence. By updating a non-informative prior with the data, which include failure and non-failure cases, Kanning calibrated a model factor m_B in the following form to account for the bias in Bligh's percolation factors:

$$H_c = \frac{cL}{m_B} \tag{3.18}$$

Kanning found that the probability distribution of the model factor is best described by the following lognormal distribution: $m_B \sim LN(1.76, 1.69)$.

SELLMEIJER

The Sellmeijer formulae, both original and revised, were derived from a more general theory developed by Sellmeijer (1988) for the following specific conditions:

1. a homogeneous aquifer underlying an impervious blanket layer, both of constant thickness;
2. no spatial variation of properties in the longitudinal direction of the dike;

Note that uncertainties originating from conditions deviating from the above are not addressed explicitly in this thesis; complete three-dimensional models for piping do not yet exist. The uncertainties are rather treated implicitly by choosing "characteristic" input values for the model. Notice that "characteristic" in this context deviates from the statistically motivated definitions of characteristic values in reliability-based design or codes of practice. It rather refers to "effective" or "equivalent".
For the revised Sellmeijer model, a model uncertainty factor was studied in Lopez de la Cruz et al. (2010) based on experimental results ranging from small to prototype scale (Van Beek and Knoeff, 2010). Figure 3.9 shows the comparison of critical head difference and critical gradient from model predictions (H_c) versus observations ($H_{c,o}$). From these results it seems reasonable to account for the model uncertainty through a model factor m_p as in the performance function (Eq. 3.14).

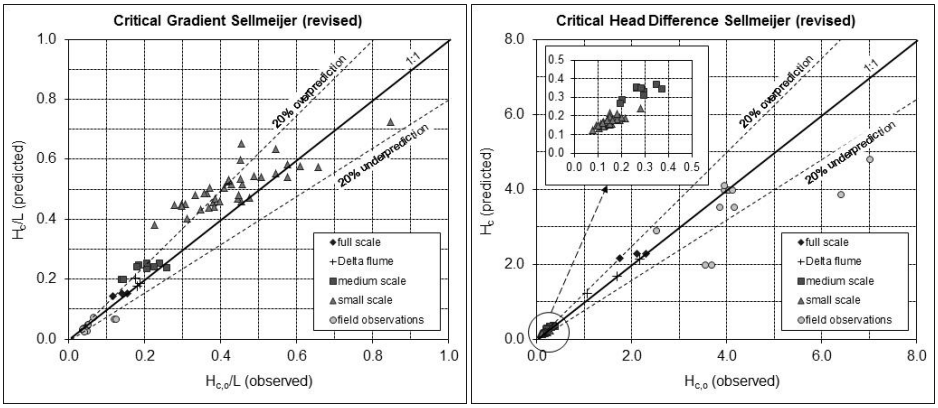

Figure 3.9: Model uncertainty Sellmeijer (revised): observed vs. predicted critical gradient (left) and critical head difference (right) (Lopez de la Cruz et al., 2010)

The results in Figure 3.9 show that the model is (practically) an unbiased estimator for the critical head difference, hence a mean value of the model factor distribution of one is used. Based on the results the model uncertainty factor is modeled with a lognormal distribution in this thesis: $m_p \sim LN(1.0, 0.12)$. Table 3.4 summarizes the distributions and values of the model parameters used in the piping performance function.

3.3.3. SITE CHARACTERIZATION

The uncertainties of geotechnical input variables are usually modeled with continuous probability distribution functions or continuous random fields. The underlying assumption is often that these properties refer to statistically homogeneous soil strata. Their parameters are determined by statistical analysis of discrete observations or expert judgement. Usually, these uncertainties refer to a given soil profile with assumptions regarding (a) stratification, (b) the existence, size and position of geological or man-made anomalies or (c) geo-hydrological conditions.

Table 3.4: Model parameters of Sellmeijer, revised version

Symbol X	Unit	Distribution Type	Mean μ_X	COV V_X	SD σ_X
m_p		Lognormal	1.0	0.12	
θ	[deg]	Deterministic	37	-	
η		Deterministic	0.25	-	
d_{70m}	[m]	Deterministic	2.08e-4	-	
ν	[m^2/s]	Deterministic	1,33e-6	-	
$(\gamma_s - \gamma_w)/\gamma_w$		Deterministic	1.65	-	

Uncertainties in these assumptions can be much more important than the uncertainties of input variables describing statistically homogeneous layer properties or model uncertainties, as will be demonstrated in section 3.5. In general, characterization uncertainty refers to the "discrete" choices made by engineers to generate model input from site investigation data combined with geological knowledge and local experience. In engineering design these choices are made implicitly by generating representative cross sections or 3D-subsoil models in a cautious fashion, for example, by choosing worst case scenarios or making conservative assumptions. In reliability analysis, these uncertainties can be dealt with explicitly by generating scenarios and assigning likelihoods to them. In Schweckendiek and Calle (2010) an attempt was made to explicitly treat this type of uncertainty in design practice by introducing a "safety factor for geotechnical characterization". A few illustrative, though strongly simplified examples are presented below. The (mutually exclusive sets of) stratification scenarios in the case studies in this thesis refer to such uncertainties in site characterization.

STRATIFICATION

Inferring stratification from borings requires interpretation and engineering judgement. There are usually several plausible "scenarios" for the real stratification which "generated" the bore logs. Figure 3.10 shows three fictitious bore logs, from which different soil profiles could be interpreted. The examples (a) and (b) show two possible interpretations. Suppose an embankment is to be built close to the boring in the middle, for which the peat layer could be a serious issue. In that case, scenario (a) would represent an optimistic interpretation, because it assumes that the peat layer is not present at the site. On the other hand, scenario (b) would be a pessimistic scenario because it assumes the peat layer to be present even though not indicated in the boring. A possible reason to choose scenario (b) in a design context could be that there are interpretation errors in the borelogs themselves. Furthermore, the non-existence of the layer may be highly implausible based on local geological experience. The approach proposed in Schweckendiek and Calle (2010) shows a way to deal with this situation in designs and safety assessments.

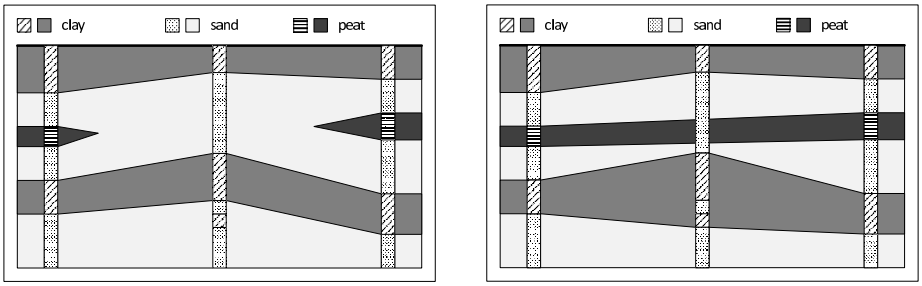

(a) Optimistic Interpretation (b) Pessimistic Interpretation

Figure 3.10: Illustration of geological uncertainties: different stratification scenarios inferred from the same borings. Supposing a levee would were to be built at the center boring, the left-hand side interpretation (a) would be optimistic in terms of expected settlements, whereas (b) would be pessimistic.

GEOLOGICAL AND MAN-MADE ANOMALIES

Similarly, geological and man-made anomalies need to be considered in the characterization of the ground conditions. As for stratification, we are only interested in anomalies that may influence the structural performance, such as:

1. For uplift and piping, shallow sand lenses (e.g., old river channels) can be major threats. These usually sandy and highly permeable features may lead to high pore pressure penetration under the levee and the blanket layer, which can also be thinner where these channels cut through it.
2. Pipelines (with inappropriate or missing seepage screens) may create preferential flow paths.

Notice that the stratification scenarios in the examples and case studies in this thesis can reflect geological anomalies or adverse geological details. Man-made anomalies are just mentioned for the sake of completeness here; they are not treated in the remainder.

GEO-HYDROLOGICAL CONDITIONS

As the limit states discussed in this chapter show, pore pressures and hydraulic gradients play an important role in piping reliability as they do for other geotechnical failure mechanisms of levees. The shear strength of soil decreases with increasing pore pressures (i.e., effective stress concept) and hydraulic gradients are the drivers for ground water flow and, therefore, internal erosion processes like piping.

In order to assess the hydro-geological conditions we need to assess, for example, whether or not a river is in (direct) contact with the aquifer and, if so, where. Figure 3.11 illustrates that variations in the thickness of a blanket layer can result in uncertainties of so-called entry points. At some locations the river side blanket may be so thin (as interpreted from the available site investigation data) that there may be hydaulic contact between the river and the aquifer. The position of these entry points determines not only the groundwater flow and, hence, the pore pressure fields but also the length of the seepage path (L). Similar to stratification and anomalies, the potential entry points may

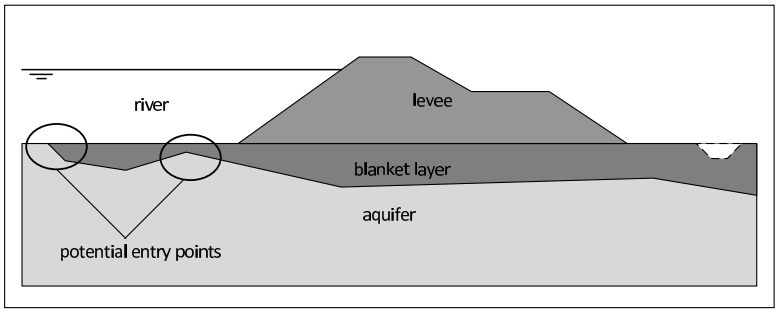

Figure 3.11: Illustration of uncertainties in hydro-geological conditions (potential entry points)

be modeled by scenarios. In fact, entry points may be considered as a special case of stratification and anomalies.

3.4. RELIABILITY ANALYSIS

IN reliability analyses (e.g., for safety assessments) and reliability-based design, the aforementioned uncertainties need to be accounted for properly. This section provides theory and definitions for how to apply reliability analysis to uplift, heave and piping. More elaborate information on the actual (numerical) reliability analysis techniques used throughout this thesis is provided in appendix B.

3.4.1. FAILURE (UNDESIRED EVENT)

Failure refers to an unwanted event, not necessarily to collapse of a structure, which we model by means of a (continuous) performance function $Z = g(\mathbf{X})$ such that the performance function assuming negative values represents the failure domain:

$$F = \{Z < 0\} = \{g(\mathbf{X}) < 0\} \tag{3.19}$$

where $\mathbf{X}$ is the vector of random variables.

3.4.2. PROBABILITY OF FAILURE

According to the definition of failure and the performance function, the probability of failure (i.e., unwanted event) is given by:

$$P(F) = P(Z < 0) = P(g(\mathbf{X}) < 0) = \int_{g(\mathbf{X})<0} f_{\mathbf{X}}(\mathbf{x})\, d\mathbf{x} \tag{3.20}$$

where $f_{\mathbf{X}}(\mathbf{x})$ is the probability density function (PDF) of $\mathbf{X}$.

3.4.3. FRAGILITY CURVES

Fragility curves are the probability of failure conditioned on a dominant load variable s:

$$P(F|s) = \int_{g(\mathbf{R},s)<0} f_{\mathbf{R}}(\mathbf{r})\,d\mathbf{r} \tag{3.21}$$

where $\mathbf{R}$ is the vector of resistance variables (or, exactly speaking, all variables except s). If the total uncertainty in the resistance can be expressed in terms of one random variable R this simplifies to:

$$P(F|s) = F_R(s) \tag{3.22}$$

where F_R is the CDF of R.

3.4.4. SYSTEM RELIABILITY

If failure is not just defined for one structural element or limit state, but by several limit state functions $g_i(\mathbf{x})$, $i = 1...m$, the failure domain can be defined by the following expression:

$$F = \left\{ \min_{1\le k\le K} \left[\max_{i\in C_1} g_i(\mathbf{x}), ..., \max_{i\in C_k} g_i(\mathbf{x}) \right] \le 0 \right\} \tag{3.23}$$

where C_k is an index set denoting the k-th cut set. For $m = 1$, this is a component reliability problem; for $K = 1$, it is a parallel system reliability problem; and when each cut set contains only one index, it is a series system reliability problem.

Hence, the parallel system problem of uplift, heave and piping ($F = \{F_u \cap F_h \cap F_p\}$) can be formulated as:

$$F = \left\{ \max\left[g_u(\mathbf{x}), g_h(\mathbf{x}), g_p(\mathbf{x}) \right] \le 0 \right\} \tag{3.24}$$

3.4.5. STRATIFICATION SCENARIOS

As discussed in 3.3.3, some ground-related uncertainties, in particular the stratification, will be modeled as (discrete) scenarios E_i. The total probability of failure over all (mutually exclusive and collectively exhaustive: $\sum P(E_i) = 1$) scenarios is given by the law of total probability:

$$P(F) = \sum_i P(F|E_i)P(E_i) \tag{3.25}$$

3.5. APPLICATION EXAMPLE: MASTENBROEK

PIPING, amongst other failure modes, was subject to a reliability analysis in the Dutch VNK2-project (Jongejan et al., 2013), on which the prior probabilities used in the following example are based. For the sake of clarity, the input has been reduced to the main contributing uncertainties. For example, the number of stratification scenarios has been reduced from eight to four. Furthermore, the limit state models used in this report are based on more recent insights. For example, heave is included in the failure definition considered, whereas it is not in VNK2, and the revised Sellmeijer model is used as compared to the original one in VNK2[5]. Therefore, the resulting probabilities of failure cannot be compared directly. It is emphasized that the example does not aim at evaluating the safety of the dike setion in question but at at illustrating the effects of uncertainty reduction measures in the subsequent chapters for a realistic example.

3.5.1. LOCATION

The dike reach is located along the river IJssel in the south-western part of dike ring 10 (Mastenbroek, VNK2 ID: Vak 03 HM 1,4 - HM 2,8). While the reach is about 1.4 km long, the analysis refers to an 250 m long subreach. This location was chosen due to its relatively large contribution to the probability of failure of the dike ring due to uplift and piping in VNK2.

Figure 3.12: Location of the application example: dike Reach 03 from the VNK2-project in the South-Western Part of Dike ring 10

[5]At the time of writing the VNK2-project (Jongejan et al., 2013) was re-analysing dike ring 10 with new data, the presented results are based on the first analysis made in the project as available at the time of the analysis

3.5.2. INPUT DATA

Tables 3.5 and 3.6 show the most relevant input parameters; detailed information on the input and results is provided in appendix H. The scenario probabilities as presented in table 3.6 in the VNK-project were determined by spatial statistical analysis of a large number of shallow (classified) borelogs in the surroundings of the locations in question (Wiersma et al., 2011).

Table 3.5: Input data application example for field observations, dike ring 10 (Mastenbroek) - prior distributions of the scenario-independent random variables (based on VNK2 data). The seepage length L, input to the piping limit state function, is defined as $L = L_f + B + x_{exit}$.

Symbol	**Unit**	**Type**	**Mean** (Par1)	**Std** (Par2)
D	[m]	Lognormal	μ_{D,E_i} *	0.2μ
k	[m/s]	Lognormal	μ_{k,E_i} *	0.7μ
d_{70}	[m]	Lognormal	$2.1E-4$	0.15μ
θ	[deg]	Deterministic	37	
h	[m]	Gumbel	$a_h = 1.362$	$b_h = 5.747$
h_b	[m]	Gaussian	0.3	0.1
d	[m]	Lognormal	μ_{d,E_i} *	0.3μ
x_{exit}	[m]	Lognormal	30.0	0.5
L_f	[m]	Lognormal	10.0	2.4
B	[m]	Deterministic	37.0	
L_h	[m]	Deterministic	$1.0E+4$	
k_h	[m/s]	Lognormal	$1.0E-6$	1.0μ
γ_{sat}	[kN/m^3]	Gaussian	23.0	3.5
γ_w	[kN/m^3]	Deterministic	10.0	

* *defined in Table 3.6*

Table 3.6: Input data application example for field observations, dike ring 10 (Mastenbroek) - prior distributions of the scenario-dependent random variables (based on VNK2 data, E_i is the ith scenario)

scenario **i**	$\mathbf{P(E_i)}$	$\mu_{\mathbf{d,E_i}}$ [m]	$\mu_{\mathbf{D,E_i}}$ [m]	$\mu_{\mathbf{k,E_i}}$ [m/s]
1	17.6%	2.90	20.0	$3.4E-4$
2	62.4%	2.90	96.0	$1.8E-4$
3	4.4%	0.00	24.5	$3.4E-4$
4	15.6%	0.00	100.5	$1.8E-4$

The main difference between the scenarios, besides the mean permeability and aquifer thickness, is that in scenarios 1 and 2 there is an (effective) blanket layer ($\mu_{D,E_i} > 0$), whereas in scenarios 3 and 4 the blanket layer is assumed to be absent or not effective (e.g., there may be wholes in the blanket). We will see that the two types will behave differently, especially for field observations as discussed in chapter 5.

3.5.3. PRIOR RELIABILITY

A summary of the prior reliability analysis results is presented in Table 3.7, more detailed results are provided in appendix H. The scenarios without blanket (3 and 4) are the main contributors to the (total) annual probability of failure of $P(F) = 1.9E-3$. Figure 3.13 shows the fragility curves (see 3.4.3) for uplift, heave and piping and failure for scenario E_1. It clearly demonstrates parallel system effect: (a) the 'system' probability of failure is always smaller than the smallest probability of failure of the separate failure mechanisms and (b) the system effect is largest where the mechanism probabilities are of about the same magnitude (i.e., the difference of the system probability and the mechanism probabilities is largest).

Notice that all fragility curves eventually approach 1.0 for increasing water levels; only the heave curve can remain at a lower level, which is due to the effect of the limit potential or gradient. The heave curve has a horizontal asymptote at $P(i_g < i_{c,h})$, where is this case the limit gradient is the critical uplift gradient ($i_g = i_{c,u}$).

Table 3.7: Application example for field observations, dike ring 10 (Mastenbroek) - prior analysis results summary (annual probabilities)

i	**P(E_i)**	**Uplift P(F_u|E_i)**	**Heave P(F_h|E_i)**	**Piping P(F_p|E_i)**	**Failure P(F|E_i)**	**P(E_i)P(F|E_i)**
1	17.6%	$1.8E-2$	$1.0E-1$	$4.8E-4$	$1.4E-4$	$2.5E-5$
2	62.4%	$2.8E-2$	$1.7E-1$	$5.7E-4$	$2.2E-4$	$1.3E-4$
3	4.4%	$1.0E-0$	$1.0E-0$	$8.9E-3$	$8.9E-3$	$3.9E-4$
4	15.6%	$1.0E-0$	$1.0E-0$	$8.3E-3$	$8.3E-3$	$1.3E-3$
total	100.0%				$P(F) =$	$1.9E-3$

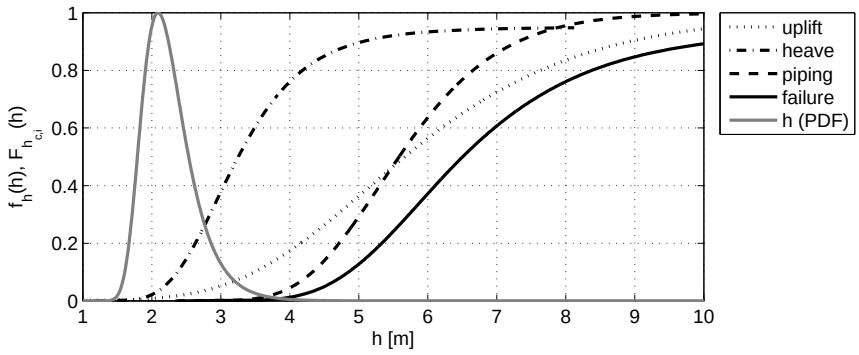

Figure 3.13: Application example dike ring 10 - prior fragility curves for uplift, heave, piping and failure and probability density of the water level (normalized) for stratification scenario E_1

Figure 3.14: Sand bags around a sand boil, source: TAW (1994)

3.6. FLOOD FIGHTING

BESIDES emergency flood fighting measures like closing dike breaches with sand bags there are specific techniques to mitigate piping. Traditionally, when sand boils are observed in the Netherlands, rings of sand bags are built around the well (see Fig. 3.14; this mitigation measure is called *opkisten* in Dutch). By decreasing the head difference between water side and land side - the driving force of the piping mechanism - the erosion should stop.

In principle, the effect of flood fighting measures could be accounted for in a reliability-based safety standard by accepting higher probabilities of failure or higher head differences. In the Netherlands, incorporation of mitigation measures in safety targets has been rejected so far on the grounds that their effectiveness is highly uncertain (Lendering et al., 2014). There are considerable doubts about the number of locations where mitigation would be necessary in extreme conditions. When wells are sand-bagged, new wells often appear in the vicinity. Therefore, the emergency measures are not taken into account in the target reliability. The same approach is followed in this thesis for sake of practical applicability of the results in the Dutch context - flood fighting measures are ignored. On the other hand, when analyzing field observations, emergency measures need to be accounted for, if they have an effect on the observation (see chapter 5).

3.7. CONCLUDING REMARKS

THIS chapter has introduced the conceptual and operational definitions of the uplift, heave and piping failure mode and the respective reliability analysis. Piping is an internal backward erosion mechanism that can lead to levee failure. Since piping cannot occur without uplift and heave, all are considered a parallel system.

The most important uncertainties are associated with the water level h (i.e., the loading), the hydraulic conductivity of the aquifer k, the blanket layer thickness d and the models themselves (accounted for by the model factors). Since the uncertainty in the water level is practically irreducible, efforts to reduce uncertainties should focus on the remaining three.

The main observations from this chapter with implications for the envisaged applications in this thesis are:

1. The fact that the mechanisms uplift, heave and piping act as a parallel system creates opportunities to focus on one of the mechanisms for uncertainty reduction or retrofitting, wherever the effect on the reliability or cost is greatest. Another, more physically motivated interpretation is that one can either try to prevent the initiation of piping or its progression.

2. The main categories of uncertainties involved in assessing piping safety are input variable and model uncertainties as well as uncertainties in stratification and anomalies. Most of these can, in principle, be reduced by measurements, monitoring or other kinds of observations, as long as they are of (pre-dominantly) epistemic nature.

3. Uncertainties concerning stratification and anomalies can be much more dominant than parameter uncertainties, especially in data-sparse regions where the stratification models are largely based on geological expert knowledge. While much of the recent literature has dealt with heterogeneity in terms of spatially varying properties within (statistically homogeneous) strata, this thesis explicitly deals with stratification uncertainties and anomalies, because their influence on the reliability is significant.

4. Flood fighting measures and their effect on the reliability with respect to uplift and piping are not included in the safety assessment. However, they may need to be accounted for when updating reliability using field observations.

Finally, it is pointed out that the length-effect (see e.g. Kanning, 2012) is not treated explicitly in this thesis; all analyses are for statistically independent levee sections with lengths in the same order of magnitude as the relevant scales of fluctuation.

4

RELIABILITY UPDATING AND DECISION ANALYSIS

"A decision was wise, even though it led to disastrous consequences, if the evidence at hand indicated it was the best one to make; and a decision was foolish, even though it led to the happiest possible consequences, if it was unreasonable to expect those consequences."

Herodotus, around 500 BC

This chapter elaborates the proposed approach for updating piping-related uncertainties and reliability, building upon the background, objectives and restrictions presented hitherto. Bayesian posterior and decision analysis form the very basis of the approach proposed in this thesis. After a brief review of the essential aspects of the theory, specific methods for reliability updating and pre-posterior analysis will be discussed, addressing the specific requirements posed by the applications envisaged in this thesis. The theory and methods described in this chapter will be applied in the remaining application-related chapters 5 to 7.

Contents

4.1. BAYESIAN DECISION ANALYSIS

4.1.1. UTILITY THEORY

Utility theory, developed by Von Neumann and Morgenstern (1947), formalizes the rational choice based on a decision maker's preferences. Suppose there is a set of possible *events* (or *outcomes*) E_i ($i = 1...n$). The set is ordered such that events with higher values of index i are preferred over events with lower index values. Choosing an *action* a_j will lead event E_i to assume probability $p^j_{(i)}$. Note that this requires the probabilities for all events per action to be an exhaustive set:

$$\sum_i p_i^{(j)} = 1 \tag{4.1}$$

Under the condition that the preferences (i.e., the ordering of the events) fulfil a number of consistency requirements, a numerical index u_i called *utility* can be assigned to the events E_i such that an action (i.e., decision) is preferred to another, if and only if it has a larger expected utility:

$$E[u(a_j)] = \sum_i p_i^{(j)} u_i(a_j) \tag{4.2}$$

Thus, expected utility provides a formal basis for comparing alternative actions. Van Dantzig (1953) and Benjamin and Cornell (1970) were among the first to apply the theory to engineering problems, Ditlevsen (2003) furthermore addresses issues like *risk aversion* and the valuation of human lives in engineering decision problems.

4.1.2. BAYESIAN DECISION THEORY

Building upon classical decision theory as developed by Von Neumann and Morgenstern (1947), Raiffa and Schlaifer (1961) provide formal procedures to take into account the preferences and judgments of decision makers. To this end a decision maker needs to be capable of

1. assigning a unique utility to each identified possible outcome that may result from the decisions taken (i.e., formalization of preferences),

2. assigning a (possibly subjective) probability to all uncertain variables involved.

Bayesian Decision Analysis forms the fundamental basis for optimizing reassessment and site investigation planning in this thesis. Even though the use of subjective probabilities and preferences is controversial, it is the only way to make decision-making consistent for this type of problems (Raiffa and Schlaifer, 1961; Savage, 1974). The main benefit of the approach lies in its consistency and transparency, for in the formalized process decision-makers need to state their preferences and judgment rather than their decisions right away. This way, discussions can focus on the critical decision parameters rather than on the result and arbitrariness can be avoided as much as possible.

Furthermore, the following chapters will show that the degree of subjectivity in judgment can be reduced substantially by involving "objective" information (i.e., observations) and by formalizing the procedures to arrive at judgment (e.g., geological assessments) as much as possible. The critics of subjective probabilities should recognize

that strictly seen nothing in life is objective in its purest sense, this is especially true in geotechnical engineering. The term "data interpretation" speaks for itself in this context. Yet, where decisions need to be made for the community, for example the citizens of a flood-prone area, the author believes it is their right to have their agents invest their tax-payers' money as consistently and transparently as reasonably achievable.

4.1.3. PRIOR DECISION ANALYSIS

Prior decision analysis is about decisions with given information (see Benjamin and Cornell, 1970). If θ is the true, yet unknown state of nature described by the PDF $f_\Theta(\Theta)$, the optimal decision a^* is the one that maximizes the expected utility:

$$a^* : \max_a E[u(a,\theta)] = \max_a \int u(a,\theta) f_\Theta(\theta) d\theta \tag{4.3}$$

Notice that in contrast to Eq. 4.2 here the decision space is continuous.

4.1.4. POSTERIOR DECISION ANALYSIS

Posterior analysis only differs from prior analysis in that new information (i.e., evidence) ε is accounted for by Bayesian Updating:

$$a^* : \max_a E[u(a,\theta)] = \max_a \int u(a,\theta) f_\Theta(\theta|\varepsilon) d\theta \tag{4.4}$$

where $f(\theta|\varepsilon)$ is the posterior (i.e, updated) PDF of the state of nature, which can be obtained as discussed in the next section.

4.1.5. PRE-POSTERIOR ANALYSIS

Site investigation or monitoring decision analysis is about acquiring new information and subsequently updating the existing information with it. In order to take the new but as yet unknown information into account, the posterior analysis can be carried out with the prior probabilities of the observations. In the so-called pre-posterior analysis, in abstract terms the expected utility to be maximized changes to:

$$E[u(S,\varepsilon,a,\Theta)] = E[u(S,\varepsilon,d(S,\varepsilon),\Theta)] \tag{4.5}$$

where

S	the information acquisition strategy: all decision parameters regarding measurements, monitoring or experiments in terms of type, number, location, time etc.
ε	the evidence or sample outcomes: for example results of in-situ and laboratory testing, geological anomaly detection or monitoring
a	the terminal acts: possible actions after obtaining new information such as reinforcement or do nothing
$d(S,\varepsilon)$	decision rule to determine the terminal action based on the inspection strategy and the inspection results
Θ	the true but unknown state of nature (e.g., failure)

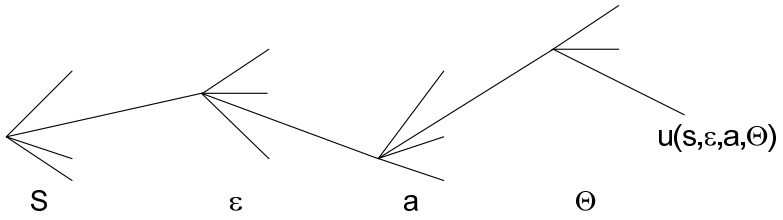

Figure 4.1: Decision tree of pre-posterior analysis, after Raiffa and Schlaifer (1961)

The decision tree in Figure 4.1 shows the ingredients and steps involved in pre-posterior decision analysis. Note that the terminal act is determined by the decision rule $a = d(S, \varepsilon)$, which can is a deterministic function after integrating out the (remaining) uncertainties. In fact, the decision rule is obtained by carrying out posterior analysis (see 4.2) conditional on the possible inspection results. Furthermore it is important to realize that the sample outcomes ε depend on the state of nature Θ. Raiffa and Schlaifer (1961) distinguish between the normal and the extended form of (statistical decision) analysis. Both types of analysis are different ways to obtain the same optimal decision or strategy, this thesis applies the normal form, which is rather common in risk-based inspection and maintenance planning. Recent examples

In contrast to the classical decision problems typically involving the costs or benefits involved with the state of nature (e.g., in risk analysis the consequences of an unwanted event such as the failure of a flood defense), this thesis works with (risk-based) reliability constraints (see 4.4.1). Furthermore, it is important to notice that the expected future posterior reliability is the same as the prior without any actions or interventions (see Box 1 below for illustration).

Box 1: Expected Posterior Reliability Index for Z = R - s

The following example illustrates that the expected reliability after a posterior analysis in the future based on the prior uncertainties is the prior reliability itself. To this end, we recur to the popular example of $Z = R - s$ where the resistance $R \sim N(\mu_R, \sigma_R)$ is a Gaussian random variable and the load s is deterministic. The prior reliability index equals: $\beta = \mu_Z/\sigma_Z = (\mu_R - s)/\sigma_R$. Suppose, we can measure R with a measurement error $e_m \sim N(0, \sigma_{e_m})$, which implies that future measurement values of the resistance can be modeled as $R_m = R + e_m$, the distribution of which is $R_m \sim N(\mu_R, \sqrt{\sigma_R^2 + \sigma_{e_m}^2})$. The correlation between the limit state function and the measurement is:

$$\rho_{Z,R_m} = \frac{COV(Z,R_m)}{\sigma_Z \sigma_{R_m}} = \frac{\sigma_R^2}{\sigma_R \sigma_{R_m}} = \frac{\sigma_R}{\sigma_{R_m}}$$

For updating the reliability with a measured value r_m, we transform the measured value to standard normal space ($u_m = (r_m - \mu_R)/\sigma_{R_m}$) and we condition a bivariate standard Normal distribution on the transformed measurement u_m (see also appendix G):

$$\mu_{v|u_m} = \rho u_m = \rho \frac{(r_m - \mu_R)}{\sigma_{R_m}} \qquad \sigma_{v|u_m} = \sqrt{1-\rho^2}$$

Now we back-transform to real space;

$$\begin{aligned} \mu_{Z|r_m} &= \mu_{v|u_m}\sigma_z + \mu_Z = \rho \frac{(r_m - \mu_R)}{\sigma_{R_m}}\sigma_Z + \mu_Z \\ \sigma_{Z|r_m} &= \sigma_{v|u_m}\sigma_Z = \sqrt{1-\rho^2}\sigma_Z \end{aligned}$$

With these ingredients we can express the posterior reliability index as a function of an arbitrary measurement as follows:

$$\beta'' = \frac{\mu_{Z|r_m}}{\sigma_{Z|r_m}} = \frac{\rho(r_m - \mu_R)/\sigma_{R_m} + \beta}{\sqrt{1-\rho^2}}$$

Given the uncertainty in the measurement, also the posterior reliability index can be considered uncertain with:

$$\mu_{\beta''} = \frac{\beta}{\sqrt{1-\rho^2}} \qquad \sigma_{\beta''} = \frac{\rho}{\sqrt{1-\rho^2}}$$

In order to obtain a Bayesian estimator for β'', the uncertainty can be integrated out with the limit state function $Z_\beta = \beta'' - u$, where u is a standard Normal random variable. The corresponding mean and standard deviation are:

$$\mu_{Z_\beta} = \mu_{\beta''} = \frac{\beta}{\sqrt{1-\rho^2}} \qquad \sigma_{Z_\beta} = \sqrt{\sigma_{\beta''}^2 + 1^2} = \sqrt{\frac{\rho^2}{1-\rho^2} + 1} = \frac{1}{\sqrt{1-\rho^2}}$$

That implies that the pre-posterior reliability index equals the prior β.

4.2. POSTERIOR ANALYSIS

POSTERIOR analysis, also called "Bayesian Updating", is a key element in (Bayesian pre-posterior) decision analysis. This section discusses several issues with and aspects of posterior analysis which will play an important role in the application chapters.

Bayes' Rule (Bayes, 1763) forms the basis for updating probabilities with new evidence:

$$P(E|\varepsilon) = \frac{P(\varepsilon|E)P(E)}{P(\varepsilon)} \tag{4.6}$$

where E is the event to be predicted and ε the observed event or evidence. Similarly, a vector of random parameters Θ can be updated by:

$$f_\Theta(\theta|\varepsilon) = \frac{P(\varepsilon|\theta)f_\Theta(\theta)}{\int P(\varepsilon|\theta)f_\Theta(\theta)d\theta} \propto \mathbb{L}(\theta)f_\Theta(\theta) \tag{4.7}$$

where $f_\Theta(\theta)$ is the prior PDF of the parameters and $\mathbb{L}(\theta)$ is the likelihood function expressing the probability of observing the evidence given the parameters or the state of nature ($\mathbb{L}(\theta) = P(\varepsilon|\theta)$). There are two important distinctions for the implementation of posterior analysis for the envisaged applications. Firstly, we distinguish:

1. *Indirect Reliability Updating*: The distribution of the basic random variables is updated first, before the uncertainty or reliability analysis is re-done with the posterior distribution.

2. *Direct Reliability Updating*: The direct method exploits the definition of conditional probability and avoids updating the basic random variables first.

Secondly, we distinguish two general types of information in posterior analysis:

1. *Inequality type*: observations where it is only known that the observed variable is greater or less than some limit (e.g., incomplete load capacity tests): $h(\mathbf{x}) < \mathbf{0}$

2. *Equality type*: value has been measured directly or indirectly, measurement and transformation errors are known and modeled as random variables: $h(\mathbf{x}) = \mathbf{0}$

Both updating methods and information types are discussed in more detail below. subsequently, additional information on updating discrete scenarios is provided.

4.2.1. INDIRECT RELIABILITY UPDATING

One way of updating a probability of failure is using Bayes' Rule (Eq. 4.7) to update the probability distributions of the basic random parameters and recalculate the reliability with these posterior probability distributions. Having updated the parameters, the updated probability distribution of the random variables is found by:

$$f_{\mathbf{X}}(\mathbf{x}|\epsilon) = \int_{-\infty}^{\infty} f_{\mathbf{X}}(\mathbf{x}|\theta)\, f_{\Theta}(\theta|\epsilon)\, d\theta \tag{4.8}$$

where $f_{\mathbf{X}}(\mathbf{x}|\theta)$ is the probability distribution of the random variables. Consequently, the posterior (i.e., updated) probability of failure (F) is obtained by:

$$P(F|\varepsilon) = \int_{g(\mathbf{x})<0} f_{\mathbf{X}}(\mathbf{x}|\epsilon)\, d\mathbf{x} \tag{4.9}$$

where $g(\cdot)$ is the limit state function. While updating the parameters of the distribution of Θ is necessary, if we assume an underlying "true" distribution of Θ (i.e., random process), posterior analysis can be carried out directly on the distribution of the random variables $\mathbf{x}$ (i.e. by applying equation 4.7 to $\mathbf{x}$ instead of θ), if their probability distribution describes epistemic uncertainty regarding a true but unknown value. The latter approach is followed in this thesis for resistance properties of flood defenses, unless stated otherwise.

4.2.2. DIRECT RELIABILITY UPDATING

Direct reliability updating exploits the definition of the conditional probability of failure F given the evidence ε, which is

$$P(F|\varepsilon) = \frac{P(F \cap \varepsilon)}{P(\varepsilon)} \tag{4.10}$$

While the direct and indirect updating are mathematically equivalent, the direct method is easier to implement, especially with simulation type of reliability analysis methods such as Monte Carlo simulation (MCS). Schweckendiek (2010) showed that the indirect method implemented with numerical integration indeed gives the same results as the direct method with MCS. In this thesis the direct method is preferred, mainly due to its flexibility and ease of implementation.

If implemented with simulation techniques, often also the updated distributions of the basic random variables can be inferred, too. While this is very useful for interpretation of the results, using the updated distributions for further analysis must be treated with caution. Correlations between the variables are introduced or changed through the updating, which would need to be accounted for properly.

4.2.3. INEQUALITY INFORMATION

As mentioned earlier, there are two types of information that are distinguished mainly due to the difference in implementation for reliability updating, equality and inequality information. We are dealing with inequality information, if the evidence ε implies that our observed quantity is greater than or less than some function of the random variables of interest, which can be (re-)formulated as:

$$\varepsilon \equiv \{h(\mathbf{x}) < 0)\} \tag{4.11}$$

where $h(\cdot)$ is the observation function. Typical examples of inequality information are failure (i.e., exceedance of a limit state), survival or the loads reached in incomplete load tests, the latter being in fact some form of survival information. In terms of direct reliability updating, the posterior probability of failure can be found as follows:

$$P(F|\varepsilon) = \frac{P\left(\{g(\mathbf{X}) < 0\} \cap \{h(\mathbf{X}) < 0\}\right)}{P(h(\mathbf{X}) < 0)} = \frac{\int_{F\cap\varepsilon} f_{\mathbf{X}}(\mathbf{x})\,d\mathbf{x}}{\int_{\varepsilon} f_{\mathbf{X}}(\mathbf{x})\,d\mathbf{x}} \tag{4.12}$$

where F is (the outcome space of $\mathbf{x}$ for) failure: $F \equiv \{g(\mathbf{x}) < 0\}$. Notice that for multiple observations, the total evidence is the intersection of the individual outcome spaces:

$$\varepsilon \equiv \bigcap_k \{h_k(\mathbf{x}) < 0\} \tag{4.13}$$

4.2.4. EQUALITY INFORMATION

In contrast to inequality information, equality type of observations are described by

$$\varepsilon \equiv \{h(\mathbf{x}) = 0\} \tag{4.14}$$

In principle, the difficulty with reliability updating problems involving equality information is that surface integration is involved, which conventional reliability analysis methods are not suited for. Another problem is that the prior probability of the observation is zero (i.e., the denominator in Eq. 4.12).

One way of bypassing both problems is transforming the failure and observation random variables, $g(\mathbf{x})$ and $h(\mathbf{x})$ respectively, to Standard Normal space, for which a solution is known. Straub (2011) developed an alternative method recently, which is exact and can be used with simulation techniques directly. For a brief discussion and comparison of both methods, refer to appendix G. In essence Straub's method allows reformulating the equality in terms of inequality information.

For the envisaged problems in this thesis, we may measure a system characteristic where s_m is the measured value of the system characteristic $s(\mathbf{x})$ with error e_m, the PDF of which is denoted as $f_{e_m}(\cdot)$. In that case the likelihood function can be expressed as

$$\mathbb{L}(\mathbf{x}) = f_{e_m}[s_m - s(\mathbf{x})] \tag{4.15}$$

The key element in the the transformation to an inequality problem is rewriting the likelihood function as the following identity

$$\mathbb{L}(\mathbf{x}) = \frac{1}{c} P\left(U - \Phi^{-1}[c\mathbb{L}(\mathbf{x})] \le 0\right) \tag{4.16}$$

where U is a standard Normal random variable and c is a positive constant chosen to ensure that $0 \leq c\mathbb{L}(\mathbf{x}_g) \leq 1$. This enables expressing the likelihood function by the following equivalent (observation) limit state function

$$h_e(\mathbf{x}_g, u) = u - \Phi^{-1}[c\mathbb{L}(\mathbf{x}_g)] \tag{4.17}$$

and the corresponding (inequality) domain

$$\varepsilon_e \equiv \{h_e(\mathbf{x}_g, u) \leq 0\} \tag{4.18}$$

The conditional probability of failure is then obtained by

$$P(F|\varepsilon) = \frac{P(F \cap \varepsilon)}{P(\varepsilon)} = \frac{\int_{F \cap \varepsilon_e} f_{\mathbf{X}_g}(\mathbf{x}_g)\varphi(u)\, du\, d\mathbf{x}_g}{\int_{\varepsilon_e} f_{\mathbf{X}_g}(\mathbf{x}_g)\varphi(u)\, du\, d\mathbf{x}_g} \tag{4.19}$$

where $\varphi(\cdot)$ is the standard normal PDF. Notice that both, the numerator as well as the denominator can be evaluated straightforwardly using standard (structural) reliability analysis methods, including sampling techniques such as Monte Carlo simulation.

4.2.5. UPDATING SCENARIOS

So far, the posterior analysis has been discussed for continuous probability distributions, which are the most common representations for uncertainty in physical quantities involved in failure and observation (limit state) functions. As discussed in chapter 3, also discrete random variables play an important role for the envisaged applications, mainly in the form of stratification scenarios (see section 3.4). If the random variables per scenario are independent, the (relative) likelihood of a scenario is the probability of the observation given the scenario:

$$\mathbb{L}(E_i|\varepsilon) = P(\varepsilon|E_i) = \int_{\varepsilon} f_{\mathbf{X}_i}(\mathbf{x}_i) d\mathbf{x}_i \tag{4.20}$$

where $\mathbf{X}_i$ are the random variables in scenario E_i. For equality type of information, the integration domain changes to ε_e (using the same normalization constant c for all scenarios). A more detailed discussion and examples of survival analysis are provided in appendix D.

4.3. REDUCIBILITY OF UNCERTAINTIES

THE focus of this thesis lies on reducing uncertainties and reliability updating. In engineering problems, most random variables reflect either natural (intrinsic) variability or lack of knowledge (i.e. epistemic uncertainty), some a combination of both where, however, often one of the two is dominant. The distinction between sources and types of uncertainty (see e.g. Figure 4.2) is important, not so much for classification or semantic purposes but for the question if uncertainties can be reduced and to what degree.

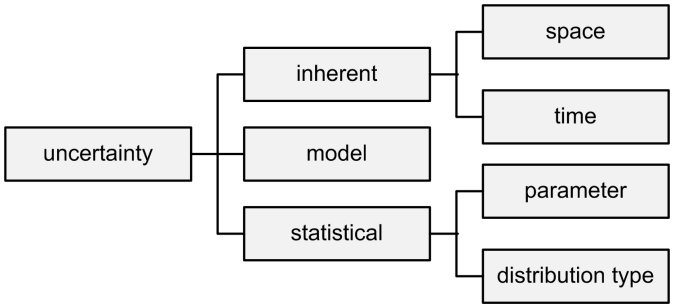

Figure 4.2: Classification of uncertainties (after Van Gelder, 2000)

The intention of this section is not to repeat or re-open the (probably never-ending) debate on types and definitions on uncertainty as held already by numerous scholars, also in engineering decision making (see e.g. Ditlevsen, 2003; Der Kiureghian and Ditlevsen, 2009), but to highlight a few relevant points one encounters when applying Bayesian posterior analysis to the envisaged applications.

4.3.1. REDUCIBILITY

As stated, the question that matters for decision making is whether uncertainties can be reduced by incorporating additional information or not. We define uncertainties as reducible, if it is feasible to acquire, interpret and incorporate information that has a significant impact on the magnitude of uncertainty. Statistical uncertainties are typically reducible.

Typical examples of reducible uncertainties related to the problems at hand are the probability distributions of stratification scenarios (introduced in section 3.3.3), including so-called anomalies or adverse geological details. These features are time-invariant, at least on an engineering scale. At the same time, information about them can be acquired by site investigation. The impact of such additional information can be significant, as we will see, because of changes in scenario probabilities and the resulting change in reliability. In specific situations scenarios can, in practical terms, even be verified or falsified (i.e., posterior probability equal to one or zero), which can have a considerable impact on the reliability and risk.

On the other hand, the uncertainty in a year's maximum river water level at a certain location would be rather of the irreducible type of uncertainty. While it is true that each

year we obtain new evidence, because each year a new maximum level is realized, such information usually does not change the probability information significantly (except for extreme events). Furthermore, we can hardly actively pursue such information; this year's measurement will not tell us much about next years.

As we may conclude from these examples, for the envisaged applications, reducibility is a matter of correlation in time.

4.3.2. AUTO-CORRELATION IN TIME

One way to interpret uncertainty and reliability updating as described above is that the parameter space for which the past observations were likely obtains more weight in the probability redistribution than parameter space for which the observations were unlikely. The latter is only possible, if we assume the random variables to be time-invariant. In other words, we consider them to be the same in the past during the observation as in the future event to be predicted. Note that statistical uncertainties are typically time-invariant.

If however, a situation we deal with has predominantly intrinsic variability (in time), we can hardly "learn" from an observation (i.e., the effect of updating is insignificant). In this case the observation and the predicted event are statistically independent in time (i.e., zero auto-correlation), practically speaking.

4.3.3. MODEL UNCERTAINTY

Conceptually, modeling model uncertainty is accounting for model error, the deviations of model predictions from true behavior. Arguably, model uncertainty will contain reducible and non-reducible elements. Some reasons are listed below.

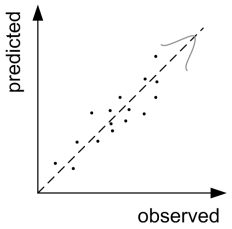

Figure 4.3: Illustration of model error estimation by comparing observed and predicted outcomes

Observed versus Predicted One way to estimate the model error is to compare model predictions with observations as illustrated in Figure 4.3. If the experiments are reproducible under controlled conditions, such as in the laboratory, the model error probably implies that the model does not perform equally well under different conditions. In such a case, we deal with a sort of local bias (i.e., local in terms of parameter space), which is reducible because it does not change from time to time.

Field versus Laboratory At the same time, we need to realize that in engineering applications the difference between controlled (laboratory) conditions and real-life behavior contributes to the discrepancy between observations and predictions. While the temperature and moisture are controlled in the laboratory, they are variable outside. While the soil in a physical model is homogeneous, heterogeneity is a reality in the field. The more these ingredients of the model error can change from event to event, the less reducible the model uncertainty is.

Site-to-site Variation The performance of a model (i.e., it's bias) may vary from site to site, essentially due to the same reasons as discussed in the point above. There may be factors influencing a characteristic of interest which are not included in the model, but which differ from site to site. This implies that only part of the (reducible portion of the) model uncertainty is also reducible from site to site. In other words, what we learn from an observation at one site is not necessarily transferable to other locations.

Event-to-event Variation Similar to the above, as already discussed for all random variables in 4.3.2, the model error may be different from event to event due to influencing factors varying in time. This part of model error is also of non-reducible nature.

In conclusion, model uncertainty typically has contributions of reducible and of irreducible nature. The modeling of model as well as other uncertainties in this thesis is discussed below in section 4.3.4.

4.3.4. MODELING APPROACH

In reality, most random variables will not belong to either category exclusively - epistemic or aleatory - and, as such will not be fully reducible nor absolutely irreducible. For the envisaged applications, however, load variables (e.g., the river water level) will typically be predominantly aleatory and irreducible. On the other hand, geotechnical properties such as the grain size distribution will be virtually time-invariant and thus predominantly of reducible. As argued in section 3.3, ground-related uncertainties are essentially statistical and, hence, epistemic, even though we sometimes resort to modeling them as random processes (e.g., random field simulation).

Although in principle the uncertainty could even be split in reducible and irreducible parts for each random variable, for the applications in this thesis we pragmatically assume each random variable to belong to either of the categories. More specifically, the variables assumed to be reducible will be modeled as "simple random variables", while the irreducible ones will be modeled as stochastic (time-varying) processes. Furthermore, for the latter category we assume no auto-correlation in time, at least not at the time scale between observations and events to be predicted. Section 4.3.5 describes how this is dealt with in the posterior analysis using Monte Carlo simulation.

Model uncertainty was assumed to be irreducible in all cases in order not to overestimate the effects of reliability updating. A thorough analysis of the distinction between the reducible and non-reducible parts of model uncertainty for uplift and piping was out of the scope of this thesis, but is certainly recommended to future research.

4.3.5. MONTE CARLO-BASED POSTERIOR ANALYSIS

As indicated in the previous section (4.3.4), for the envisaged applications we will distinguish between random variables with perfect auto-correlation in time (fully epistemic/reducible) and random processes with zero auto-correlation between the observed event and the event to be predicted (fully aleatory/irreducible). This is indicated by using two sets of random variables, $\mathbf{X}^p$ and $\mathbf{X}^f$, where p stands for the (past) observed event and f for the (future) event to be predicted. Notice that this is simplified way of modeling the random processes. Even though for some of the variables the true auto-correlation may be in between those values, the actual differences in results are speculated to be insignificant, as for example the results in chapter 5 indicate.

The steps describe a prior and subsequent posterior analysis using these definitions:

1. **Simulation of the event to be predicted** Generate n realizations of the basic random variables according to their joint probability distribution. The jth realization of the i-th random variable is denoted as X^f_{ij} and j-th the realization of the vector of basic random variables is denoted as $\mathbf{X}^f_j$.

2. **Prior probability of failure** The prior probability of uplift, heave and piping is the number of realizations where all three mechanisms fail ($\mathbf{1}[\cdot]$ is the indicator function), divided by n.

$$\hat{P}(F) = \frac{1}{n}\sum_j \mathbf{1}[g(\mathbf{X^f_j} < 0)] = \frac{1}{n}\sum_j \mathbf{1}[g_u(\mathbf{X^f_j}) < 0] \cdot \mathbf{1}[g_h(\mathbf{X^f_j}) < 0] \cdot \mathbf{1}[g_p(\mathbf{X^f_j}) < 0]$$

3. **Simulation of the observed conditions** The realizations of all variables with (fully) reducible uncertainty obtain the same value as the event to be predicted (full auto-correlation in time or time-invariance):

$$X^p_{ij} = X^f_{ij}$$

for all i where the uncertainty is assumed reducible. The random variables assumed to be intrinsically variable obtain new independent realizations (no auto-correlation in time) according to their (joint) probability distribution.

4. **Posterior probability of failure** The updating is achieved by conditioning on the observation (in general form $\varepsilon_k = \{h_k(\mathbf{X^p}) < 0\}$,) and evaluating the following term:

$$\hat{P}(F|\varepsilon) = \frac{\sum_j \mathbf{1}[g_u(\mathbf{X^f_j} < 0)] \cdot \mathbf{1}[g_h(\mathbf{X^f_j} < 0)] \cdot \mathbf{1}[g_p(\mathbf{X^f_j}) < 0] \cdot \prod_k \mathbf{1}[h_k(\mathbf{X^p_j}) < 0]}{\sum_j \prod_k \mathbf{1}[h_k(\mathbf{X^p_j}) < 0]}$$

Similar procedures can be used for updating the distributions of basic random variables and fragility curves. The term $\prod_k \{h_k(\mathbf{X^p_j} < 0\}$ implies that an observation can imply several limit states (i.e., inequality types of information) and/or several observations. For equality information, the equivalent inequalities can be used (see 4.2.4).

Adaptation of the implementation with Monte Carlo sampling as described above to more more computationally efficient methods such as Importance Sampling, Directional Sampling or Subset Simulation is straightforward.

4.4. DECISIONS IN PIPING SAFETY ASSESSMENTS

THIS section discusses the constraints and criteria applicable to decisions in piping safety assessments in a Dutch context. To this end, we combine the search for the strategy maximizing the expected utility (section 4.1) with the constraints imposed by the requirements from the safety assessment (chapter 2).

4.4.1. RELIABILITY CONSTRAINT

An important assumption in this thesis is that the safety requirement is expressed in terms of an annual acceptable probability of failure p_T (per levee reach or structure) as discussed in chapter 2. The flood defense is considered safe, if

$$P(F) < p_T \tag{4.21}$$

An alternative way of expressing acceptable probabilities of failure is the target annual reliability index $\beta_T = \Phi^{-1}(1 - p_T)$, where $\Phi^{-1}(\cdot)$ is the inverse of the Standard Gaussian CDF.

Note that working with reliability constraints means treating the consequences of failure implicitly rather than explicitly. In this respect, the problem at hand and the solution approaches are slightly different from classical risk-based decision problems.

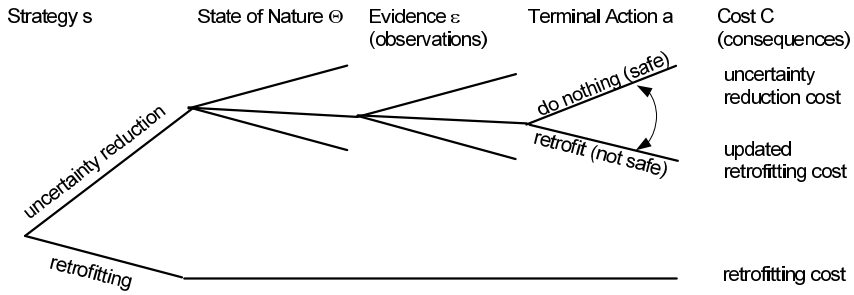

Figure 4.4: Decision tree for safety assessments of flood defenses

4.4.2. DECISION OPTIONS

The situation considered in this thesis is a levee that failed to meet the target reliability for piping based on a-priori uncertainties (i.e., $P(F) > p_T$), which implies that action needs to be taken. The conventional way of achieving an acceptably safe situation would be retrofitting or reinforcing the levee. As illustrated in the decision tree (Figure 4.4), taking measures to reduce uncertainties is an alternative to retrofitting right away.

In general, site investigation or acquiring additional information (e.g., through monitoring) will reduce uncertainties. As a result, the retrofitting design and the associated cost may change and in very favorable conditions retrofitting can even be avoided. For

piping, retrofitting can mean the construction or extension of a berm, the insertion of seepage screens or the use of relief wells.

The main characteristics, advantages and drawbacks of the alternative measures to reduce piping-related uncertainties are summarized in Table 4.1; more details are discussed below.

FIELD OBSERVATIONS

The first, and probably least costly alternative is incorporating field observations from past flood events (see chapter 5). This option is about incorporating readily available information from performance observations during past loading events through posterior analysis. In this context, performance observations are defined as observations that can be interpreted in terms of (non-)exceedance of limit states which are related to the failure of a levee such as via sand boils.

If well-documented data from historical floods are available, a posterior analysis will always provide results as if the response of the levee to a test loading were analyzed. Naturally, to be of significance, the loading needs to have been considerable in the sense that the response is representative for the conditions under which failure could occur.

MONITORING

In contrast to field observations, which work with readily available data, monitoring a levee's response to loading (e.g., the piezometric head in the aquifer) as discussed in chapter 6 requires installation and maintenance of sensors as well as waiting for a flood which leads to sufficiently significant loading of the levee to measure a representative response. This implies that the time to a useful measurement is uncertain and may well be in the order of years.

SITE INVESTIGATION

In contrast to the precious two, site investigation or exploration does not depend on extreme load conditions but can take place virtually anytime. Insitu or laboratory tests provide direct or indirect measurements of ground properties. Most insitu-techniques, furthermore, allow inferring the local stratification. The main drawback is that measurements are usually local and due to heterogeneity a rather high sampling density is required.

	Field Observations	**Monitoring**	**Site Investigation**
Characteristics	visually observe performance observed flood events partial (non-)failure response to test loading	measure a system state future flood events instrumentation needed response to test loading	measure ground properties not flood-related in-situ or laboratory mostly indirect measurements
Advantages	+ inexpensive (desk study) + always gives results	+ measures response directly + focus on quantities of interest	+ execution flood-independent + focus on important ground parameters
Disadvantages	- scarce/incomplete records - requires extreme loading	- requires extreme loading - extrapolation to extremes is not always possible - maintenance of equipment	- heterogeneity - high density needed (expensive) - uncertain transformation models

Table 4.1: Characteristics, advantages and disadvantages of the basic decision options to reduce uncertainties

4.4.3. OPTIMAL DECISIONS

Knowing our options to solve a safety issue with a levee section by either retrofitting, reducing uncertainties or a combination of both, we will now discuss how to analyse and identify the optimal or preferable decisions.

In this thesis, we assume a risk neutral decision maker (see section 4.5), which implies that the optimal decision is the one with the lowest expected total cost of all decision alternatives. Below we discuss the different elements, in terms of costs, decisions and uncertainties that constrained optimization problem entails. The explanation below focuses on the necessary ingredients for specific problem at hand, which fit very well in the more generic framework for decision analysis of inspection problems using Value of Information concepts described by Straub (2014). Recent examples of applications from related disciplines are described in Faber et al. (2000), Straub and Faber (2004), Thoens and Faber (2013), Garre and Friis-Hansen (2013) or Corotis et al. (2005).

PRIOR RETROFITTING COST

The starting point considered in this study is an unsafe levee (i.e., $P(F) > p_T$), for which we would need to invest the so-called retrofitting cost C_r based on prior knowledge. Without including any additional information, the optimal retrofitting cost $C_r^{'}$ is the minimum cost for which the reliability becomes acceptable (i.e., constrained optimization, $s.t.$ stands for subject to):

$$C_r^{'} = \min_{\Omega} C_r(\Omega, f(x)) \tag{4.22}$$

$$s.t. \quad P(F) \leq p_T$$

where $f(x)$ represents the prior uncertainties of the state of nature (i.e., the prior distribution of the basic random variables) and Ω is the set of design variables. In this case, $\arg\min_{\Omega} C_r(\Omega, f(x))$ are the optimal design values. Design variables can be continuous, such as the length of a seepage berm, or discrete (or even binary) such as the decision whether or not to install a seepage screen or pressure relief installations (e.g., relief wells or toe drains).

SITE INVESTIGATION COST

For the sake of simplicity, we will denote all costs involved with uncertainty reduction as site investigation cost $C_s(\Psi)$, which is a function of the site investigation parameters Ψ. As the retrofitting parameters, site investigation parameters can be continuous or discrete. Examples for continuous parameters are the distance between soundings (e.g., CPT) or exploration depths; examples for discrete ones are the choice of a site investigation or monitoring technique or, most importantly, the main decision (parameter) of whether or not to invest in site investigation or monitoring at all.

In this thesis, we only consider situations where the entire scope of site investigation is decided beforehand. That means that we do not consider staged investigations where follow-up activities depend on the outcomes of preceding activities, even though the problem is conceptually very similar. Hence, the site investigation cost are considered known a-priori and deterministic.

POSTERIOR RETROFITTING COST

Measures to reduce uncertainties lead to new information or evidence ε, which is used to update our state of knowledge in form of the posterior probability distribution of the random variables $f(x|\varepsilon)$ and the posterior probability of failure $P(F|\varepsilon)$. Hence, the optimal design and retrofitting cost changes to:

$$C_r''(\varepsilon) = \min_{\Omega} C_r(\Omega, f(x|\varepsilon)) \tag{4.23}$$

$$s.t. \quad P(F|\varepsilon) \leq p_T$$

where $P(F|\varepsilon) = \int_{g(x)<0} f(x|\varepsilon)dx$. Hence, a-posteriori, an investment in site investigation or monitoring has paid off if the achieved saving in terms of difference in retrofitting cost ($\Delta C_r''$) exceeds the cost:

$$C_s(\Psi) < \Delta C_r'' = C_r' - C_r''(\varepsilon) \tag{4.24}$$

Notice a-priori that there is no guarantee that the posterior retrofitting cost will actually be lower than the prior, as ε is random.

PRE-POSTERIOR RETROFITTING COST

As nicely put by Herodotus (see quote at the beginning of the chapter), the crux is to make decisions with uncertain future outcomes rather than evaluating their results a posteriori. In our case that means that at the moment we need to decide, we do not yet know the outcomes of our actions to reduce uncertainty (ε) and, hence, we do not know beforehand what the posterior probability of failure $P(F|\varepsilon)$ and the posterior retrofitting cost $C_r''(\varepsilon)$ will be. As discussed in 4.1.5, the way to deal with this in Bayesian decison analysis is pre-posterior analysis, in which we assume the future evidence to be uncertain with distribution:

$$f(\varepsilon|\Psi) = \int f(\varepsilon|\Psi, x) f(x) dx \tag{4.25}$$

where $f(\varepsilon|\Psi, x)$ represents the conditional probability of the evidence given the site investigation parameters Ψ and the random variables x.

Hence, in pre-posterior analysis, we use our prior degree of belief to estimate what the future evidence (e.g., outcomes of experiments) will be, including uncertainty. With that, we can obtain an expected value of the posterior retrofitting cost by:

$$E[C_r''(\Psi)] = \int \min_{\Omega} C_r(\Omega, f(x|\varepsilon)) f(\varepsilon|\Psi) d\varepsilon \tag{4.26}$$

$$s.t. \quad P(F|\varepsilon) \leq p_T$$

Notice that $f(\varepsilon)$ is actually a function of the prior uncertainties $f(x)$, thus, the optimization essentially depends on our prior degree of belief.

OPTIMAL STRATEGY

Since the optimal decision was defined as the one with the lowest total cost (except failure cost), it will be the strategy with decision parameters Ψ^* that minimizes the sum of the cost of measures to reduce uncertainties and expected retrofitting cost:

$$\begin{aligned} \Psi^* &= \arg\min_{\Psi}\{C_s(\Psi) + E[C_r^{''}(\Psi)]\} \\ &= \arg\min_{\Psi}\{C_s(\Psi) + \int \min_{\Omega} C_r(\Omega, f(x|\varepsilon)) f(\varepsilon|\Psi, x) f(x) dx\} \\ s.t. \quad & P(F|\varepsilon) \leq p_T \end{aligned} \tag{4.27}$$

In contrast to fully pre-determined site investigation strategies as treated here, the cost of staged strategies depend on the outcomes of intermediate phases.

Another potentially metric would the probability of a successful measure in the sense that there is a probability of the actual savings exceeding the costs given by:

$$P(\Delta C_r^{''} > C_s(\psi)) = \int \mathbf{1}\left[\Delta C_r^{''} - C_s(\psi) > 0\right] f(\varepsilon|\Psi, x) f(x) dx \tag{4.28}$$

A probability of success is especially useful in situations where the cost savings are either all or nothing, for example, when a certain retrofitting measure required a-priori can be avoided entirely by uncertainty reduction. In such cases, usually the savings in case of success are guaranteed (i.e., $\Delta C_r^{''} > C_s(\psi)$) and the probability of success becomes the probability of achieving a safe situation with uncertainty reduction only:

$$P(P(F|\varepsilon) < p_T) = \iint \mathbf{1}\left[\int_{\varepsilon} \mathbf{1}\left[g(x) < 0\right] f(x|\varepsilon) dx\right] \leq p_T \Bigg] f(\varepsilon|\Psi, x) f(x) dx \tag{4.29}$$

For such cases with known costs, in the framework considered in this thesis one would invest, if $P(P(F|\varepsilon) < p_T)\Delta C_r^{''} > C_s(\psi)$. In a fully risk-based decision framework without reliability constraints, the approach and the results would be different.

Box 2 on the next page illustrates both the approach with a target reliability as well as a fully-risk based approach by means of a simplified example of an investment decision in inspection. By comparing the decision trees, one can easily see that using a target reliability is simpler because there is no need to account for the consequences of failure explicitly.

Box 2: Simple Example Decision Analysis: Inspection versus Retrofitting

The following simplified example illustrates the type of decision analysis envisaged in this thesis. Suppose in our levee section under consideration there may be a weak spot with a probability of 0.1. While the conditional annual probability of failure with a weak spot would be 10^{-1}, the probability of failure without a weak spot would be much lower with 10^{-5}. The resulting annual probability of failure would be: $p_f = 0.1 \cdot 10^{-1} + 0.9 \cdot 10^{-5} \approx 10^{-2}$. The levee section is considered unsafe because the target annual probability f failure is 10^{-4} and retrofitting up to 10^{-5} (i.e., mitigating the effect of the anomaly and meeting the target reliability) would cost 1M€. Furthermore, assume that we could use an inspection technique costing 10k€ which could tell us for sure, if an anomaly is present (i.e., no measurement error). Would we invest the inspection?

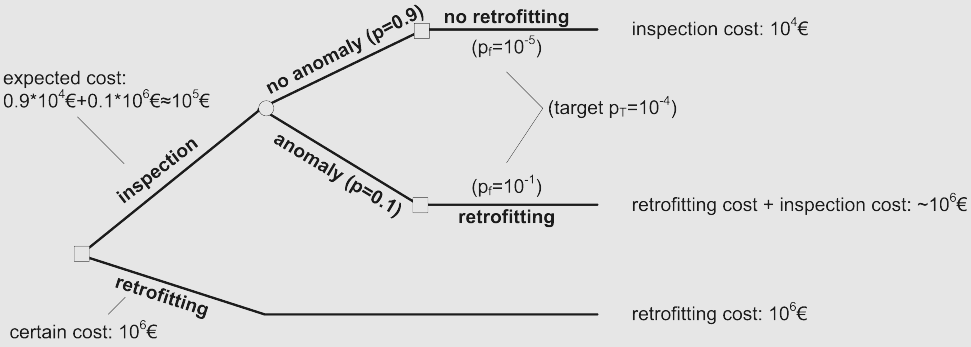

The decision tree above illustrates how we can determine the expected costs for the basic decision options of doing retro-fitting right-away or doing inspection (and possibly retrofitting afterwards). Solving a decision tree works from the consequences to the initial decision (here from right to left), while the squares represent decision nodes and the circles represent the state of nature.

If we choose for the inspection strategy and we detect no anomaly, retrofitting can be avoided (the probability of failure is lower than the target) and the only costs are the inspection costs. Based on our prior belief, the respective probability is 0.9. On the other hand there is a probability of 0.1 that we find an anomaly and have to pay for the retrofitting and the inspection. Hence, the expected cost of the inspection strategy is roughly 10^5€, which is less than choosing for retrofitting right-away with a certain cost of 10^6€.

The conclusion of the example is that a risk-neutral decision maker would opt for the inspection strategy, because the potential savings together with the corresponding probability outweigh the risk of paying the inspection cost on top of the retrofitting cost. One could say we can buy the probability of saving money.

In fully risk-based decisions without target reliability constraints we need to take into account the consequences of failure. For comparison, the decision tree corresponding to this example, where the assume that failure of the levee would cause damages of 10M€, is shown in appendix E.

4.5. LIMITATIONS

TOGETHER with the considerations regarding the target reliability in chapter 2 and the theory for reliability analysis as discussed in chapter 3, the theory presented in this chapter forms the basis for the applications treated in the remainder of this thesis. Clearly, choices and assumptions have been made to keep the scope manageable. The most important general limitations are listed below, specific limitations are addressed in each application-related chapter.

INTERIM RISK

Data acquisition by monitoring or site investigation requires time, during which the risk for a flood defense considered unsafe is, in principle, unacceptably high. Yet reinforcing a levee reach usually takes roughly ten years from initiation to completion. Thus monitoring or site investigation campaigns, of say one year duration, fall well within the standard preliminary design period. As long as the time of a reinforcement project is not extended significantly by measures to reduce uncertainty, we assume no cost of (additional) risk-bearing. An exception are long-term monitoring strategies as described in section 5.2.

RISK NEUTRALITY

In this study the decisions are based on comparing the expected costs of decision alternatives. In utility theory this implies that the utility is assumed linear with respect to monetary units, also called "risk-neutral" behavior. Is this justifiable?

All costs and benefits valued in this study are actual costs, namely the costs of measures to reduce uncertainties (e.g., data acquisition or monitoring) and the costs of reinforcing levees. There is no necessity for estimation of direct or indirect economical damage nor for valuation of human lives, because the consequences of failure (i.e., flooding) are treated implicitly in the reliability constraint(see chapter 2 and section 4.4.1).

The main reason for a decision maker to act risk-aversely instead of risk-neutrally would be if the the total costs would be of such magnitude that the public budget[1] could require significant amendments in case of adverse outcomes. This is not the case with levee reinforcement measures in the Dutch context. Furthermore, in a portfolio of levees there will be some "averaging" of positive and adverse outcomes. Hence, there is no (financial) reason for a public authority to act risk-aversely or risk-seeking and the assumptions of a risk-neutral decision maker seem reasonable for the envisaged application. Similarly, Benjamin and Cornell (1970) come to the conclusion that expected cost is an appropriate decision criterion in most in civil engineering problems and discuss the related issues in more detail.

[1] Keeping primary flood defenses up to the safety standards is a tasks carried out by public entities in the Netherlands.

UNKNOWN UNKNOWNS

Posterior and pre-posterior analysis can only act on our relative degrees of belief in identified potential states of nature; unknown unknowns cannot be revealed by Bayesian Analysis. As the term "relative likelihood" suggests, posterior analysis is a relative reweighting exercise. Even if all considered potential explanations for the evidence are very implausible, Bayesian posterior analysis will just make the most plausible ones more likely.

The latter does not only hold for the considered random variables and their distributions, it is also true for the physical process or limit state models considered in the analysis. All conclusions are conditional on the model (and the considered model uncertainty). This is not restricted to the mathematical models involved but entails all sorts of modeling choices made such as representative input values.

RATIONALITY AND OBJECTIVITY

Decision-analytical approaches are often said to lead to objective decision-making. However, decision analysis being the principal theoretical framework in this thesis requires the assessment of probabilities of events with uncertain outcomes. A considerable part of the uncertainty is epistemic (i.e., lack of knowledge); this is especially true for ground-related problems. Consequently, subjectivity can impossibly be avoided and is inherent to site characterization as it is to most engineering problems.

Despite all the difficulties with removing subjectivity, we can make rational decisions. Rationality (in a practical sense) only implies that we make choices based on our stated preferences and we choose the actions based on the maximum expected utility (Raiffa and Schlaifer, 1961)). That means that, even though objectivity would be desirable, the work in this thesis cannot contribute to making decisions totally objective, but it can help to reduce subjectivity. In any case, the proposed framework will contribute to making site investigation decisions more explicit and justifiable and therefore, hopefully, more effective.

REDUCIBILITY

Uncertainties can be reducible or irreducible (see 4.3). Which random variables or which parts of the uncertainty belong to which category is not a result of Bayesian posterior analysis but input to it. In this thesis, random variables will be assumed to belong to either category based on engineering judgment.

MULTI-STAGE STRATEGIES

Multi-stage site investigation strategies are not treated in this thesis, only strategies where the entire scope and parameters of the measures to reduce uncertainties are decided a-priori.

4.6. SUMMARY

IN safety assessments with explicit reliability constraints we may identify unsafe dike reaches based on prior information. The two essential strategies to improve the safety of such reaches are (a) reducing uncertainties and (b) structural reinforcement measures or a combination of both. Uncertainty can be reduced by incorporating information on past performance, by monitoring the structural response to loading or by site investigation. Bayesian Decision Analysis provides an adequate theoretical basis for optimizing strategies to improve piping safety. The objective is to minimize the total expected cost of measuring, monitoring and/or structural reinforcement measures. How information from the mentioned sources can be incorporated quantitatively and how the respective strategies can be analyzed is the subject of the remaining chapters, which are dedicated to specific applications.

Some of the listed limitations to the proposed approach as listed above give rise to recommendations for further research:

1. As most random variables contain both reducible and irreducible uncertainty, we need to investigate to which degree a random variable belongs to either category. There are different strategies, like treating the reducible and irreducible parts as separate random variables. However, there may be more efficient approaches.

2. The issue in item (1) above is particularly interesting for model uncertainty, since it not only concerns the residuals between model predictions and experimental observations, but also the differences between experiments and reality.

3. The cost-effectiveness of multi-stage site investigation strategies may be considerably higher than one-stage strategies. This needs further study.

While the presented decision theoretical approach itself is not new, the related original contributions in this thesis will be in the applications in the remaining chapters, where further more specific recommendations will be formulated.

5

FIELD OBSERVATIONS

Data never speak for themselves.

De Finetti

Figure 5.1: Landside ponding due to seepage through a river levee (source: Rijkswaterstaat)

Observations of a levee's performance in the field, from here on denoted simply as field observations are a source of information often neglected in reliability assessments. For example, the Dutch river dikes experienced high river discharges in 1993 and 1995, both events with return periods of approximately 100 years. How do we incorporate the information provided by such observations in reliability analyses? That is the question this chapter strives to answer by applying Bayesian posterior analysis as described chapter 4 to uplift, heave and piping reliability as introduced in chapter 3.

Some of the material in this chapter has been published in: Schweckendiek, T., Vrouwenvelder, A.C.W.M. & Calle E.O.F. (2014): Updating Piping Reliability with Field Performance Observations, Structural Safety 47, p.13-23.

Contents

DURING floods, we often make observations in the field that are related to failure modes. The simplest type of observation is the survival of the extreme load event; for levees this would mean non-exceedance of one or several (failure) limit states conditional on the observed flood stage. In fact, such a survived loading has strong analogy with incomplete load tests (i.e. loading not up to failure) such as pile bearing capacity tests (Zhang, 2004; Ching et al., 2011). Calle (1999, 2005) and Zhang et al. (2011) have demonstrated how survival information can be incorporated by means of Bayesian Updating for slope stability. The result of such analyses is an updated (i.e, posterior) reliability, which in case of survival information is always higher than the prior. Depending on the method, updated distributions of the basic random variables can also be obtained.

Besides survival there are other field observations that can be related to failure modes of levees, which can be used in a similar fashion. For example, sand boils indicate that piping-related processes (i.e., under-seepage or backward internal erosion) are ongoing. The information provided by these observations regarding the ground conditions and, ultimately, reliability is largely neglected. Only recently, rather pragmatic approaches have been developed by the US Army Corps of Engineers (USACE, 2011) using so-called likelihood ratios in a Bayesian framework with a base failure rate as prior. This approach uses expert judgment to obtain both the prior base rate (i.e., probability) of failure as well as the likelihood ratios, which modify the base rate based on observations of past performance such as seepage or fracturing. The objective of this chapter is to develop a more objective approach, consistent with the reliability analysis methods and the level of detail as applied for reliability analysis of flood defense systems in the Netherlands (Jongejan et al., 2013; Van Manen and Brinkhuis, 2005), for which a first step was made in Schweckendiek (2010).

The chapter commences by elaborating a simple example of survival analysis in section 5.1, for the sake of illustration. Subsequently, section 5.2 shows how the concept can be extended by accounting not only for past observations but also for (expected) future observations, an important element in decision analysis. After clarifying the general concept, section 5.3 applies the theory to piping using Bligh's rule, before section 5.4 discusses how uplift-, heave- and piping-related observations such as sand boils can be incorporated in state-of-the-art reliability analysis, including system reliability aspects. In the last section (5.5 the impact of the different (potential) observations for a recent flood in 2011 is demonstrated using the application example introduced in section 3.5.

5.1. SURVIVAL OF EXTREME LOADS

THIS section illustrates the concept of updating resistance variables and reliability with observed survivals of loads for the simple limit state function $Z = r - s$, where r represents the resistance and s the load. Notice that many reliability problems can be reformulated this way. For example, river levee-related failure models most models can provide a critical water level h_c (resistance) which is compared to the water level h (load).

5.1.1. PRIOR RELIABILITY

The prior probability of failure ($F = \{Z < 0\}$) is given by:

$$P(F) = P(Z < 0) = P(R - S < 0) = P(R < S) \tag{5.1}$$

It can be computed by integrating the joint PDF of R and S (which are assumed independent) over the failure domain or by integrating the fragility curve F_R weighted by the probability density of the load f_S:

$$P(F) = \iint_{r<s} f_R(r) f_S(s)\, dr\, ds = \int F_R(s) f_S(s)\, ds \tag{5.2}$$

5.1.2. RESISTANCE DISTRIBUTION AND PARAMETERS

Now we assume R Normal-distributed with $R \sim N(\mu_R, \sigma_R)$. The estimated parameters of the distribution of R are assumed to have the following properties:

- The prior distribution of (the estimate of) the mean resistance $\hat{\mu}_R$ is $f(\mu_R)$, assumed as $\hat{\mu}_R \sim N(\mu, \sigma)$.
- The variance σ_R represents the intrinsic within-site variability of the resistance which is assumed to be known in this example and non-reducible.

Thus, the total prior variance of the resistance is the sum of σ^2 (reducible) and σ_R^2 (non-reducible). Consequently, the prior (Bayesian) distribution of R is given by:

$$f_R(r) = \frac{1}{\sqrt{2\pi(\sigma^2 + \sigma_R^2)}} \exp\left\{ -\frac{1}{2} \left(\frac{\mu - r}{\sqrt{\sigma^2 + \sigma_R^2}} \right)^2 \right\} \tag{5.3}$$

Note that, if measurements of the resistance property are available, μ may be estimated as the average of the data for the prior distribution, whilst sample variance may be used as estimate for σ_R.

The prior distribution of $\hat{\mu}_R$ is straightforward

$$f_{\hat{\mu}_R}(\xi) = \frac{1}{\sqrt{2\pi}\sigma} \exp\left\{ -\frac{1}{2} \left(\frac{\mu - \xi}{\sigma} \right)^2 \right\} = \frac{1}{\sigma} \varphi\left(\frac{\mu - \xi}{\sigma} \right) \tag{5.4}$$

where $\varphi(\cdot)$ is the Standard Normal PDF.

5.1.3. LIKELIHOOD FUNCTION

Suppose that survival of the load $\acute{s}$ has been observed (i.e., the evidence is $\varepsilon = \{R > \acute{s}\}$). In order to update the distribution of μ_R and subsequently R and the probability of failure using the indirect method (see 4.2), the following likelihood function of μ_R is formulated:

$$\mathbb{L}(\mu_R|\varepsilon) = P(R > \acute{s} \mid \mu_R) = \int_{\acute{s}}^{\infty} \frac{1}{\sqrt{2\pi}\sigma_R} \exp\left\{-\frac{1}{2}\left(\frac{r-\mu_R}{\sigma_R}\right)^2\right\} dr \tag{5.5}$$

$$\mathbb{L}(\mu_R|\varepsilon) = \Phi\left(-\frac{\acute{s}-\mu_R}{\sigma_R}\right) \tag{5.6}$$

where $\Phi(\cdot)$ is the standard normal CDF. This is the probability of observing the evidence ε (here: survival), given the parameter assumes μ_R [1].

For the sake of illustration we consider the special case where there is no irreducible within-site variability (i.e., $\sigma_R = 0$), in which case the resistance uncertainty can be fully reduced and the likelihood function becomes:

$$\mathbb{L}(\mu_R|\varepsilon) = \begin{cases} \lim\limits_{\sigma_R \to 0} \Phi\left(-\dfrac{\acute{s}-\mu_R}{\sigma_R}\right) = \Phi(-\infty) = 0 & \text{if } \mu_R < \acute{s} \\ \lim\limits_{\sigma_R \to 0} \Phi\left(-\dfrac{\acute{s}-\mu_R}{\sigma_{site}}\right) = \Phi(+\infty) = 1 & \text{if } \mu_R > \acute{s} \end{cases} \tag{5.7}$$

which may also be formulated as a uniform distribution with limits: $U(\acute{s}, +\infty)$. In this special case survival tells us with certainty that the resistance cannot be less than the observed load $\acute{s}$ and the likelihood is uniform above that value.

5.1.4. POSTERIOR ANALYSIS

POSTERIOR MEAN RESISTANCE

The posterior distribution of μ_R can be determined using Bayes' rule (Eq. 4.7):

$$f_{\mu_R|\varepsilon}(\xi) \sim \mathbb{L}(\mu_R|\varepsilon)\, f_{\mu_R}(\xi) = \Phi\left(-\frac{\acute{s}-\xi}{\sigma_R}\right) \frac{1}{\sqrt{2\pi}\sigma} \exp\left\{-\frac{1}{2}\left(\frac{\xi-\mu}{\sigma}\right)^2\right\} \tag{5.8}$$

For the special case without irreducible (inherent) uncertainty ($\sigma_R = 0$), the posterior distribution becomes a truncated normal distribution as illustrated in Figure 5.2):

$$f_{\mu_R|\varepsilon}(\xi) = \frac{\frac{1}{\sigma}\varphi\left(\frac{\xi-\mu}{\sigma}\right)}{1-\Phi\left(\frac{\acute{s}-\mu}{\sigma}\right)}, \quad \xi \geq \acute{s} \tag{5.9}$$

[1] Notice that the standard deviation used in the likelihood function is σ_R, i.e. the inherent or irreducible part of σ_R. This is due to the fact that the likelihood function represents the probability of observing the evidence, in this case survival, given the mean μ_R is known (i.e., $\sigma = 0$).

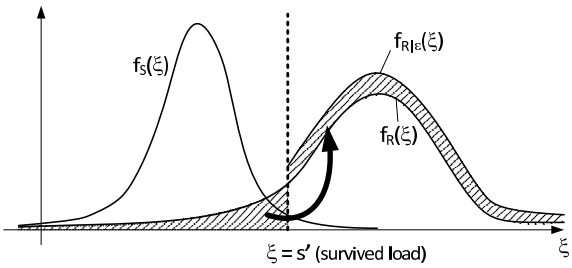

Figure 5.2: Illustration of resistance updating for the special case without inherent uncertainty ($\sigma_R = 0$) and without measurement uncertainty

POSTERIOR RESISTANCE

The posterior distribution of the resistance R (quantity of interest) is obtained by integrating out the uncertainty of μ_R:

$$f_{R|\varepsilon}(r) = \int_{-\infty}^{\infty} f_R(r|\xi)\ f_{\mu_R|\varepsilon}(\xi)\ d\xi \tag{5.10}$$

POSTERIOR PROBABILITY OF FAILURE

Using the indirect method (4.2), the posterior (updated) probability of failure is obtained by using the posterior resistance in Eq. 5.2 instead of the prior:

$$P(F|\varepsilon) = \iint_{r<s} f_{R|\varepsilon}(r) f_S(s)\ dr\ ds = \int F_{R|\varepsilon}(s) f_S(s)\ ds \tag{5.11}$$

where $F_{R|\varepsilon}$ would be the updated or posterior fragility curve.

5.1.5. NUMERICAL EXAMPLE

Assume the following (a-priori) properties:

- prior distribution of the local average resistance: $\mu_R \sim N(\mu, \sigma) = N(5, 1)$
- within-site variance (inherent, non-reducible): $\sigma_R = 1$
- prior distribution of resistance: $R \sim N(\mu \sqrt{\sigma^2 + \sigma_R^2}) = N(5, \sqrt{2})$

POSTERIOR RESISTANCE

Figure 5.3 shows the likelihood and posterior distribution of the estimated mean resistance based on the survival of an observed load $\acute{s} = 4$ (we do not consider measurement uncertainty in this example) according to Eq. 5.8. Integrating out the uncertainty in the estimated mean gives the posterior distribution of the resistance (Eq. 5.10) as presented in Fig. 5.4.

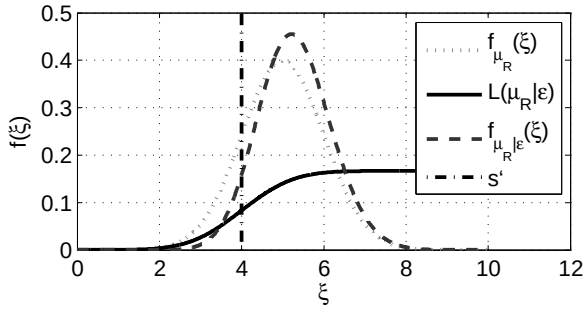

Figure 5.3: Example: Survival analysis with Normal-distributed resistance - posterior mean resistance after survival of load $\hat{s} = 4$

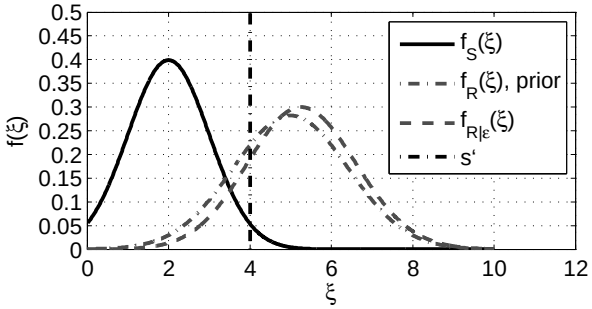

Figure 5.4: Example: Survival analysis with Normal-distributed resistance - load vs. posterior resistance

PROBABILITY OF FAILURE

The prior probability of failure for the given example can by computed by:

$$F(F) = P(R - S < 0) = \Phi\left(-\frac{\mu - \mu_S}{\sqrt{\sigma^2 + \sigma_R^2 + \sigma_S^2}}\right) = \Phi\left(-\frac{5-2}{\sqrt{1^2+1^2+1^2}}\right) \approx 4.2\ \%$$

Solving the posterior probability of failure analytically is not trivial. Numerical integration of Eq. 5.11 results in a posterior probability of failure about a factor 2 lower than the prior with:

$$P(F|\varepsilon) = \int F_{R|\varepsilon}(s)\ f_S(s)\ ds \approx 2.3\%$$

Evaluating the effect of updating, one should bear in mind that the prior probability of failure at the observed water level was $P(R < \hat{s}) = 0.24$, which means that the load was rather high compared to characteristic loads in civil engineering. Figure 5.5 shows the dependence of the posterior probability of failure and the corresponding reliability index respectively.

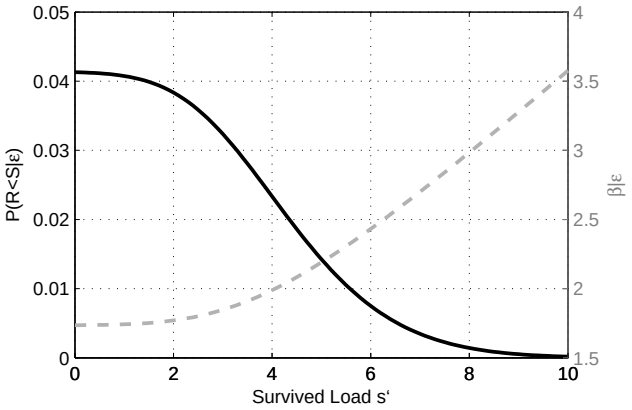

Figure 5.5: Example: Survival analysis with Normal distributed resistance - posterior probability of failure and reliability index as functions of the observed load

5.1.6. GENERALIZATION

The approach illustrated so far for a single resistance parameter can be generalized to multi-dimensional problems as follows. The likelihood function is the the probability of survival given the parameters θ, which is the complement of the probability of failure given the parameters:

$$\mathbb{L}(\theta|\bar{F}|\acute{s}) = P(Z(\mathbf{X},\acute{s}) > 0|\theta) = 1 - \int_{Z(\mathbf{x},\acute{s})<0} f_{\mathbf{X}}(\mathbf{x}|\theta)\, d\mathbf{x} \tag{5.12}$$

where $\bar{F}|\acute{s} = \{Z(\mathbf{X},\acute{s}) > 0\}$ is a short-hand notation for survival given load $\acute{s}$. Hence, the reliability analysis techniques for determining the probability of failure (see 3.4 and appendix B) are also useful in computing the likelihood for survival observations.

Whereas the likelihood is required for the indirect method, we can also update the probability of failure $P(F)$ with an observation ϵ using the direct method as discussed in 4.2 in the following way:

$$P(F|\epsilon) = \frac{P(F \cap \epsilon)}{P(\epsilon)} = \frac{P(F \cap \bar{F}^p|\acute{s})}{P(\bar{F}^p|\acute{s})} = \frac{\{P(Z(\mathbf{X},S) < 0\} \cap \{Z(\mathbf{X}^p,\acute{s}) > 0\})}{P(Z(\mathbf{X}^p,\acute{s}) > 0)} \tag{5.13}$$

where superscript ^{p} (past) indicates indicates the survived event in the past. Notice that there is only an effect of updating, if the past and future random variables are correlated. The effect is maximum for perfect correlation between the two, which would imply time-invariance (see 4.3.2) being a reasonable assumption for many geotechnical properties. Calle (1999, 2005) provides a first-order approximation approach with examples for slope stability problems; the theory is provided in appendix F.

5.2. EXPECTED DEVELOPMENT OF RELIABILITY OVER TIME

WHILE the previous section illustrated incorporating readily available information from survival of extreme loads, this section[2] discusses what future development of the reliability can be expected based on the probability distribution of the load.

5.2.1. EXPECTED PROBABILITY OF FAILURE

Let the extreme annual load in year i be S_i and the resistance in the same year be denoted as R_i. Consequently, failure in year i and the corresponding probability are denoted as $F_i = \{R_i < S_i\}$ and

$$P(F_i) = P(R_i < S_i) \tag{5.14}$$

If the survival of the (known) load $\acute{s}_j$ in year j is denoted as $\bar{F}_j = R_j > \acute{s}_j$, the posterior probability of failure in year i ($i > j$) is given by:

$$P(F_i|\bar{F}_j) = P(R_i < S|R_j > \acute{s}_j) \quad i > \max j \tag{5.15}$$

For pre-posterior analysis, we may only have a probability distribution for the future load $\acute{S}_j$, not the exact value. Accounting for this uncertainty, the (pre-)posterior probability of failure in year i is obtained by integrating over the probability density of $\acute{S}_j$ of the uncertain survived load event:

$$P(F_i|\bar{F}_j) = \iint P(R_i < s_i|R_j > \acute{s}_j)\ f_S(\acute{s}_j)\ f_S(s_i)\ d\acute{s}_j\ ds_i \tag{5.16}$$

For several known survivals, the evidence is the intersection of the observed survivals and Eq. 5.15 changes to:

$$P(F_i|\bigcap \bar{F}_j) = P(R_i < S_i|\bigcap \{R_j > \acute{s}_j\}) \quad i > \max j \tag{5.17}$$

Contemplating a series of consecutive years, the expected or pre-posterior probability of (first-time) failure in year N depends on the conditional probability of failure in that year and the probability of survival (non-failure) of the previous years:

$$p_f(N) \equiv P(F_N \cap \bigcap_{j=1}^{N-1} \bar{F}_j) = P(F_N|\bar{F}_{N-1}) \cdot \prod_{j=1}^{N-2} P(\bar{F}_{j+1}|\bar{F}_j) \cdot P(\bar{F}_1) \tag{5.18}$$

$$= P(F_N|\bar{F}_{N-1}) \cdot (1 - P(F_{N-1})) \tag{5.19}$$

$$\approx P(F_N|\bar{F}_{N-1}) \tag{5.20}$$

For low probabilities of failure the survival term is approximately equal to 1. Notice that this is a Markov process, i.e., the conditional probability of year N only depends on year $N-1$, not on all previous years.

[2] Some of the material presented in this section was published in Schweckendiek (2010).

If the uncertainty in the resistance is time-invariant and, consequently, purely epistemic and fully reducible, we have a special case similar to Fig. 5.2: Updating in that case means truncating the resistance distribution at the highest survived load; loads smaller than the highest one have zero probability of causing failure. The conditional probability for several observations can then be simplified to:

$$\begin{aligned} P(F_N|\bar{F}_{N-1}) &= \iint P(R_N < S|R > S_{N-1}) f_{S_{N-1}}(\acute{s}) f_S(s)\, d\acute{s} ds \\ &= \int F_{R|\tilde{S}_{N-1}}(s) f_S(s)\, ds \end{aligned} \tag{5.21}$$

where $f_{S_N}(\acute{s}_N)$ is the (extreme value) distribution of the maximum of load S in N years ($S_N = \max(S_i), i = [1, N]$). Thus, the probability of failure in any year N in the future only depends on the distribution of the maximum load that has occurred until the previous year $N-1$. For many distribution types this extreme value distribution can be determined analytically (Ang and Tang, 2007). Multiplying with the probability of survival until year $N-1$ we obtain the probability of failure in year N:

$$p_f(N) = (1 - P(F_{N-1})) \int F_{R|\tilde{S}_{N-1}}(s)\, f_S(s)\, ds \approx \int F_{R|\tilde{S}_{N-1}}(s)\, f_S(s)\, ds \tag{5.22}$$

This is computationally very attractive , since there is no need for computing the probability of survival for the whole time series.

5.2.2. EXAMPLE: PIPING (SIMPLIFIED MODEL)

The following example illustrates the effect of accounting for future survivals in the expected probability of failure for a simplified piping model with the limit state function is: $Z_p = H_c - H$. While the head difference H [m] is characterized by a Gumbel (extreme value, type I) distribution, the critical head difference is described by means of a Normal Distribution with coefficient of variation of $V_{H-c} = 0.2$, which is a realistic value for the overall uncertainty in the piping resistance.

N-YEARS EXTREME VALUE LOAD DISTRIBUTION

If yearly maxima of H are described by a Gumbel distribution in this form:

$$F_H(h) = \exp\left[-\exp\left(-\frac{h-\alpha}{\beta}\right)\right] \tag{5.23}$$

the distribution of the maximum in N years can be written as[3]

$$F_{H_N}(h) = \left\{\exp\left[-\exp\left(-\frac{h-\alpha}{\beta}\right)\right]\right\}^N = \exp\left[-\exp\left(-\frac{h-\alpha+\beta\ln(N)}{\beta}\right)\right] \tag{5.24}$$

Thus, $F_{H_N}(h_N)$ is also Gumbel-distributed with parameters $\alpha_N = \alpha + \beta\ln(N)$ and $\beta_N = \beta$; the yearly distribution is shifted to the right by $\beta\ln(N)$.

[3] We use the fact that $N = \exp[\ln(N)]$.

LOAD AND RESISTANCE PARAMETERS

Typical values of load parameters can be found by contemplating design water levels (MHW, in Dutch: "Maatgevend Hoogwater"), which correspond with region-specific protection levels expressed in terms of exceedance probabilities (F_{exc}, see Rijkswaterstaat (2007)). Combining the exceedance probability with the so-called decimate height h_{dec} (water level difference that reduces F_{exc} by a factor 10), the local Gumbel parameters, β (spread) and α (location), can be derived using the expressions described in appendix C. The three parameter sets used in this example are presented in Table 5.1 for yearly, 5-year and 50-year maxima. Five years is the typical safety assessment interval and 50 years a common design life time.

For the present example, the mean values of the critical head difference μ_{H_c} per load parameter set have been chosen such that the prior probability of failure equals the corresponding exceedance frequency F_{exc}.

Location	H_d [m]	$1/F_{exc}$ [1/yr]	h_{dec} [m]	β	α	α_5	α_{50}
Rivers (upstream)	3.0	1,250	0.70	0.304	0.83	1.05	1.35
Rivers (downstream)	5.0	4,000	0.35	0.152	3.74	3.85	4.00
Coast, estuaries	5.5	10,000	0.75	0.326	2.50	2.73	3.05

Table 5.1: Typical hydraulic load conditions for piping in the Netherlands ($H_d = MHW - h_b$ is the design value for the head difference).

POSTERIOR RESISTANCE

For sake of illustration, we assume resistance uncertainty to be entirely epistemic and reducible. Thus, the updated resistance distribution is a Truncated Normal distribution with the maximum observed water level[4] $\acute{h_N}$ (so far in N years) as lower bound:

$$f_{H_c}(h_c|H_c > \acute{h_N}) = \frac{1}{\sigma_{H_c}}\phi\left[\frac{h_c - \mu_{H_c}}{\sigma_{H_c}}\right] / \left(1 - \Phi\left[\frac{\acute{h_N} - \mu_{H_c}}{\sigma_{H_c}}\right]\right) \tag{5.25}$$

In the absence of an analytical expression we denote the posterior fragility curve as $F_{H_c}(h_c|H_c > \acute{h_N})$.

EXPECTED PROBABILITY OF FAILURE DUE TO PIPING

As discussed, the expected probability of failure in year N is approximately equal to the conditional probability of failure in year N:

$$p_f(N) \approx P(F_N|\bar{F}_{N-1}) \tag{5.26}$$

$$\approx \iint F_{H_c}(h|H_c > \acute{h_N})\, f_H(\acute{h_N}|\alpha_N, \beta_N)\, f_H(h|\alpha, \beta)\, d\acute{h}_N\, dh \tag{5.27}$$

where $f_H(\acute{h_N}|\alpha_N, \beta_N)$ is a Gumbel distribution with parameters α_N and β_N for the distribution of the maximum load in N years and $f_H(h|\alpha, \beta)$ is the PDF of the annual maximum water load.

[4] Notice that the water level h in this example corresponds with the generic load s in the preceding theoretical considerations.

Figure 5.6 shows the expected development of the probability of failure over time. The difference in decrease of $p_{f,p}(i)$ between the different parameter sets is remarkable. They may be due to the relative contributions of load and resistance to the total uncertainty and, furthermore, in the absolute level of the probability of failure. The decrease in $p_p(i)$ in 50 years is between a factor 2 and 100 for the assumption of a time-invariant resistance with fully reducible uncertainty.

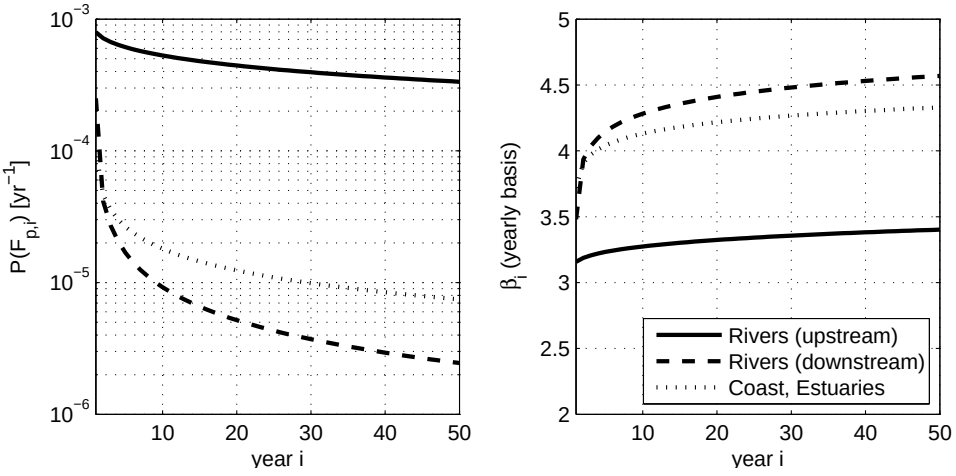

Figure 5.6: Expected probability of failure due to piping with a (simplified model) over time. Notice that this expected value includes the possibility of intermediate failure, however, since the level of probability of failure is low, the influence is insignificant.

The behavior exhibited in Figure 5.6 is similar to what Hoeg (1996) found for dam failures and to the results of a more conceptual study by Vrijling and Gelder (1998). Most dam failures occur in the first years after construction. The most important or design load for a reservoir dam is a full reservoir, which usually occurs in the first years after construction, often on purpose. Hence, the (test) loading of the dams in the early years reduces epistemic uncertainty significantly and the failure probability of the dams that survived decreases considerably. Levees, on the other hand, usually experience loads close to their design load much later if at all. Therefore, also the expected decrease of probability of failure is slower than for dams.

5.3. SURVIVAL WITH BLIGH'S RULE

WHILE the previous sections illustrated the effect of probability updating based on survival information for a single resistance variable, this section shows that the same principles are valid updating various resistance variables. To this end, the theory is applied for Bligh's rule:

$$Z_p = m_B \frac{L}{c} - H \tag{5.28}$$

where m_B is the model uncertainty factor by Kanning (2012) based on a Bayesian Analysis of dike failures and survivals, while c is considered deterministic, if the grain size (class) is known (see Table 3.1).

5.3.1. EXAMPLE 1: DETERMINISTIC OBSERVATION

INPUT PARAMETERS

The effects are best illustrated by an example, the input parameters of which are presented in Table 5.2. In this example we consider the seepage length L to be uncertain

X_i	Unit	Distribution	Parameters
L	[m]	Normal	$\mu = 50$, $\sigma = 2.5$
H	[m]	Gumbel	$\alpha = 0.53$, $\beta = 0.406$
m_B	[-]	Lognormal	$\mu = 1.76$, $\sigma = 1.69$
c	[-]	Deterministic	$c = 18$

Table 5.2: Example survival analysis with Bligh's rule: input parameters

but reducible (see section 4.3). The same assumption is made for the model uncertainty factor m_B (see section 4.3.3).

If we observe a head difference with a 100 year return period to be $\acute{H} = 2.4$m and no piping failure has occurred, the evidence may be expressed as:

$$\varepsilon = \left\{ Z_p(L, m_B, c, \acute{H}) > 0 \right\} = \left\{ m_B \frac{L}{c} > \acute{H} = 2.4m \right\} \tag{5.29}$$

LIKELIHOOD AND POSTERIOR DISTRIBUTIONS

Correspondingly, the likelihood function can be formulated as:

$$\mathbb{L}(m_B, L|\varepsilon) = P\left(m_B \frac{L}{c} > \acute{H} | m_B, L \right) \tag{5.30}$$

$$= \begin{cases} 1 & \text{if } m_B \frac{L}{c} \geq \acute{H} \\ 0 & \text{if } m_B \frac{L}{c} < \acute{H} \end{cases} \tag{5.31}$$

That means that the parameter space not complying with this condition becomes impossible (likelihood equal to zero) and the probability mass is re-distributed over the feasible parameter space proportional to the prior, as clearly shown in Fig. 5.7.

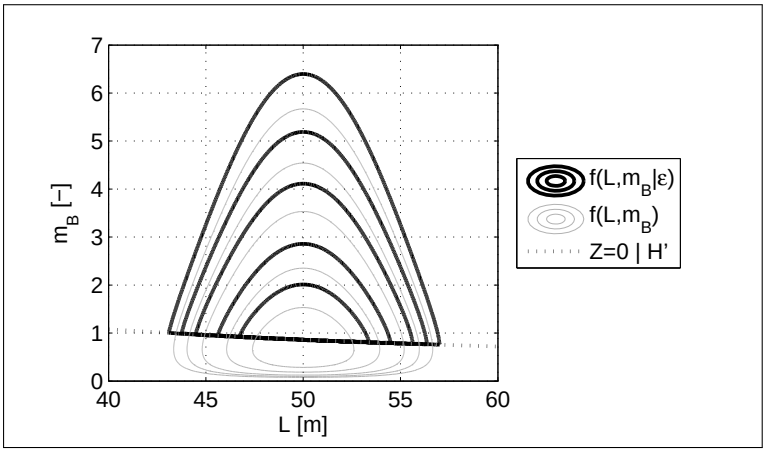

Figure 5.7: Prior and posterior JPDF of seepage length and Bligh model factor

The fact that the joint PDF is truncated does not imply that the marginal distributions are truncated as well, as demonstrated in Fig. 5.8. Even though the posterior distribution of m_B seems almost truncated, it has, in fact been redistributed. Please notice that the posterior random variables (m_B and L) are not independent anymore, even though the priors were; the updating has introduced correlation.

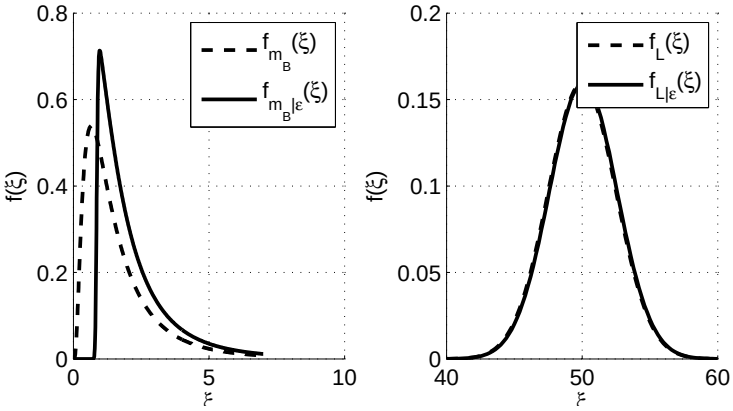

Figure 5.8: Prior and posterior PDF of seepage length and bligh model factor

PRIOR AND POSTERIOR RELIABILITY AND FRAGILITY CURVES

The fragility curve represents the CDF of the critical water level F_{H_c} with:

$$H_c = m_B \frac{L}{c} \tag{5.32}$$

Figure 5.9 shows the prior and posterior fragility curves. As expected the posterior curve is zero up to the observed survived load in this example with fully reducible resistance uncertainty. Clearly, the effect is greatest close to the observed value. This implies that the effect of updating is even more important for future flood event management for events similar to the historical one than for safety assessments, which also consider even more extreme events (Schweckendiek, 2010).

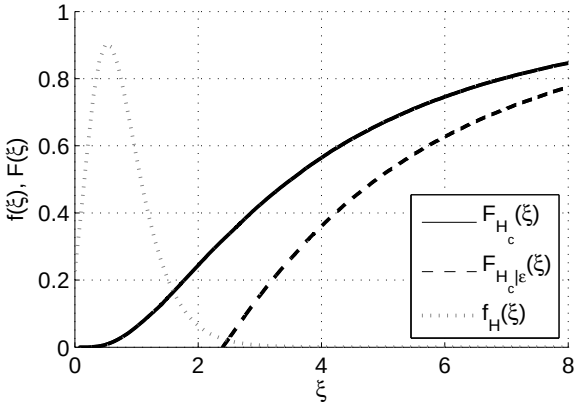

Figure 5.9: Prior and posterior fragility curves for Bligh parameters updated with survived head difference of $\acute{H} = 2.4$m

Table 5.3 contains the prior and posterior reliability, the probability of failure decreases by roughly a factor 40.

	Prior	Posterior
Probability of Failure ($P(H_c < H)$)	$4.9E-2$	$1.2E-3$
Reliability Index (β)	1.66	3.03

Table 5.3: Example survival analysis with Bligh's rule - annual prior and posterior probabilities of failure for a deterministic observation

5.3.2. EXAMPLE 2: UNCERTAIN OBSERVATION

The second example builds upon the first by using the same limit state function and input parameters. However, the observed head difference is assumed to be uncertain, modeled with a Normal Distribution with a standard deviation of $\sigma_{\acute{H}} = 0.3$m (i.e., $\acute{H} \sim N(2.4, 0.3)$). In contrast to the previous example, the uncertain observation leads to a likelihood function that is no longer just zero or one:

$$\mathbb{L}(m_B, L|\varepsilon) = P\left(m_B \frac{L}{c} > \acute{H}|m_B, L\right) \tag{5.33}$$

$$= \Phi\left(\frac{m_B L/c - \mu_{\acute{H}}}{\sigma_{\acute{H}}}\right) \tag{5.34}$$

Consequently, the posterior joint PDF in Figure 5.10 is not truncated anymore.

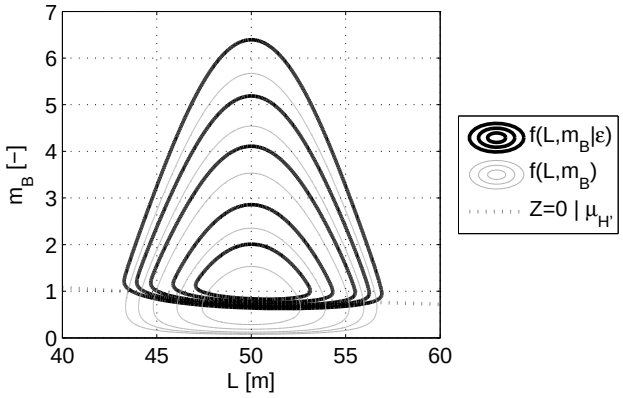

Figure 5.10: Prior and posterior JPDF of seepage length and Bligh model factor for an uncertain observation

As opposed to the first example, the posterior fragility curve is not zero up to the observed survived load (Figure 5.11), even though in this example the resistance uncertainty is fully reducible. Either uncertain observations (e.g., measurement error) or intrinsically variable and, hence, non-reducible resistance uncertainties can cause this effect - past survived loads are not necessarily survived in the future with certainty.

Table 5.4 contains the prior and posterior reliability, the probability of failure decreases by roughly a factor 30, hence less than for the deterministic observation.

	Prior	Posterior
Probability of Failure ($P(H_c < H)$)	$4.9E-2$	$1.6E-3$
Reliability Index (β)	1.66	2.95

Table 5.4: Example survival analysis with Bligh's rule - annual prior and posterior probabilities of failure for an uncertain observation

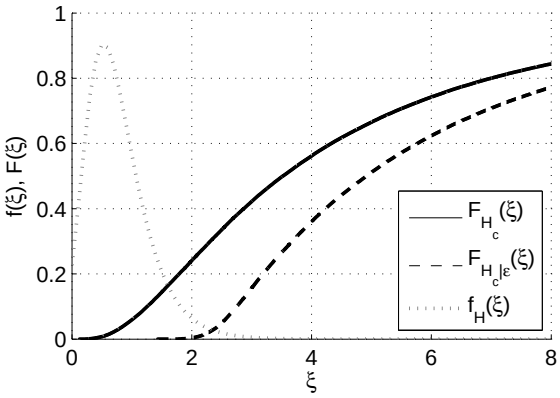

Figure 5.11: Prior and posterior fragility curves for Bligh parameters updated with uncertain survived head difference of $\acute{H} \sim N(2.4, 0.3)$ [m]

5.4. PIPING-RELATED FIELD OBSERVATIONS

IN contrast to the previous sections, which contemplated rather simple examples for sake of illustration, this section develops a more elaborate approach extending the concept (a) by looking at uplift, heave and piping together as a parallel system and (b) by analyzing more types of field observations than just survival.

During floods, when a levee experiences extreme loading by high water levels, visual inspection and / or instrumented monitoring may observe several piping-related phenomena which may influence the piping reliability. This section relates these field observations to the phenomena uplift, heave and piping (see Figure 3.1) and to the respective limit states to enable quantitative analysis.

In the following, $\acute{h}$ denotes the water level at which field observations were made and $\mathbf{X}^p$ denotes the random variables at the time of the observation (superscript p stands for "past"), which is usually the maximum flood stage reached an extreme event. The following shorthand notations are introduced for exceedance of the uplift, heave and piping limit state respectively:

$$F_u^p|\acute{h} \equiv \{g_u(\mathbf{X}^p|h=\acute{h})<0\} \tag{5.35}$$
$$F_h^p|\acute{h} \equiv \{g_h(\mathbf{X}^p|h=\acute{h})<0\} \tag{5.36}$$
$$F_p^p|\acute{h} \equiv \{g_p(\mathbf{X}^p|h=\acute{h})<0\} \tag{5.37}$$

Superscript p stands for the past observed event, meaning the exceedance of the respective limit state with the realizations of the random variables in the past. This distinction between past observed event and future event to be predicted is important if time-variant (i.e., non-reducible) variables are involved. The complement (i.e., non-exceedance of the limit state or non-failure) is denoted as $\bar{F}_i^p|\acute{h}$.

5.4.1. NO SEEPAGE (NO UPLIFT)

If no excessive seepage is observed during extreme flood stages, we may conclude that no uplift has occurred (i.e., the landside blanket is still intact). In quantitative terms we may interpret that as the uplift limit state not having been exceeded up to the observed river water level. Consequently, the evidence becomes:

$$\varepsilon = \bar{F}_u^p | \acute{h} \tag{5.38}$$

Since without uplift neither heave nor piping can be observed, this observation cannot be related directly to their limit states.

For ground conditions without blanket layer, we suppose that excessive seepage should always be observed during extreme flood stages. And vice versa, if no seepage is observed there must be a blanket present.

5.4.2. SEEPAGE (UPLIFT)

When (significant) seepage is observed, we may conclude that the pore pressures under the blanket layer have led to its rupturing (see Figure. 3.2, phase b). Hence, the conclusion is that the uplift limit state has been exceeded (or that there was no intact blanket layer), leading to the evidence:

$$\varepsilon = F_u^p | \acute{h} \tag{5.39}$$

Even though no erosion is observed at the same time, we cannot conclude that the heave limit state has not been exceeded, because heave is considered a necessary but not a sufficient criterion for erosion. The observation does not allow us to conclude anything about the (non-)exceedance of the piping limit state either.

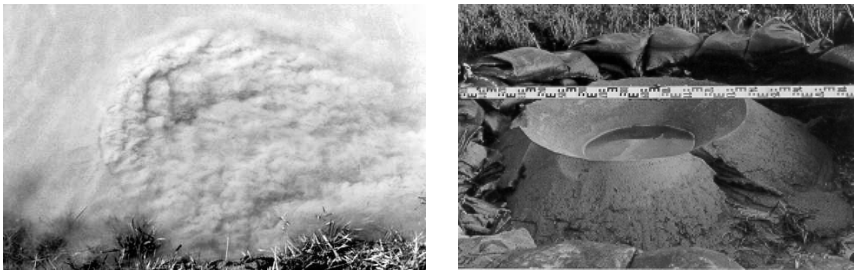

Figure 5.12: Sand boils (left: active during flood; right: post-flood crater; source: Rijkswaterstaat)

5.4.3. SAND BOILS (UPLIFT & HEAVE)

Sand boils (see Figure 3.2, phase c and Figure 5.12) are characterized by sand transport to the surface through the blanket layer. If we observe excessive seepage and erosion, the conclusion is that the uplift limit state has been exceeded and so has the heave limit state. The combined evidence is given by:

$$\varepsilon = \{F_u^p \cap F_h^p\} | \acute{h} \tag{5.40}$$

It is conservative to not neglect that no piping has occurred ($\bar{F}_p^p$) because piping could not occur in the future at the same water level. One reason is that the piping process takes time and a future flood may last longer, while flood duration is not captured in the Sellmeijer model on which the piping limit state is based. Another reason is that it is yet unclear if piping exhibits memory or cumulative effects (i.e., formed pipes remain intact after the flood). For a more detailed discussion and sensitivity analysis refer to Schweckendiek and Rijneveld (2012).

5.4.4. FLOOD FIGHTING

Sand bags are a common mitigation measure (Figure 5.13), when water or sand boils are observed by dike inspection during extreme events. Even though such measures influence the head difference over the structure, such flood fighting measures are taken after detecting seepage and/or erosion. Hence, their effect on the head difference does not need to be accounted for uplift and heave-related information.

Figure 5.13: Sand bags around an active sand boil (source: Rijkswaterstaat)

5.4.5. SUMMARY

Table 5.5 summarizes the types of observations and the information they provide for situations. For situations where there is no blanket on the landside of the levee, the main information provided is on the scenario likelihoods themselves. The probability of observing no seepage at extreme flood stages without a blanket is zero; the probability of observing seepage or sand boils is one. The reason for observing seepage but no erosion may be that there is no concentrated outflow.

	Limit state exceeded?		
Observation	**Uplift**	**Heave**	**Piping**
No seepage	no ($\bar{F}_u^p \mid \acute{h}$)	n/a	n/a
Seepage & No Erosion	yes ($F_u^p \mid \acute{h}$)	n/a	n/a
Seepage & Erosion (sand boils)	yes ($F_u^p \mid \acute{h}$)	yes ($F_h^p \mid \acute{h}$)	n/a

Table 5.5: Relations of observations with uplift, heave and piping limit states for situations with blanket layer (summary). For situations without blanket layer only the likelihood of the scenarios is affected, which becomes zero for "no seepage" and one for "seepage" and "sand boils".

5.5. APPLICATION EXAMPLE: MASTENBROEK

THIS section applies the theory as developed above to the application example which was introduced in section 3.5, where also the prior reliability with respect to uplift, heave and piping is discussed.

5.5.1. OBSERVED WATER LEVEL

The river IJssel experienced relatively high flood stages in mid-January 2011. The location of interest as described in section 3.5 is about 18 km downstream of measurement station Wijhe and 12 km upstream of measurement station Kampen. Interpolating between the maximum water levels at Wijhe and Kampen which were 4.7 m and 1.5 m respectively, the maximum water level at the dike reach under consideration on January 18, 2011 was estimated to be $\acute{h} = 2.8$m, which is an event with a return period of roughly 11 years. To put the observation into a context, the design water level for the considered dike ring is based on an annual exceedance frequency of $5 \cdot 10^{-4}$ (1/2000).

5.5.2. POSTERIOR ANALYSIS

In the following, the effect of updating using the different types of observations will be demonstrated. Even though, only "no seepage" (i.e., no uplift) was observed at the studied location during the analyzed flood, all types of observation are contemplated to show what their occurrence would have implied. Per observation, the results and illustrations for stratification scenario are presented below as well as an overview of the most important results for all scenarios. For the detailed results, see appendix H.

With respect to the reducibility of uncertainty, the choice of how much of the uncertainty per random variable is actually reducible can be somewhat arbitrary as pointed out in section 4.2. The main aspect in posterior analysis based on field observations is to consider if a variable is time-invariant and, if not, how much of its variance can be attributed to intrinsic variability. For this example the pragmatic choice was to assume all basic random variables as epistemic (i.e., reducible) except the following: the hinterland water level (h_b), the permeability of the hinterland blanket (k_h) and all model uncertainty factors (see discussion in section 4.3).

NO SEEPAGE

Observing no uplift at $\acute{h} = 2.8$ m water level shifts down the fragility curves for uplift and piping (see Figure 5.14). The effect is most obvious for uplift. Note that because there is some intrinsic, non-reducible uncertainty involved, the probability of uplift below $\acute{h}$ is not zero. Since the limit state functions for uplift, heave and piping have common random variables, also the probabilities of heave and piping are affected by the observation, as is the (system) probability of failure, though not significantly. Interestingly, the fragility curve for heave is shifted upwards slightly. The reason is that a lower probability for uplift implies higher limit gradients (i_g) at the exit point (see Eq. 3.9).

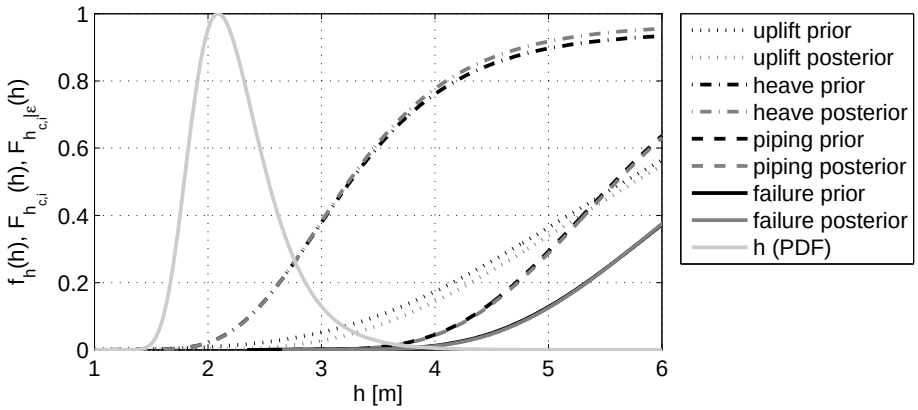

Figure 5.14: Application example for field observations, dike ring 10 (Mastenbroek) - posterior fragility curves for "no seepage"-observation, Stratification Scenario E_1

Figure 5.15 shows the changes in probabilities for the stratification scenarios. The likelihood of a scenario is the prior conditional probability of the observation for that scenario. For uplift that means that E_1 and E_2 had a prior probability of about 95% of exhibiting no uplift at the observed water level. Notice that E_3 and E_4 are scenarios without blanket layer. Since for these seepage should have been observed clearly, they obtain a likelihood zero (i.e., the observation was impossible) and, hence their posterior probability becomes zero, too.

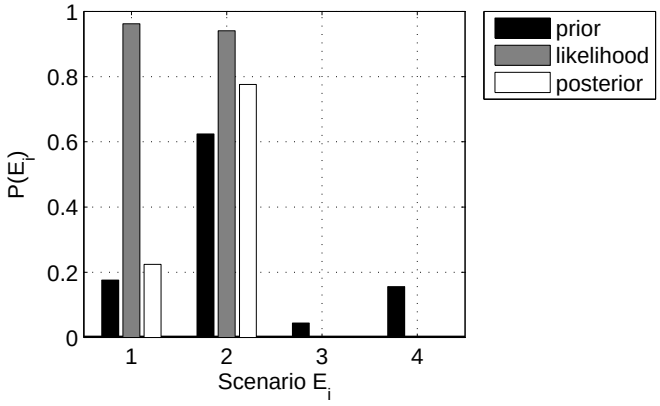

Figure 5.15: Application example for field observations, dike ring 10 (Mastenbroek) - prior and posterior scenario probabilities for "no seepage"-observation

Furthermore, Table 5.6 shows that the posterior probability of failure is more than a factor 10 lower than the prior, which can be mainly attributed to the "exclusion" of the scenarios without blanket layer.

Table 5.6: Application example for field observations, dike ring 10 (Mastenbroek) - posterior analysis results summary, no seepage

PRIOR ANALYSIS					**P(F) =**	**1.9E − 3**
i	**P(E_i)**	**Uplift P(F_u|E_i)**	**Heave P(F_h|E_i)**	**Piping P(F_p|E_i)**	**Failure P(F|E_i)**	**P(E_i)P(F|E_i)**
1	17.6%	$1.8E-2$	$1.0E-1$	$4.8E-4$	$1.4E-4$	$2.5E-5$
2	62.4%	$2.8E-2$	$1.7E-1$	$5.7E-4$	$2.2E-4$	$1.3E-4$
3	4.4%	$1.0E-0$	$1.0E-0$	$8.7E-3$	$8.9E-3$	$3.9E-4$
4	15.6%	$1.0E-0$	$1.0E-0$	$8.3E-3$	$8.3E-3$	$1.3E-3$
POSTERIOR - NO SEEPAGE					**P(F) =**	**1.4E − 4**
i	**P(E_i|ε)**	**P(F_u|E_i,ε)**	**P(F_h|E_i)**	**P(F_p|E_i,ε)**	**P(F|E_i,ε)**	**P(E_i|ε)P(F|E_i,ε)**
1	22.4%	$6.3E-3$	$1.0E-1$	$4.3E-4$	$1.0E-4$	$9.6E-5$
2	77.6%	$8.7E-3$	$1.7E-1$	$5.2E-4$	$1.5E-4$	$4.0E-4$
3	0.0%	$1.0E-0$	$1.0E-0$	$8.7E-3$	$8.9E-3$	0.0
4	0.0%	$1.0E-0$	$1.0E-0$	$8.3E-3$	$8.4E-3$	0.0

Similar to the fragility curves, the posterior distributions of the (reducible) basic random variables can be compared to the priors in order to get an impression of the impact of the observation. Figure 5.16 illustrates that in stratification scenario E_1 there is hardly any effect, only a slight change in the distribution of volumetric weight of the blanket layer γ_{sat}. This is unsurprising, since the prior probability of the observation was high.

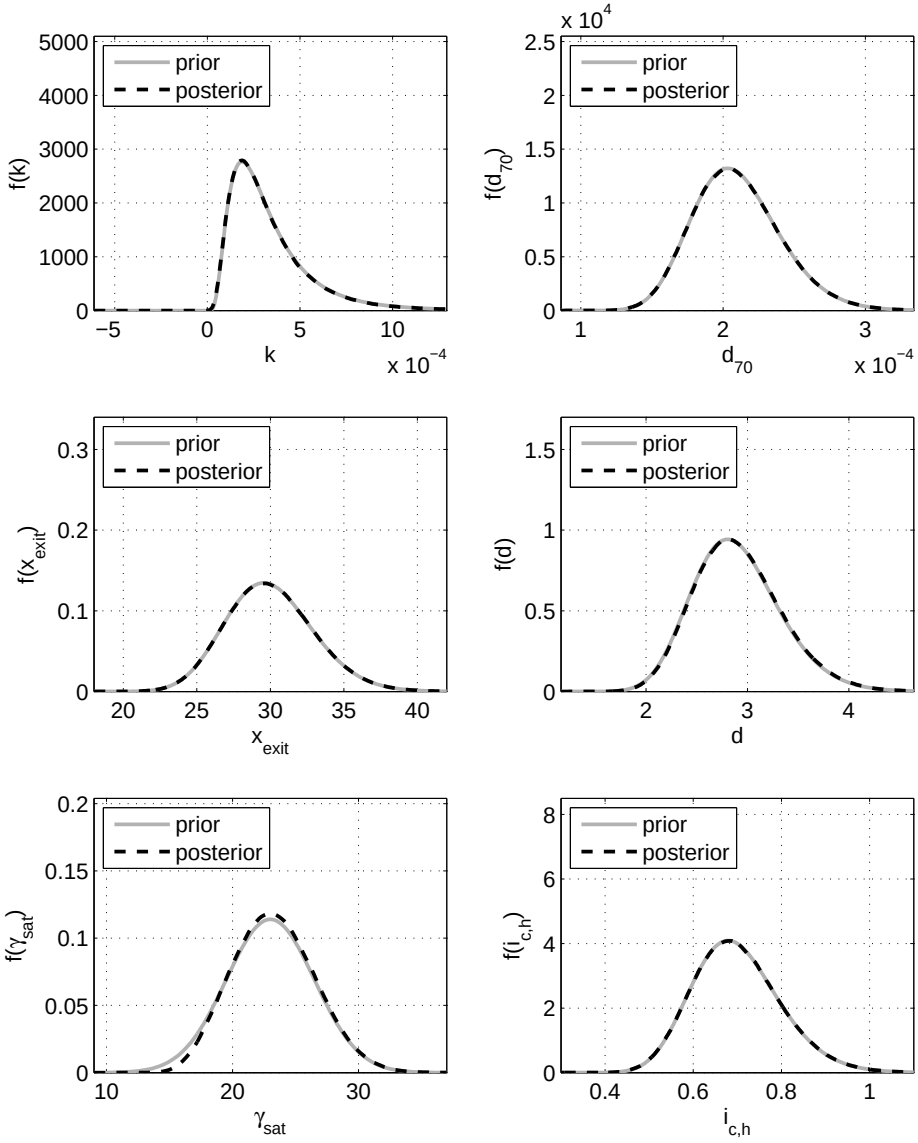

Figure 5.16: Application example for field observations, dike ring 10 (Mastenbroek) - posterior distributions for "no seepage"-observation, stratification scenario E_1

SEEPAGE (UPLIFT)

Observing seepage and no erosion implies that the probability of uplift increases significantly (see Figure 5.17), which implies that the probability of reaching the limit potential increases, or equivalently, the probability distribution of the limit potential shifts towards lower values. This effect is reflected in the heave fragility curve shifting upwards for low water levels while the asymptote goes down. The asymptote reflects the probability that the critical heave gradient is lower than the limit gradient. Through the parallel system behavior, the fragility curve for failure is at the same level (only for theoretically possible water levels with very low probability of exceedance).

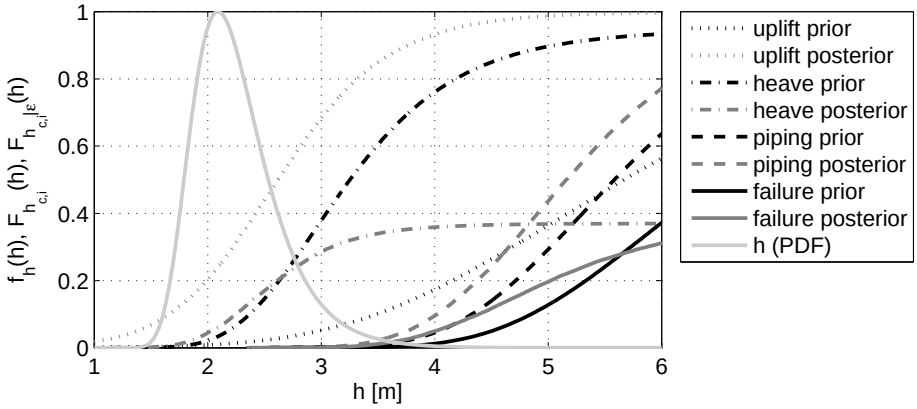

Figure 5.17: Application example for field observations, dike ring 10 (Mastenbroek) - posterior fragility curves for the "seepage"-observation, stratification scenario E_1

Figure 5.18 shows that the probability mass is significantly shifted to the stratification scenarios without blanket layer (E_3 and E_4), for which the likelihood equals one. From Table 5.7 we may conclude that the increase of the probability of failure by approximately a factor 4 is due to both changes in scenario probabilities and changes in the conditional probabilities of failure per scenario.

The posterior distributions in Fig. 5.19 show that the most affected random variables are the permeability of the aquifer k as well as the blanket thickness d and the volumetric weight γ_{sat} (i.e., the blanket weight). Interestingly, the change in the volumetric weight appears to be more significant than the permeability. This demonstrates how Bayesian inference in essence analyses the the plausibility of observations. Apparently, the best explanation for the observation is that γ_{sat} is lower than estimated a-priori.

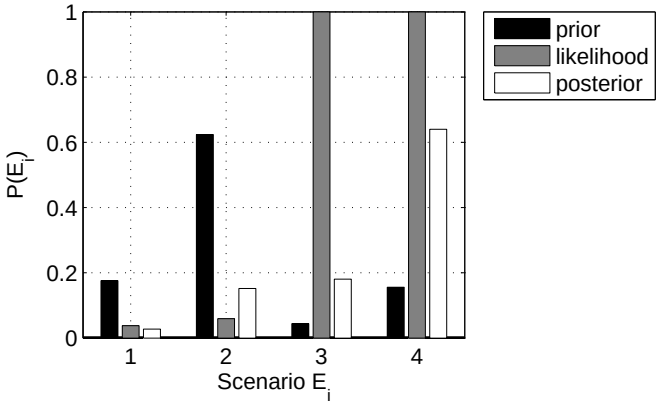

Figure 5.18: Application example for field observations, dike ring 10 (Mastenbroek) - prior and posterior scenario probabilities for the "seepage"-observation

Table 5.7: Application example for field observations, dike ring 10 (Mastenbroek) - posterior analysis results summary, seepage

PRIOR ANALYSIS					**P(F) =**	**1.9E − 3**
i	**P(E$_i$)**	**Uplift P(F$_u$|E$_i$)**	**Heave P(F$_h$|E$_i$)**	**Piping P(F$_p$|E$_i$)**	**Failure P(F|E$_i$)**	**P(E$_i$)P(F|E$_i$)**
1	17.6%	$1.8E-2$	$1.0E-1$	$4.8E-4$	$1.4E-4$	$2.5E-5$
2	62.4%	$2.8E-2$	$1.7E-1$	$5.7E-4$	$2.2E-4$	$1.3E-4$
3	4.4%	$1.0E-0$	$1.0E-0$	$8.7E-3$	$8.9E-3$	$3.9E-4$
4	15.6%	$1.0E-0$	$1.0E-0$	$8.3E-3$	$8.3E-3$	$1.3E-3$
POSTERIOR - SEEPAGE					**P(F) =**	**7.1E − 3**
i	**P(E$_i$|ε)**	**P(F$_u$|E$_i$,ε)**	**P(F$_h$|E$_i$)**	**P(F$_p$|E$_i$,ε)**	**P(F|E$_i$,ε)**	**P(E$_i$|ε)P(F|E$_i$,ε)**
1	2.7%	$3.3E-1$	$1.1E-1$	$1.1E-3$	$6.3E-4$	$3.1E-5$
2	15.2%	$3.4E-1$	$1.9E-1$	$8.8E-4$	$4.9E-4$	$1.3E-4$
3	18.1%	$1.0E-0$	$1.0E-0$	$8.7E-3$	$8.7E-3$	$1.6E-3$
4	64.0%	$1.0E-0$	$1.0E-0$	$8.4E-3$	$8.4E-3$	$5.4E-3$

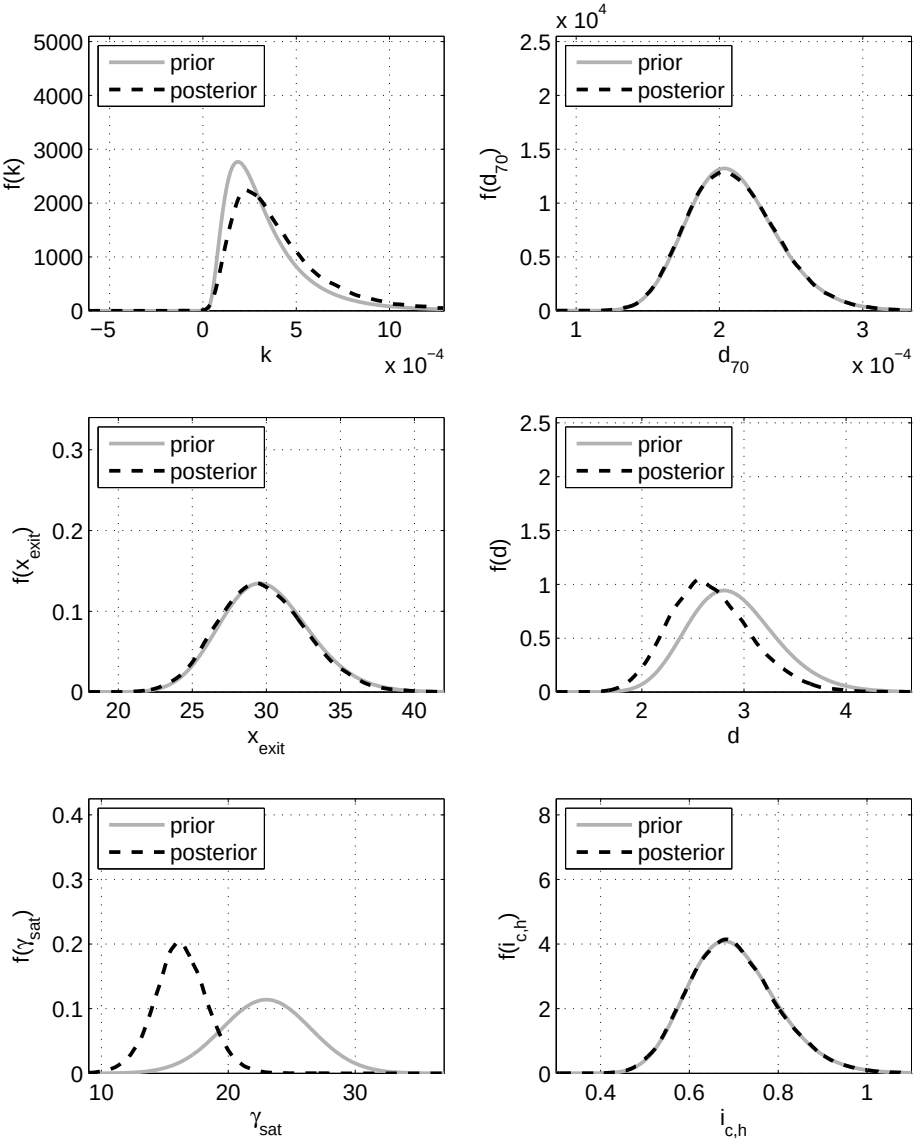

Figure 5.19: Application example for field observations, dike ring 10 (Mastenbroek) - posterior distributions for "seepage"-observation, stratification scenario E_1

SAND BOILS (UPLIFT & HEAVE)

For observing sand boils (i.e. uplift and heave) Figure 5.20 shows that all posterior fragility curves are shifted upwards with respect to their priors. In contrast to the previous case (seepage and no erosion) also the heave fragility curve increases without asymptote below one. As a consequence, the probability of failure is now dominated by the piping fragility curve, which is by far the lowest probability of the three mechanisms.

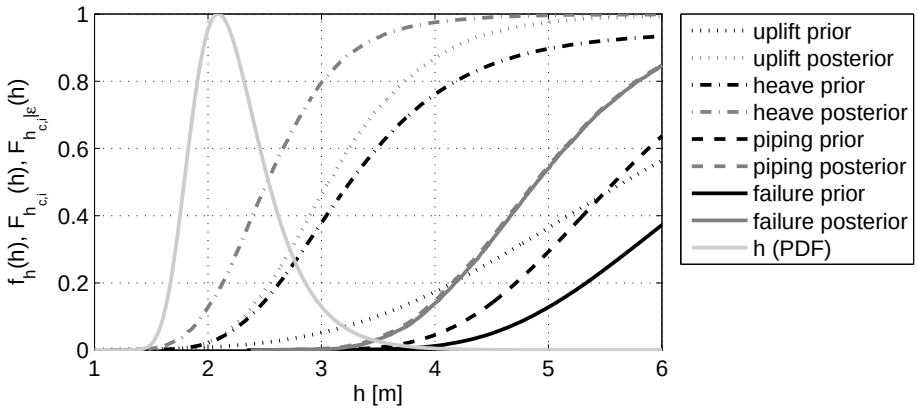

Figure 5.20: Application example for field observations, dike ring 10 (Mastenbroek) - posterior fragility curves for "sand boils"-observation, stratification scenario E_1

As for seepage, Figure 5.21 shows that the probability mass is significantly shifted to the stratification scenarios without blanket layer (E_3 and E_4), for which the likelihood equals one. This effect is even more pronounced, because observing uplift and heave for scenarios E_1 and E_2 (with blanket) was even less likely based on the priors than observing uplift and no piping. Table 5.8 shows that the increase of the probability of failure is approximately by a factor 4.

The posterior distributions in Figure 5.22, too, show that the random variables important for the uplift and heave limit states are most affected, namely the permeability of the aquifer k, which affects uplift pressure, and the blanket thickness d as well as the volumetric weight γ_{sat}. As opposed to the previous case, the change in permeability is much more pronounced, because now it explains both uplift and heave under the observed conditions. As heave is involved, we also observe a change in the distribution of the critical heave gradient $i_{c,h}$.

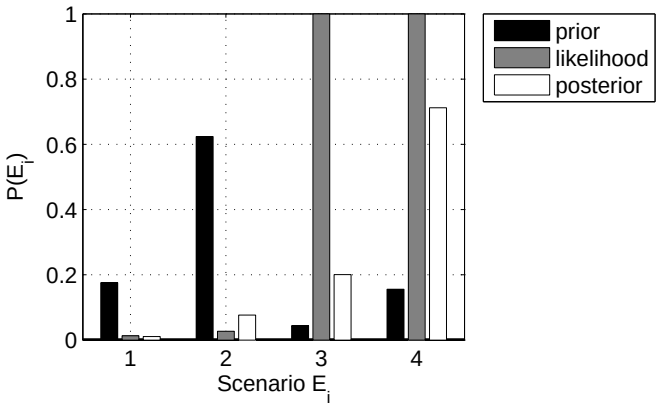

Figure 5.21: Application example for field observations, dike ring 10 (Mastenbroek) - prior and posterior scenario probabilities for "sand boils"-observation

Table 5.8: Application example for field observations, dike ring 10 (Mastenbroek) - posterior analysis results summary, sand boils

PRIOR ANALYSIS					**P(F) =**	**1.9E−3**
i	**P(E_i)**	**Uplift P(F_u|E_i)**	**Heave P(F_h|E_i)**	**Piping P(F_p|E_i)**	**Failure P(F|E_i)**	**P(E_i)P(F|E_i)**
1	17.6%	$1.8E-2$	$1.0E-1$	$4.8E-4$	$1.4E-4$	$2.5E-5$
2	62.4%	$2.8E-2$	$1.7E-1$	$5.7E-4$	$2.2E-4$	$1.3E-4$
3	4.4%	$1.0E-0$	$1.0E-0$	$8.7E-3$	$8.9E-3$	$3.9E-4$
4	15.6%	$1.0E-0$	$1.0E-0$	$8.3E-3$	$8.3E-3$	$1.3E-3$
POSTERIOR - SAND BOILS					**P(F) =**	**7.9E−3**
i	**P(E_i|ε)**	**P(F_u|E_i,ε)**	**P(F_h|E_i)**	**P(F_p|E_i,ε)**	**P(F|E_i,ε)**	**P(E_i|ε)P(F|E_i,ε)**
1	1.1%	$1.2E-1$	$3.1E-1$	$2.0E-3$	$1.7E-3$	$2.1E-5$
2	7.7%	$1.6E-1$	$4.0E-1$	$1.2E-3$	$1.0E-3$	$9.4E-5$
3	20.1%	$1.0E-0$	$1.0E-0$	$8.9E-3$	$8.7E-3$	$1.7E-3$
4	71.2%	$1.0E-0$	$1.0E-0$	$8.4E-3$	$8.4E-3$	$6.0E-3$

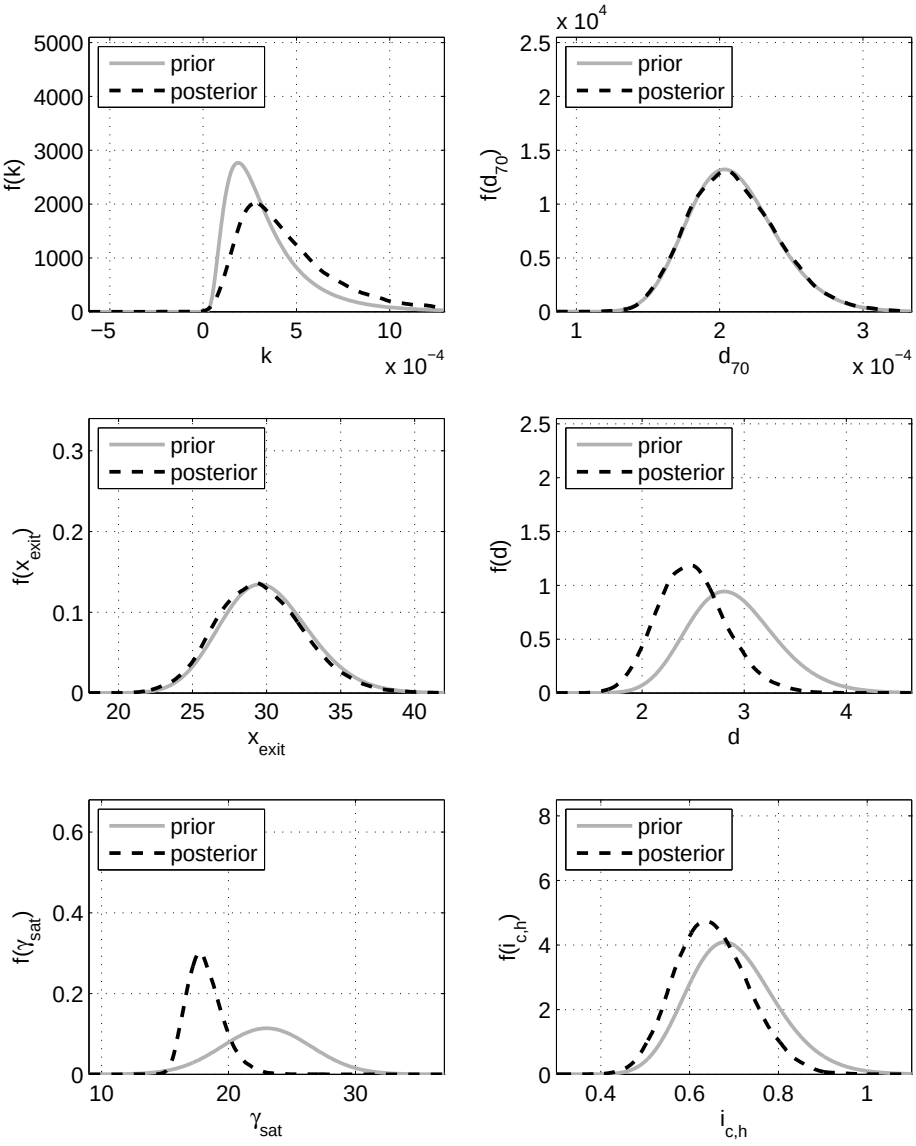

Figure 5.22: Application example for field observations, dike ring 10 (Mastenbroek) - posterior distributions for "sand boils"-observation, stratification scenario E_1

5.5.3. SUMMARY

There is a significant shift in stratification scenario probabilities for each observation type towards the scenarios with blanket layer for "no seepage" and towards the scenarios without blanket layer for observations that do include uplift (and heave). This effect can dominate the overall change in the (unconditional) probability of failure. The uplift-related observations do not only affect the uplift fragility curve (and, hence, the conditional probability of uplift) but also the piping fragility curve through their correlation induced by the random variables they have in common. Only observing essentially no signs of failure (no seepage) decreases the conditional probability of failure per scenario. Observing seepage but no erosion (uplift) increases it and observing sand boils (uplift and heave) results in an even higher increase.

Table 5.9: Application example for field observations, dike ring 10 (Mastenbroek) - prior and posterior analysis results summary

PRIOR ANALYSIS					**P(F) =**	**1.9E−3**
i	**$P(E_i)$**	**Uplift $P(F_u\|E_i)$**	**Heave $P(F_h\|E_i)$**	**Piping $P(F_p\|E_i)$**	**Failure $P(F\|E_i)$**	**$P(E_i)P(F\|E_i)$**
1	17.6%	$1.8E-2$	$1.0E-1$	$4.8E-4$	$1.4E-4$	$2.5E-5$
2	62.4%	$2.8E-2$	$1.7E-1$	$5.7E-4$	$2.2E-4$	$1.3E-4$
3	4.4%	$1.0E-0$	$1.0E-0$	$8.7E-3$	$8.9E-3$	$3.9E-4$
4	15.6%	$1.0E-0$	$1.0E-0$	$8.3E-3$	$8.3E-3$	$1.3E-3$
POSTERIOR - NO SEEPAGE					**P(F) =**	**1.4E−4**
i	**$P(E_i\|\varepsilon)$**	**$P(F_u\|E_i,\varepsilon)$**	**$P(F_h\|E_i)$**	**$P(F_p\|E_i,\varepsilon)$**	**$P(F\|E_i,\varepsilon)$**	**$P(E_i\|\varepsilon)P(F\|E_i,\varepsilon)$**
1	22.4%	$6.3E-3$	$1.0E-1$	$4.3E-4$	$1.0E-4$	$9.6E-5$
2	77.6%	$8.7E-3$	$1.7E-1$	$5.2E-4$	$1.5E-4$	$4.0E-4$
3	0.0%	$1.0E-0$	$1.0E-0$	$8.7E-3$	$8.9E-3$	0.0
4	0.0%	$1.0E-0$	$1.0E-0$	$8.3E-3$	$8.4E-3$	0.0
POSTERIOR - SEEPAGE					**P(F) =**	**7.1E−3**
i	**$P(E_i\|\varepsilon)$**	**$P(F_u\|E_i,\varepsilon)$**	**$P(F_h\|E_i)$**	**$P(F_p\|E_i,\varepsilon)$**	**$P(F\|E_i,\varepsilon)$**	**$P(E_i\|\varepsilon)P(F\|E_i,\varepsilon)$**
1	2.7%	$3.3E-1$	$1.1E-1$	$1.1E-3$	$6.3E-4$	$3.1E-5$
2	15.2%	$3.4E-1$	$1.9E-1$	$8.8E-4$	$4.9E-4$	$1.3E-4$
3	18.1%	$1.0E-0$	$1.0E-0$	$8.7E-3$	$8.7E-3$	$1.6E-3$
4	64.0%	$1.0E-0$	$1.0E-0$	$8.4E-3$	$8.4E-3$	$5.4E-3$
POSTERIOR - SAND BOILS					**P(F) =**	**7.9E−3**
i	**$P(E_i\|\varepsilon)$**	**$P(F_u\|E_i,\varepsilon)$**	**$P(F_h\|E_i)$**	**$P(F_p\|E_i,\varepsilon)$**	**$P(F\|E_i,\varepsilon)$**	**$P(E_i\|\varepsilon)P(F\|E_i,\varepsilon)$**
1	1.1%	$1.2E-1$	$3.1E-1$	$2.0E-3$	$1.7E-3$	$2.1E-5$
2	7.7%	$1.6E-1$	$4.0E-1$	$1.2E-3$	$1.0E-3$	$9.4E-5$
3	20.1%	$1.0E-0$	$1.0E-0$	$8.9E-3$	$8.7E-3$	$1.7E-3$
4	71.2%	$1.0E-0$	$1.0E-0$	$8.4E-3$	$8.4E-3$	$6.0E-3$

5.5.4. SENSITIVITY TO TIME-INVARIANCE ASSUMPTIONS

As pointed out in section 4.3.2, all (resistance) random variables were assumed time-invariant except the hinterland water level (h_p), the permeability of the hinterland blanket (k_h) and model uncertainty factors (m_ϕ, m_u and m_p). It is hard to determine to what degree these are correlated in time. The assumption made in the analyses led to the minimum updating effect possible regarding these variables. In order to explore how the effect on reliability updating we explore assumption of all variables being time-invariant and fully reducible, the results being presented in Table 5.10. The results indicate that the updating effect is indeed stronger for this assumption, but not considerably. The likely reason is that other uncertainties dominate the problem at hand.

Table 5.10: Application example for field observations, dike ring 10 (Mastenbroek) - prior and posterior analysis results summary for the assumption of all random variables being time-invariant (sensitivity analysis)

PRIOR ANALYSIS	$P(F) =$	$1.9E-3$
POSTERIOR - NO UPLIFT	$P(F) =$	$1.3E-4$
POSTERIOR - UPLIFT & NO PIPING	$P(F) =$	$7.3E-3$
POSTERIOR - UPLIFT & HEAVE	$P(F) =$	$8.1E-3$

5.6. CONCLUSIONS

THIS chapter has demonstrated how field performance observations can be used to update the probability distributions of the basic resistance random variables and the probability of failure by means of Bayesian posterior analysis. First, the concept was illustrated for a simple example of one load and one resistance variable (i.e., $Z = R - S$), which was also extended to (uncertain) observations in the future. Subsequently, the method was extended to a multi-variate resistance problem by applying it to Bligh's rule. And, ultimately, the method was elaborated for state-of-practice uplift, heave and piping models including system reliability aspects. For the latter, different types of field observations of limit states of uplift, heave and piping were used in order to use them as inequality type of information in the posterior analysis.

The findings in this chapter have led to the following observations and conclusions:

1. Field performance observations from historical loadings are valuable information for the estimation of reliability of a flood defense (in fact for any kind of structure for which the probability of failure is dominated by large uncertainties in resistance properties). So far, field observations have hardly been exploited consistently in reliability analyses. The presented method enables using not only mere survival information but also more specific field observations as long as these can be related to an observation (limit state) which is correlated to the failure limit state in question.

2. In posterior analysis, attention needs to be paid to distinguishing between reducible and non-reducible uncertainties. Since data are usually scarce, the deci-

sion on what (part of) uncertainty is reducible may need to be based on judgment. The more uncertainty is reducible, the larger are the effects of updating.

3. If not all resistance uncertainty is reducible (i.e., time-invariant), there is no guarantee that a previously survived load level will be survived again in the future. The reason is that the parameters with intrinsic (i.e., non-reducible) uncertainties may be less favorable in future events than during the observed event. Notice that this holds also for non-degrading resistance.

4. For decision analysis purposes, we can estimate the effects of yet uncertain future observations as illustrated in section 5.2. A simplified analysis with realistic numbers for typical Dutch conditions regarding piping reliability has illustrated that the expected decrease of probability of failure during the a design life time of 50 years can be one order of magnitude or more, if the resistance is assumed time-invariant and fully reducible. A substantial part of the decrease is realized in the first 10 years.

5. The application of the theory with Bligh's rule has demonstrated the method for a multi-dimensional problem and also the effect of an uncertain observation, the latter unsurprisingly weakening the effect of updating.

6. Three types of observations have been defined and related to the limit states for uplift, heave and piping: (a) observing no excessive seepage is interpreted as no uplift having occurred, (b) observing excessive seepage is interpreted as the uplift limit state being exceeded and (c) observing sand boils (i.e., sand erosion) is interpreted as the uplift and heave limit states having been exceeded. Notice that with sand boils assuming that the piping limit state has not been exceeded would imply further unconservative assumptions (see 5.4).

7. The application example essentially demonstrates (a) that the probability of failure can decrease or increase by roughly a factor 10, (b) that the change in scenario probabilities can be significant and dominate the posterior probabilities and (c) that observing signs of (partial) failure can outweigh the effects of not having observed piping.

8. Though not thoroughly analyzed, it seems that the prior level of reliability would influence the (expected) impact of the updating based on field observations. The relative importance of the reducible part of the resistance certainly does. Future studies are advised to study these aspects more systematically.

9. Field performance observations should be taken into account for decision-making in inspection and maintenance or in design of newly built structures. Neglecting the information may lead either to over-investments in structures which are more reliable than based on prior data only or to under-investments in structures that are less reliable than initially thought. In both cases, incorporating the information leads to cost-savings either in terms of lower construction cost or in terms of lower risk.

6

HEAD MONITORING

Things should be made as simple as possible but not any simpler than that.

Albert Einstein

Figure 6.1: What you can see of an observation well at the surface.

As opposed to passive observations of field performance as described in the previous chapter, this chapter investigates the cost-effectiveness of actively monitoring pore pressure. In chapter 2 geohydrological uncertainties were shown to be important in piping reliability. Pore pressures are directly related to geohydrological parameters such as the permeability of the aquifer, its thickness or the seepage length. This chapter investigates how monitoring pore pressures affects uncertainties and reliability. After outlining the theoretical approach, the basic idea and features are first illustrated by means of an example with a simplified uplift model, followed by a case study on realistic data using the models applied in Dutch safety assessments.

Some of the material in this chapter has been published in: Schweckendiek, T. & Vrouwenvelder, A.C.W.M. (2013). *Reliability Updating and Decision Analysis for Head Monitoring of Levees*, Georisk, 7(2).

Contents

6.1. PRE-POSTERIOR ANALYSIS FOR MONITORING PLANNING

THE previous section highlighted important features of reliability updating for a simplified uplift model; this section elaborates a more realistic modeling approach including (a) uplift, heave and piping, (b) the influence of the position of the monitoring device and (c) the dependence of the retrofitting cost on the monitoring and reliability updating outcome. The latter is based on the idea that the closer the posterior reliability is to the target, the less retrofitting is needed.

6.1.1. POSTERIOR ANALYSIS

Using the definitions from chapter 3, the prior probability of failure is given by:

$$P(F) = P(F_u \cap F_h \cap F_p) = P(\{Z_u < 0\} \cap \{Z_h < 0\} \cap \{Z_p < 0\}) \tag{6.1}$$

where Z_u, Z_h and Z_p are the limit state functions as described in section 3.2.

The goal of posterior analysis is to incorporate the evidence ε provided by the pore pressure measurements in the reliability:

$$P(F|\varepsilon) = \frac{P(F \cap \varepsilon)}{P(\varepsilon)} = \frac{P(F_u \cap F_h \cap F_p \cap \varepsilon)}{P(\varepsilon)} \tag{6.2}$$

The posterior probabilities of uplift, heave and piping ($P(F_u|\varepsilon)$, $P(F_h|\varepsilon)$ and $P(F_p|\varepsilon)$, can be computed accordingly.

The monitoring provides a measured head, "equality type" of information which is treated using the approach by Straub (2011) (see 4.2.4). Similar to the example in the previous section the likelihood is expressed as a function of the measurement error for the difference between the measured and the real value of the head $\phi(\mathbf{x}, \acute{h})$ (for the observed water level $\acute{h}$):

$$\mathbb{L}(\mathbf{x}) = f_{e_m}\left(\phi_m - \phi(\mathbf{x}, \acute{h})\right) \tag{6.3}$$

and the equivalent inequality domain can be expressed as:

$$\varepsilon_e = \{h_e(\mathbf{x}, u) < 0\} = \left\{u - \Phi^{-1}\left[c\mathbb{L}(\mathbf{x})\right] < 0\right\} \tag{6.4}$$

Whereas the simplified example in section 6.2 uses a damping factor approach for the head $\phi(\mathbf{x}, \acute{h})$, the application example in sections 6.3 and 6.3, employs the groundwater flow model described in appendix A. Notice that in the latter we can take the position of the monitoring device into account, too, and the heave and piping probabilities will be affected indirectly through the common random variables in the respective limit states.

6.1.2. MONITORING DESIGN AND COST

The principal design parameters in pore pressure monitoring design are (a) the number and (b) the position of devices. For the sake of illustration, here we contemplate only the installation of one device. The preferable position is where its updating effect is greatest.

In principle, the total cost of monitoring consists of mobilization cost and unit cost (e.g., cost of maintenance and readings per year). For the sake of simplicity, we will not distinguish between these cost items explicitly and only consider a lump sum monitoring cost $C_{monitor}$ [€].

The decision analysis for the monitoring design consists of finding the optimal configuration (i.e., position) and comparing the expected costs or benefit-cost ratios (BCR) of the decision options for that design.

6.1.3. PRE-POSTERIOR ANALYSIS

In contrast to posterior analysis with readily available monitoring data (6.1.1), in pre-posterior analysis the future measurements are yet unknown and, hence, uncertain. Not only is the measurement uncertain due to the uncertainties in ground properties and the measurement error, in this case also the future water level (i.e., loading) triggering the pore pressure response needs to be modeled as a random variable. That implies that the measured head ϕ_m used in the likelihood function in the posterior analysis (Eq. 6.3) becomes a random variable itself:

$$\mathbb{L}(\mathbf{x}) = f_{e_m}\left(\phi_m(\mathbf{X}, \acute{h}, e_m) - \phi(\mathbf{x}, \acute{h})\right) \tag{6.5}$$

Notice that $\mathbf{X}$ is the vector of random variables, while $\mathbf{x}$ is a dummy vector, and that here $\acute{h}$ and e_m are random variables in contrast to Eq. 6.3 from posterior analysis.

As to updating the scenario probabilities, in principle, the same method for posterior analysis is applicable as for inequality type of information (Eq. 4.20); the only difference is that the observation or evidence space ε is replaced by the equivalent observation space ε_e.

Furthermore, notice that since the likelihood is a random variable, the future updated reliability will be a random variable and, hence, so are the required retrofitting cost, as will be investigated in the following example.

6.2. EXAMPLE SIMPLIFIED UPLIFT MODEL

To illustrate updating with monitoring (i.e., equality type) information, an example with a simplified uplift model is elaborated below.

6.2.1. SIMPLIFIED UPLIFT MODEL

In contrast to the analytical, Dupuit-based model presented in section 3.2.2 and appendix A, the simplified model in this example only uses a damping factor λ, without considering the underlying permeabilities etc. The damping factor is supposed to be estimated directly in this case, for example, by expert judgement or based on measurements.

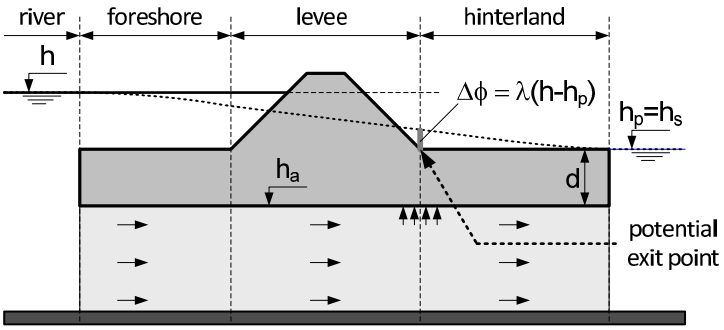

Figure 6.2: Damping factor λ for predicting the head at the exit point

Notice that in the following all surface and phreatic levels are denoted as h (with a subscript), whereas the ϕ stand for hydraulic heads in the aquifer.

LIMIT STATE FUNCTION

The limit state function is formulated basically as the critical head difference minus the predicted head difference:

$$Z_u = g_u(\mathbf{x}) = m_u \Delta\phi_{c,u} - \Delta\phi \tag{6.6}$$

where m_u is the resistance model factor, $\Delta\phi_{c,u} = \phi_{c,u} - h_s$ is the critical head difference [m] with respect to surface level h_s and $\Delta\phi = \phi - h_s$ is the corresponding (estimated) head difference [m].

CRITICAL HEAD DIFFERENCE (RESISTANCE)

The phreatic (polder) level h_p [m] is assumed to be at surface level (i.e. $h_p = h_s$). Hence, the critical head is given by the (total) weight of the blanket in terms of meters of water column above the bottom level of the blanket h_a [m]:

$$\phi_{c,u} = h_a + d\frac{\gamma_{sat}}{\gamma_w} = h_s - d + d\frac{\gamma_{sat}}{\gamma_w} \tag{6.7}$$

where d = blanket thickness [m], γ_{sat} = volumetric saturated weight of the blanket layer [kN/m^3] and γ_w = volumetric weight of water [kN/m^3]. As the critical head difference is defined with respect to h_p, it is given by

$$\Delta\phi_{c,u} = d\left(\frac{\gamma_{sat}}{\gamma_w} - 1\right) \tag{6.8}$$

HEAD DIFFERENCE (LOAD)

The head itself is estimated using the damping factor λ by

$$\phi = h_p + \lambda(h - h_p) \tag{6.9}$$

where h = (river) water level [m]. Consequently, the corresponding head difference is given by

$$\Delta\phi = \lambda(h - h_p) \tag{6.10}$$

Estimating λ can be done by either judgement, monitoring or modelling.

CRITICAL WATER LEVEL

Inserting the load (Eq. 6.10) and resistance (Eq. 6.8) in the limit state function results in

$$Z_u = g_u(\mathbf{x}) \quad = \quad m_u d\left(\frac{\gamma_{sat}}{\gamma_w} - 1\right) - \lambda(h - h_p) \tag{6.11}$$

Equating to zero and solving for the water level gives the critical water level for uplift $h_{c,u}$:

$$h_{c,u} \quad = \quad \frac{d\left(\gamma_{sat}/\gamma_w - 1\right)}{\lambda} + h_p \tag{6.12}$$

Notice that $F_{h_{c,u}}(\xi)$ is the uplift fragility curve.

6.2.2. INPUT PARAMETERS AND PRIOR RELIABILITY

The input example parameters as presented in Table 6.1 are fictitious but realistic; the values are similar to the example from section 5.5. The annual prior probability of failure obtained by Monte Carlo simulation is $P(F_u) = 3.9 \cdot 10^{-2}$ (the convergence is shown in Figure 6.3), which corresponds to an annual reliability index of $\beta = 1.76$.

X_i	Unit	Distribution	Parameters
h	[m]	Gumbel (annual)	$\alpha = 3.0$, $\beta = 0.3$
h_p	[m]	Normal	$\mu = 1.0$, $\sigma = 0.1$
d	[m]	Lognormal	$\mu = 4.0$, $\sigma = 0.4$
m_u		Lognormal	$\mu = 1.0$, $\sigma = 0.1$
γ_{sat}	[m]	Normal	$\mu = 20.0$,$\sigma = 1.0$
λ		Lognormal	$\mu = 0.8$, $\sigma = 0.1$
e_m	[m]	Normal	$\mu = 0.0$, $\sigma = 0.1$

Table 6.1: Example uplift monitoring: input parameters

6.2.3. OBSERVATION

We suppose that monitoring during a 100-year flood stage of 4.4 m ($\acute{h} = F_h^{-1}(1-1/100) = 4.4$m) has resulted in a measured head in the aquifer at the dike toe of $\phi_m = 2.8$ m. The duration of the reached flood stage is assumed sufficient for a near steady-state pore pressure response in the aquifer, which means that the models from appendix A are applicable. Furthermore, the measurement is supposed to be unbiased with a standard error $e_m \sim N(0, 0.1)$ [m].

6.2.4. POSTERIOR ANALYSIS

The equality information for this example is given by:

$$h(\mathbf{x}, e_m) = \phi(\mathbf{x}, \acute{h}) + e_m - \phi_m = 0 \tag{6.13}$$

Following the approach by Straub (2011) (see 4.2.4), we formulate the likelihood function as the probability of the measurement error for the difference between the measured and the real value of $\phi(\mathbf{x}, \acute{h})$:

$$\mathbb{L}(\mathbf{x}) = f_{e_m}\left(\phi_m - \phi(\mathbf{x}, \acute{h})\right) \tag{6.14}$$

That implies that the equivalent inequality domain can be expressed as:

$$\varepsilon_e = \{h_e(\mathbf{x}, u) < 0\} = \left\{u - \Phi^{-1}\left[c f_{e_m}\left(\phi_m - \phi(\mathbf{x}, \acute{h})\right)\right] < 0\right\} \tag{6.15}$$

Now, according to equation 4.19, the updated probability of uplift failure is determined by:

$$P(F_u|\varepsilon) = \frac{P(F_u \cap \varepsilon)}{P(\varepsilon)} = \frac{\int_{F_u \cap \varepsilon_e} f_{\mathbf{X}}(\mathbf{x})\varphi(u)\, du\, d\mathbf{x}}{\int_{\varepsilon_e} f_{\mathbf{X}}(\mathbf{x})\varphi(u)\, du\, d\mathbf{x}} \tag{6.16}$$

where $F_u = \{g(\mathbf{x}) < 0\}$.

Since the evaluation of the limit states for uplift, heave and piping is computationally inexpensive, we can obtain (asymptotically) exact results by using Monte Carlo simulation, which are summarized in Table 6.2. Incorporating the monitoring observation causes the probability of failure to decrease by a factor 10.

	Probability of Failure	Reliability Index
Prior	$P(F_u) = 3.9 \cdot 10^{-2}$	$\beta = 1.76$
Posterior	$P(F_u\|\varepsilon) = 4.0 \cdot 10^{-3}$	$\beta = 2.65$

Table 6.2: Example uplift monitoring: annual prior and posterior probability of failure

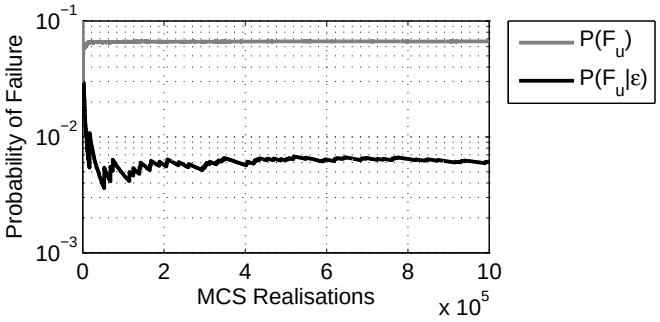

Figure 6.3: Example uplift monitoring: convergence of the prior and posterior annual probabilities of failure

Figure 6.3 illustrates that, even though the prior and posterior probability are not extremely low, the posterior analysis takes a large number of MCS-realisations to converge. Decisive here is the numerator term of equation 6.16, $P(F_u \cap \varepsilon)$, which can be orders of magnitude lower than $P(F_u|\varepsilon)$ itself. Subset Simulation (SubSim) (Au and Beck, 2001) provides a workable alternative for cases, where this poses computational problems. For the given problem, the same results were obtained by SubSim with roughly a factor 10 to 100 less realizations.

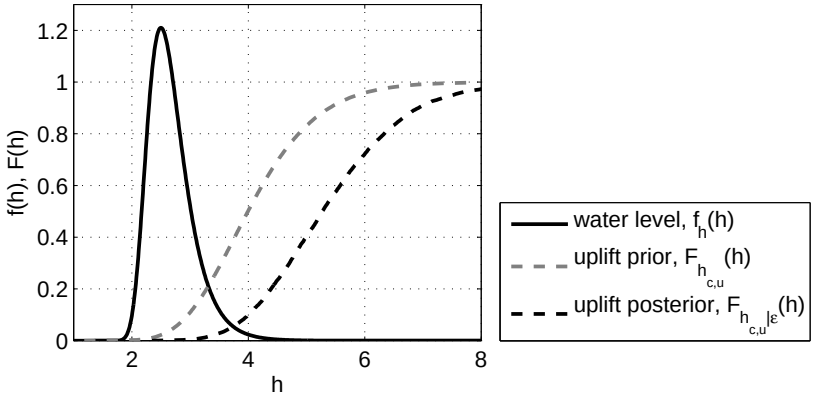

Figure 6.4: Example uplift monitoring: prior and posterior critical water level and head at exit point expressed as probability densities ($f(\cdot)$) and fragility curves ($F(\cdot)$)

An important difference with the preceding chapter 5 is illustrated in Figure 6.5. In survival type of analysis as for field observations, basically all random variables are updated. Here only the random variables that influence the measurement are updated. While the fragility curve of the critical head difference $\Delta\phi_c$ does not change at all, the fragility curve of the critical water level $h_{c,u}$ changes significantly. The reason is that $\Delta\phi_c$ does not contain any (load) variables that influence the pore pressure at the exit point. On the other hand, $h_{c,u}$ does contain those variables; it contains all random variables except h.

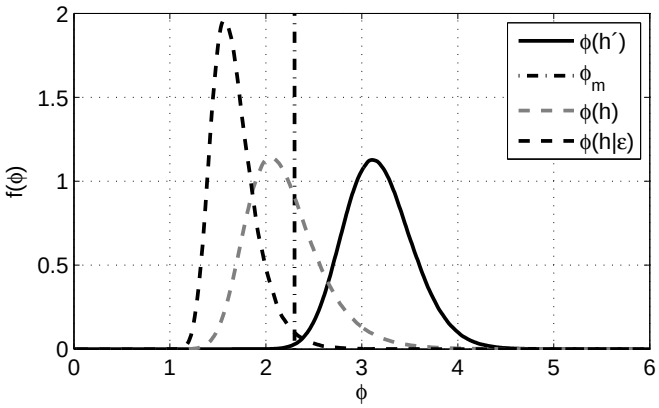

Figure 6.5: Example uplift monitoring: prior and posterior distributions (PDF) of the unconditional head ($\phi(h)$) and the head conditional on the observed 100-year flood level ($\phi(\acute{h})$)

In Figure 6.5, the gray dashed line represents the prior PDF of the head distribution at the exit point, while the black solid line shows the head distribution conditioned on the observed water level $\acute{h}$. The observed head ϕ_m (dotted line) is thus relatively high with respect to the yearly (unconditional) distribution, but it is a rather low value for the observed event. This means that the posterior load characteristics are lower than the prior ones, which is another explanation for the increase in reliability after updating.

Similar conclusions can be drawn from the posterior PDFs for individual variables of shown in Figure 6.6. Only h_p and λ, the variables influencing the head ϕ (remember: $\phi = h_p + \lambda(h - h_p)$), are updated. While the PDF of h_b only slightly shifts to the left, the distribution of λ shifts significantly and the spread decreases considerably, too. This is plausible, because with the head based on the mean values of h_p and λ and for $\acute{h}$ would have been: $\phi = \mu_{h_p} + \mu_\lambda(\acute{h} - \mu_{h_p}) \approx 3.6$m; the measured value was significantly lower with $\phi_m = 2.8$m. Notice that the posterior distributions can be correlated even though the prior distributions were uncorrelated as illustrated in Figure 6.7.

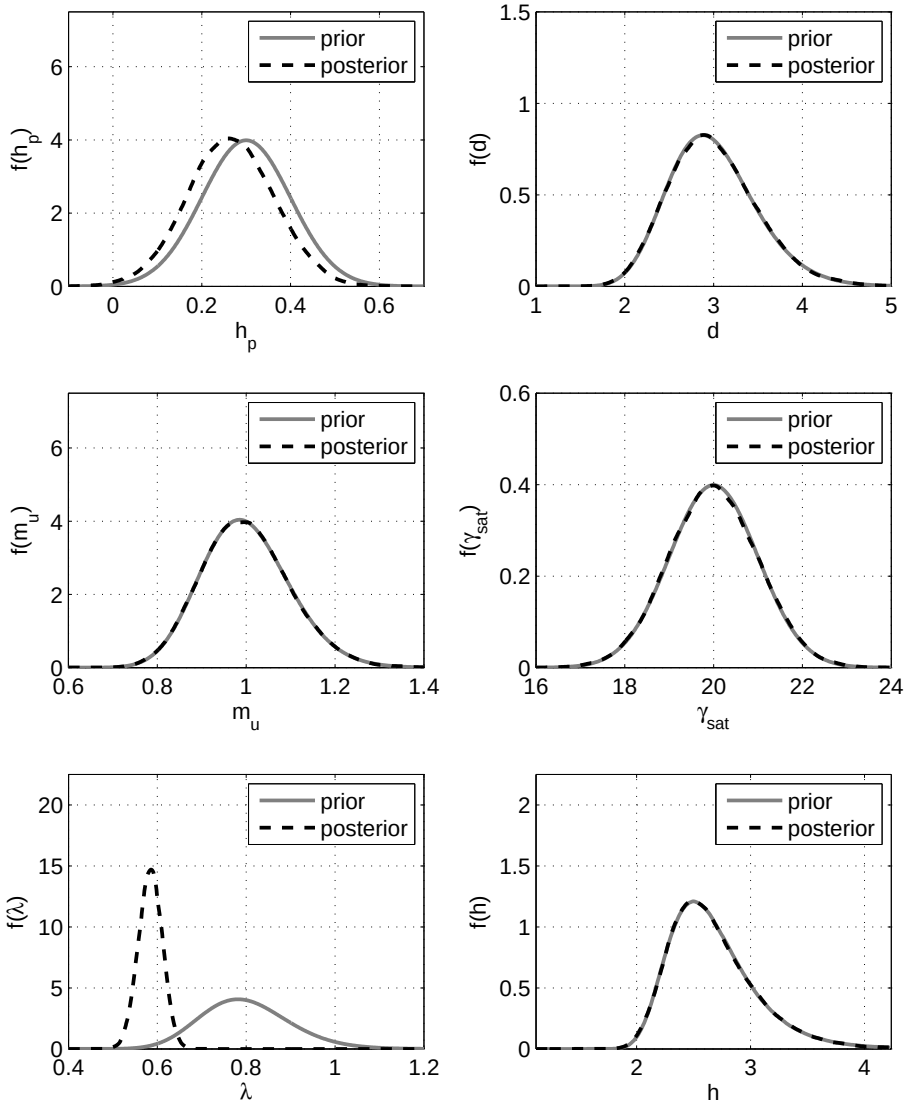

Figure 6.6: Example uplift monitoring: posterior probability density functions

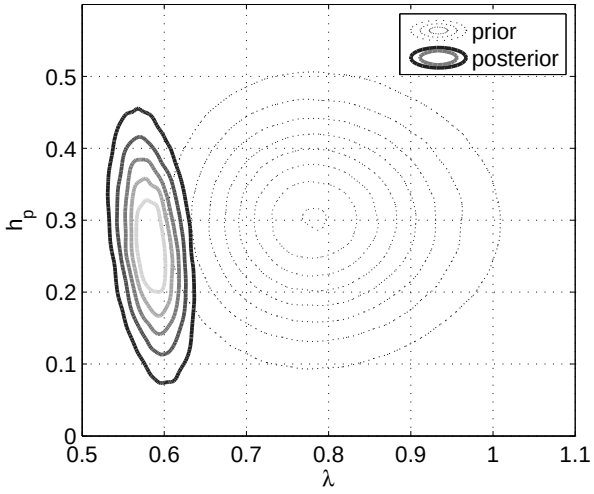

Figure 6.7: Example uplift monitoring: posterior JPDF of the damping factor and the landside phreatic level

6.2.5. SENSITIVITY ANALYSIS

Below we investigate the sensitivity of the outcomes to the following observation related parameters:

1. σ_e (the measurement error),
2. ϕ_m (the measured head at the potential exit point),
3. $\acute{h}$ (the observed water level, at which the measurement was taken)

Finally, some qualitative consideration on additional variables will be given.

MEASURED HEAD ϕ_m AND OBSERVED WATER LEVEL $\acute{h}$

Figure 6.8 is a contour plot showing the posterior reliability index for combinations of the observed water level ($\acute{h}$) and the measured head (ϕ_m) for a given measurement error of $\sigma_e = 0.1$m. Such a representation helps in quick interpretation of observations and can be used as "pre-compiled" results in pre-posterior analysis as shown in the subsequent section.

MEASUREMENT ERROR σ_e

Figure 6.9 demonstrates that the updating effect vanishes with increasing measurement error.

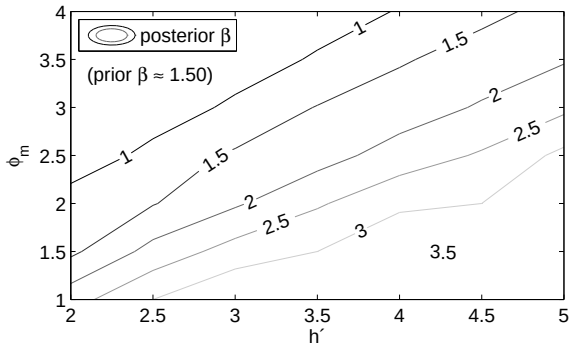

Figure 6.8: Example uplift monitoring: posterior reliability as a function of the measured head ϕ_m and the observed water level $\acute{h}$ (for a measurement error of $\sigma_e = 0.1$m, annual reliability)

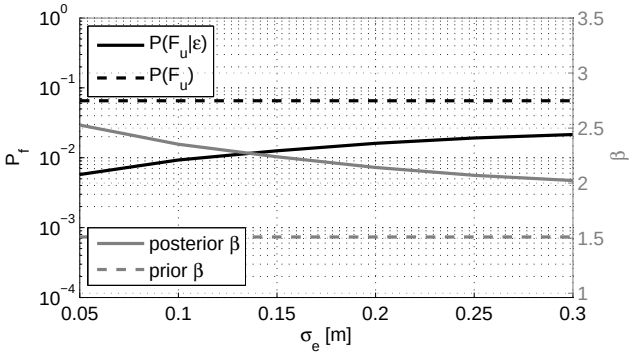

Figure 6.9: Example uplift monitoring: sensitivity of the posterior reliability with respect to the measurement error σ_e (for a measured head of $\phi_m = 2.8$m and a 100-year flood stage $\acute{h} = 4.4$m, probabilities on an annual basis)

OTHER PARAMETERS

While the considerations above cover the most relevant parameters, the effect of other parameters can be inferred qualitatively. For example, if the observed water level is not known deterministically (e.g., due to measurement error), the updating effect will be weaker in a comparable fashion as for the measurement error of the head (σ_e). After all, both make the observation more uncertain. Similarly, the lower the prior variance of λ, the the smaller the effect of updating and vice versa.

6.2.6. INVESTMENT DECISION PROBLEM

After contemplating the effects of posterior analysis for a given measurement, we now turn to the problem of monitoring planning. Suppose our fictitious levee needs to comply with a target reliability for uplift of $p_{T,u} = 10^{-2}$ a^{-1}, which it currently does not ($P(F_u) = 3.9 \cdot 10^{-2}$ a^{-1}). Furthermore, assume that the levee needs to be reinforced up to compliance level, unless monitoring during the next year leads to updated reliability which does comply.

For the current example, the decision boils down to whether or not to invest in monitoring as illustrated in the decision tree in Figure 6.10.

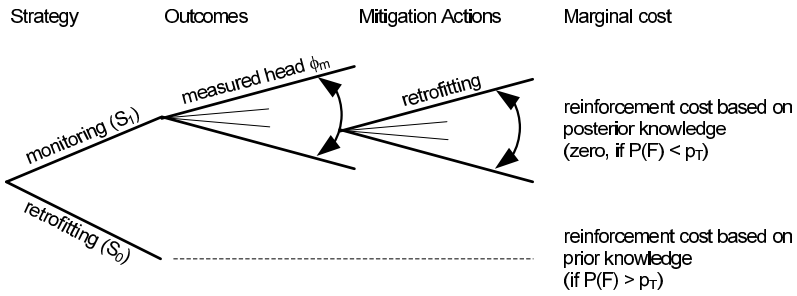

Figure 6.10: Example uplift monitoring: decision tree for a simple uplift monitoring example in a safety assessment situation

PRE-POSTERIOR ANALYSIS

The essential difference with posterior analysis is that we don't know the water level $\acute{h}$ that will occur during the monitoring year and we do not know the outcome of the pore pressure measurement ($\phi_m(\acute{h})$) either. With the uncertainty in the water level to be observed described by the PDF of the yearly maximum water level ($f_{\acute{h}}(\xi) = f_h(\xi)$), the head to be measured becomes a function of $\acute{h}$ (which now is a random variable) and the other parameters influencing the head:

$$\phi_m(\mathbf{X}, \acute{h}) = \phi(\mathbf{X}, \acute{h}) + e_{m,obs} \tag{6.17}$$

where $\phi(\mathbf{X}, \acute{h})$ is the real head and $e_{m,obs}$ is the measurement error at the observation[1].

The uncertainty in the future observation leads to uncertainty in the reliability after posterior analysis, which is illustrated by the distribution of the resulting posterior reliability index (Figure 6.11). The latter is based on the prior distribution of the random variables and also called "pre-posterior distribution". The pre-posterior distribution of the reliability index shows that the expected reliability after the measurement will be higher than a-priori. We would expect this because the general effect of measuring is uncertainty reduction. On the other hand, there is a considerable chance (~ 30%) that

[1] Notice that it is necessary to distinguish between $e_{m,obs}$ and e_m, since the future measurement error is independent of the error at the time of the observation

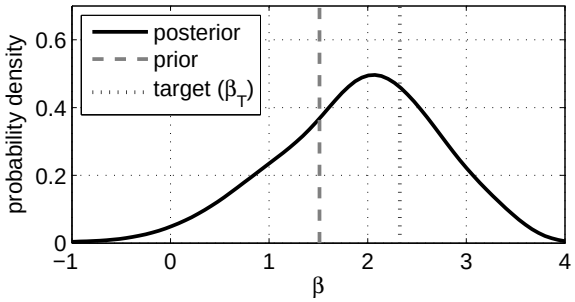

Figure 6.11: Example uplift monitoring: Pre-posterior distribution of the posterior annual reliability index β after one year of monitoring

the posterior reliability is lower than the prior, for example due to "measuring" resistance properties such as the damping factor λ to be lower than the expected value.

From a decision theoretical point of view, at least now there is a chance that after one year of monitoring the dike section under consideration may comply with the uplift safety assessment criteria (the target reliability β_T) and retrofitting becomes unnecessary. This probability of "success" is given by:

$$P[P(F_u|\varepsilon) < p_{T,u}] \approx 41.1\% \tag{6.18}$$

That means that there is a 41% chance that retrofitting becomes unnecessary and a 59% chance that retrofitting is still required on top of the investment in monitoring. This information in itself is insufficient to take a well founded decision, since the difference of monitoring and retrofitting cost is also important as we will see below.

STRATEGY COSTS AND DECISION CRITERION

As illustrated in Figure 6.10, the strategy options as to choose for retrofitting directly or to choose for monitoring will be called strategies S_0 and S_1 respectively.

For the sake of illustration, in this simplified example we use a simple cost function. Since berm with cost C_{berm} needs to be built if the reliability target ($p_{T,u}$) is not met, the retrofitting costs are:

$$C_r = C_{berm} \tag{6.19}$$

Thus, for S_0 (no monitoring, direct retrofitting) the expected cost equals the retrofitting cost: $E[C_{S_0}] = C_r = C_{berm}$.

The monitoring strategy S_1 involves monitoring cost $C_{monitor}$ and the retrofitting cost will depend on the observation ε. The cost is thus given by:

$$C_{S_1} = C_{monitor} + C_{berm} \cdot \mathbf{1}[P(F_u|\varepsilon) > p_{T,u}] \tag{6.20}$$

which means we have only monitoring cost, if after monitoring the probability of failure drops below the target and we have monitoring and berm cost, if it remains unacceptably high.

The expected cost of S_1 depends on the probability of the evidence $f(\varepsilon)$ and is denoted as:

$$E[C_{S_1}] = C_{monitor} + C_{berm} \cdot P[P(F_u|\varepsilon) > p_{T,u}] \tag{6.21}$$

where $P[P(F_u|\varepsilon) > P_{T,u}]$ is the probability that the posterior probability of uplift failure will (still) be larger than the target, which is computed by:

$$P[P(F_u|\varepsilon) > P_{T,u}] = \int_{P(F_u|\varepsilon) > p_{T,u}} f(\varepsilon) d\varepsilon \tag{6.22}$$

where $P(F_u|\varepsilon)$ is determined based on equation 6.16, in which the ϕ_m and $\acute{h}$ are random variables as described above. In words, this means that we consider all possible observations (ε) weighted by their probability based on prior uncertainties and integrate over the observation space that would lead to "failure" - a reliability problem in essence.

Having determined the costs and probabilities involved, the (risk-neutral) decision is based on the comparison of the expected costs per strategy. One would choose to invest in monitoring (S_1), if

$$E[C_{S_1}] < E[C_{S_0}] \tag{6.23}$$

$$\Leftrightarrow \quad C_{monitor} + C_r P[P(F_u|\varepsilon) > p_{T,u}] < C_r \tag{6.24}$$

$$\Leftrightarrow \quad C_{monitor} < C_r P[P(F_u|\varepsilon) < p_{T,u}] \tag{6.25}$$

$$\Leftrightarrow \quad \frac{C_{monitor}}{C_r} < P[P(F_u|\varepsilon) < p_{T,u}] \tag{6.26}$$

which means in words that if the monitoring investment is lower that the expected savings (potential savings = C_{berm} times probability of "success") we would decide to invest. Or, equivalently, if the ratio of investment over potential saving is lower than the probability of achieving the saving, the decision would be to invest. For the given case a reasonable indication for the orders of magnitude of monitoring and retrofitting cost in the Netherlands would be 10^4€ and 10^6€ respectively, which makes the ratio approximately 1%. Hence, despite a considerable probability of "failure" (i.e., not avoiding investments in retrofitting), in this specific example investing in monitoring would make sense.

BENEFIT-COST RATIO

Another way to present the decision support information is Benefit-Cost Ratio (BCR). While a risk-neutral decision maker would come the same conclusion via BCR as via expected cost, BCR may be more appealing to decision makers, since it shows the expected return on investment.

In the present example it seems appropriate to define the monitoring cost as costs and the expected value of the reduction in retrofitting cost as benefits:

$$BCR = \frac{C_{berm} P\left[P(F_u|\varepsilon) < P_{T,u}\right]}{C_{monitor}} \approx \frac{4.11 \cdot 10^5}{10^4} = 41.1 \approx 40 \tag{6.27}$$

The BCR being (considerably) greater than unity shows that monitoring is a viable option and should be preferred over S_0 which has no cost but no benefit either according to the chosen definition.

DECISION TREE

As the considerations regarding strategy cost and BCR, the decision tree in Figure 6.12 illustrates that the monitoring strategy is preferred, for its expected cost is roughly 30% lower.

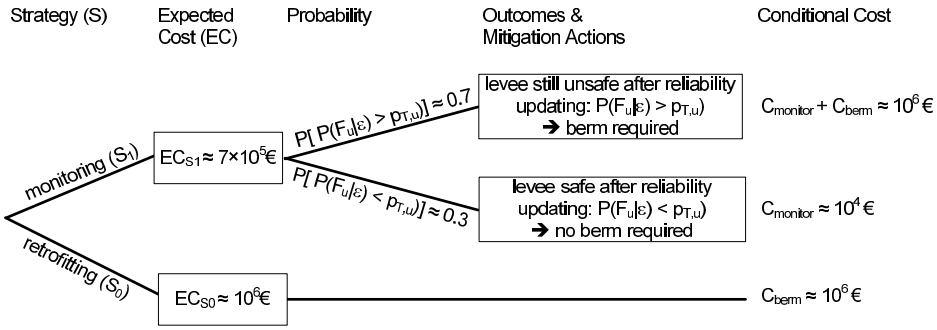

Figure 6.12: Example uplift monitoring: decision tree with the results regarding (expected) cost and probabilities

6.2.7. DISCUSSION

Besides the specific noteworthy aspects below, this simple example illustrates some general features of reliability updating with pore pressure monitoring and the respective investment decisions:

1. The posterior analysis confirms that only uncertainties of variables affecting the measured variable can be updated. Since the head at the toe is not affected by resistance properties such the blanket thickness or weight, these uncertainties persist. Hence, the effect of reliability updating depends largely on the relative importance of the observation-driving variables.

2. Figure 6.5 demonstrates the importance of knowing the water level belonging to the measured head in the aquifer. If we only had a measured head but no information on the corresponding water level, we would need to assume the probability distribution of the water level as a sort of measurement uncertainty. Figure 6.5 shows that for an unknown water level the measured head would have been rather expected, while it it was a very low value for the observed water level.

3. The sensitivity analysis shows how the posterior reliability changes with respect to varying the measured head, the measurement error and the observed water level. Furthermore, it illustrates how posterior analysis results can be precompiled for use in pre-posterior analysis.

4. The more (a-priori) unlikely an observation is, the larger is the difference between prior and posterior reliability.

5. The pre-posterior reliability (i.e., after integrating out prior uncertainties) is practically equal to the prior. After all, a-prior we expect to measure according to our expectation (prior probabilities) and in that case the effect of updating is rather small. On the other hand, if the prior uncertainty in the observation-driving variables is considerable, the uncertainty in the posterior distribution will be large, too. Hence, even though the expected posterior reliability is not much different from the prior, the decision can be influenced significantly. In the example, even a rather small chance of "success" of about 1% would have made the monitoring strategy the preferable choice.

6. The ratio of investment cost and potential savings drives the decision, together with the probability of realising the savings - the "chance of success". That means that investments even with a rather low probability of success can be worthwhile, if they are relatively low-cost, for example monitoring with respect to retrofitting.

7. The computations for this example were based on Monte Carlo simulation (MCS).Even though the probability of failure is not very small, in the posterior analysis the number of required MCS-realisations can be very high (i.e., much higher than in the prior analysis). The reason is that the (equivalent) observation space can be very small, especially for small measurement errors. The problem also increases, if several observations are considered simultaneously. More efficient techniques with full system reliability capabilities like Subset Simulation Au and Beck (2001) also provide a solution.

6.3. APPLICATION EXAMPLE - POSTERIOR ANALYSIS

THIS section applies the theory developed in this chapter to the application example which was introduced in section 3.5 and further elaborated on in terms of field performance observations in section 5.5. We contemplate the same location, observed water level and assumptions regarding the reducibility of uncertainty as described in these sections. This enables comparing the relative effects of reliability updating with the two different sources of information (i.e., field observations vs. head monitoring).

Below the results and illustrations for stratification scenario E_1 are presented as well as an overview of the most important results for all scenarios. For the detailed results for all scenarios the reader is referred to appendix H.

6.3.1. OBSERVATION

The effect of reliability updating with pore pressure measurements is demonstrated with a fictitious measurement here. We assume that at a 100-year flood stage of $\acute{h} = 3.5$m a head of $\phi_m = 2.1$m was measured (with measurement error $\sigma_e = 0.1$m)).

6.3.2. POSTERIOR FRAGILITY CURVES

The posterior fragility curves in Figure 6.13 indicate that the observation has led our degree of belief in failure to decrease; all curves shift downwards.

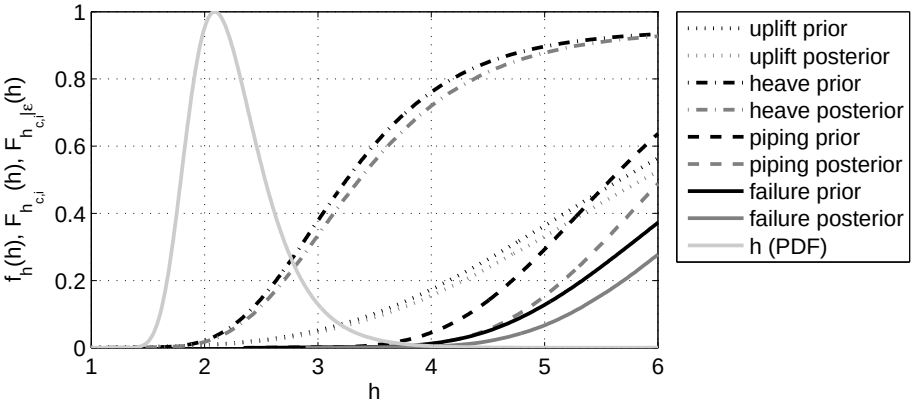

Figure 6.13: Application example head monitoring: water level (h) PDF and posterior versus prior fragility curves for uplift ($h_{c,u}$), heave ($h_{c,h}$), piping ($h_{c,p}$) and failure (h_c), stratification scenario E_1

Figure 6.14 confirms that the measured head ϕ_m was lower than expected a-priori for the observed water level. The expected value was approximately $E[\phi(\mathbf{x}, \acute{h})] \approx 2.5$m, whereas the measured value was roughly one standard deviation lower.

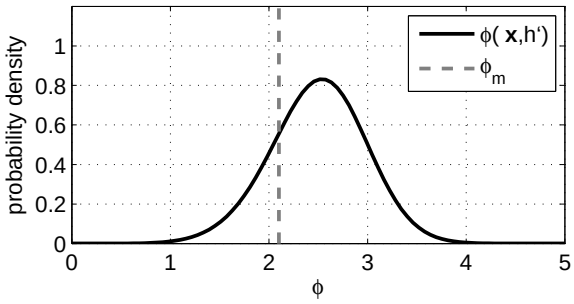

Figure 6.14: Application example head monitoring: prior distribution of the head at the measured location, stratification scenario E_1

It is important to realize that through the common variables in the failure limit states and the load model (i.e., the parameters affecting the observed head) all three, uplift, heave and piping are affected. This illustrates an important advantage of failure models which involve physically interpretable and (directly or indirectly) measurable parameters as opposed to empirical models. The advantage is that observations can be related to these physically interpretable parameters in order to update our degree of belief of the state of nature, the model bias and failure.

6.3.3. POSTERIOR SCENARIO PROBABILITIES

The likelihoods and posterior probabilities of the stratification scenarios in Figure 6.15 show that (a) the observation changes our relative belief between the scenarios with blanket layer (E_1 and E_2) and it provides evidence that (b) the scenarios without blanket layer are highly unrealistic and practically attain a posterior probability of zero. The explanation for the latter is rather simple; if there were no blanket layer, the measured head should be close to h_p, which it is not.

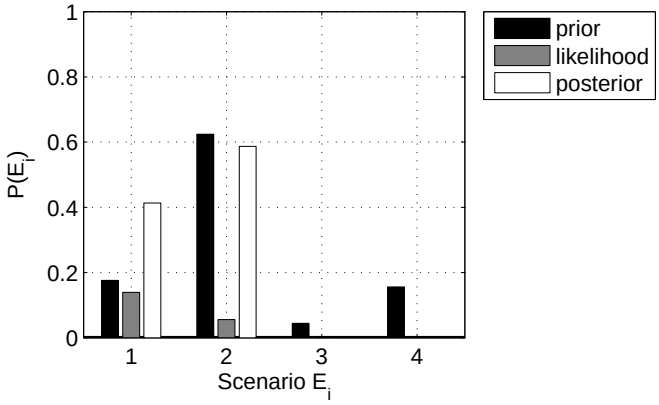

Figure 6.15: Case study field observations: prior and posterior scenario probabilities

6.3.4. POSTERIOR ANALYSIS SUMMARY

The comparison of prior and posterior probabilities in Table 6.3 shows that the observation has led to a significantly lower overall probability of failure (almost two orders of magnitude). The main contribution to that reduction was the "exclusion" of the two stratification scenarios without blanket layer, whereas a-priori these scenarios were the main contributors to the probability of failure. For the scenarios with blanket layer (E_1 and E_2), the reduction in probability of failure was most significant for piping, mainly through the change in the distribution of the permeability k (see posterior distributions for scenario E_1 in Figure 6.16).

Table 6.3: Application example head monitoring, dike ring 10 (Mastenbroek) - prior and posterior analysis results summary (annual probabilities)

PRIOR ANALYSIS					**P(F) =**	**1.9E−3**
i	**P(E_i)**	**Uplift P(F_u|E_i)**	**Heave P(F_h|E_i)**	**Piping P(F_p|E_i)**	**Failure P(F|E_i)**	**P(E_i)P(F|E_i)**
1	17.6%	$1.8E-2$	$1.0E-1$	$4.8E-4$	$1.4E-4$	$2.5E-5$
2	62.4%	$2.8E-2$	$1.7E-1$	$5.7E-4$	$2.2E-4$	$1.3E-4$
3	4.4%	$1.0E-0$	$1.0E-0$	$8.7E-3$	$8.9E-3$	$3.9E-4$
4	15.6%	$1.0E-0$	$1.0E-0$	$8.3E-3$	$8.3E-3$	$1.3E-3$
POSTERIOR ANALYSIS					**P(F) =**	**3.3E−5**
i	**P(E_i|ε)**	**P(F_u|E_i,ε)**	**P(F_h|E_i)**	**P(F_p|E_i,ε)**	**P(F|E_i,ε)**	**P(E_i|ε)P(F|E_i,ε)**
1	41.3%	$1.6E-2$	$8.8E-2$	$1.5E-4$	$5.0E-5$	$2.1E-5$
2	58.7%	$2.4E-2$	$1.5E-1$	$2.4E-5$	$1.8E-5$	$1.1E-5$
3	0.0%	n/a	n/a	n/a	n/a	0.0
4	0.0%	n/a	n/a	n/a	n/a	0.0

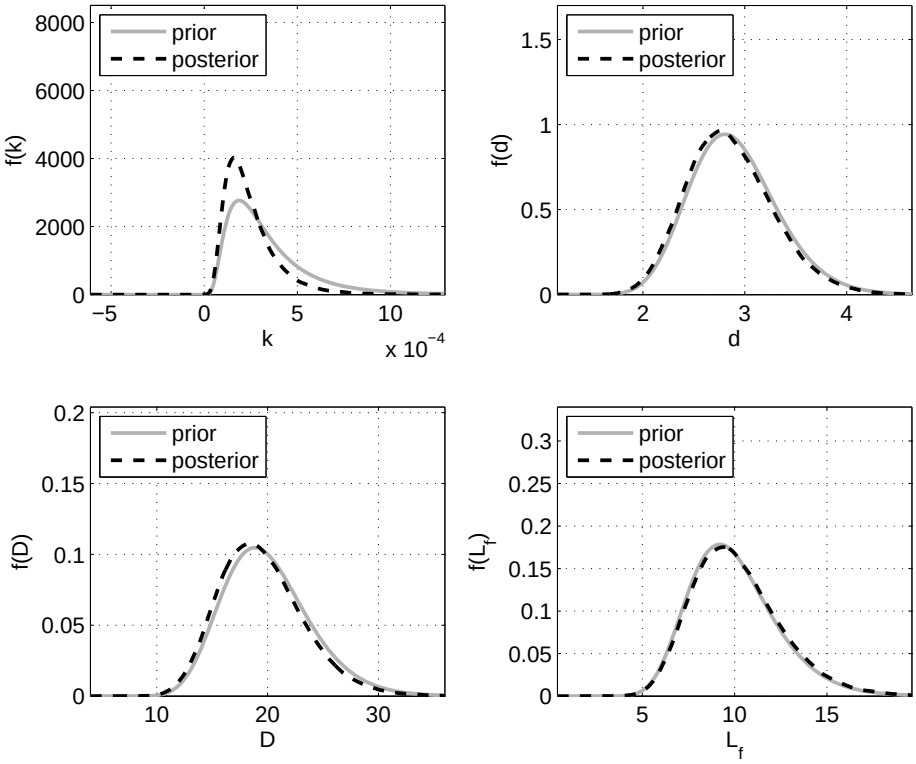

Figure 6.16: Application example head monitoring: posterior distributions of random variables affecting the observation, stratification scenario E_1

6.4. APPLICATION EXAMPLE - PRE-POSTERIOR ANALYSIS

THIS section will elaborate the (pre-posterior) decision analysis for the present example. Instead of using readily available monitoring data as in posterior analysis, we have to estimate the expected measurement outcome and its effect on the updated reliability as well as the respective costs or savings based on our prior knowledge.

6.4.1. PRE-POSTERIOR MEASURED HEAD ϕ_m

As outlined in 6.1.3, in pre-posterior analysis our measurement outcome also becomes a random variable ($\phi_m(\mathbf{X}, \acute{h}, e_m)$), because the water level $\acute{h}$ (i.e., the forcing for the observation), the ground properties and the measurement error are all random variables themselves. Figure 6.17 shows that for the present case study, the pre-posterior distribution of the (future) measured head is bi-modal. The reason is that scenarios E_3 and E_4 would lead to measured heads practically equal to the hinterland surface level h_s, which represents the left-hand part of the distribution, while scenarios E_3 and E_4 "generate" the right-hand part. The set of realisations underlying the ϕ_m-distribution, together with the corresponding (future) observed water levels form the input to the pre-posterior analysis below.

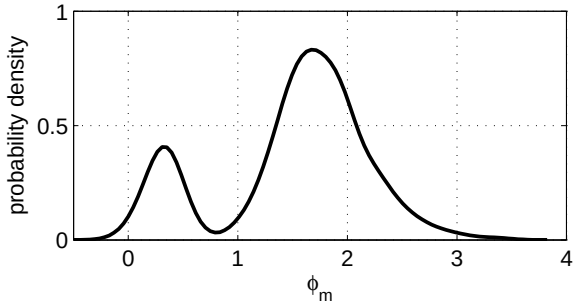

Figure 6.17: Application example head monitoring: probability distribution of the future measured head ϕ_m [m] based on prior distributions of the random variables

6.4.2. DEALING WITH HIGHLY UNLIKELY OBSERVATIONS

As Figure 6.17 illustrates, the distribution of future observations is actually divided in two parts with little overlap. One part stems from the stratification scenarios with and the other part without blanket layer. Using these observations in posterior analysis leads to highly unlikely events, namely the measured ϕ_m coming from blanket-scenarios are highly unlikely for no blanket-scenarios and vice versa. Computationally, this introduces the following issue: The equivalent inequality domain ε_e is in parameter subspace with very low probability density of the basic random variables, which results in very low probability values for the term $P(\varepsilon_e)$ (i.e, lower than 10^-6) and even lower values for $P(F_u|\varepsilon_e)$ and $P(F_p|\varepsilon_e)$. As a result, the amount of required MCS-realisations becomes computationally intractable. Fortunately, if $P(\varepsilon_e)$ is orders of magnitude lower than the

total and the target probability of failure, the posterior probability of the respective stratification scenario $P(E_i|\varepsilon) \sim P(\varepsilon_e|E_i)P(E_i)$ will also be that small that its contribution to the total probability of failure $P(F|\varepsilon) = \sum P(F|E_i,\varepsilon)P(E_i|\varepsilon)$ becomes insignificant.

Computationally, we can use this reasoning to keep computations tractable by first evaluating $P(\varepsilon_e)$ and skipping the evaluation of the conditional posterior probabilities of failure (i.e., $P(F_j|E_i,\varepsilon)$ for very low values of for example $P(\varepsilon_e) < 10^{-6}$. At the same time, the posterior scenario probabilities are set to zero. Table 6.4 illustrates how this approach works out for the present case study. The highly unlikely observations use to be the ones where in the posterior analysis of a scenario with blanket layer the observation was "generated" by a scenario without blanket and vice versa. Note that the same holds for other types of scenarios as described in 3.3.3 as for example the uncertain in the location of a potential entry point.

Table 6.4: Case study field observations: posterior stratification scenario probabilities and the influence of a blanket layer

	OBSERVATION-GENERATING SCENARIO	
ANALYZED SCENARIO	blanket	no blanket
blanket	normal analysis	$P(E_i|\varepsilon) = 0$
no blanket	$P(E_i|\varepsilon) = 0$	normal analysis

6.4.3. RELIABILITY INDEX PER STRATIFICATION SCENARIO

Figure 6.18 shows the pre-posterior distributions of the reliability indices for uplift,heave, piping and failure per stratification scenario for observations with a significant likelihood as explained in section 6.4.2. Consequently, only the realisations of the future measurements from scenarios with blanket layer influence each other, the same holds for the no blanket layer scenarios. As a result, the expected value of the reliability index in E_1 is lower than the prior because it is influenced by scenario E_2, which is characterized by more unfavorable conditions (i.e., a higher prior probability of failure.). The inverse is true for E_2. Qualitatively, the same holds for scenarios E_3 and E_4, only that the mean posterior reliability index stays much closer to the prior.

An important observation for the decision analysis is that there is significant spread in the posterior βs as already illustrated in section 6.2.6. Roughly speaking, the likely range of change in terms of reliability index is plus minus 0.5, which is equivalent to a range of one order of magnitude in terms of probability of failure.

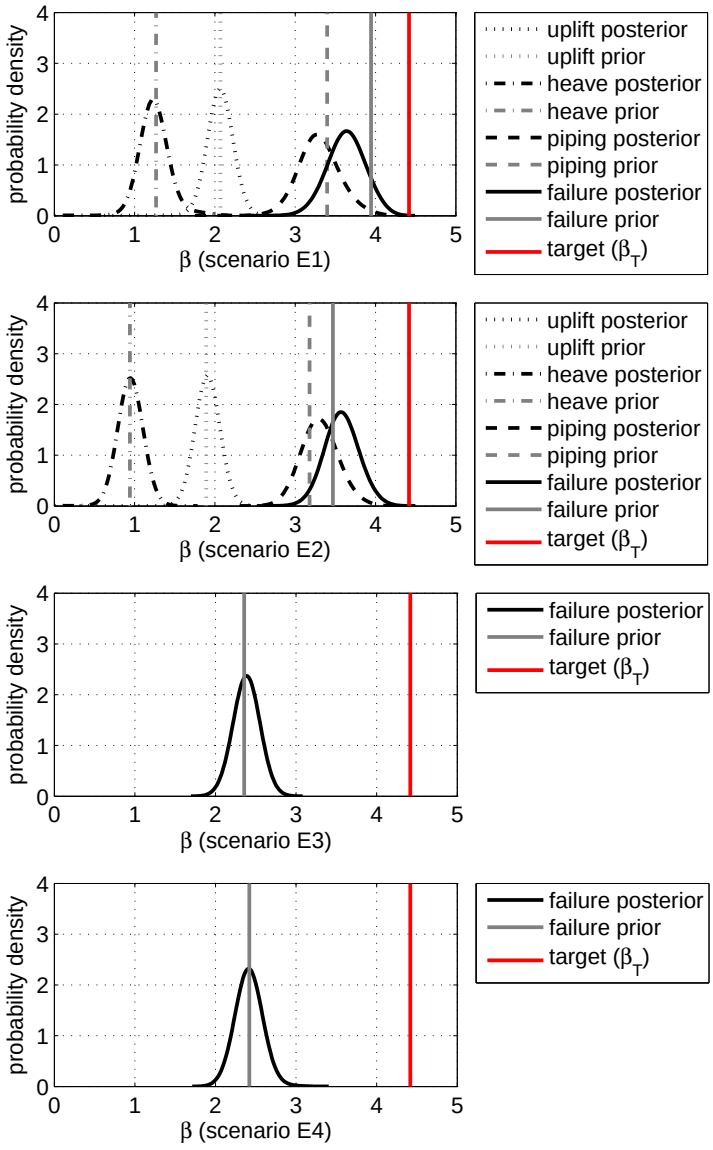

Figure 6.18: Application example head monitoring: density plots of pre-posterior realisations of posterior reliability indices per stratification scenario for a random future water level and measurement error (1 year of monitoring).

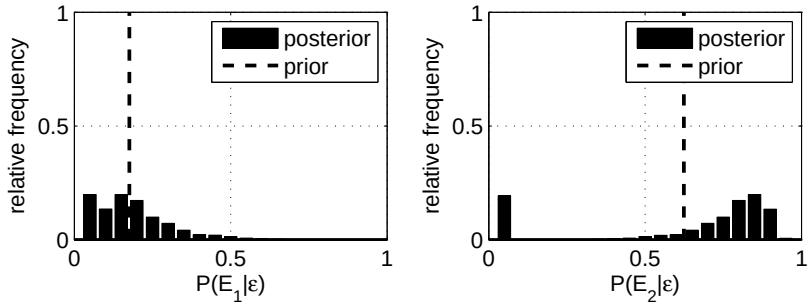

(a) Stratification Scenario E_1 (b) Stratification Scenario E_2

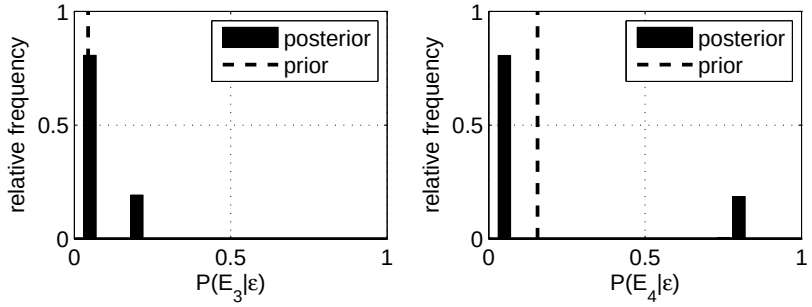

(c) Stratification Scenario E_3 (d) Stratification Scenario E_4

Figure 6.19: Application example head monitoring: realisations of posterior scenario probabilities for a random future water level (1 year of monitoring)

The pre-posterior stratification probabilities in Figure 6.19 also reflect the importance of the shifts in scenario probabilities, especially due to highly unlikely observations as outlined in 6.4.2. The histograms of all scenarios show a significant bin with zero posterior probabilities, which can be explained as follows. Both, E_1 and E_2 exhibit approximately a 20% probability of "being excluded" by the posterior analysis. That is exactly the sum of the prior probabilities of scenarios E_3 and E_4 ($P(E_3) + P(E_4) \approx 0.2$). As explained earlier observations generated from no blanket-scenarios lead to practically zero likelihood for scenarios with blanket. Again, the inverse holds for E_3 and E_4, which obtain zero posterior probability with an 80% chance. This implies that after posterior analysis there are only two scenario sets left, either E_1 and E_2 or E_3 and E_4.

Furthermore, subfigures (c) and (d) of Figure 6.19 show no variation in the posterior scenario probabilities (except for the zero probabilities). This results from the fact that for both scenarios one would measure the same head, namely the surface level ($\phi_m = h_s$). Hence, a measurement cannot help to distinguish between the two scenarios in terms of relative likelihood. The only effect is that $P(E_3)$ and $P(E_4)$ are normalized to

sum up to one. This is different for E_1 and E_2, where the measured head is more plausible for one scenario than for the other. Also notice that, except for the zero probabilities, the histograms of E_1 and E_2 and of E_3 and E_4 are mirror images of each other, which makes sense because they need to sum up to one (to be proper PMF of mutually exclusive scenarios).

6.4.4. PRE-POSTERIOR RELIABILITY

The distributions of the "total" pre-posterior reliability indices (i.e., "weighted" by the scenario probabilities) reflect the combination of the conditional posterior reliability indices per scenario and the and the posterior scenario probabilities. All distributions, for uplift, piping and failure are two-modal, reflecting the differences between blanket- and no blanket-scenarios[2]. The left modes of the piping and failure distribution stem from scenarios E_3 and E_4, while the right part comes from E_1 and E_2.

Notice that integrating out the uncertainty in the posterior reliability we obtain a Bayesian estimate of the posterior reliability, which is exactly the same as the prior (as discussed and exemplified in 4.1.5). However, for the decision analysis, we conclude that there is a 5% probability that the posterior reliability will comply with the target value:

$$P[P(F_u|\varepsilon) < P_{T,u}] \approx 5\%$$

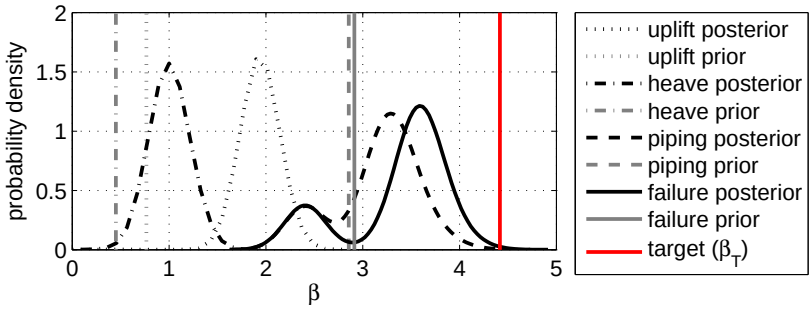

Figure 6.20: Application example head monitoring: density plots of pre-posterior realisations of posterior reliability indices for all scenarios for a random future water level and measurement error (1 year of monitoring). A part of the density of the pre-posterior uplift reliability $\beta_u|\varepsilon$ is below zero and left out for better representation of the relevant β-regions.

[2] Notice that as indicated in the figure caption the left part of the posterior uplift reliability index distribution is not displayed in the figure, it is somewhere around -5.

6.4.5. INVESTMENT DECISION

The general approach to the decision analysis based on expected cost and benefit-cost ratio has already been discussed in 6.2.6 and is not repeated here. However, in a realistic setting we should consider the following additional aspects:

1. The retrofitting cost may vary depending on the "degree of lack of safety" (i.e., the difference between posterior and target reliability).

2. The retrofitting cost may also depend on the changes in scenario probabilities, since for specific scenarios, the retrofitting options may differ considerably between the two. For example, while for some scenarios an increase in berm length may be effective, in other cases vertical seepage screens can be the better option.

There is no general recipe for analyzing these cost aspects other than consequently applying pre-posterior and decision analysis while using appropriate cost (functions) for the situation at hand. In the Monte Carlo approach followed in this thesis, this implies finding a optimal design for each pre-posterior realization and computing its (expected) cost.

6.4.6. PRE-POSTERIOR ANALYSIS SUMMARY

The pre-posterior analysis nicely illustrates that based on prior knowledge, the expected future measurement is rather uncertain, especially due to the different stratification scenarios. In the spre-posterior analysis with the uncertain future observation this leads to "highly unlikely observations" or ranges of measurements. For measurements in a certain range, some stratification scenarios are highly implausible and obtain a posterior probability of practically zero. This confirms our intuition that if we have scenarios that would lead to considerably different measurement outcomes, monitoring helps in "ruling out" some of them. As pointed out earlier, this discrete type of uncertainty again proves to be more important than the uncertainty in resistance properties "within" a scenario (i.e., the conditional probability distributions given a scenario).

Furthermore, this realistic case demonstrates that investments in monitoring can pay out because there is a reasonable chance that the levee section under consideration can be proven to fulfil the target reliability. The main effects are the "ruling out" of scenarios and the considerable differences in monitoring versus retrofitting cost.

6.5. CONCLUSIONS

THIS chapter has demonstrated how pore pressure monitoring can be used for reliability updating and how decisions on monitoring investments can be supported by pre-posterior analysis. First, the concept was illustrated for a simplified uplift model with an expert judgment damping factor. Subsequently, the method was elaborated for state-of-the-art uplift and piping models including system reliability aspects. In contrast to chapter 5, pore pressure measurements provide equality type of information, for which the method by Straub (2011) was applied in the reliability updating.

The following conclusions are based on the findings in this chapter:

1. Uplift, heave and piping reliability are very sensitive to pore pressure information, because the geohydrological conditions - the main drivers of these mechanisms - are usually highly uncertain. Both, the simplified example (6.2) as well as the application example (6.3 and 6.4) show that reliability updating based on monitoring can change the probability of failure up to orders of magnitude, depending on the degree of prior uncertainty.

2. It is important to realize that an observation is not only the pore pressure measurement itself but also the loading which triggered it, in this case the water level. That implies that measurement uncertainties of both the measured head and the water level need to be accounted for. The higher the measurement error, the weaker the information and the smaller the change in reliability.

3. As shown in the simplified example, only the variables affecting the observation are updated. The reliability updating method takes care of this inherently. On the other hand, the analyst himself needs to take care that only reducible uncertainties are updated. For example, the water level distribution needs to remain unaffected in posterior analysis. This implies that it needs to be modelled as a random process rather than most soil properties, which are usually treated as time-invariant random variables.

4. The posterior analysis method to deal with equality type of information presented by Straub (2011) has proven to be easy to implement and work very well with the Monte Carlo approach followed in this thesis. The only drawback with (crude) MCS is that high reliability together with rather unlikely observations lead to even more unlikely intersection terms (i.e., $P(failure \cap observation)$), which can lead to very high numbers of required realisations. In those situations, the use of more efficient techniques such as Subset Simulations is recommendable.

5. Observing the unexpected causes significant changes in posterior probability, where unexpected means unlikely based on prior uncertainties. Where the prior uncertainties include scenarios that lead to very different geohydrological responses, an observation is most likely unexpected for at least some of these scenarios, which can then be "ruled out". Similarly, the uncertainty in highly uncertain geohydrologically important parameters (within scenarios) can be reduced significantly as shown in 6.2.

6. Since in pre-posterior analysis we use prior probabilities as input, we actually expect to observe the expected. In fact, integrating out the uncertainties in the future posterior reliability leads to the prior reliability. However, the spread or distribution of the (pre-)posterior reliability can make a significant difference for the decision, because the consequences (here: cost) for each posterior reliability can vary considerably.

7. Since the difference between monitoring and retrofitting cost uses to be large (i.e., several order of magnitude), even a small chance of "success", which in this case is avoiding retrofitting or reducing its cost, can make monitoring very cost-effective.

7

SOUNDINGS

You pay for a site investigation, whether you have one or not.

Institution of Civil Engineers (1991)

Figure 7.1: CPT-cone

The most obvious form of reducing ground-related piping uncertainties is site investigation. Since stratification is very important, this chapter focuses on in-situ soundings (e.g., CPT, borings). The objective is to show how they can reduce uncertainties and how they can be planned cost-effectively. After an overview of the piping-relevant information provided by soundings in section 7.1, two types of investigation are addressed in detail. The first one is detection of anomalies (adverse geological details). An example addressing the potential existence of sand lenses in section 7.2 highlights the most important features in anomaly detection. Section 7.3 elaborates on uncertainties in the blanket thickness and the related location of potential entry or exit points as well as the seepage length. A fictitious but realistic example demonstrates how such these uncertainties can be reduced by using Kriging analysis and conditional random field simulation to update the reliability.

Some of the material in this chapter has been published in: Schweckendiek, T., Gelder, P.H.A.J.M. van & Calle, E.O.F. (2011). *On risk-based geotechnical site investigation of flood defenses.* In Faber, Koehler, & Nishijima (Eds.), Applications of Statistics and Probability in Civil Engineering (ICASP 11), Zurich, Switzerland.

Contents

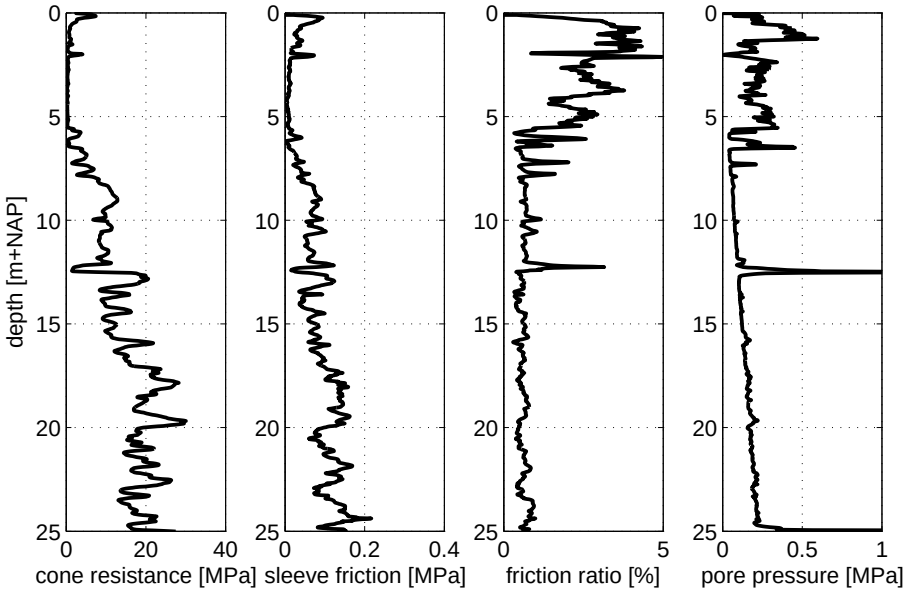

Figure 7.2: Typical CPT-data from the Dutch riverine area indicating a low-permeability blanket overlying an aquifer (sand).

7.1. INFORMATION PROVIDED BY SOUNDINGS

THIS section gives a brief overview of the information provided by CPTs (see Figure 7.2) and borings which can be used for inference of piping-relevant properties, the most important of which is certainly the stratification.

7.1.1. STRATIFICATION

The most important and straightforward information to obtain from soundings with respect to piping is the mapping of aquitards (low permeability) and aquifers (high-permeability).

INFERENCE OF STRATIFICATION FROM CPT

There are various methods in the literature which allow the identification and delineation of geological deposits, at least in terms of the main types of soft soils, i.e. sand, clay and peat, based on tip resistance, sleeve friction and/or pore pressures. An extensive overview is provided by Fellenius and Eslami (2000); Figure 7.3 shows an example of a widely-used CPT interpretation or profiling chart by Robertson (1990).

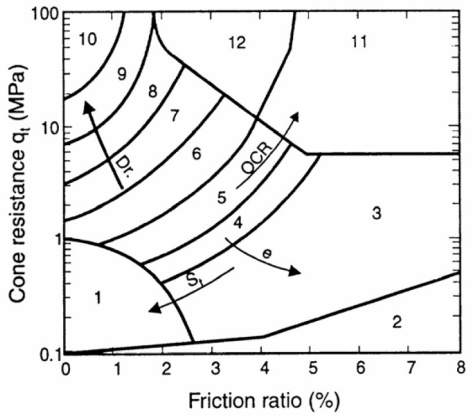

Zone	Soil Behavior Type
1	Sensitive fine grained
2	Organic material
3	Clay
4	Silty clay to clay
5	Clayey silt to silty clay
6	Sandy silt to clayey silt
7	Silty sand to sandy silt
8	Sand to silty sand
9	Sand
10	Gravelly sand to sand
11	Very stiff fine grained*
12	Sand to clayey sand*

*Overconsolidated or cemented

Figure 7.3: CPT profiling chart per Robertson (1990) based on cone resistance and friction ratio

The method most commonly used in the Netherlands is the one described in CUR (1992), which in essence boils down to that cone resistance values above roughly 2 MPa are interpreted as sand, while for lower values the distinction between clay and peat is made based on the friction ratio (i.e. low values indicate clay whereas high values indicate peat or organic material).

GEOMETRY OF STRATA BOUNDARIES

Being able to identify or at least distinguish soil deposits based on CPTs or bore logs, we also have information on the boundaries between those geological units, at least at the location of the sounding (i.e., along a vertical line). In order to infer 2D or 3D geometrical models of the subsurface, we need to interpolate between the exploration points in some way. Ideally, (engineering) geologists are involved in order to introduce (local) geological knowledge in the interpolation as much as possible.

Where either the available data or expert knowledge allow for a spatial statistical characterization, techniques such as Kriging (e.g., Krige, 1951; Cressie, 1990) or random field simulation (Vanmarcke, 1983) can be used for estimation, reliability analysis or decision support. As we have seen so far, in terms of subsurface geometry, the most influential uncertain variable is the thickness of the blanket layer. Sections 7.4 and 7.5 will provide the theory and an exemplary case respectively on how such techniques can be used for uncertainty reduction and reliability updating using CPT-data, as well as how decision analysis can be used in site investigation planning, for example by optimizing sampling grids.

DETECTION OF ANOMALIES

Anomalies, also called adverse geological details, are a special case of the identification and localization as described above because of their local nature in an otherwise predominantly horizontally layered environment. As pointed out in section 3.3.3, the most important type of anomaly for piping is a sand lens, usually an old river channel, which

causes thin, weak spots in the cohesive blankets or even shortens the length of the seepage path. In section 7.2 we will see how anomaly detection problems can be approached by means of pre-posterior analysis.

7.1.2. SOIL PROPERTIES

The piping-relevant soil properties in terms of the models described in chapter 3 are:

- γ_{sat} [kN/m^3]: saturated volumetric weight of the blanket layer
- d_{70} [m]: 70%-fractile of the grain size distribution of the piping-sensitive layer
- k [m/s]: specific conductivity of the aquifer
- k_h [m/s]: specific conductivity of the hinterland blanket

While most of these properties can be analyzed using laboratory testing on samples obtained by borings, the correlations of CPT data with these properties are highly uncertain. For the properties of interest, the only parameter which can reasonably be inferred from CPT is permeability (e.g., Robertson, 2010), even though we need to bear in mind that the corresponding techniques are suitable to estimate permeability rather locally, while for piping we would need the representative value for a larger volume. Of course, one may infer parameters indirectly, by combining local geological knowledge with CPT logs in order to identify the stratification first (e.g., Cetin and Ozan, 2009) and assign values to the respective units or strata based on local or regional experience.

7.1.3. SUMMARY

Since we expect most impact from incorporating information on the blanket thickness, the seepage length and the related anomaly issues, the remainder of this chapter will focus on stratification-related uncertainties rather than on updating of soil properties, the inference of which from in-situ soundings is highly uncertain.

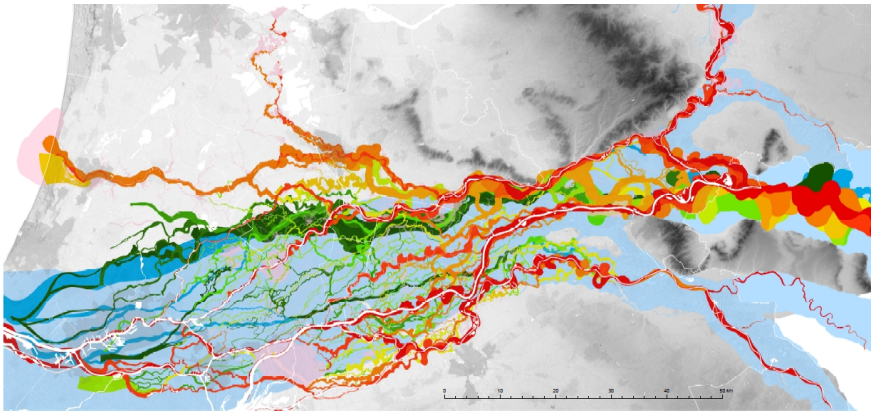

Figure 7.4: Overview of sand channels in the Dutch Rhine-Meuse delta. The warmer colors indicate younger deposits. Source: Universiteit Utrecht, Dept. Fysische Geografie, K.M. Cohen & E. Stouthamer, 2012.

7.2. DETECTION OF SAND LENSES

As pointed out in 3.4, adverse geological details such as shallow sand lenses or channels (Figure 7.4) can dominate the probability of failure. Both the conditional probability of failure as well as the probability of their presence have an influence on the relative importance of such phenomena in piping reliability. Both can be influenced by site investigation.

The following example addresses the detection of adverse geological details or, in fact, the updating of the probability of their existence. The example is simplified for the sake of illustrating the basic concepts and features in reliability updating for this kind of problem. The goal is to determine the optimal sounding interval using pre-posterior analysis and to decide whether investing in (additional) soundings is sensible at all.

7.2.1. EXAMPLE DESCRIPTION AND PARAMETERS

Figure 7.5 illustrates the hypothetical conditions in this example: subfigure a) represents the ground profile interpreted from site investigation where a blanket layer is (continuously) present in the levee section under consideration while subfigure b) shows a situation where a shallow sand lens cuts through the blanket. The latter is a weak spot for piping. We consider a levee reach of 1 km length, suppose that the conditional annual probabilities of failure for that reach are $P(F|\bar{A}) = 10^{-5}$ and $P(F|A) = 10^{-1}$, where A (anomaly) stands for the stratification scenario with sand lens and $\bar{A}$ for its complement, the stratification without sand lens.

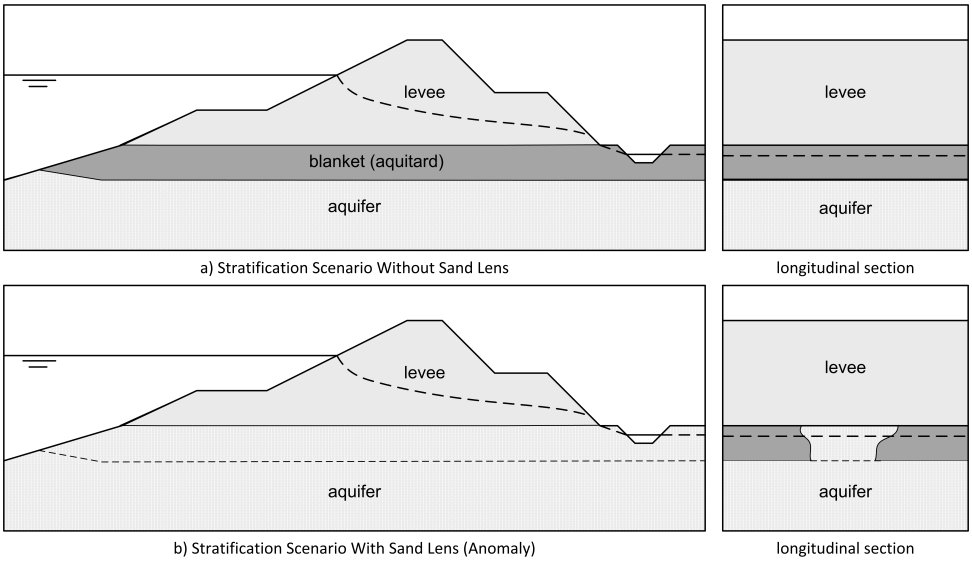

Figure 7.5: Anomaly detection example - possible ground profiles for a piping assessment

Suppose that the target annual probability of failure is $p_T = 10^{-3}$ so that dike would be safe without sand lens ($\bar{A}$) and unsafe with it (A). The probability of such an anomaly in the given reach is estimated (e.g., by engineering geologists) to be $P(A) = 0.1$, which implies that the current situation is considered unsafe, since

$$P(F) = P(F|\bar{A})P(\bar{A}) + P(F|A)P(A) \approx 10^{-2} > p_T = 10^{-3} \tag{7.1}$$

We consider two options to improve piping safety: site investigation with soundings to detect potential sand lenses or building a berm which would provide sufficient safety regardless of the presence of a sand lens. Figure 7.6 illustrates the considered decision problem:

1. *Do Nothing*: As discussed, doing nothing is not acceptable, as the current (prior) reliability does not meet the target.
2. *Retrofitting*: Reinforcing the dike by building a berm in order to make it safe regardless of the presence of sand lenses would cost $C_{berm} = 500$ k€. For the sake of illustration, we assume that the berm is built over the entire length.
3. *Site Investigation*: The cost of doing site investigation by means of soundings with an interval d_s [m] would be $C_{CPT} = 1000/d_s$ [k€] (supposing the cost of one CPT to be 1 k€). The cost of this decision option depends on the outcome:
   - *No Detection* ($\bar{D}$): If no sand lens is detected, there is only the site investigation cost;
   - *Detection* (D): If a sand lens is detected, the total cost will be the cost of site investigation plus the cost of the berm.

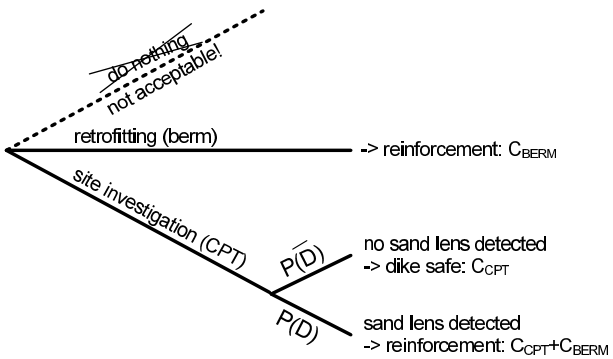

Figure 7.6: Anomaly detection example - decision tree

The potentially present sand lens is characterized by a detectable[1] width B with mean value $\mu_B = 50$ m and standard deviation $\sigma_B = 15$ m (i.e., $V_B = 30\%$). We neglect the possibility of several sand lenses being present in the reach.

[1] Notice that sand lenses like old river channels can cross the levee in any direction, not only perpendicular. That means the the detectable width may be greater than the actual width of the lens or channel.

Based on the information provided, the following issues will be discussed in the remainder of this section:

1. How can the probability of the stratification scenarios be influenced by posterior analysis using the outcomes of soundings (i.e., $P(A|\bar{D})$)?

2. What is the optimal sounding interval d_s?

3. What are the expected costs of the two decision options (site investigation versus retrofitting)?

7.2.2. PROBABILITY OF DETECTION (POD)

For the posterior analysis we need to assess the updated probability of an anomaly, given no sand lens is detected[2], which is given by Bayes' rule: $P(A|\bar{D}) \propto P(\bar{D}|A)P(A)$. That means that we need to assess the probability of missing a sand lens $P(\bar{D}|A)$ or its complement, the probability of detection $P(D|A)$, commonly abbreviated as PoD.

Figure 7.7 illustrates our geometrically motivated probabilistic detection model, in which the PoD is the probability that the sum of the distance to the closest sounding a [m] (on the left) and the lens width B [m] exceed the inter-sounding distance d_s [m]:

$$P(D|A) = P(a + B > d_s) \tag{7.2}$$

In the absence of information on the location of a sand lens relative to the closest sound-

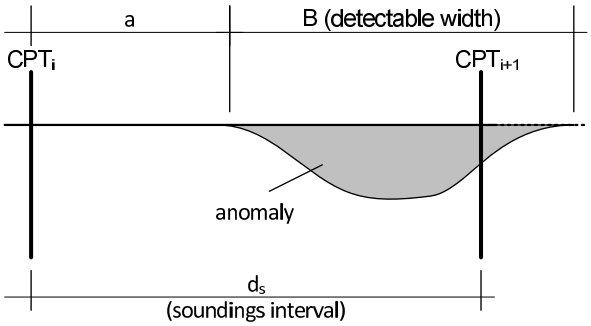

Figure 7.7: Anomaly detection example - definitions for the probability of detection (PoD)

[2] Notice that we assume perfect accuracy for detecting sand lenses with the soundings, i.e. no false positives nor false negatives, which implies that the probability of an anomaly in case of detection equals one.

ing, the PDF of a is uniform between 0 and d_s (i.e., $f_a(\xi) = 1/d_s$) and the PoD becomes

$$P(D|A) = \begin{cases} 1 & B > d_s \\ B/d_s & B \leq d_s \end{cases} \tag{7.3}$$

$$= P(B > d_s) + \int_0^{d_s} \frac{\xi}{d_s} f_B(\xi) d\xi \tag{7.4}$$

$$= 1 - F_B(d_s) + \int_0^{d_s} \frac{\xi}{d_s} f_B(\xi) d\xi \tag{7.5}$$

where $f_B(\xi)$ is the PDF of the detectable width B. Consequently, the probability of missing the sand lens is

$$P(\bar{D}|A) = 1 - P(D|A) = F_B(d_s) - \int_0^{d_s} \frac{\xi}{d_s} f_B(\xi) d\xi \tag{7.6}$$

Figure 7.8 shows how the probability of missing a potentially present sand lens decreases with decreasing sounding interval d_s for different types of probability distributions (see analytical derivations in appendix I) attributed to the detectable width B. The Normal distribution exhibits some unrealistic behaviour for very small distances, which is avoided by choosing a distribution that have zero probability below zero distance like Truncated Normal or Lognormal. The remainder of the example will work with a Lognormal distribution, since that seems the most realistic choice (i.e., non-negative and small probabilities for short intervals).

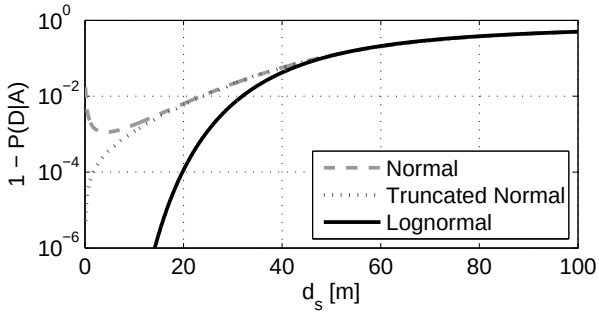

Figure 7.8: Probability of missing a sand lens with width B ($\mu_B = 50$m, $\sigma_B = 15$m]) as function of the sounding interval d_s for different PDF assumptions of B.

7.2.3. POSTERIOR ANOMALY PROBABILITY

The change of the probability of failure as a function of the soil investigation outcome can be considered by using the updated scenario probability of a sand lens (given no detection) in Bayes' rule:

$$P(A|\bar{D}) = \frac{P(\bar{D}|A)P(A)}{P(\bar{D})} \tag{7.7}$$

where $P(\bar{D})$ is the (prior) probability of the observation (i.e, of not detecting any sand lens),which itself can be determined using the law of total probability:

$$P(\bar{D}) = P(\bar{D}|A)P(A) + P(\bar{D}|\bar{A})P(\bar{A}) = P(\bar{D}|A)P(A) + P(\bar{A}) \tag{7.8}$$

Notice that $P(\bar{D}|\bar{A}) = 1$,since where there is no sand lens none will be detected. Thus, the posterior probability of a sand lens only depends on the probability of detection $P(D|A)$ and on the prior $P(A)$. Figure 7.9 shows that the updated probability of a sand lens ($P(A|\bar{D})$) drops with increasing investigation density (i.e., decreasing d_s). The decrease in probability becomes very noticeable for $d_s < \mu_B$. For $d_s = 100$m, a value often used in site investigations for Dutch levees, the probability of a sand lens with the assumed dimensions would be hardly affected.

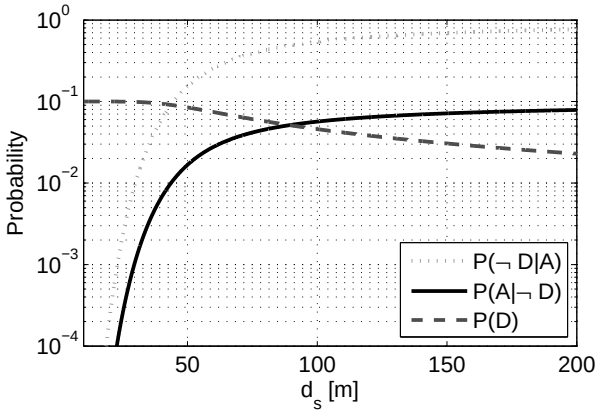

Figure 7.9: Anomaly detection example - posterior probability of non-detection (given an anomaly), of a sand lens (width $B \sim LN(50,15)$) and of detection as functions of the sounding interval (¬ in the legend is the negation sign)

7.2.4. POSTERIOR PROBABILITY OF FAILURE

The probability of failure, our actual quantity of interest, strongly depends on the probability of a sand lens as equation 7.9 illustrates.

$$P(F) = P(F|A)P(A) + P(F|\bar{A})P(\bar{A}) \tag{7.9}$$

where $P(A)$ is either the prior probability of a sand lens for a prior assessment or $P(A|\bar{D})$ for a posterior assessment in case nothing is detected (and $P(\bar{A})$ similarly). Opting for

site investigation only makes sense if the probability of failure can drop below the target value p_T, which implies:

$$P(F|\bar{D}) < p_T \quad \Leftrightarrow P(A|\bar{D}) < \frac{p_T - P(F|\bar{A})}{P(F|A) - P(F|\bar{A})} \tag{7.10}$$

Planning a site investigation unable to meet the requirement stated in Eq. 7.10 is not sensible, because retrofitting would be needed even though no anomaly is detected. For the present example, the requirement is $P(A|\bar{D}) < 9.9 \cdot 10^{-3}$ (annual probability). If the probability of failure without anomaly is very small (i.e., $P(F|\bar{A} \ll p_T)$, the required $P(A|\bar{D})$ approaches the ratio $p_T / P(F|A)$.

The continuous black line in Figure 7.10 represents the posterior probability of failure conditional on non-detection $P(F|\bar{D})$ (in the figure denoted as $P(F|\neg D)$). At a sounding interval of $d_s \approx 44m$ $P(F|\bar{D})$ drops below the target value, which represents the minimum site investigation density, or the maximum inter-sounding distance. At the same distance of $d_s = 44$m, the posterior probability of an anomaly is approximately $P(A|\bar{D}) \approx 10^{-2}$, which corresponds with equation 7.10.

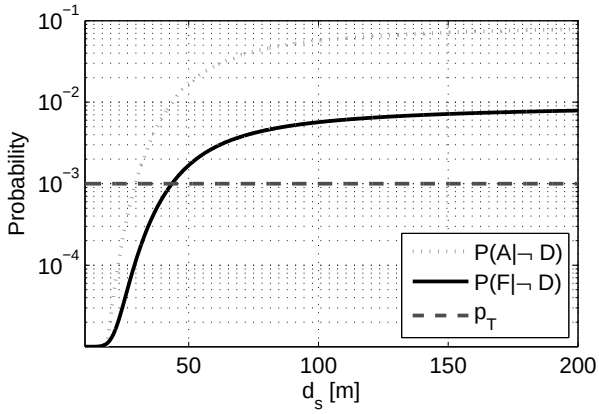

Figure 7.10: Anomaly detection example - updated probability of failure as a function of the sounding interval (anomaly width $B \sim LN(50,15)$; ¬ in the legend is the negation sign)

7.2.5. EXPECTED COSTS

From the previous section (7.2.4) we know what our maximum sounding interval is and by simple reasoning we can conclude that the same interval will also be the optimum value. Working with $d_s \approx 44$m and not finding an anomaly will already lead to meeting the target reliability, higher sampling density will only lead to higher site investigation cost but cannot lower the retrofitting cost any further[3].

[3]The independence of the retrofitting cost of the site investigation density is a simplifying assumption in this example; in reality there may well be a dependence. Therefore the conclusion that there is a minimum site investigation density equal to the optimum cannot be generalized based on the present findings.

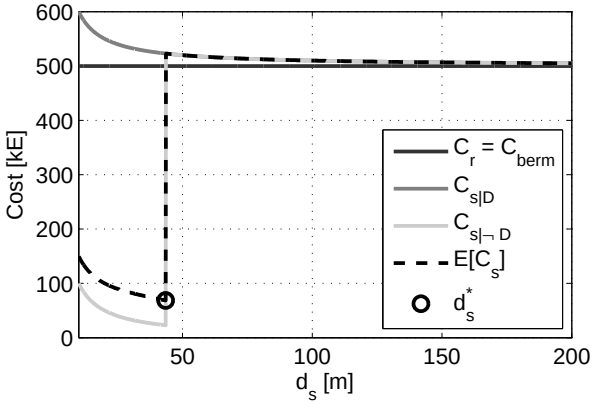

Figure 7.11: Anomaly detection example - costs as a function of the sounding interval (anomaly width $B \sim LN(50,15)$). The black and dark grey represent the cost of the berm and the cost of the berm plus soundings respectively. The light-grey line shows the total cost for the decision option site investigation (SI) provided no anomaly is detected. The dashed black line is the expected cost of the decision option SI including the probability of detection. The optimum is found at the lowest expected cost (black circle).

Though unnecessary for finding the optimal sounding interval d_s^*, it is instructive to investigate the conditional and expected cost for the considered decision options. The medium gray line in Figure 7.11 shows the conditional cost of the decision option to do site investigation for detecting an anomaly, which is the sum of the site investigation cost (C_{CPT}) and the retrofitting cost (C_{berm}). For non-detection the conditional cost of the site investigation option $C_{s|\bar{D}}$ is equal to the outcome with detection for values of d_s greater than 44m due to the reason discussed earlier. It drops, however to only the site investigation cost below 44m. The dashed black line shows the expected cost for choosing site investigation, thus including the probability of non-detection: $P(\bar{D})$ (i.e., the "probability of success"). Clearly, the minimum expected cost is confirmed to be at the optimum sounding interval of $d_s \approx 44$m.

For the sake of clarification, we approach the same problem also from a mathematical-analytical point of view. The expected cost of site investigation (see also the decision tree in Fig. 7.6) is given by:

$$E[C_s] = \begin{cases} C_{CPT}P(\bar{D}) + (C_{CPT} + C_{berm})P(D) = C_{CPT} + C_{berm}P(D) & d_s \leq d_s^* \\ C_{CPT} + C_{berm} & d_s > d_s^* \end{cases} \tag{7.11}$$

where

$$d_s^* = \arg\max_d \left[P(F|\bar{D}) < p_T\right] \tag{7.12}$$

For $d_s \leq d_s^*$, the probability of non-detection is the probability of success. Also note that both, C_{CPT} and $P(D)$ depend on d_s, $P(D)$ being defined by:

$$P(D) = P(D|A)P(A) + P(D|\bar{A})P(\bar{A}) = P(D|A)P(A) \tag{7.13}$$

The optimum CPT-distance is found to be $d_s^* \approx 44m$, for which the expected cost is $E[C_s](d_s^*) \approx 450$ k€. As the expected cost of site investigation is lower than the cost of retrofitting, a risk-neutral decision maker would prefer to "take his chances" with site investigation over the "safe" option of retrofitting right away.

7.2.6. BENEFIT-COST RATIO (BCR)

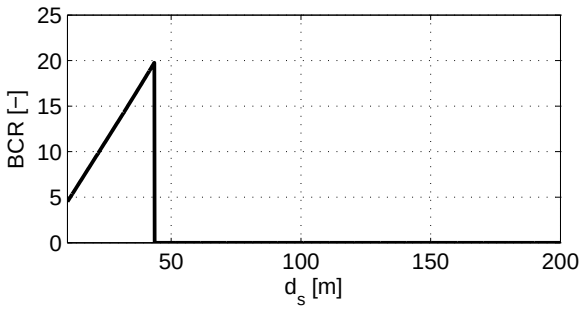

Figure 7.12: Anomaly detection example - benefit-cost ratio (BCR) as a function of the sounding interval (anomaly width $B \sim LN(50,15)$)

Benefit-cost ratios (BCR) are an alternative way to express the cost-effectiveness of investments. In order to estimate BCRs, we need to define what we consider as costs and benefits, which is rather arbitrary. Considering site investigation as the investment, hence cost, the benefit would be the avoided unnecessary retrofitting cost. Using this approach, the present values of the benefits (PVB) and the costs (PVC) and their ratio for doing site investigation can be defined as:

$$BCR = \frac{PVB}{PVC} = \frac{P(\bar{D})C_r}{C_s} \tag{7.14}$$

where PV stands for "present value", even though in this example discounting is assumed negligible, because both benefits and costs would be realised practically immediately. While the cost in this definition is certain, the benefit is uncertain and depends on the outcome of the soundings. Figure 7.12 shows the BCR as function of the sounding interval, which assumes its maximum value of $BCR = 19.8$ at the previously determined optimum d_s^*.

7.2.7. OPTIMAL SITE INVESTIGATION DENSITY

Considering the insights hitherto regarding the minimal and, at the same time, optimal site investigation density, for the assumptions in this example a shorter and more elegant way to determine the optimal distance d_s^* is the following inverse reasoning:

1. Determine the maximum acceptable posterior probability of a sand lens (given no detection):
$$P_{A|\bar{D},T} = \frac{p_T - P(F|\bar{A})}{P(F|A) - P(F|\bar{A})} \tag{7.15}$$
where $P(F|\bar{A}) < P_{A|\bar{D},T} < P(F|A)$.

2. The maximum acceptable probability of missing a sand lens is then given by:
$$P_{\bar{D}|A,T} = \frac{P_{A|\bar{D},T}P(\bar{D})}{P(A)} = \frac{P_{A|\bar{D},T}\left(P(\bar{D}|A)P(A) + P(\bar{A})\right)}{P(A)} \tag{7.16}$$

3. Combining Eqs. 7.6 and 7.16 it follows that d_s^* is the maximum d_s satisfying the constraint:
$$P_{A|\bar{D},T} = \frac{P(A)\int_0^{d_s} \frac{d_s-\xi}{d_s} f_B(\xi)\,d\xi}{P(\bar{A}) + P(A)\int_0^{d_s} \frac{d_s-\xi}{d_s} f_B(\xi)\,d\xi} \tag{7.17}$$

This demonstrates that under specific conditions an optimal site investigation density or scope can be found rather directly. The above derivation is in fact the elaboration of Equation 7.12.

7.2.8. SENSITIVITY ANALYSIS

The optimal distance d_s^* and the corresponding (minimum) expected cost depend on the prior probability $P(A)$. Since determining $P(A)$ necessarily involves subjectivity, it is interesting to examine the sensitivity of the results with respect to it. Figure 7.13 shows d_s^* as well as the conditional and expected cost of the decision option site investigation as functions of the prior $P(A)$. This illustrates that the whole decision problem becomes trivial, if $P(A) < P_{A|\bar{D},adm} \approx 0.009$, because, neither site investigation nor reinforcement are necessary. Furthermore, choosing site investigation is practically always the better choice, because its expected cost is lower than the cost of reinforcement. Only if we were quite sure from the beginning to encounter a sand lens ($P(A) \gtrsim 0.92$), immediate retrofitting is preferable from a cost-effectiveness point of view.

Of course, the results are also sensitive to the (probability distribution of the) anomaly width. The results cannot be generalized for any type and size of anomaly.

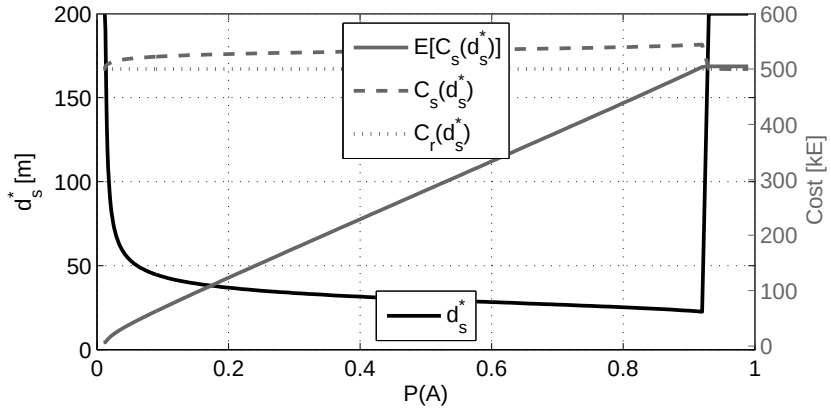

Figure 7.13: Dependence of the optimal CPT-distance and the expected costs on the prior probability of a sand lens (width $B \sim LN(50, 15)$)

7.2.9. DISCUSSION

This simplified fictitious example has demonstrated conceptually how soundings can be used for anomaly detection. The basic trade-off is that an investment in site investigation can lower the cost of retrofitting[4] with a certain chance of success. Using our prior beliefs, we can analyze the problem in a pre-posterior way to optimize the site investigation and to decide whether the investment is cost-effective at all.

It is important to realize that the probability of "false negatives", here the probability of non-detection given the presence of an anomaly $P(\bar{D}|A)$, drives the decision rather than the probability of "true positives", which would be the probability of detection $P(D|A)$. This is interesting because intuitively we tend to do our best to detect of phenomena rather than making sure they are really not there.

Even though the sampling density needs to be rather high in this example with the sounding distance close to the mean value of the anomaly width, the benefit-cost ratio is still high (almost twenty). Furthermore, the probability of "success" (i.e., non-detection) is almost 90%, which means that using soundings to confirm the likely outcome of the absence anomalies would be a sensible decision.

We conclude this example with a critical note. The simplifications in the assumptions have led to a paradoxical situation, namely that we would never choose to do more site investigation than strictly needed (d_s^*). Even if soundings were free of cost, the expected cost of the decision option site investigation increases with decreasing d_s. This is an artifact of working with admissible probabilities of failure. The benefits of risk reduction by a higher reliability than required by the norm are not quantified in this framework, which is a clear limitation leading to suboptimal decision compared to fully risk-based approaches.

[4] Notice that, while in the example the possibilities were full or zero retrofitting cost only, in real-world examples the cost may also be anything in between (or even higher than the a-priori retrofitting cost in case of unfavorable outcomes of the site investigation).

7.3. BLANKET THICKNESS AND SEEPAGE LENGTH

APART from adverse geological details and stratification scenarios addressing the geohydrology and the aquifer, the next most important uncertainty in piping to be reduced by soundings may be in the blanket thickness on the land-side of the levee, as this affects the location of potential exit points and the length of the seepage path. This section elaborates on modeling the blanket thickness as a two-dimensional random field and on reliability updating with additional soundings using Kriging and conditional simulation. While in the previous section rather simplistic assumptions were made for the probability of piping failure, this section develops a more realistic approach using the actual reliability models as discussed in chapter 3.

7.3.1. RANDOM FIELD MODELING OF THE BLANKET

The aim of this section is to show how uplift, heave and piping reliability can be modeled taking into account the spatial variability of a statistically homogeneous blanket layer (in terms of thickness). This will be demonstrated by a realistic but fictitious example; the modeling of the scale of fluctuation and the random fields is discussed below. The general theory on random field modeling in a geotechnical context has been extensively discussed in the literature (see e.g. Vanmarcke 1983; Fenton and Griffiths 2008) and is not repeated here; the sections below only provide the most important definitions and concepts to understand the example treated in sections 7.4 and 7.5.

Wide-sense Stationarity The horizontal 2D random field used to represent the spatial variability of the thickness of the blanket layer is assumed modeled as wide-sense stationary, implying that (a) the mean and variance of the field are constant and (b) that the correlation between two points is solely a function of their separation distance.

Isotropy in the horizontal plane Furthermore, the random field is assumed to be isotropic in the horizontal plane, which implies that the auto-correlation distance or scale of fluctuation is equal for all directions in the horizontal plane, i.e. it is invariant under rotation. In fact, isotropy implies wide-sense stationarity.

Gaussian Correlation Function We will apply the Gaussian autocorrelation function with lag τ [m] and correlation distance δ [m], $\rho(\tau) = \exp -(\tau/\delta)^2$, which seems to have several advantages for the envisaged application (Kanning, 2012). The correlation distance is not the same as the scale of fluctuation δ_0 (Vanmarcke, 1983), which for the Gaussian model would be: $\delta_0 = \delta\sqrt{\pi}$.

Given the modeling assumptions above, the covariance function of a random field of property d can be denoted as:

$$C_d[d(\mathbf{t}_1), d(\mathbf{t}_2)] = C_d(|\mathbf{t}_1 - \mathbf{t}_2|) = C_d(|\tau|) = \sigma_d^2 \rho_d(|\tau|) = \sigma_d^2 \exp -\left(\frac{\tau}{\delta}\right)^2 \tag{7.18}$$

where $\mathbf{t}_1$ and $\mathbf{t}_2$ are the respective two-dimensional coordinates of two points (i.e., $\mathbf{t}_i$ has components $t_{i,x}$ and $t_{i,y}$) and τ is the vector representing their difference. Kanning (2012) also showed that a correlation distance for the thickness of the blanket layer of

200m is a reasonable assumption for Dutch conditions. This value will be used for the fictitious examples.

7.3.2. SIMULATION AND UPDATING

The modeling of the thickness of the blanket layer as a two-dimensional random field will imply unconditional as well as conditional simulation along with kriging. This section provides a brief description of the applied techniques.

All figures showing plots of random fields in this section are top views of the blanket layer thickness from the levee toe landward as illustrated in Figure 7.14.

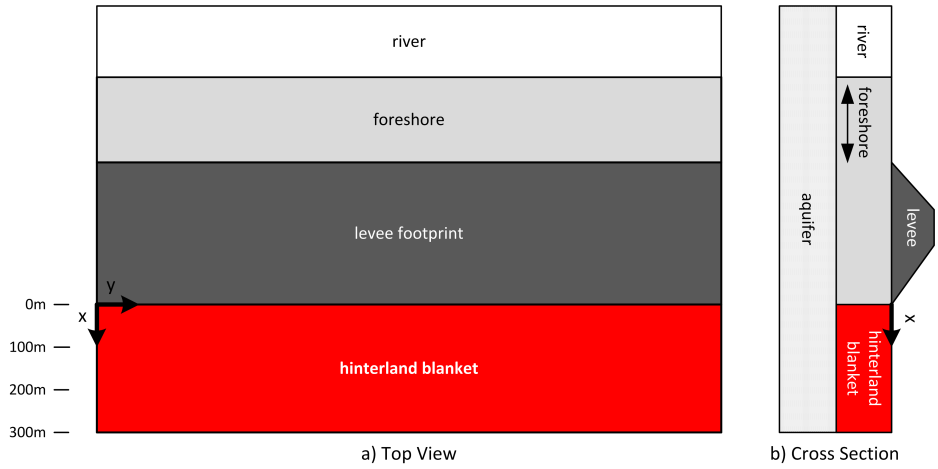

Figure 7.14: Position of the random field of the blanket thickness (red) with respect to the levee in (a) top view and (b) cross section.

UNCONDITIONAL SIMULATION

We speak of unconditional simulation when generating realisations of the random field solely based on the field parameters (i.e., mean, variance and correlation distance) without any local observations. The respective technique used in this thesis is Local Average Subdivision (LAS; Fenton 1990). Figure 7.15 shows an unconditional realisation of a random field with properties as described in section 7.3.1 above.

Unconditional simulation may be useful in reliability analysis, where no local prior information is available but the field parameters of interest can be estimated from regional data or expert elicitation. Where local data are available, geostatistical techniques like Kriging or conditional simulation are more appropriate.

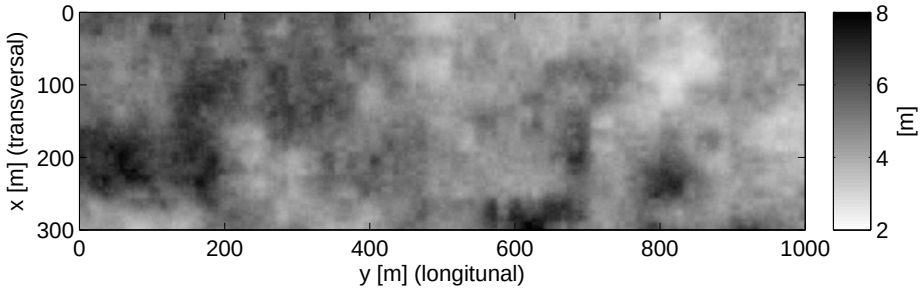

Figure 7.15: Unconditional Realisation of a Random Field with Mean μ =5.0m, Standard Deviation σ =1.0m and Correlation Distance δ =200m (Top View, Levee Toe at $y = 0$m)

KRIGING

Kriging is a BLUE (Best Linear Unbiased Estimator) which allows us to estimate a property at an arbitrary location based on observations of the same property at other locations in a statistically homogeneous field with known or estimated field parameters. The estimate and variance for Simple Kriging for our quantity of interest, the thickness of the blanket layer, are given by:

$$\hat{d}(\mathbf{x}) = \mu_d + \sum_i \lambda_i \left(d(\mathbf{x}_i) - \mu_d\right) \tag{7.19}$$

$$Var[\hat{d}(\mathbf{x}) - d(\mathbf{x})] = \sigma_d^2 - \sum_i \lambda_i C_d(\mathbf{x}_i - \mathbf{x}) \tag{7.20}$$

where $\mathbf{x}_i$ ($i = 1...n$ are the locations of known property values, C_d is the covariance function and λ_i are the Kriging weights (i.e., Lagrange multipliers) obtained by solving the so-called Kriging System:

$$\sum_j \lambda_j C_d(\mathbf{x}_i - \mathbf{x_j}) = C_d((\mathbf{x}_i - \mathbf{x}) \tag{7.21}$$

In the examples and cases in this thesis we will use Simple Kriging (when the field mean is assumed to be known) and Ordinary Kriging (when the field mean is assumed to be unknown). For descriptions of Kriging techniques the reader is referred to the literature (e.g., Journel and Huijbregts, 1978).

In order to illustrate spatial estimation with Kriging, suppose the field in Figure 7.15 is the true field and we have measurements from a regular grid every 50m (in both directions). Figure 7.16 illustrates that the kriged field looks similar to the supposed true field only less variable, as it represents the best estimate not the spatial variability.

Kriging is computationally relatively inexpensive, however, it is commonly applied to so-called "point processes". Where the function to be estimated depends not only on the value of a property locally but also on its values elsewhere), the use of Kriging is not straightforward (sometimes impossible) but instead we can apply conditional simulation in order to simulate random fields yet using the available data (e.g., from measurements).

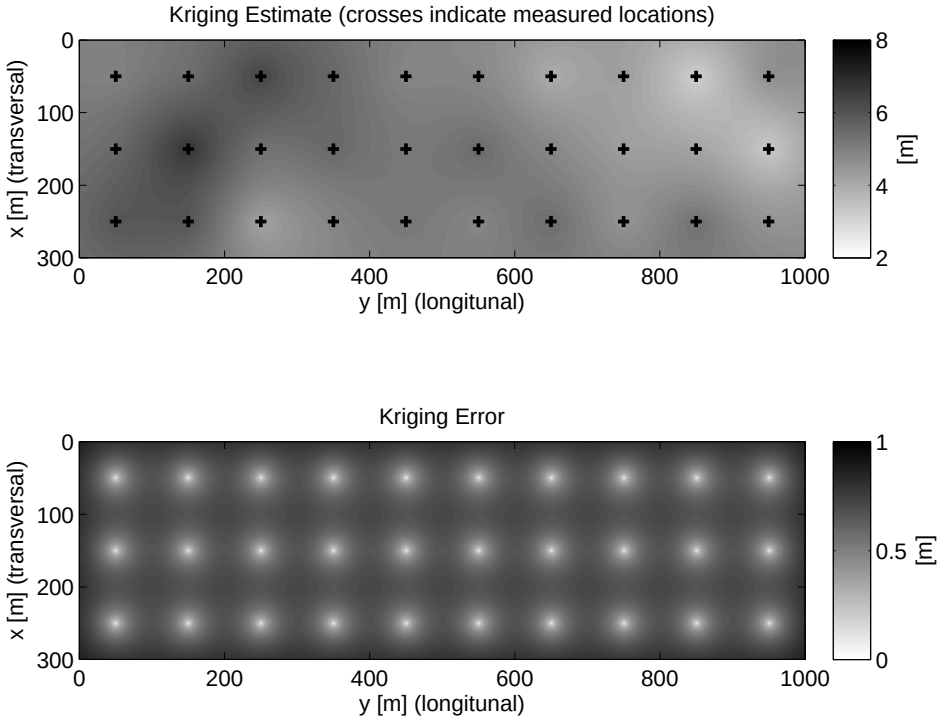

Figure 7.16: Illustration Kriging estimate and error assuming the field in figure 7.15 as true and the properties to be known at the indicated locations (top view, levee toe at $x = 0$m)

CONDITIONAL SIMULATION

For processes which depend not just on the property at one point in the field (so-called "point processes") we may use conditional simulation (see Appendix J) to condition the simulations on the measurements such that each still has the appropriate characteristics in terms of variability and correlation structure as illustrated in Figure 7.17 for two dimensions. Notice that the average of a large number of conditional realizations converges to the Kriging estimate.

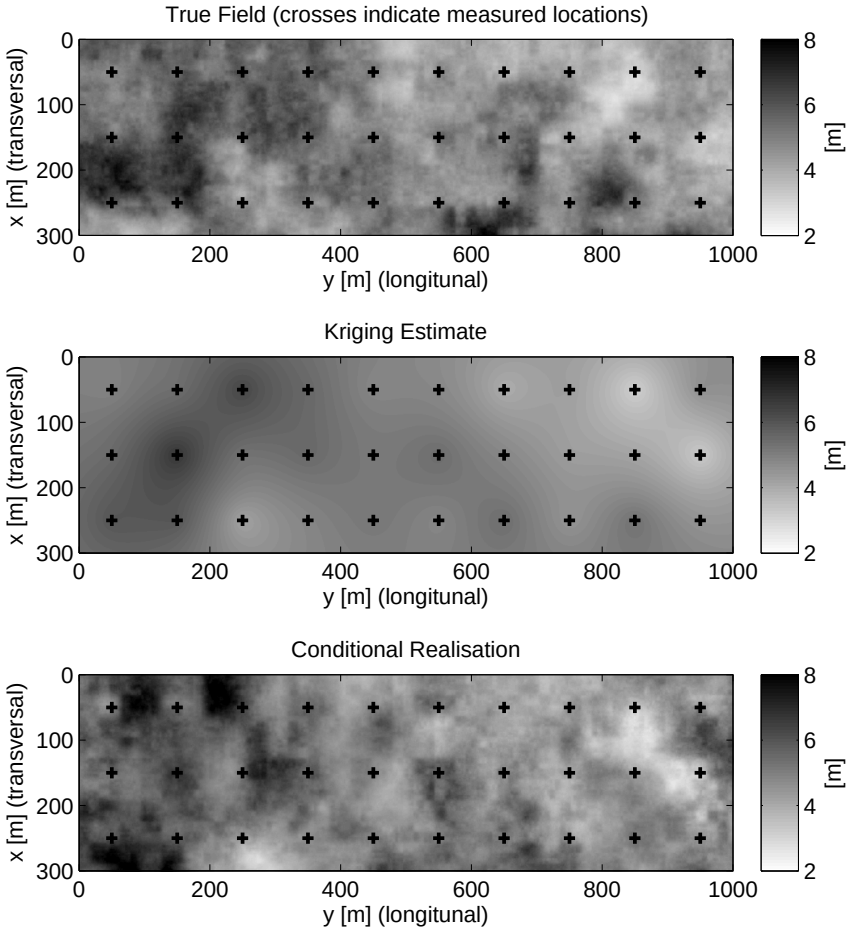

Figure 7.17: Example conditional simulation, from top to bottom: (a) unconditional realisation, (b) Kriging estimate, (c) conditional realisation (top view, levee toe at $y = 0$m)

7.3.3. CRITICAL SEEPAGE LENGTH

In order to work with the Sellmeijer model for piping (see 3.2.4) when we do not work with cross sections representative for a levee reach but model the blanket explictly as a 2D-random field, we need to choose an operational definition for the seepage length:

> The seepage length L [m] is the distance between an entry and an exit point in the considered reach[5].

This definition will be used in a deterministic setting, namely in (conditional) random field realizations of the blanket (thickness), where the potential entry or exit points are either the foreshore or hinterland boundaries or blanket defects caused by uplift as illustrated in Figure 7.18.

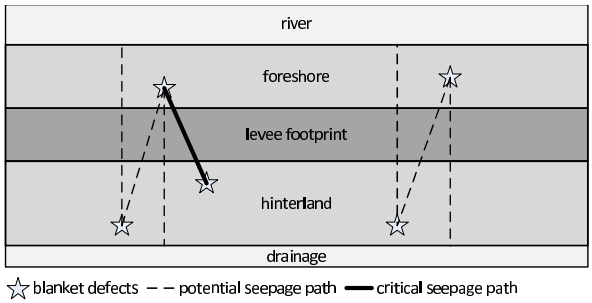

Figure 7.18: Illustration of the critical seepage path between the closest entry and exit points (top view)

There are 4 relevant situations to be distinguished:

1: No defect in foreshore or hinterland blanket The seepage length is the distance between the river and the far boundary of the hinterland.

2: Defect in foreshore, but not in hinterland blanket The seepage length is the distance between the defect in the foreshore blanket and the far boundary of the hinterland.

3: No defect in foreshore, but in the hinterland blanket The seepage length is the distance between the river and the defect in the hinterland blanket.

4: Defect in foreshore and hinterland blanket The seepage length is the distance between defects in the foreshore and hinterland blanket.

In the illustrations in the remainder of this chapter we will assume an intact foreshore (i.e., no defects leading to hydraulic contact) and potential defects by rupturing of the hinterland blanket due to uplift, which implies that we either deal with situation 1 or 3.

[5] Notice that this definition does not entirely match the original assumptions of the Sellmeijer model, which works in a vertical plane and assumes homogeneous conditions in the longitudinal direction of the levee. Nevertheless, this model is used in this chapter for the sake of illustration in order to be consistent with the other applications in this thesis. As for all applications in this thesis, the same concepts and techniques as presented are also applicable to other or more sophisticated models such as internal erosion models implemented in numerical analysis environments.

The seepage length L and the (local) blanket thickness d will be evaluated with the Sellmeijer model for all potential seepage paths to evaluate the potential for piping. The critical seepage path is defined as the one with the lowest performance function value, which does not necessarily coincide with the shortest seepage path (both L and d influence the performance function).

7.4. EXAMPLE UPLIFT

THIS section discusses a fictitious case which investigates the effect of soundings on the reliability with respect to uplift heave and piping, applying the theory presented hitherto. While this section will focus on uplift, section 7.5 will include piping as well. This allows us to illustrate some specific aspects of working with just one local mechanism (i.e., point process) first, before scaling up to the full mechanism and highlighting other features for that situation.

7.4.1. EXAMPLE DESCRIPTION AND PARAMETERS

We consider a fictitious levee reach of length 1km assuming all variables to be uniform in space (see Table 7.1) except the blanket thickness, which is modeled as a stationary random field with correlation length $\delta = 200$m. For the sake of illustration, the assumed true but unknown field of the blanket thickness is shown in Figure 7.22. As in previous chapters, the limit state functions and groundwater flow model are the ones described in section 3.2.

Designation	**Symbol**	**Unit**	**Type**	**Mean** (Par1)	**Std** (Par2)
aquifer thickness	D	[m]	Lognormal	20.0	2.0
hydraulic conductivity	k	[m/s]	Lognormal	$1.0E-4$	$5.0E-5$
grain size	d_{70}	[m]	Lognormal	$2.0E-4$	$3.0E-5$
bedding angle	θ	[deg]	Deterministic	37	
water level	h	[m]	Gumbel	$a_h = 4.0$	$b_h = 3.0$
landside phreatic level	h_p	[m]	Gaussian	1.0	0.1
blanket thickness	d^*	[m]	Lognormal	6.0	0.5
foreshore width	L_f	[m]	Lognormal	30.0	3.0
levee footprint	B	[m]	Deterministic	50.0	
hinterland width	L_h	[m]	Deterministic	$1.0E+4$	
blanket permeability	k_h	[m/s]	Lognormal	$5.0E-7$	$5.0E-7$
sat. vol. weight blanket	γ_{sat}	[kN/m^3]	Gaussian	18.0	1.0

* *The correlation length of the blanket thickness d, the only parameter treated as a random field, is $\delta = 200$.*

Table 7.1: Soundings example: input parameters for uplift, heave and piping.

Though technically straightforward, we do not consider stratification scenarios as in earlier instances, as the focus is on the influence of soundings on the blanket thickness (estimate). Notice that not all parameters are necessary when only uplift is considered, but they will be used for the extension of the problem to heave and piping in section 7.5.

Starting point for the example is that the field parameters (i.e., statistics) of the blanket thickness are assumed to be known (e.g., by expert judgment), but no local information is available.

7.4.2. PRIOR RELIABILITY

In the current example contemplating uplift only, we consider all random variables to be homogeneous (i.e., fully correlated in space) except the blanket thickness, which is modeled as a two-dimensional stationary random field. We may reformulate the limit state function such that we compare the actual blanket thickness d [m] (resistance) with the critical blanket thickness $d_{c,u}$ [m], which contains all random variables except d. To this end, we equate the Eq. 3.5 to zero and solve for d:

$$d_{c,u} = \frac{m_\phi(\phi(x_{exit}) - h_p)}{m_u(\gamma_{sat}/\gamma_w - 1)} \tag{7.22}$$

Assuming both d and $d_{c,u}$ are lognormal-distributed, the local uplift reliability per grid cell can be determined using the following analytical approach:

$$\beta_u = \frac{\lambda_d - \lambda_{d_c}}{\sqrt{\zeta_d^2 + \zeta_{d_c}^2}} \tag{7.23}$$

where β_u is the uplift reliability index, λ_d, ζ_d^2, λ_{d_c} and $\zeta_{d_c}^2$ are the mean and standard deviations of the exponents of the actual and the critical blanket thickness respectively (i.e, the lognormal-transformated parameters).

Figure 7.19 shows how a-priori the mean blanket thickness is constant, while the mean critical thickness (the equivalent load variable) decreases with increasing distance from the toe. Consistently, the resulting reliability index increases with increasing distance from the toe, that is the probability of uplift decreases.

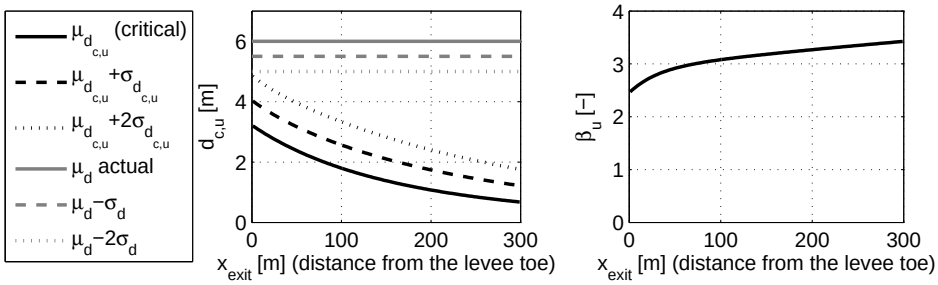

Figure 7.19: Soundings example: critical versus actual blanket thickness as function of the distance from the levee toe (left) and prior annual reliability index for uplift assuming the load to be homogeneous in longitudinal direction (right).

Notice that in the absence of additional information the statistics of the critical and actual blanket thickness as well as the prior uplift reliability are constant in the longitudinal direction of the levee.

7.4.3. POSTERIOR RELIABILITY

This section illustrates the effect of additional soundings on our estimate of d locally. Figure 7.21 illustrates how the Kriging estimate resembles the true field more and more as we increase the site investigation density.

Since we are ultimately interested in not only the best estimate of d, we can use the same approach as in the previous section to obtain the local reliability by first-order approximation (see Eq. 7.23), using Kriging estimate and variance for the probability distribution of d. Figure 7.22 shows how Kriging based on a CPT-distance of 100m influences the reliability with respect to uplift. Subfigure d) clearly depicts that by updating the uplift reliability can increase as well as decrease locally. In essence, uncertainty is replaced by "known" strong and weak spots (see subfigure a)). The effect of updating is more pronounced close to the levee toe than far away from it, or in other words, the effect is greater in the regions of an a-priori relatively high probability of failure. Similarly, Figure 7.20 shows that the longitudinally averaged annual posterior reliability index does not move away significantly from the prior.

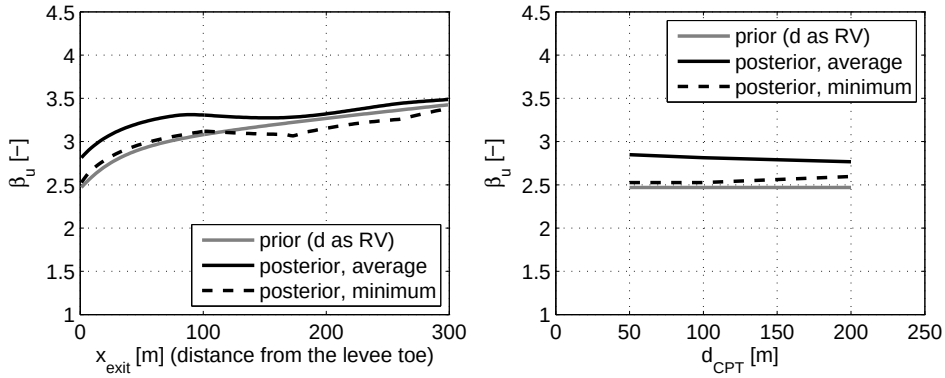

Figure 7.20: Soundings example: prior and posterior annual uplift reliability index obtained by Kriging based on regular grids. Left: as function of the distance to the levee toe for a CPT-distance of 100m, right: as function of the CPT-distance at the levee toe. The continuous line shows the average in longitudinal direction, the dashed line shows the minima.

The dashed lines in Figure 7.20 highlight another issue so far neglected in this thesis by working with so-called representative values for the whole levee reach for each random variable - the effect of spatial variability on the probability of failure. The dashed lines show the minima of the posterior reliability indices in longitudinal direction. The minima are what we actually need to consider, when analysing the reliability of a levee section, as failure will occur at the weakest spots. For the example at hand, the result is that the update of the mean, which decreases in some locations, has more impact than the reduction of the variance.

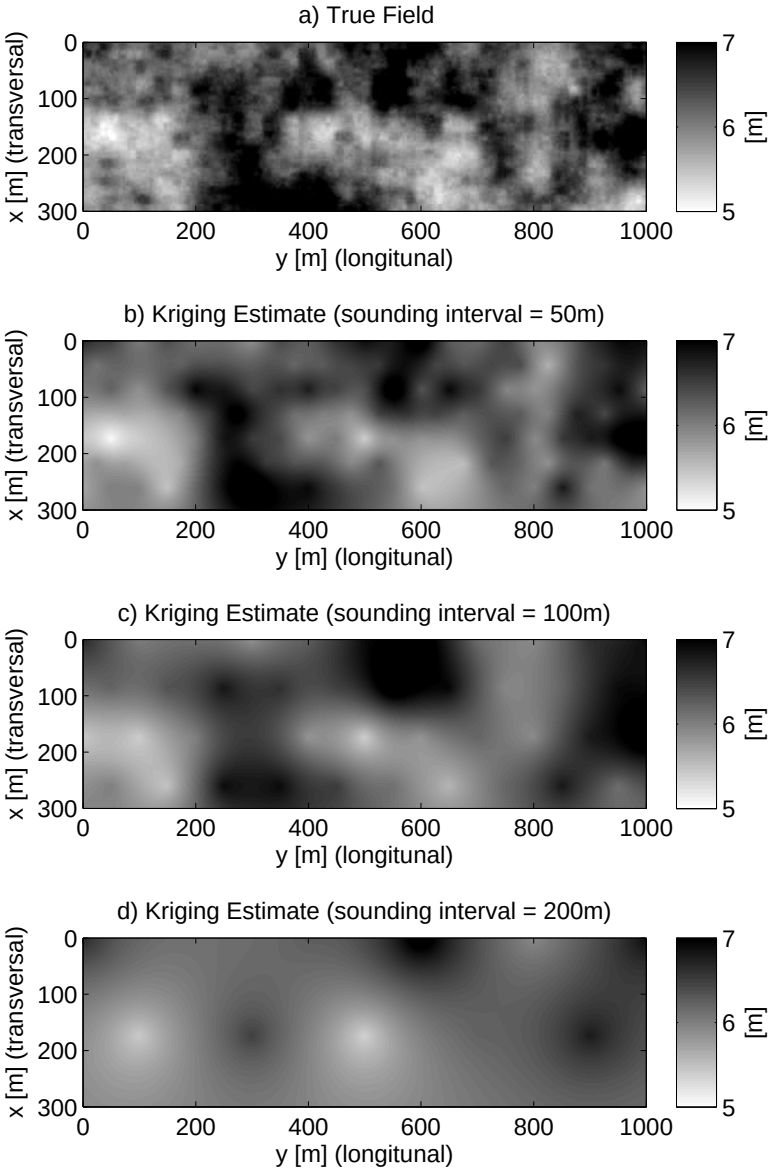

Figure 7.21: Soundings example: Kriging estimates of the blanket thickness for different CPT-distances (50m, 100, and 200m, regular triangular grid) assuming zero measurement error (top view, levee toe at $y = 0$m).

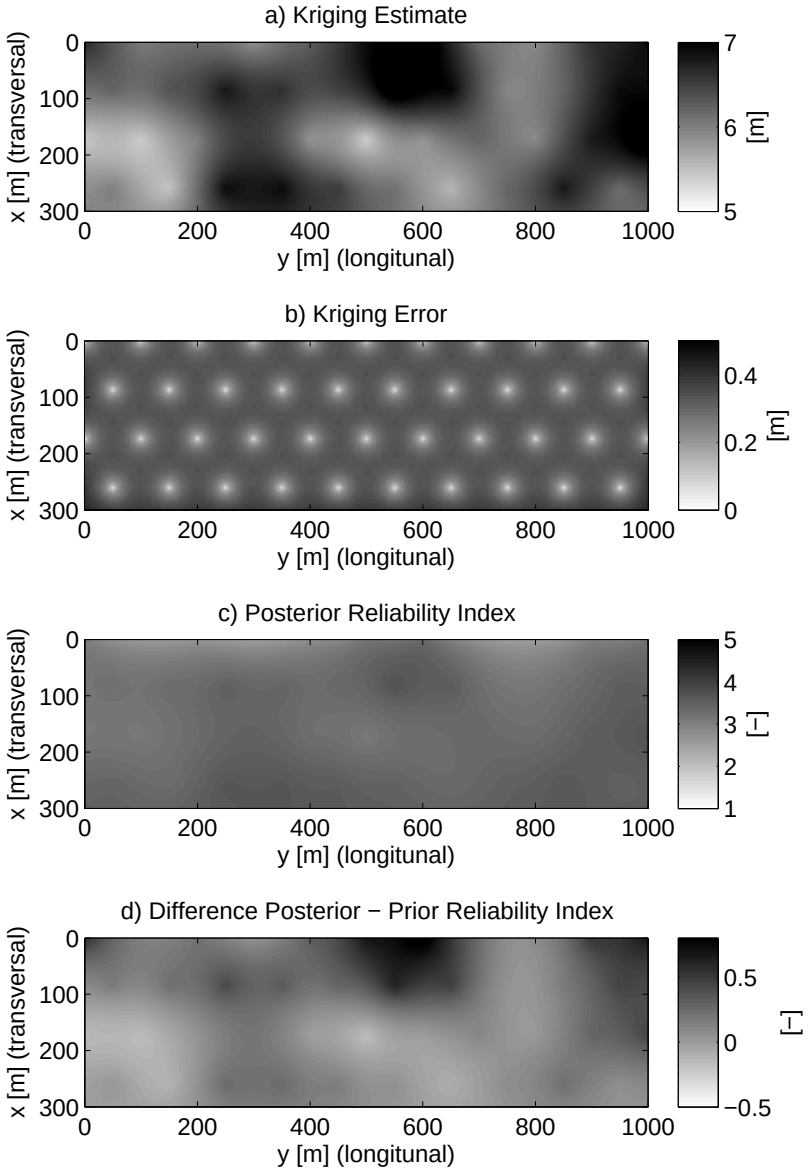

Figure 7.22: Soundings example: posterior uplift reliability index based on soundings with a distance of 100m assuming zero measurement error (top view, levee toe at $y = 0$m).

7.4.4. PRE-POSTERIOR ANALYSIS

As indicated in the previous section, we cannot expect much from pre-posterior analysis in the given setting, unless local measures could be applied at the weak spots only (e.g. by increasing the blanket weight locally). While in the next section we will go deeper into this including heave and piping also, in this simplified uplift example we will only show what the effect of total information (regarding d) would be.

Suppose we assume perfect information on d but all other random variables to be uncertain as represented by their a-priori distributions. Furthermore, suppose we simulate a large number of MCS-realizations for the latter and propagate them through Eq. 7.22 to obtain the critical blanket thickness ($d_{c,u}(x_{exit})$). Now we can check per realization, if uplift occurs in at least one grid cell. The number of realizations with uplift failure divided by the total number of realizations is the prior probability of uplift failure for the entire reach given perfect information on d, which happens to correspond to a reliability index of $\beta_u = 2.4$. Interestingly, that is very close to the minimum posterior value we obtained for closely spaced soundings (see Figure 7.20).

7.4.5. CONCLUDING REMARKS

The example has shown that even for uplift, in principle a point process (i.e., only dependent on local conditions not the whole field), FORM analysis based on Kriging as discussed in section 7.4.2 is not enough to obtain a posterior probability of failure for the whole levee section. Furthermore, the Kriging results and the benchmark analysis with the true field show that observations from soundings just replace unknown variability by known weak spots. Hence, if the uncertainty at hand represents only spatial variability and not epistemic uncertainty, additional investigation is unlikely to pay off, unless local measures can be taken at the weak spots which are less costly than an overall rehab design. In the next section, we will revisit and extend this example by including heave and piping (i.e., non-point process) and by including (reducible) epistemic uncertainty.

7.5. EXAMPLE UPLIFT, HEAVE AND PIPING

THIS section extends the fictitious example from the previous section by introducing or including the following features:

1. In addition to uplift, we also consider heave and piping (see 7.3.3).
2. In order to treat the spatial variability of the blanket properly, instead of Kriging we will work with random field simulation in the prior analysis (unconditional) as well as the posterior analysis (conditional).
3. In addition to spatial variability, epistemic uncertainty for the blanket thickness will be considered by modeling the mean value as a random variable (i.e., reducible uncertainty).
4. In the pre-posterior decision analysis we will compare an a-priori design for the whole reach with a locally adapted design according to what is required a posteriori after updating with additional data.

The example parameters are identical to the uplift example described in section 7.4; the parameters are given in Table 7.1.

7.5.1. PRIOR RELIABILITY AND IMPORTANCE SAMPLING

This example is computationally relatively expensive, because in posterior and especially in pre-posterior analysis large numbers of reliability analyses need to be carried out. Therefore, we will apply Importance Sampling using a sampling distribution for the water level as displayed in Figure 7.23 in order to reduce the required number of realizations.

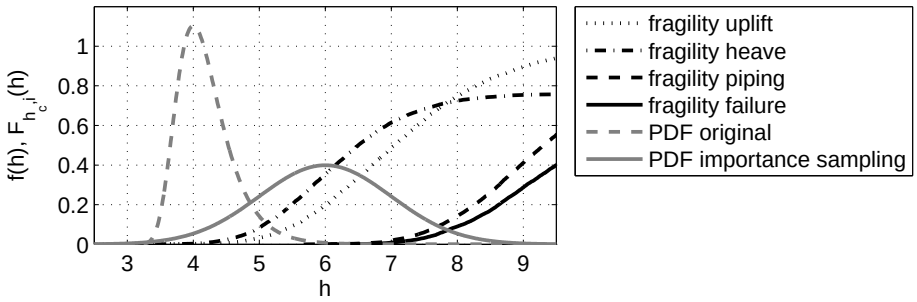

Figure 7.23: Soundings example: fragility Curves, water level and importance sampling distribution for the water level $f_{h,IS}(h)$ with parameters $h_{IS} \sim N(6,1)$

Notice that in the context of this example (7.5) the fragility curves in Figure 7.23 are merely for the sake of illustration of the suitability of the importance sampling distribution. They are meaningless for other purposes as they include d as a simple random

variable and not as a random field, whereas we use random field simulation to contemplate uplift, heave and piping simultaneously. Nevertheless, the sampling distribution for the water level will clearly generate more failure samples than the original one.
For each realisation i, of the (load-related) random variables and the random field of the blanket layer, we

1. identify the grid cells of the random field where uplift failure occurs,
2. count a realisation as uplift failure (F_u), if at least one grid cell fails due to uplift
3. check all grid cells failed due to uplift for heave failure,
4. count a realisation as heave failure(F_{uh}), if at least one grid cell fails due to heave,
5. check all grid cells failed due to heave and uplift for piping failure,
6. count a realisation as piping failure (F_{uhp}), if at least one grid cell fails.

As the water level h is assumed independent of the remaining random variables, the probability of failure are obtained by

$$P(F) = \frac{1}{n}\sum_i \mathbf{1}_{F_i}\left[\frac{f_h(h_i)}{f_h^{IS}(h_i)}\right] \tag{7.24}$$

where $f_h(h_i)$ is the PDF of the (annual maximum) water level as specified in Table 3.5 and $f_h^{IS}(h_i)$ the the importance sampling distribution, which in this example is a Normal distribution with mean 6m and standard deviation 1m. The resulting reliability indexes are presented in Table 7.2. Notice that the interpretation of these probabilities is slightly different than in all previous examples on uplift, heave and piping, as the probability of heave is actually the probability of uplift and heave and the probability of piping is the parallel system probability of all three sub-mechanisms failing together. We see that for this example the probability of heave is lower than uplift, which is plausible looking at the realisations of critical blanket thicknesses for uplift ($d_{c,u}$) and heave ($d_{c,h}$) in Figure 7.24. They are similar, the critical heave gradients being slightly higher on average. Furthermore, the probability of piping failure is orders of magnitude lower than heave and uplift.

β_i	Uplift	Heave	Piping (Failure)
Prior	2.36	2.65	4.24

Table 7.2: Soundings example: prior reliability indices for uplift, heave and piping

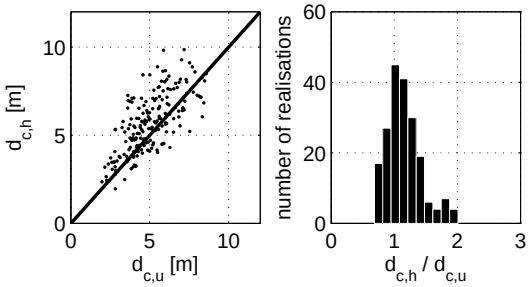

Figure 7.24: Soundings example: comparison of the critical thicknesses for uplift ($d_{c,u}$) and heave ($d_{c,h}$) for the realizations generated by Importance Sampling (left: scatter plot, right: histogram of the ratio).

7.5.2. POSTERIOR RELIABILITY

This section illustrates the effect of sampling the blanket thickness by means of soundings from the (fictitious) true field using regular grids with different inter-sounding distance (d_{CPT}). The prior and posterior probabilities for uplift, heave and piping are summarized in Table 7.3. In the current setting, the fact that the prior uplift reliability is lower than shown for the shortest distance to the toe in Figure 7.20 demonstrates that the serial system or length effect is implicitly accounted for in this type of analysis.

β_i	Uplift	Heave (and uplift)	Piping (Failure)
Prior	2.36	2.65	4.24
Posterior, $d_{CPT} = 50m$	2.59	3.10	4.51
Posterior, $d_{CPT} = 100m$	2.52	3.00	4.51
Posterior, $d_{CPT} = 200m$	2.53	2.98	4.37

Table 7.3: Soundings example: prior and posterior reliability indexes for uplift, heave and piping for different sounding intervals.

There is no clear trend in the posterior reliability in a sense that a denser sampling grid would always lead to a clearly higher reliability. This was expected, as the uncertainty in the blanket thickness was entirely attributed to spatial variability, in which case the additional information just helps to replace the uncertainty by "known" weak and strong spots.

The effect of updating (i.e., conditioning the random field realizations on the sampling data) is also illustrated in Figure 7.25, which shows an unconditional and a conditional random field realization for the same realization of the remaining (load) variables. The grid cells marked in red represent the locations where uplift and heave occur for this particular realization, i.e. the exit points for internal erosion, which determine the seepage length for the piping sub-mechanism. In this particular case, the additional information leads to a reduction of the area where uplift and heave occurs.

In real life, the high density of sampling points used in this synthetic example will

be hardly encountered. That raises the questions which amount of soundings would be cost-optimal for the present type of problem. To this end, we need to involve the retrofitting cost and how it is influenced by the additional information as will be discussed in the remainder of this section.

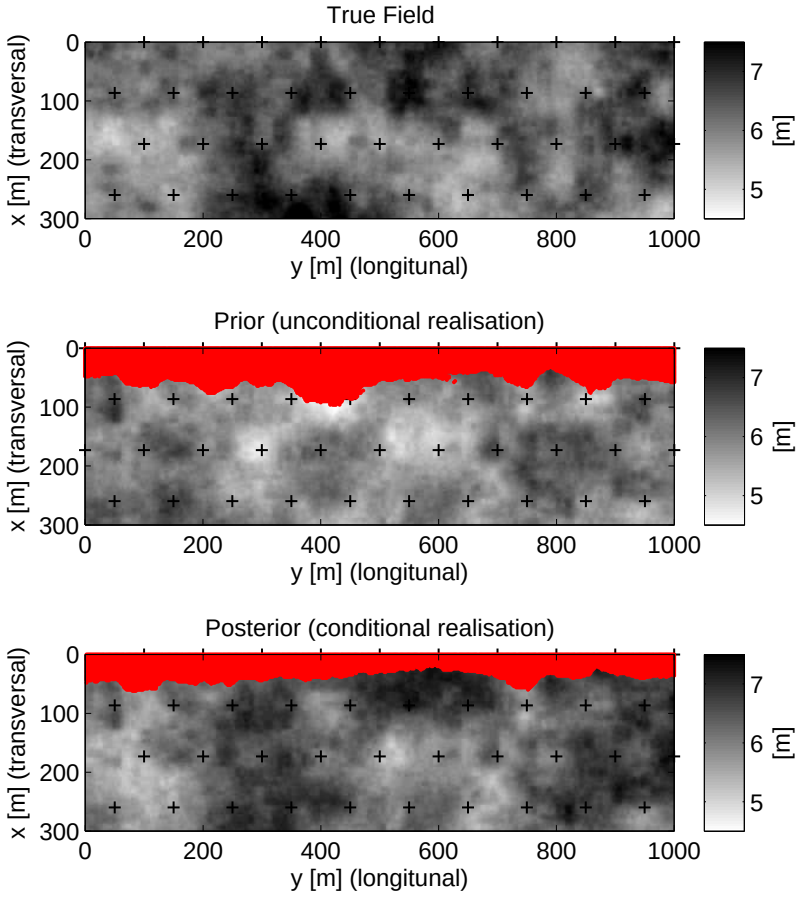

Figure 7.25: Soundings example: unconditional and conditional random field realisation indicating uplift and heave locations (marked in red, obtained with Importance Sampling) based on a triangular sampling grid with a sounding interval of $d_{CPT} = 100$m (top view, levee toe at $y = 0$m).

7.5.3. PRE-POSTERIOR ANALYSIS

If we do not have data from a readily carried out site investigation, the question is how much we should invest in such a campaign, if at all. That depends on how much we can get in return in terms of optimizing the retrofitting design and ultimately saving retrofitting cost. In the ideal scenario, the uncertainty reduction achieved by the site investigation would even make retrofitting unnecessary.

In order to demonstrate how pre-posterior analysis can be applied to such a decision analysis, this subsection introduces a simplified design approach and an associated cost model to be able to estimate the retrofitting cost after posterior analysis. Subsequently, to make the case more realistic, we introduce an uncertainty in the mean (field) value of the blanket thickness. The pre-posterior analysis is then used to optimize (a) the inter-sounding distance in longitudinal direction d_{CPT}, (b) the number of rows in the sampling grid in transverse direction (one or two) and (c) the transverse distance between the rows, if applicable (see Figure 7.30).

The example parameters are the same as described in section 7.4 and Table 7.1, except for the fact that the mean thickness is modeled as a (epistemic) random variable as well: $\mu_d \sim N6.0, 0.3$. Notice that for the whole field the epistemic part can theoretically be reduced to zero by sampling, while the spatial variability part can be reduced locally but the field variance (considered over the entire area of interest being a multiple of the relevant correlation distances) will persist.

TARGET RELIABILITY AND DECISION PROBLEM

The target annual reliability index in this fictitious example is $\beta_T = 5.0$, which refers to the total probability of failure (i.e., uplift, heave and piping) for the entire reach. Given that the prior reliability is significantly lower than the target, doing nothing is not an option. Similar to the example on anomaly detection (see 7.2), the decision tree for the situation at hand (Figure 7.26) comprises the decision whether or not to do site investigation at all and the optimization of the site investigation parameters. In contrast to the example on anomaly detection, the retrofitting cost in this example is not a fixed value (or zero) but instead the retrofitting design adjusts to the a-posteriori knowledge based on the sampling outcome as discussed below.

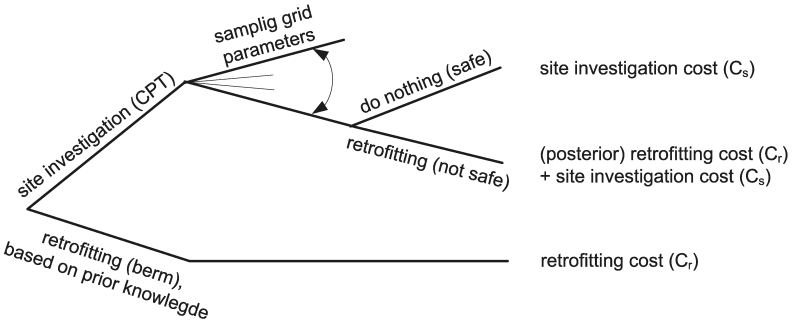

Figure 7.26: Soundings example: decision tree.

DESIGN AND COST OF RETROFITTING

While in reality there are many options to mitigate piping such as seepage screens, relief wells or filters (CIRIA, 2013), in this example we only consider the construction of a landside berm for the sake of illustrating the effect of additional information on the cost of retrofitting. The considered retrofitting design model is as follows:

1. For the berm width we apply the following (fictitious) design rule, which is assumed to ensure sufficient reliability to meet the target β_T: The berm width per sub-reach of 200m length is determined by the distance of the grid cell farthest from the levee which has an annual reliability index for heave and heave lower than $\beta_{T,uh} = 3.4$ (see Figure 7.27).
2. The cost of retrofitting by means of berm construction C_r [k€/km] is composed of mobilisation cost and variable cost as represented by the following cost function: $C_r = 1000 + 20 \cdot w$, where w [m] is the berm width. Figure 7.28 illustrates that the cost of berm construction varies between 1M€/km for small berm up to 5M€/km for very wide berms of over 200m.

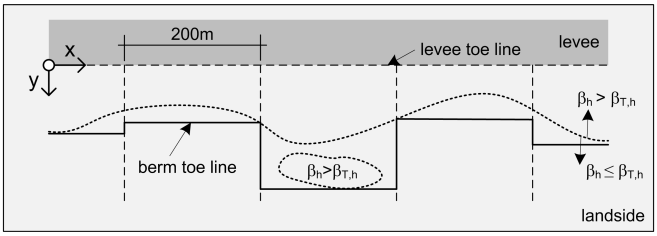

Figure 7.27: Soundings example: Illustration of the simplified design model to determine the cost of retrofitting based on prior and posterior data (top view).

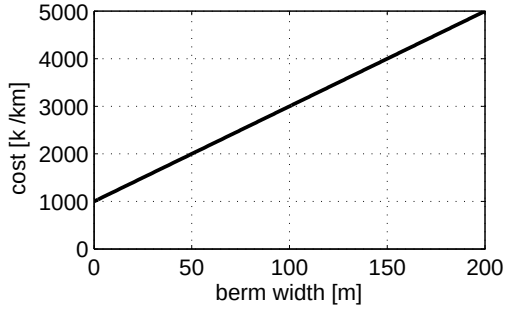

Figure 7.28: Cost function (fictitious) for berm construction as function of the berm width

The fact that only a berm is considered as retrofitting measure does not mean that a berm is the only possible measure nor that it is the one to be preferred. The berm is merely used to estimate the cost depending on the amount of information. Other measures are possible and can be treated accordingly. Furthermore, notice that the target reliability index for design based on uplift and heave can be different to the target reliability index in a safety assessment.

A-PRIORI DESIGN AND COST

In order to explore the decision option of retrofitting without any (additional) soundings, we determine the required berm width and the associated cost as explained above. To this end we need to use the total uncertainty in the blanket thickness, $\sigma_{d,total} = \sqrt{\sigma_{\mu_d}^2 + \sigma_d^2}$, and the critical thickness for uplift and heave (i.e., the load term), $d_{c,uh} = \min\left[d_{c,u}, d_{c,h}\right]$. Figure 7.29 shows the resulting prior annual reliability index for uplift and heave as a function of the distance from the levee toe. The required berm length is given by the distance from the toe where the target reliability ($\beta_{T,u,h,} = 3.4$) is met, here resulting in $w = 184m$ with a total cost of $C_r = 4.7$ M€.

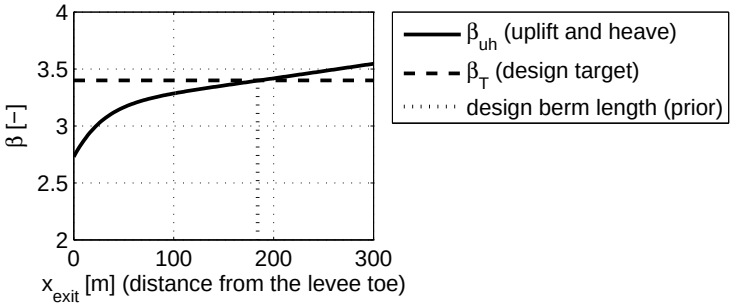

Figure 7.29: Soundings example: prior annual reliability index for uplift and heave (β_{uh}) as function of the distance to the levee toe (x_{exit}) assuming the load to be homogeneous in longitudinal direction. The berm design width is determined by the target reliability (β_T).

OPTIMIZATION OF DESIGN PARAMETERS

In this section, we will use the cost function described above in a pre-posterior analysis for different combinations of the design parameters to illustrate how the cost of site investigation and the expected retrofitting cost change with them. If one pursues only the optimal site investigation design, it is convenient and efficient to minimize the total expected cost by means of global optimization techniques (e.g., genetic algorithms) or to treat the problem as an augmented reliability problem (Au, 2005; Wang et al., 2011).

Here we will use brute force and discretise the design parameters, which besides finding the optimal design also provides insights into sensitivities with respect to the design parameters (see Figure 7.30):

- d_{CPT} (longitudinal spacing of the soundings)
- $d_{CPT,x}$ (transversal distance between rows of soundings)
- n_{rows} (number of rows)

Notice that for a given d_{CPT} combinations with $n_{rows} = 2$ and small values of $d_{CPT,x}$ should behave similarly as just one row (n_{rows}=1) with half the spacing (i.e., $d_{CPT}/2$).

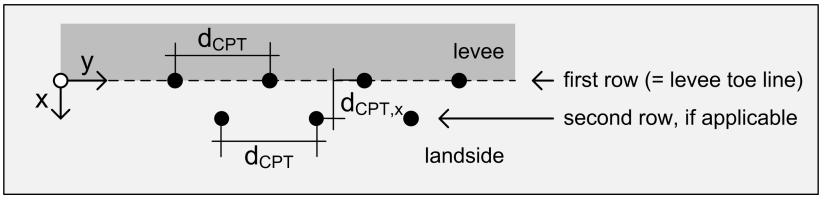

Figure 7.30: Soundings example: sampling grid parameters to be optimized with pre-posterior analysis (top view).

COMPUTATIONAL FRAMEWORK

The computational framework for the pre-posterior analysis is shown in Figure 7.31, which depicts the role of pre-posterior analysis in the optimization of the design parameters for the site investigation and and its nested structure. The "outer loop" uses Monte Carlo simulation (here with Importance Sampling) for representing the prior knowledge of the state of nature, in this case of the blanket thickness in particular. Per realisation, a posterior analysis is carried out, based on which a retrofitting design is made and the respective cost is determined.

The pre-posterior analysis needs to be repeated for as many combinations of site investigation design parameters as required for the optimisation and it delivers the expected retrofitting cost for these combinations. Combining this with the site investigation cost gives the expected total cost.

In general, the retrofitting design could be a reliability-based design (RBD) where the design parameters are optimized in an internal loop of reliability analyses with posterior knowledge. However, as discussed above, in this example we apply a simplified design rule based on the posterior probability of uplift and heave, which makes only one posterior analysis per pre-posterior realisation necessary and we can use Kriging for this purpose. On the one hand, this makes the problem computationally much less expensive, on the other hand this is also a situation more likely to be encountered in (Dutch) reality. For example, in the Netherlands, safety assessments may apply reliability analysis to show that the target values are met, however in design more often than not we resort to simpler and more "robust[6]" approaches.

[6]The use of the word "robust" is ambiguous in the context of structural design. The meaning here is that the designs obtained by robust approaches have a high probability of producing designs meeting the target reliability, often at the expense of being less economical than a reliability-optimized design.

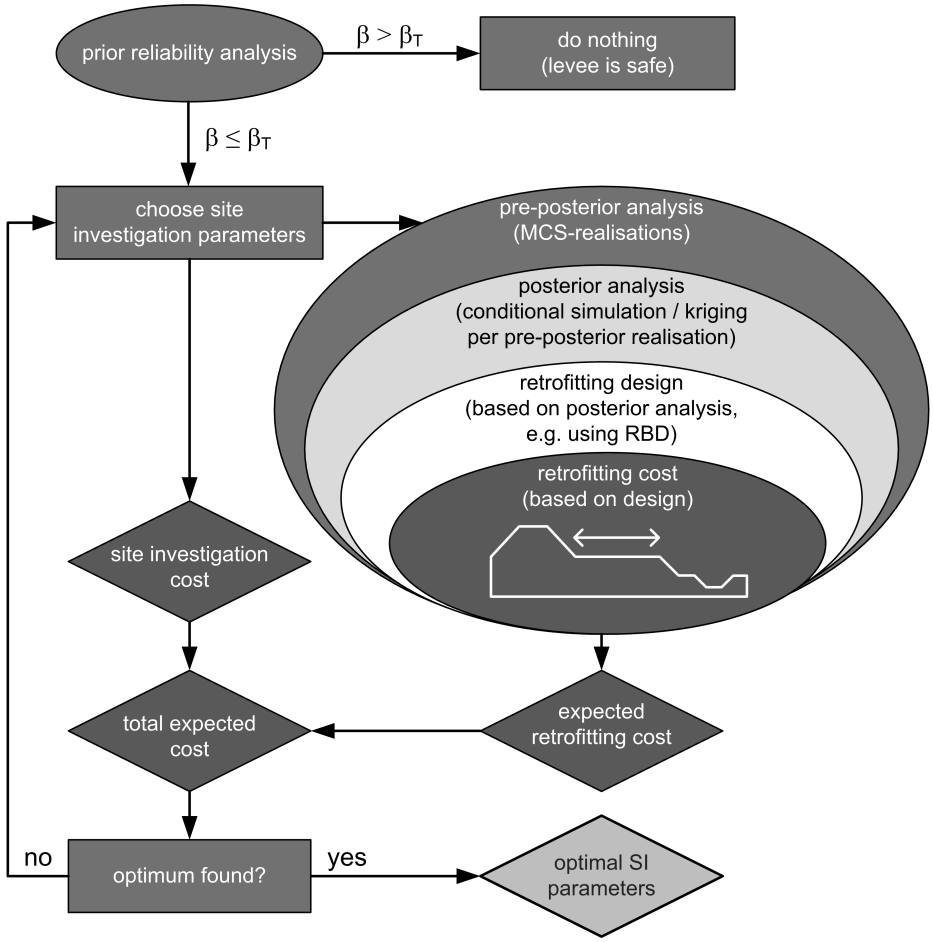

Figure 7.31: Computational framework for the pre-posterior analysis.

ONE ROW OF SOUNDINGS EVERY 100M

Before addressing the optimal choice of site investigation parameters, we first contemplate the specific case of one row of soundings at the levee toe with a distance of d_{CPT} = 100m and the insights that pre-posterior analysis can provide.

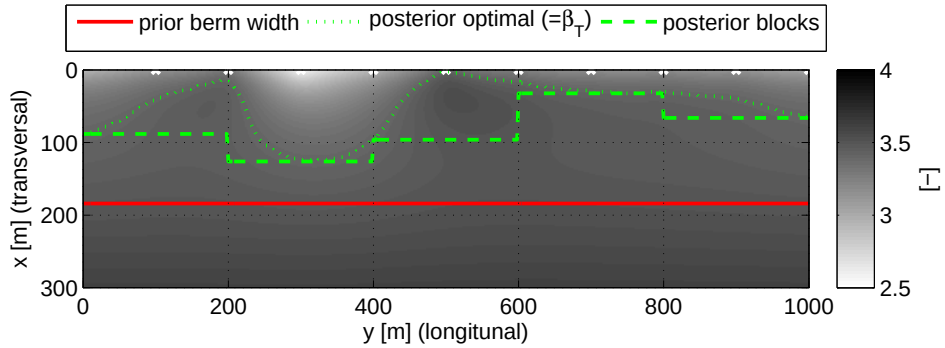

Figure 7.32: Soundings example: illustration of the prior, posterior optimum and posterior berm width per subberm of length 200m. The 2D field shows the posterior reliability index for uplift and heave for an arbitrary pre-posterior realisation (top view, levee toe at y = 0m).

First of all, Figure 7.32 illustrates the berm design based on the posterior (kriged) field of the blanket thickness. For the arbitrary pre-posterior realisation in the figure, the posterior required berm (green, dashed line) is narrower than a-priori (red, continuous line), and locally the difference can be significant. Two effects play a role, (a) the mean thickness varies in each realisation and may be rather high here (i.e., epistemic contribution) and (b) the uncertainty around the sampling points is reduced.

Without reducible or epistemic uncertainty the probability of avoiding retrofitting entirely would be virtually zero, because the considered length (1km) is a multiple of the correlation distance (200m), for which there is a very high probability of a weak spot somewhere in the reach. However, with the epistemic uncertainty and, hence, the possibility of encountering a higher field mean in reality, the probability of avoiding retrofitting can become substantial (in terms of the decision problem). For 2 out of 1000 pre-posterior realisations no berm was necessary at all, so the probability of avoiding retrofitting entirely is in the order of 10^{-3}.

The pre-posterior distributions of the berm cost and (average) width in Figure 7.33 exhibit a rather wide range of outcomes reflecting the (large) uncertainties in the example. Comparison with the prior values (4.68M€and 184m) results in a larger probability of saving cost than spending more. This is confirmed by the expected cost values in Table 7.4, a risk-neutral decision maker faced with the option of doing soundings every 100m or nothing at all should opt for investing in site investigation. The benefit-cost ratio (BCR) is very high (<70), which means that even for a much lower cost function (e.g., in rural areas) a BCR in the order of 10 is not unrealistic.

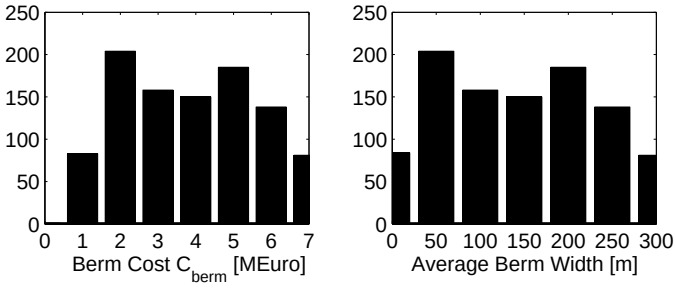

Figure 7.33: Soundings example: histograms of pre-posterior retrofitting cost (left) and berm width (left) for one row of soundings at the levee toe with distance d_{CPT} = 100m.

	$E[C_r]$ [k€]	C_s [k€]	$E[C]$ [k€]	BCR
d_{CPT} = 100m	3870	11	3881	72.6
no soundings	4680	0	4680	0

Table 7.4: Soundings example: expected cost and BCR for one row of soundings at the levee toe with distance d_{CPT} = 100m.

OPTIMAL SITE INVESTIGATION

In order to find the optimal combination of site investigation parameters, a parametric study has been carried out in which the site investigation design parameters have been varied systematically:

- d_{CPT} (longitudinal sounding distance),
- number of rows (i.e., one or two),
- $d_{CPT,x}$ (distance between rows, if applicable).

The expected total cost (Figure 7.34) shows a minimum for just one row of soundings with a distance around d_{CPT} = 200m, which is close to the correlation distance. The optimum expected cost is roughly 1M€lower than the prior value (4.68M€). The expected average berm width is roughly 130m, as compared to 184m a-priori.

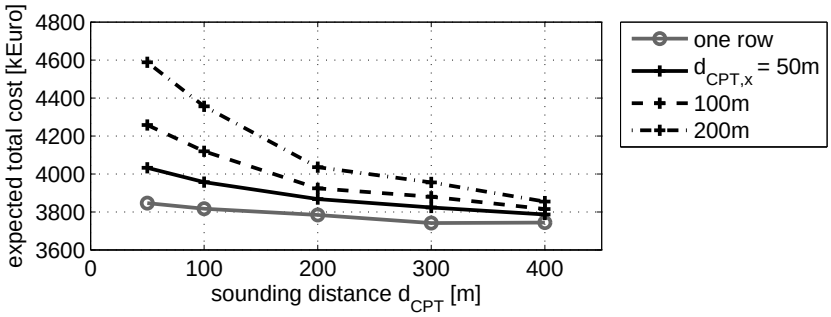

Figure 7.34: Soundings example - parametric study: expected total cost versus SI-design parameters.

Figure 7.34 also exhibits that, apparently, adding another row of soundings reverses the savings effect increasingly with increasing distance from the levee toe (where the first row is located). For closely spaced soundings in longitudinal direction and the second row 200m from the toe, both expected cost and width are close to the prior values again.

Considering the probability of avoiding retrofitting (i.e., no berm necessary after posterior analysis) as displayed in Figure 7.35, a plausible explanation for the increasing expected cost with more site investigation coverage would be the following. We need a couple of soundings to reduce the epistemic uncertainty around the field mean value. Additional information from closely spaced soundings only increase the likelihood of encountering a weak spot, which may "reintroduce" the need for retrofitting. This effect is very similar to what we encountered in the example on anomaly detection (see 7.2) and it is an effect that can occur when working with target reliabilities (i.e., omitting the cost of failure in the risk considerations).

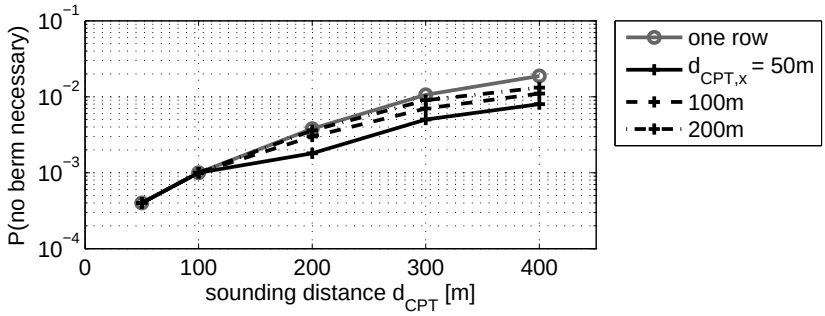

Figure 7.35: Soundings example - parametric study: probability of avoiding the berm (i.e., $C_r = 0$) versus SI-design parameters.

Figure 7.36 gives an impression of the BCR encoutered for this example, ranging from close to zero up to over 200. The fact that the BCR keeps on increasing with larger longitudinal spacing whereas there is a minimum for the expected cost demonstrates that the BCR can be a poor parameter to base decisions on. The fact that the cost of soundings may decrease at a higher rate than the savings in berm should not lead to the conclusion of doing less soundings, because the overall cost is important in the end, not the "relative return on investment".

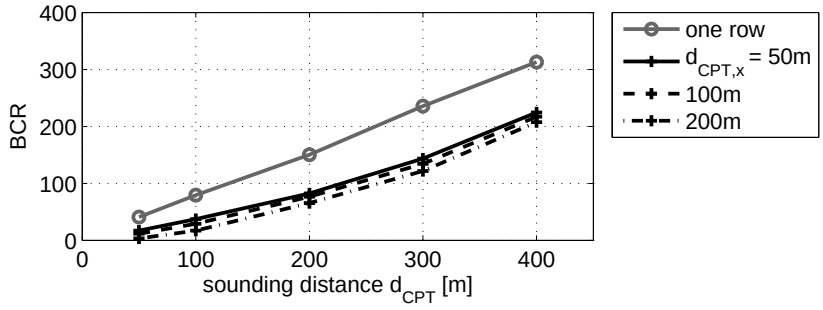

Figure 7.36: Soundings example - parametric study: benefit-cost ratio (BCR) versus SI-design parameters.

7.5.4. CONCLUDING REMARKS ON THE EXAMPLE

This section has extended the concepts elaborated so far in this chapter to the failure modes uplift, heave and piping. In order to obtain the reliability for the entire reach of interest, conditional simulation is applied for posterior reliability analysis, because Kriging is only suitable for so-called point-processes to determine the probability of failure(unless the probabilities are combined accounting for their mutual correlations, which is cumbersome). Importance Sampling on the water level was used to reduce the computational burden. The example on posterior analysis (7.5.2) showed that, if we only deal with uncertainty stemming from spatial variability, the impact of observations on the reliability is negligible, as the uncertainty is only replaced by known weak and strong spots.

In the extension of the example to (pre-posterior) decision analysis, we introduced an epistemic uncertainty in the mean blanket thickness. The decision problem is similar to the one on anomaly detection (7.2), as the essence is to optimize the site investigation design parameters and to assess, whether an investment in site investigation is cost-effective at all. The main differences are, though, (a) the more elaborate failure model, (b) the more refined retrofitting cost model (i.e., the berm width can vary in longitudinal direction), (c) the spatial variability is described by a (continuous) random field instead of stratification scenarios and (d) there are more site investigation design parameters than just the soundings interval in longitudinal direction.

The computational framework has a layered structure with several nested loops, from outer to inner loop being (a) the optimization of site investigation parameters, (b) the pre-posterior analysis , (c) the posterior analysis by means of Kriging or conditional simulation per pre-posterior realization and (d) the retrofitting design and cost based on posterior knowledge. The outcomes include the pre-posterior distributions of berm width and cost as well as the probability of avoiding retrofitting at all, the latter depending mainly on the epistemic uncertainty around the mean blanket thickness.

The main conclusion of the parametric study of the site investigation parameters is that just one row of soundings at the levee toe with an interval close to the correlation distance seems the optimal setup. More rows of soundings or smaller intervals only increase the cost and increase the probability of encountering a weak spot. The effect here is similar to the one encountered in the example on anomaly detection as discussed in section 7.2.9. In the adopted framework of working with target probabilities of failure, wherein the benefits of risk reduction through higher reliability are not accounted for, the incentives are to achieve the target reliability level at minimum cost or with the highest probability. We essentially do not want to know more than necessary.

7.6. SYNOPSIS

THIS chapter has demonstrated how soundings can be used to for reliability updating and how the cost-effectiveness of investments in site investigation can be assessed by decision analysis. First, piping-relevant types of information to be obtained from soundings were described. Subsequently, a simple example on anomaly detection highlighted the most important features of pre-posterior analysis. Finally, blanket layer geometry and its relation with the seepage length were chosen for a more realistic elaboration of reliability updating and pre-posterior analysis, the effects of which were

demonstrated in a fictitious example. The following are the main conclusions based on the findings in this chapter:

1. Soundings like CPT and borings provide information on several parameters relevant to piping such as the permeability of aquifers (e.g., by dissipation tests) or the grain size distribution (by sieve analysis of samples retrieved by borings). However, the most important information to be inferred from soundings is the stratification in terms of identification of soil strata, blankets and aquifers as well as their geometry.
2. Bayesian posterior analysis can be applied to update the probability of anomalies as well as for updating the uncertainty of properties that can be modeled by means of continuous random fields such as the blanket thickness. Whereas analytical solutions are still tractable for (discrete) anomaly detection problems, for the random fields we need to resort to techniques like Kriging or simulation.
3. Pre-posterior decision analysis provides not only the optimal decision (here for a risk-neutral decision maker) but provides also insights into the uncertainty of the pre-posterior retrofitting designs and costs.
4. Site investigation can be very cost-effective for anomaly detection problems, if the conditional probability of failure given the presence of an anomaly dominates the overall probability of failure. The cost of site investigation is usually orders of magnitude lower than the cost of retrofitting.
5. Similarly, site investigation can be very cost-effective for reducing the uncertainty in the blanket thickness. This is especially true, when the epistemic uncertainty leads to a considerable probability that retrofitting can be avoided and the mobilization cost is relatively high.
6. The proposed approach works well within the chosen framework. However, working with target reliabilities and neglecting the cost of failure is a simplification which implies trade-offs. From safety standards we know that target reliabilities are suboptimal because they need to cover a wide range of inhomogeneous conditions; risk optimization would be more economic. Similarly, working with a target reliability can provide wrong incentives for site investigation decisions. As pointed out in both pre-posterior examples in this chapter, gathering more information than enough to meet the target is not rewarded in this framework, though the additional risk reduction may outweigh the additional cost.

Staged site investigation strategies have not been investigated, but the extension is straightforward, though computationally even more expensive.

8

CONCLUSION

Plans are worthless, but planning is indispensable.

Dwight D. Eisenhower

Thomas Bayes (1701-1761)

This thesis presents an approach to increase the reliability of flood defenses to an acceptable level by reducing piping-related uncertainties through incorporating information from different sources consistently using Bayesian inference considering the a-posterior necessary retrofitting (cost). Furthermore, it was demonstrated how obtaining such information by means of site investigation or monitoring can be planned in a cost-effective way using decision theory in a framework with a prescribed target reliability. While detailed conclusions and recommendations were already discussed in the respective chapters, this chapter synthesizes the main findings (8.1), states the main recommendations for future research and practice (8.2) and concludes with some closing words (8.3).

8.1. MAIN FINDINGS

PIPING UNCERTAINTIES

The failure mode considered consists of the three failure mechanisms uplift, heave and piping. In reliability terms, these mechanisms can be modeled as a parallel system, as all three are necessary (but not sufficient) conditions for failure. The mechanisms are correlated through common variables, the most influential ones being the water level on the loading side, the seepage length, the hydraulic conductivity of the aquifer, as well as the blanket thickness on the resistance side. Even more important than the uncertainties in soil properties can be uncertainties in the stratification and in the geo-hydrological system, which in this thesis have been modeled by discrete scenarios. The examples and case studies have demonstrated that the latter category, e.g., the presence of adverse geological details or the position of the so-called entry and exit points can be the dominant uncertainties. Nevertheless, in contrast to the variability of soil properties within a statistically homogeneous layer, often modeled by means of random field theory, the discrete type of uncertainties has been paid little attention in the literature so far.

RELIABILITY UPDATING

Bayesian posterior analysis was adopted for updating prior degrees of belief by incorporating additional information from the various sources of information studied in this thesis. The Monte Carlo simulation framework used for posterior analysis is capable of handling both discrete scenarios (e.g., stratification) as well as the uncertainties in the loads and resistance properties, modeled with continuous probability density functions at the same time. Also the correlations between the failure modes as well as between different load events are dealt with appropriately. The computational approach followed is (asymptotically) exact and can serve as a benchmark for computationally more efficient approaches. Some demonstrations of more efficient techniques such as Subset Simulation or Importance Sampling have been given in the application-oriented chapters.

It is important to point out that the proposed approach is only as good as the models and the scenarios or prior uncertainties identified by the modeler. Inherently, Bayesian posterior analysis is incapable of detecting previously unidentified conditions or mechanisms which, nevertheless may contribute to the probability of failure. Only in case of large prior model uncertainties and evidence contradicting the prior beliefs is model bias adjusted. However, if a priori the model uncertainty is not dominant, the Bayesian analysis will "look for" the most plausible explanation of the evidence in other uncertain variables. The inability of handling "black swans" (Taleb, 2007) is a clear limitation of the approach we need to be aware of. Everything is conditional on the model.

Another aspect with considerable impact is the distinction between reducible (epistemic) uncertainties and irreducible (aleatory) uncertainties. For the applications treated in this thesis, time-invariant variables (e.g., blanket thickness) essentially fall into the reducible category whereas variables modeling (intrinsice) variability in time (e.g., the water level) fall into the irreducible category. The larger the share of reducible uncertainty in a problem, the greater the effect of updating. Whether uncertainty is reducible is an input to the analysis, not an outcome. As discussed in chapter 4, it is not straightforward to allot model uncertainty to either category, as it always contains contributions of both.

DECISION ANALYSIS FRAMEWORK

The decision analysis framework adopted in this thesis has two main ingredients. First, the optimal investment strategy is determined by the minimum (pre-posterior) expected total cost, i.e., the cost of uncertainty reduction (e.g., monitoring or site investigation) plus the cost of retrofitting. Working with expected costs implies that we assume a risk-neutral decision maker, which seems justified in situations where governmental organizations deal with a large portfolio of similar but uncorrelated projects and the potential costs in a single project do not give rise to risk-averse behavior. Secondly, our search for the optimal strategy is constrained by a prescribed target reliability as outlined in chapter 2. The choice to work with target reliabilities was made to provide results that are realistically applicable in systems like the Dutch flood protection standards (or the Eurocode), where such target reliability values have been established legally.

Bayesian pre-posterior analysis allows us to estimate the cost-effectiveness of investments in uncertainty reduction a-priori and it provides us with an impression of the range of uncertainty in the potential outcomes in terms of required retrofitting measures and costs. We can also assess the probability of achieving a certain amount of cost savings with respect to the a-priori necessary retrofitting cost. Though not fully risk-based (i.e., not accounting for the cost or consequences of failure explicitly), pre-posterior analyses provides meaningful information to support decision making and to justify investments in uncertainty reduction.

FIELD OBSERVATIONS

The work in chapter 5 has shown that only considering survival as observation of levees that do not fail during extreme load events (in Dutch: "bewezen sterkte") is an overly simplistic view, because it neglects more detailed visual observations of good or poor performance that are typically made during these events. Including observations like (heavy) seepage or sand boils has provided new insights in this respect. Whereas reliability updating based on pure survival information (i.e., no signs of poor performance) will always lead to an increase in reliability, incorporating the information from observations of poor performance always leads to a lower posterior reliability. Both ways, the change can be roughly one order of magnitude depending on the prior (reducible) uncertainties and on how unexpected the observation was (i.e., observations with a low prior probability have a high impact and vice versa). Again, the discrete uncertainties like stratification can be the most important ones causing the most significant changes.

Another related common misconception is that the probability of failure up to the highest observed and survived water level is zero. This is an assumption often made in simplified survival analyses, which is only true if all resistance uncertainties were time-invariant (i.e., fully reducible). Arguably this is not the case; for example, the groundwater conditions in the future situation to be assessed can be much more unfavorable than the conditions at the time of the observed survived water level. The respective sensitivity analyses in chapter 5 have demonstrated that the assumption of time-invariant resistance can be very unconservative as may lead to severe overestimation of the reliability.

For flood defenses with relatively high reliability, on the long term we expect the structures to survive a few significant loadings, by which their reliability is expected to

increase autonomously. One can think about this as the flood defense surviving (incomplete) load tests, the effect of which is that epistemic uncertainty is reduced. While this may sound appealing to decision makers in a sense that they may like to adopt a "wait and see"-strategy, we need to bear in mind that the next significant load event may be still years ahead and that there is a risk of failure to be considered.

HEAD MONITORING

The main driver for uplift, heave and piping is groundwater flow in the aquifer underlying the levee and the resulting pore pressures. Chapter 6 has demonstrated that monitoring the response of the hydraulic head in the aquifer to flood loading enables us to reduce geo-hydrological uncertainties, both for simplified models working with so-called damping factors as well as for groundwater flow models. The effect of updating can be considerable again depending on prior uncertainties, especially the uncertainty related to stratification.

The example on pre-posterior analysis showed that with considerable prior uncertainties there can be a significant probability that the posterior reliability meets the target. Since the difference between retrofitting and monitoring cost is usually several orders of magnitude, even a relatively low probability of meeting the target and realizing savings in retrofitting cost can make investments in monitoring attractive.

SOUNDINGS

The main information provided by soundings in terms of piping reliability is on the stratification (i.e., subsurface geometry and the presence of geological details) and on the thickness of the blanket layer. The latter is crucial for uplift and heave and plays an important role in the location of the exit point and, consequently, in the seepage length.

For anomaly detection it has been shown that the site investigation density can be optimized based on the (uncertain) anomaly size and the effect of the presence of an anomaly on the reliability. As for monitoring, due to the considerable difference between site investigation cost and retrofitting cost even a small probability of achieving savings can be enough to justify investments in soundings.

Similarly, gathering information on the thickness of the blanket layer in the hinterland of the levee enables us to optimize the design of a berm. Even though the overall (expected) cost may not always differ considerably, additional site investigation can ensure that the retrofitting design is adapted to the revealed weaker and stronger sections.

Though valuable decision support information can be generated for site investigation planning with pre-posterior analysis, chapter 7 has also revealed shortcomings of a framework with target reliabilities in which the consequences of failure are not included explicitly. It can provide wrong incentives in site investigation decisions, as gathering more information than enough to meet the target is not rewarded in this framework, though the additional risk reduction may outweigh the additional cost. The optimal strategies found may be suboptimal in an overall risk sense.

8.2. RECOMMENDATIONS

FUTURE RESEARCH

Spatial Variability and Length-effect The variability of properties in statistically homogeneous units (e.g., soil properties) was treated in an implicit fashion by so-called representative values in this thesis. The proposed method should be extended by accounting for spatial variability explicitly by means of random field theory. This would enable us to account, among others, for the length-effect. For the Dutch context, the first step should be to include the variability of properties in longitudinal direction of the levee (i.e., one-dimensional) to enable comparisons with results from reliability analyses as carried out in the Dutch VNK2-project (Jongejan et al., 2013).

Multiple Sources of Information and Staged Strategies The work in this thesis treated one source of information at a time and applied decision analysis to single stage monitoring and site investigation. For further optimization, we would want to combine the information provided from different sources of information at the same time. For example, we may consider using the information from field observations and monitoring data from the same or several historical floods altogether. Conceptually and technically the extension should be straightforward, as "today's posterior is tomorrow's prior". In the implementation, care needs to be taken of the correlation between different observations to avoid "double-counting" of essentially the same information (e.g. observations with a common cause). Similarly, the decision analysis approach for site investigation and monitoring can be extended to staged strategies, in which decisions on subsequent investigation stages are optimized based on the findings in previous stages.

Time to Next Significant Flood An implicit assumption in this thesis was that each future flood provides information regarding the resistance properties of the levee. In reality, we often see non-linear behaviour in a levee's response to hydraulic loading. For example, there may be a threshold at which the response changes because the winter bed is flooded and the hydraulic contact points with the aquifer shift closer to the levee, leading to decreased damping. Since for reliability we are most interested in the resistance properties under conditions close to failure, only the floods exceeding such a threshold provide meaningful information for reliability updating. This implies that there may be a considerable waiting time for a significant flood event which can be used for reliability updating purposes. For such situations the waiting time or the probability of a significant flood in the monitoring period needs to be included in the decision analysis.

Reducibility of Uncertainties Reducibility of uncertainties and the implications for reliability updating were discussed extensively in chapter 4. The relevance of distinguishing between reducible and irreducible uncertainties has also been discussed in the literature (e.g., Der Kiureghian and Ditlevsen, 2009) and we know how to deal with the two types in computational procedures. While for the characterization of geotechnical properties, Phoon and Kulhawy (1999) do distinguish between

inherent variability and measurement error, they do not explain what this distinction implies for the reducibility of either type (the aim of the paper was to provide methods for establishing prior uncertainties and reasonable ranges). Especially the question to what degree model uncertainty is reducible deserves more attention in the literature, as does the quantification of model uncertainty in general.

Transient Groundwater Flow While the steady-state groundwater flow model applied in this thesis may be applicable to long-lasting river floods, an extension to transient groundwater flow modeling is recommended for future research. This will be not only recommended but necessary, if the approach is to be applied in coastal areas and estuaries, where the pore pressure response can be far from the steady state due to tidal influence and relatively short storm durations.

ENGINEERING PRACTICE

The results in this thesis are promising in the sense that we may expect site investigation and monitoring to be cost-effective in many situations. A common complaint by geotechnical engineers is that is is hard to convince clients of investing (more) in site investigation. Practitioners are encouraged to use the methodology to underpin their argument quantitatively by presenting the (expected) monetized benefits to their clients.

Since practitioners will find it hard to use the fully probabilistic approach presented in this thesis directly, we need to provide simplified approaches for reliability updating as well as for site investigation and monitoring planning. Just like semi-probabilistic design and safety assessment methods, the simplified methods for reliability updating and decision analysis can be calibrated using fully probabilistic benchmarks.

In this context, it would be appropriate in the Dutch context to extend the technical report "Actuele sterkte van dijken"[1] by (a) simplified methods for the failure mechanism piping similar to the ones already provided for slope stability and (b) by fully probabilistic examples for piping as well as slope stability in order to provide a better understanding of the underlying concepts and assumptions to the potential users.

POLICY

A reliability-based framework for safety assessment and design provides much more flexibility in doing out-of-the-box (i.e., non-standard) analyses such as the reliability updating approach presented in this thesis. Working with (target) reliabilities instead of semi-probabilistic or deterministic approaches gives opportunities for optimization and, hence, better use of resources. The risk-informed, reliability-based framework for safety assessment of flood defenses which is envisaged to be implemented in 2017 in the Netherlands is a step in the right direction and should not be abandoned.

The work in this thesis has also exhibited shortcomings of working with (derived) target reliabilities instead of working with a fully risk-based approach with explicit risk acceptance criteria. For the long-term, working with acceptable risk directly may be the most efficient approach, though this option seems hardly workable for the foreseeable future due to many technical challenges yet to be solved.

[1] Technisch Rapport Actuele sterkte van dijken, Expertise Netwerk Waterveiligheid, March 2009.

8.3. CLOSING WORDS

INCORPORATING additional information from field observations, monitoring or site investigation was demonstrated to have a considerable effect on the reliability, especially for the large uncertainties in geotechnical engineering. The proposed approach helps to decide where related investments make sense and how we can optimize our uncertainty reduction strategy. The examples and cases elaborated in this thesis suggest that often such investments are indeed worthwhile.

In fact, the following simplified reasoning points in the same direction. Site investigation and monitoring cost are typically in the order of tens of thousands of Euros (10^4€). At the same time, the retrofitting cost for a levee reach of several kilometers easily exceeds the tens of millions of Euros (10^7€). If our site investigation or monitoring program gives us just a 10% chance of saving 10% of the retrofitting cost, which would imply savings in the order of hundreds of thousands of Euros (10^5€), the investment would already pay off. On the other hand, geotechnical engineers and contractors usually have difficulties of convincing their clients of the benefits of site investigation. Hopefully, the work in this thesis can help to make steps in demonstrating the effectiveness of uncertainty reduction measures and to provide useful information to take better decisions to minimize the overall societal cost of flood protection, because underpinning the probabilities of potential savings is not always straightforward.

Having stated all the potential benefits of investing in uncertainty reduction, this may never be an excuse for a decision maker to put preparations for retrofitting or mitigation measures on hold "until we know for sure". If a situation is considered unsafe based on the current state of knowledge (i.e., prior uncertainties), society bears a higher level of risk than acceptable. It is the responsibility of the decision maker to take measures to achieve a level of acceptable risk as soon as reasonably possible.

In this context, lately people have been suggesting to use innovative reinforcement measures (i.e., not yet proven or widely accepted technology) in combination with monitoring in order to save costs. While this makes sense, it needs to be pointed out that monitoring alone is not enough to warrant sufficient reliability of these measures. When implementing monitoring strategies we may not forget to plan (emergency) measures in case of monitoring outcomes deviating from our expectations as already discussed by Peck (1969) in the ninth Rankine Lecture on the "observational method". The entire package consisting of the principal measure, the monitoring and the actions in case of alarming monitoring outcomes needs to meet the target reliability.

Finally, pre-posterior analysis is more than mathematics and number-crunching. It is a rational approach to decision making, which should be adopted more often in practical problems. The essence is that we make an estimate of the situation at hand, think of experiments to verify, falsify or just better estimate it and then think through what the measurement outcomes could be and what we would do in case of any outcome. That is thinking through the possibilities and weighing them with our prior beliefs. As the quote at the chapter beginning suggests, many of these possibilities will become obsolete after our experiment, yet we need to have a plan.

BIBLIOGRAPHY

Allsop, W., Kortenhaus, A., and Morris, M. (2007). Failure Mechanisms for Flood Defence Structures. Technical Report T04-05-01.

Ang, A. H. S. and Tang, W. H. (1990). *Probability Concepts in Engineering Planning and Design, Volume II: Decision, Risk and Reliability*. Wiley, New York.

Ang, A. H. S. and Tang, W. H. (2007). *Probability Concepts in Engineering*. Wiley, New York, 2nd edition.

Au, S. (2005). Reliability-based design sensitivity by efficient simulation. *Computers & Structures*, 83(14):1048–1061.

Au, S.-K. and Beck, J. L. (2001). Estimation of small failure probabilities in high dimensions by subset simulation. *Probabilistic Engineering Mechanics*, 16(4):263–277.

Baecher, G. B. (1972). *Site Exploration: A Probabilistic Approach*. Phd thesis, Massachusetts Institute of Technology.

Baecher, G. B. (1979). Analyzing Exploration Strategies. Site Characterization and Exploration. Technical report, Massachusetts Institute of Technology.

Baecher, G. B. and Christian, J. T. (2003). *Reliability and Statistics in Geotechnical Engineering*. Wiley, West Sussex, UK.

Baecher, G. B. and Christian, J. T. (2008). Spatial variability and geotechnical reliability. In Phoon, K. K., editor, *Reliability-based design in Geotechnical Engineering*, chapter 2, pages 77–133. Taylor & Francis, London and New York.

Ball, D. J. and Floyd, P. J. (1998). Societal risks. Technical report, Health and Safety Executive, United Kingdom.

Bayes, T. (1763). An Essay towards solving a Problem in the Doctrine of Chances. *Biometrika*, 45:293–315.

Bazant, Z. (1953). Stability of a non-cohesive soil under elleptic upward seepage.

Beck, J. L. and Au, S.-K. (2002). Bayesian Updating of Structural Models and Reliability using Markov Chain Monte Carlo Simulation. *Journal of Engineering Mechanics*, 128(4):380–391.

Benjamin, J. R. and Cornell, C. A. (1970). *Probability, Statistics and Decision for Civil Engineers*. McGraw-Hill, New York.

Bierkens, M. F. P. and Van der Gaast, J. W. J. (1998). Upscaling hydraulic conductivity: theory and examples from geohydrological studies. *Nutrient Cycling in Agroecosystems*, 50:193–207.

Bligh, W. G. (1907). *Practical Design of Irrigation Works, First Edition*.

Bligh, W. G. (1910). Dams, barrages and weirs on porous foundations. *Engineering News*, 64(Dec.):708.

Bligh, W. G. (1915). Submerged weirs founded on sand. In *Dams and Weirs*, pages 151–159. American Technical Society, Chicago.

Bourinet, J.-M., Mattrand, C., and Dubourg, V. (2009). A review of recent features and improvements added to FERUM software. *10th International Conference on Structural Safety and Reliability (ICOSSAR'09), Osaka, Japan*.

Buijs, F. A., van Gelder, P. H. A. J. M., Vrijling, J. K., Vrouwenvelder, A. C. W. M., Hall, J. W., Sayers, P. B., and Wehrung, M. J. (2003). Application of Dutch reliability-based flood defence design in the UK. In *ESREL - European Safety and Reliability Confrence 2003*, Maastricht, The Netherlands.

Calle, E. O. F. (1999). Proven Strenghth - Comparison of Deterministic and Probabilistic Approach, GeoDelft (now Deltares), report no. 385640/18. Technical Report report 385640/18, Delft.

Calle, E. O. F. (2001). Assessment of Safety against Slope Failure of existing Earth Structures. Number March, pages 1001–1007.

Calle, E. O. F. (2005). Observed strength of dikes (in Dutch: Bewezen sterkte bij dijken). *Geotechniek*, 2005(1).

Calle, E. O. F. (2010). Technisch Rapport Grondonderzoek en Grondmechanisch Schematiseren bij Dijken, Deltares report no. 1001411-010-GEO-0001. Technical report.

CBS (2009). One third of Dutch economy in jeopardy in case of flood disaster.

Cetin, K. and Ozan, C. (2009). CPT-based probabilistic soil characterization and classification. *Journal of Geotechnical and Geoenvironmental Engineering*, 135(1):84–107.

Ching, J., Chen, J.-R., Yeh, J.-Y., and Phoon, K. K. (2012). Updating Uncertainties in Friction Angles of Clean Sands. *Journal of Geotechnical and Geoenvironmental Engineering*, 138(2):217–229.

Ching, J. and Hsieh, Y.-H. (2006). Updating Reliability of Instrumented Geotechnical Systems Via Simple Monte Carlo Simulation. *Journal of GeoEngineering*, 1(2):71–78.

Ching, J., Lin, H. D., and Yen, M. T. (2011). Calibrating resistance factors of single bored piles based on incomplete load test results. *ASCE Journal of Engineering Mechanics*, 137(5):309–323.

Ching, J. and Phoon, K.-K. (2011). A quantile-based approach for calibrating reliability-based partial factors. *Structural Safety*, 33(4-5):275–285.

Ching, J. and Phoon, K. K. (2012). Establishment of generic transformations for geotechnical design parameters. *Structural Safety*, 35:52–62.

Chugaev (1965). On the Determination of Erosion Resistance of the Subsoil under Dams (in Russian). *Gydrotechnicskoe stroitelstro*, 35(2):34–37.

CIRIA (2013). International Levee Handbook (ILH). Technical report, CIRIA, London, UK.

Corotis, R. B., Hugh Ellis, J., and Jiang, M. (2005). Modeling risk-based inspection, maintenance and life-cycle cost with partially observable Markox decision processes. *Structure and Infrastructure Engineering*, (1):75–84.

CRBE (1994). Sampling Strategies for Contaminated Land. Technical Report CLR Report

No. 4.

Cressie, N. (1990). The Origins of Krigin. *Mathematical Geology*, 22:239–252.

CUR (1992). *Construeren met grond (CUR 162) - Grondconstructies op en in weinig draagkrachtige en sterk samendrukbare grond (in Dutch)*. Civieltechnisch Centrum Uitvoering Research en Regelgeving.

Dasaka, S. M. and Babu, P. G. L. S. (2005). *Probabilistic Site Characterization and Reliability Analysis of Shallow Foundations and Slopes*. PhD thesis, Bangalore.

Davidenkoff, R. (1956). Zur Berechnung des hydraulischen Grundbruches. *Wasserwirtschaft*, 46.

Davidenkoff, R. (1970). *Unterlaeufigkeit von Stauwerken*. Werner-Verlag, Duesseldorf.

Deltacommissie (1960). Delta Committee Final Report and Interim Advice.

Deltacommissie (2008). Working Together with Water - Findings of the Deltacommissie 2008 - Summary and Conclusions.

Der Kiureghian, A. and Ditlevsen, O. (2009). Aleatory or epistemic? Does it matter? *Structural Safety*, 31(2):105–112.

Ditlevsen, O. (1979). Narrow Reliability Bounds for Structural Systems. *Journal of Structural Mechanics*, 7(4):453–472.

Ditlevsen, O. (1996). *Structural Reliability Methods*. John Wiley & Sons, Chichester, UK, edition 2. edition.

Ditlevsen, O. (2003). Decision Modelling and Acceptance Criteria. *Structural Safety*, 25(2):165–191.

Ditlevsen, O., Tarp-Johansen, N. J., and Denver, H. (2000). Bayesian soil assessments combining prior with posterior censored samples. *Computers and Geotechnics*, 26:187–198.

DNV (2007). Statistical Representation of Soil Data (Recommended Practice DNV-RP-C207). Technical Report DNV-RP-C207, Det Norske Veritas.

Dupuit, J. (1863). *Estudes Theoriques et Pratiques sur le mouvement des Eaux dans les canaux dècouverts et a travers les terrains permeables (Second Edition ed.)*. Paris.

EN1990 (2002). Eurocode 0 - Basis of Structural Design, CEN (European Committee for Standardization).

EN1997-1 (2005). Eurocode 7 - Geotechnical design - Part 1: General Rules, CEN (European Committee for Standardization).

EN1997-2 (2007). Eurocode 7 - Geotechnical design - Part 2: Ground investigation and testing, CEN (European Committee for Standardization).

Faber, M. H. (2007). Assessing and Managing Risks due to Natural Hazards. In *ISGSR2007 First International Symposium on Geotechnical Safety and Risk*, pages 53–70, Shanghai, China.

Faber, M. H. (2008). Interpretation of Uncertainties and Probabilities in Civil Engineering Decision Analysis (Background document no. 2 on risk assessment in engineering).

Faber, M. H. (2012). *Statistics and Probability Theory*, volume 18 of *Topics in Safety, Risk,*

Reliability and Quality. Springer, Dordrecht, Netherlands.

Faber, M. H., Engelund, S., Sorensen, J. D., and Bloch, A. (2000). Simplified and generic risk based inspection planning. In *19th Offshore mechanics and arctic engineering conference, New Orleans, ASME*.

Faber, M. H., Maes, M. A., Baker, J. W., Vrouwenvelder, T., and Takada, T. (2007). Principles of risk assessment of engineered systems. In *10th International Conference on Application of Statistic and Probability in Civil Engineering (ICASP10)*.

Fauchard, C. and Meriaux, P. (2004). Geophysical and geotechnical methods for diagnosing flood protection dikes.

Fellenius, B. H. and Eslami, A. (2000). Soil Profile Interpreted From CPTu Data. In *"Year 2000 Geotechnics" Geotechnical Engineering Conference*, Bangkok, Thailand.

Fenton, G. A. (1990). *Simulation and Analysis of Random Fields*. PhD thesis.

Fenton, G. A. (1999a). Estimation for Stochastic Soil Models. *Journal of Geotechnical and Geoenvironmental Engineering*, 125(6):470–485.

Fenton, G. A. (1999b). Random Field Modeling of CPT Data. *Journal of Geotechnical and Geoenvironmental Engineering*, 125(6):486–498.

Fenton, G. A. and Griffiths, D. V. (2008). *Risk Assessment in Geotechnical Engineering*. John Wiley and Sons, New York.

Fenton, G. A. and Vanmarcke, E. H. (1990). Simulation of Random Fields via Local Average Subdivision. *Journal of Engineering Mechanics*, 116(8):1733–1749.

Ferguson, C. C. (1992). The Statistical Basis for Spatial Sampling of Contaminated Land. *Ground Engineering*, pages 34–39.

Finetti, B. D. (1937). Foresight: Its Logical Laws, its subjective sources. *Studies in Subjective Probability*, pages 93–158.

Finetti, B. D. (1972). *Probability, Induction and Statistics: The Art of Guessing*. New John Wiley, London.

Forchheimer, P. (1886). Ueber die Ergiebigkeit von Brunnen-Anlagen und Sickerschlitzen. *Z. Architekt. Ing.-Ver (Hannover)*, (32):539–563.

Garre, L. and Friis-Hansen, P. (2013). Using Bayesian networks and value of information for risk-based adaptation to climate change: an application of the DNV-ADAPT framework. In *11th International conference on structural safety and reliability (ICOSSAR 2013)*.

Gilbert, R. B. and Traver, R. G. (2009). Beyond Assessing and onto Managing Risk for Levees. *Journal of Contemporary Water Research and Education*, 2009(141):15–20.

Goldsworthy, J. S. (2006). *Quantifying the Risk of Geotechnical Site Investigations*. PhD thesis.

Goldsworthy, J. S., Jaksa, M. B., Fenton, G. A., Griffiths, D. V., Kaggwa, W. S., and Poulos, H. G. (2007). Measuring the Risk of Geotechnical Site Investigations. In *Geo-Denver 2007*, volume 233. ASCE.

Halim, I. S. and Tang, W. H. (1990). Bayesian Method for Characterization of Geological Anomaly. In *First International Symposium on Uncertainty Modeling and Analysis*,

number 1, pages 585–590.

Halim, I. S. and Tang, W. H. (1993). Site Exploration Strategy for Geologic Anomaly Characterization. *Journal of Geotechnical Engineering*, 119(2):195–213.

Halim, I. S., Tang, W. H., and Garret, J. H. (1991). Knowledge-assisted interactive probabilistic site characterization. In *Geotechnical Engineering Congress*, pages 264–275. ACSE.

Hanses, U., Mueller-Kirchenbauer, H., and Savidis, S. (1985). Zur Mechanik der rueckschreitenden Erosion unter Deichen und Daemmen. *Bautechnik*, 1985(5):163–168.

Harza, L. F. (1935). Uplift and seepage under dams on sand. *Transactions of the American Society of Civil Engineers*, 100:1352–1385.

Hasofer, A. M. and Lind, N. C. (1974). An Exact and Invariant First-Order Reliability Format. *ASCE*, 100(EM1):111–121.

Hastings, W. K. (1970). Monte Carlo sampling methods using Markov chains and their applications. *Biometrika*, 57:97–109.

Heisenberg, W. (1927). Ueber den anschaulichen Inhalt der quantentheoretischen Kinematik und Mechanik. *Zeitschrift für Physik*, 43:172–198.

Hoeg, K. (1996). Performance evaluation, safety assessment and risk analysis for dams. *International Journal on Hydropower and Dams*, 3(6):51–58.

Hohenbichler, M. and Rackwitz, R. (1983). First order concepts in system reliability. *Structural Safety*, 1:177–188.

Honjo, Y. (2008). Monte Carlo simulation in reliability analysis. In Phoon, K. K., editor, *Reliability-based design in Geotechnical Engineering*, chapter 4, pages 169–191. Taylor & Francis, London and New York.

Jaksa, M. B., Kaggwa, W. S., Fenton, G. A., and Poulos, H. G. (2003). A Framework for Quantifying the Reliability of Geotechnical Investigations.

Jongejan, R. B. (2008). *How safe is safe enough ?* PhD thesis, Delft University of Technology.

Jongejan, R. B., Stefess, H., Roode, N., Ter Horst, W., and Maaskant, B. (2013). The VNK2-project: a fully probabilistic risk analysis for all major levee systems in the Netherlands. *IAHS Publication*, 357: Flood.

Jonkman, S. N., Van Gelder, P. H. J. M., and Vrijling, J. K. (2003). An overview of quantitative risk measures for loss of life and economic damage. *Journal of Hazardous Materials, vol. 99(1), 1-30.*, 99(1):1–30.

Journel, A. and Huijbregts, C. (1978). *Mining Geostatistics*. Academic Press London.

Kanning, W. (2012). *The Weakest Link - Length Effects for Piping*. Phd thesis, Delft University of Technology, Delft, The Netherlands.

Kanning, W., Van Baars, S., and Vrijling, J. K. (2008). The Stability of Flood Defences on Permeable Soils: The London Avenue Canal Failures in New Orleans. In *Case Histories in Geotechnical Engineering*, Arlington, VA.

Krige, D. (1951). *A statistical approach to some mine valuations and allied problems at*

the Witwatersrand. Master's thesis, University of Witwatersrand.

Lane, E. W. (1935). Security from underseepage: Masonary dams on earth foundations. *Trans. Am. Soc. Civ. Eng.*, 100(paper no. 1919):1235–1272.

Lemaire, M., Chateauneuf, A., and Mitteau, J.-C. (2009). *Structural Reliability*. Iste, London, UK.

Lendering, K. T., Jonkman, S. N., and Kok, M. (2014). Effectiveness and reliability of emergency measures for flood prevention. Technical report, Delft University of Technology.

Lopez de la Cruz, J., Calle, E. O. F., and Schweckendiek, T. (2011). Calibration of Piping Assessment Models in The Netherlands. In *3rd International Syposium on Geotechnical Safety and Risk (ISGSR 2011)*, pages 587–595, Munich.

Lopez de la Cruz, J., Schweckendiek, T., Mai Van, C., and Kanning, W. (2010). Calibration of Partial Resistance Factors for Piping and Uplift (1202123-002-GEO-0005). Technical report, Deltares, Delft, Netherlands.

Madsen, H. O., Krenk, S., and Lind, N. C. (1986). *Methods of structural safety*. Prentice-Hall, Englewood Cliffs, NJ.

Mendell, R. C. and Elston, N. R. (1974). Multifactorial qualitative traits: genetic analysis and prediction of recurrence risks. *Biometrics*, 30:41–57.

Meriaux, P. and Royet, P. (2007). Surveillance, maintenance and diagnosis of flood protection dikes.

Metropolis, N., Rosenbluth, A. W., Rosenbluth, M. N., Teller, A. H., and Teller, E. (1953). Equation of State Calculations by Fast Computing Machines. *Journal of Chemical Physics*, 21:1087–1092.

Morgan, M. G. (1990). *Uncertainty: A Guide to Dealing With Uncertainty in Quantitative Risk and Policy Analysis*. Cambridge University Press, Cambridge, New York.

Moula, M., Toll, D. G., and Vaptismas, N. (1995). Knowledge-based systems in geotechnical engineering. *Geotechnique*, 45(2):209–221.

Mueller-Kirchenbauer, H. (1978). Zum zeitlichen Verlauf der rueckschreitenden Erosion in geschichtetem Untergrund bei Daemmen und Stauanlagen .

Nataf, A. (1962). Determination des distributions de probabilites dont les marges sont donnees. *Comptes Rendus de l Académie des Sciences A 225*, pages 42–43.

Neal, R. M. (2003). Slice Sampling. *The Annals of Statistics*, 31(3):705–741.

Niederleithinger, E. (2007). Evaluation of Geophysical Methods for River Embankment Investigation. In *EFRM*, Dresden.

Ohle, N. (2005). Fault Assessment of Flood Protecting Dikes with Remote Sensing. In *International Conference on Solutions to Coastal Disasters*, Charleston, USA.

Ozkan, S. (2003). *Analytical Study on Flood Induced Seepage Under River Levees*. PhD thesis.

Papaioannou, I. and Straub, D. (2012). Reliability updating in geotechnical engineering including spatial variability of soil. *Computers & Geotechnics*, 42:44–51.

Peck, R. B. (1969). Advantages and Limitations of the Observational Method in Applied

Soil Mechanics. *Géotechnique*, 19(2):171–187.

Peng, M., Li, X., Li, D., Jiang, S., and Zhang, L. (2013). Slope safety evaluation by integrating multi-source monitoring information. *Structural Safety*.

Phoon, K. K. (2008). *Reliability-Based Design in Geotechnical Engineering*. Taylor & Francis, Oxon, UK.

Phoon, K. K. and Kulhawy, F. H. (1995). Reliability-Based Desgin of Foundations for Transmission Line Structures. Technical report, Geotechnical Engineering Group, Cornell University.

Phoon, K. K. and Kulhawy, F. H. (1999). Characterization of Geotechnical Variability. *Canadian Geotechnical Journal*, 36:612–624.

Phoon, K. K. and Kulhawy, F. H. (2003). Evaluation of model uncertainties for reliability-based foundation design.

Phoon, K. K., Quek, S.-T., and An, P. (2003). Identification of Statistically Homogeneous Soil Layers Using Modified Bartlett Statistics. *Journal of Geotechnical and Geoenvironmental Engineering*, 129(7):649–659.

Rackwitz, R. (2000). Reviewing probabilistic soils modelling. *Computers and Geotechnics*, 26(3-4):199–223.

Raiffa, H. and Schlaifer, R. (1961). *Applied Statistical Decision Theory*. Cambridge University Press, Cambridge, Massachusetts.

Rice, J. D. and Polanco, L. (2012). Reliability-Based Underseepage Analysis in Levees Using a Response Surface–Monte Carlo Simulation Method. *Journal of Geotechnical and Geoenvironmental Engineering*, 138(7):821–830.

Rijkswaterstaat (2005). Flood Risks and Safety in the Netherlands (Floris). Technical Report DWW-2006-014, Rijkswaterstaat, Netherlands.

Rijkswaterstaat (2007). Hydraulische randvoorwaarden primaire waterkeringen. Technical report, Rijkswaterstaat, Netherlands.

Rijkswaterstaat (2008). Decimeringshoogten TMR2006. Technical Report RW1708-1-008, Rijkswaterstaat, Netherlands.

Robertson, P. (1990). Soil classification using the cone penetration test. *Canadian Geotechnical Journal*, 27(1):151–158.

Robertson, P. (2010). Estimating in-situ soil permeability from CPT & CPTu. In *2nd International Symposium on Cone Penetration Testing*.

Rosenblatt, M. (1952). Remarks on a Multivariate Transformation. *Annals of Mathematical Statistics*, 23(3):470–472.

Saucke, U. (2006). Nachweis der Sicherheit gegen innere Erosion fuer koernige Erdstoffe. *Geotechnik*, 29(1):43–54.

Savage, L. J. (1974). *The foundations of statistics*. Dover Pubilcations Inc., New York.

Schweckendiek, T. (2010). Reassessing Reliability Based on Survived Loads. In *International Conference of Coastal Engineering*, Shanghai, China.

Schweckendiek, T. (2013). Using head monitoring for reliability updating of levees. In

Geotechnical Safety and Risk IV, pages 365–370, Hong Kong.

Schweckendiek, T. and Calle, E. O. F. (2010). A Factor of Safety for Geotechnical Characterization. In *Proc. of the Seventeenth Southeast Asian Geotechnical Conference (17SEAGC)*, volume Vol. II: P, pages 227–230, Taipei, Taiwan.

Schweckendiek, T., Calle, E. O. F., and Vrouwenvelder, A. (2012a). Updating Levee Reliability with Performance Observations. In *2nd European Conference on Flood Risk Management (FLOODrisk 2012)*, Rotterdam, The Netherlands.

Schweckendiek, T. and Kanning, W. (2009). Updating piping probabilities with survived loads. In *7th International Probabilistic Workshop, Delft, The Netherlands*.

Schweckendiek, T. and Rijneveld, B. (2012). DIS: Onzekerheden Ondergrondmodelering - Part 2: Reducing Piping Uncertainties with Field Observations (Flood Control 2015, report no. 2011.07.02.1). Technical Report 2011.07.02.1.

Schweckendiek, T., van Gelder, P., and Calle, E. O. F. (2011). On risk-based geotechnical site investigation of flood defenses. In Faber, Koehler, and Nishijima, editors, *Applications of Statistics and Probability in Civil Engineering (ICASP 11)*, volume ISBN 978-0, pages 1700–1708, Zurich, Switzerland. Taylor & Francis Group, London.

Schweckendiek, T., Vrouwenvelder, A., and Calle, E. (2014). Updating piping reliability with field performance observations. *Structural Safety*, 47:13–23.

Schweckendiek, T. and Vrouwenvelder, A. C. W. M. (2013). Reliability Updating and Decision Analysis for Head Monitoring of Levees. *Georisk*, 7(2):110–121.

Schweckendiek, T., Vrouwenvelder, A. C. W. M., Calle, E. O. F., Kanning, W., and Jongejan, R. B. (2012b). Target Reliabilities and Partial Factors for Flood Defenses in the Netherlands. In Arnold, P., Fenton, G. A., Hicks, M. A., and Schweckendiek, T., editors, *Modern Geotechnical Codes of Practice - Code Development and Calibration*, pages 311–328. Taylor and Francis.

Sellmeijer, J. B. (1988). *On the Mechanism of Piping under Impervious Structures*. Phd thesis, Delft University of Technology, Delft, The Netherlands.

Sellmeijer, J. B., Lopez De La Cruz, J., Van Beek, V. M., and Knoeff, J. G. (2011). Fine-tuning of the backward erosion piping model through small-scale, medium-scale and IJkdijk experiments. *European Journal of Environmental and Civil Engineering*, 2011:1139–1154.

Stallen, P. J. M., Geerts, R., and Vrijling, J. K. (1996). Three concepts of quantified societal risk. *Risk Analysis*, 16(5).

Straub, D. (2004). *Generic Approaches to Risk-Based Inspection Planning for Steel Structures*. Phd thesis, ETH Zurich, Zuerich.

Straub, D. (2011). Reliability Updating with Equality Information. *Probabilistic Engineering Mechanics*, 26 (2011):254–258.

Straub, D. (2014). Value of Information Analysis with Structural Reliability Methods. *Structural Safety*, (in press).

Straub, D. and Faber, M. H. (2004). System effects in generic risk based inspection planning. *Journal of Offshore Mechanics and Arctic Engineering*, 126(3):265–271.

Taleb, N. N. (2007). *The Black Swan: the impact of the highly improbable*. Penguin, London.

Tang, W. H. (1971). A Bayesian Evaluation of Information for Foundation Engineering Design. In *International Conference on Applications of Statistics and Probability to Soil and Structural Engineering*, Hong Kong. Hong Kong University Press.

TAW (1994). Water tegen de dijk. Technical Report X4 94.04, Technische Adviescommissie Waterkeringen.

TAW (1995). Druk op de dijken. Technical Report X4 95.13, Technische Adviescommissie Waterkeringen.

TAW (1999). Technical Report on Sand Boils (Piping). Technical report, Technische Adviescommissie Waterkeringen.

TAW (2004). Waterspanningen bij Dijken. Technical report, Technische Adviescommissie Waterkeringen.

Terzaghi, K. (1929). Effect of Minor Geological Details on the Safety of Dams. *Bulletin of the American Institute of Mining and Metallurgical Engineers*, (TP 125):31–44.

Thoens, S. and Faber, M. H. (2013). Assessing the value of structural health monitoring. In *11th International conference on structural safety and reliability (ICOSSAR 2013)*.

UNESCO (2008). Some flood damage estimate of the world. Technical report.

USACE (1956). Investigation of Underseepage and its Control. Technical Report TM 3-424, USACE-WES, Vicksburg, MS.

USACE (2000). Design and Construction of Levees, United States Army Corps of Engineers (USACE), Engineer Manual EM 1110-2-1913.

USACE (2005). Design Guidance for Levee Under-Seepage, United States Army Corps of Engineers (USACE), Technical Letter ETL 1110-2-569.

USACE (2006). Reliability Analysis and Risk Assessment for Seepage and Slope Stability Failure Modes for Embankment Dams, United States Army Corps of Engineers (USACE), Technical Letter ETL 1110-2-561.

USACE (2011). Risk characterization for levees (Levee Safety Program), White Paper, 30 April 2011.

Van Beek, V. and Knoeff, H. (2010). SBW Piping: Hervalidatie Piping - HP5.5a Analyse en validatie full-scale proeven (in Dutch).

Van Beek, V., Knoeff, H., and Schweckendiek, T. (2011a). Piping: Over 100 Years of Experience - From Empiricism to Reliability-based Design. In *A feeling for Soil and Water A Tribute to Prof. Frans Barends*, pages 143–158. Deltares Select Series - Volume 7.

Van Beek, V. M., Knoeff, J. G., and Sellmeijer, J. B. (2011b). Observations on the process of backward erosion piping in small-, medium- and fullscale experiments. *European Journal of Environmental and Civil Engineering*, 2011:1115–1137.

Van Dantzig, D. (1953). Economic Decision Problems for Flood Prevention. *Econometrica*, 24(3):276–287.

Van den Eijnden, A. (2010). *Conditional simulation for characterising the spatial variability of sand state*. Msc thesis, Delft University of Technology.

Van der Most, H. and Wehrung, M. (2005). Dealing with Uncertainty in Flood Risk Assessment of Dike Rings in the Netherlands. *Natural Hazards*, 2005(36):191–206.

Van Gelder, P. H. A. J. M. (2000). *Statistical Methods for the Risk-Based Design of Civil Structures*. Phd thesis, Delft University of Technology, Delft.

Van Manen, S. E. and Brinkhuis, M. (2005). Quantitative flood risk assessment for Polders. *Reliability Engineering & System Safety*, 90(2-3):229–237.

Vanmarcke, E. H. (1975). On the Distribution of the First-Passage Time for Normal Stationary Random Processes. *Journal of Applied Mechanics*, 42(1):215–220.

Vanmarcke, E. H. (1977). Probabilistic modeling of soil profiles. *Journal of Geotechnical Engineering Division (ASCE)*, 103(GT11):1227–1246.

Vanmarcke, E. H. (1983). *Random Fields: Analysis and Synthesis*. The MIT Press.

Von Neumann, J. and Morgenstern, O. (1947). *Theory of games and economic behavior, Second Edition*. Princeton University Press, Princeton.

Voortman, H. G. (2003). *Risk-based design of large scale flood defences*. Phd thesis, Delft University of Technology.

Vorogushyn, S., Merz, B., and Apel, H. (2009). Development of dike fragility curves for piping and micro-instability breach mechanisms. *Natural Hazards and Earth System Sciences*, (9):1383–1401.

Vrijling, J. K. and Gelder, P. V. (1998). The Effect of Inherent Uncertainty in Time and Space on the Reliability of Flood Protection. In *Safety and Reliability (ESREL 1998)*, pages 451–456, Trondheim.

Vrijling, J. K., Hengel, W., and Houben, R. J. (1998). Acceptable risk as a basis for design. *Reliability Engineering and System Safety*, 59:141–150.

Vrijling, J. K., Kok, M., Calle, E. O. F., Epema, W. G., van der Meer, M. T., van den Berg, P., and Schweckendiek, T. (2010). Piping - Realiteit of Rekenfout? (in Dutch). Technical report, Dutch Expertise Network on Flood Protection (ENW).

Vrijling, J. K., Schweckendiek, T., and Kanning, W. (2011). Safety Standards of Flood Defenses. In *3rd International Syposium on Geotechnical Safety and Risk (ISGSR 2011)*, Munich, Germany.

Vrouwenvelder, A. and Steenbergen, H. (2003). Theoriehandleiding PC-Ring - Deel A: Mechanismebeschrijvingen. Technical Report 2003-CI-R0020, TNO, Delft, The Netherlands.

Vrouwenvelder, A. C. W. M. (1987). Probabilistic Design of Flood Defences. Technical report, Delft, The Netherlands.

Vrouwenvelder, A. C. W. M. (1997). The JCSS probabilistic model code. *Structural Safety*, 19(3):245–251.

Vrouwenvelder, A. C. W. M. (2006). Spatial effects in reliability analysis of flood protection systems. In *International Forum on Engineering Decision Making*, Lake Louise, Canada.

Vrouwenvelder, A. C. W. M. and Vrijling, J. K. (2001). Kansen, onzekerheden en hun interpretatie. Technical Report TAW-V-18.

VTV (2006). Dutch Safety Assessment Rules for Flood Defences (in Dutch: Voorschrift toetsen op veiligheid). Technical report.

Wang, Y., Au, S.-K., and Kulhawy, F. H. (2011). Expanded Reliability-Based Design Approach for Drilled Shafts. *Journal of Geotechnical and Geoenvironmental Engineering*, 137(2):140–149.

Weijers, J. B. and Sellmeijer, J. (1993). A new model to deal with the piping mechanism. In Brauns, H. b. S. e., editor, *Filters in Geotechnical and Hydraulic Engineering*, volume ISBN905410. Balkema, Rotterdam.

Weijers, J. B. A. and Barends, F. B. J. (1988). Transient Effects in Geohydrological Systems. In Kolkman, P. A., Lindenberg, J., and Pilarczyk, K. W., editors, *International Symposium on Modelling Soil-Water-Structure Interactions (SOWAS 1988)*, pages 395–401, Delft. Balkema, Rotterdam.

Wiersma, A., Vonhoegen, L., Kleine, M. D., Hoogendoorn, R., Gruijters, S., Maljers, D., and Marges, V. (2011). Rapportage bepaling ondergrondparameters piping VNK2 (in Dutch). Technical Report 1203622-000-BGS-0004, Deltares.

Wolff, T. F. (1994). Evaluating the Reliability of Existing Levees. Technical Report ETL 1110-2-556, USACE.

Wolff, T. F. (2002). Performance of Levee Underseepage Controls: A Critical Review. Technical Report ERDC/GSL TR-02-19.

Wolff, T. F. (2008). Reliability of levee systems. In Phoon, K. K., editor, *Reliability-based design in Geotechnical Engineering*, chapter 12, pages 449–496. Taylor & Francis, London and New York.

Zhang, J., Zhang, L. M., and Tang, W. H. (2011). Slope Reliability Analysis Considering Site-Specific Performance Information. *Journal of Geotechnical and Geoenvironmental Engineering*, 137(3):227–238.

Zhang, L. M. (2004). Reliability Verification Using Proof Pile Load Tests. *Journal of Geotechnical Engineering and Geoenvironmental Engineering*, 130(11):1203–1213.

Appendices

A

GROUNDWATER FLOW MODEL

This appendix describes the ground water flow model applied in this thesis to analyse uplift (3.2.2) and heave (3.2.3). For both mechanisms the head in the aquifer ϕ [m] needs to be estimated. Notice that in the following all surface and phreatic levels are denoted as h (with a subscript), whereas the ϕ stand for hydraulic heads in the aquifer.

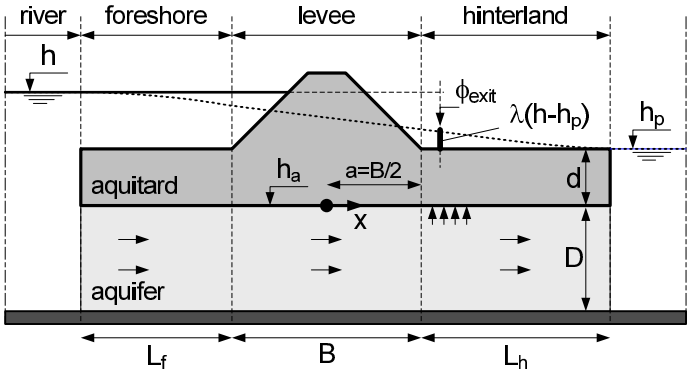

Figure A.1: Groundwater flow model for an aquifer under an impermeable levee with leakage through the foreshore and landside blanket (adopted from TAW (2004))

The most common situation in the Netherlands is an aquifer underlying a (semi-pervious) blanket layer. A blanket may be present in the hinterland as well as in the foreshore. Figure A.1 contains a schematic representation of that situation and the associated groundwater flow model.

The groundwater flow and hydraulic heads in the aquifer can be modeled by Dupuit flow (i.e., predominantly horizontal flow with vertical leakage). Assuming the levee itself to be impermeable, the hydraulic resistance of the aquifer in the section beneath the dike is given by $W = B/(kD)$ (with B [m] being the levee footprint, k [m/s] the hydraulic

conductivity of the aquifer and D [m] the aquifer thickness), while the foreshore and hinterland part of the system have the following resistances respectively

$$W_f = \frac{\lambda_f}{kD}\tanh\frac{L_f}{\lambda_f} \tag{A.1}$$

$$W_h = \frac{\lambda_h}{kD}\tanh\frac{L_h}{\lambda_h} \tag{A.2}$$

where L_f [m] and L_h [m] are the lengths of the foreshore and hinterland respectively and $\lambda_i = \sqrt{kDd_i/k_i}$ is the so-called *leakage factor* in the foreshore (i=f) and the hinterland (i=h); d_i are the respectice blanket thicknesses. Hence, the total resistance of the aquifer is given by:

$$\sum W = W_f + W + W_h \tag{A.3}$$

The head at the landside toe of the dike is:

$$\phi_t = \phi(B/2) = h_p + (h - h_p)\frac{W_h}{\sum W} \tag{A.4}$$

$$= h_p + (h - h_p)\frac{\lambda_h \tanh\frac{L_h}{\lambda_h}}{\lambda_f \tanh\frac{L_f}{\lambda_f} + B + \lambda_h \tanh\frac{L_h}{\lambda_h}} \tag{A.5}$$

The development of the head from the toe in the direction of the hinterland then be calculated by:

$$\phi(x) = h_p + (\phi_t - h_p)\frac{\sinh\frac{B/2+L_h-x}{\lambda_h}}{\sinh\frac{B/2+L_h}{\lambda_h}} \tag{A.6}$$

In order to avoid introducing unimportant variables the following assumptions seem justified for the typical conditions encountered in the Netherlands:

1. If a finite foreshore blanket is considered, it has a significant thickness ($d_f > 1m$) and is virtually impermeable ($k_f < 10^-7$). In that case L_f/λ_f will be always small and the resistance in the foreshore part simplifies to: $W_f \approx L_f/(kD)$. Hence, d_f and k_f are not required as explicit input variables.

2. If the hinterland blanket is significant and continuous (i.e., no hydraulic contact of the aquifer with a water body in the direct vicinity of the dike, its length may be assumed infinite, for the results are then insensitive to the length. In that case the resistance of the hinterland section can be approximated by $W_h \approx \lambda_h/(kD)$ and the hydraulic head can be approximated by:

$$\phi(x) \approx h_p + (\phi_t - h_p)\exp^{(B/2-x)/\lambda_h} \tag{A.7}$$

In summary, applying the assumptions as stated above, the head at the exit point may be approximated by:

$$\phi(x) \approx h_p + (h - h_p)\frac{\lambda_h}{L_f + B + \lambda_h}\exp^{(B/2-x)/\lambda_h} \tag{A.8}$$

BLANKET THEORY

The design guidance for federal levees in the US (USACE, 2000) uses a similar approach. The so-called "blanket theory equations" provide solutions of the same problem for special cases regarding the (non)existence and length of blankets on either side of the levee as well as their permeability (i.e., semi-pervious vs. impermeable). Fig. A.2 gives an overview of the equations; more details are provided in (USACE, 2000) as for example the determination of the equivalent permeability of a blanket composed of several substrata.

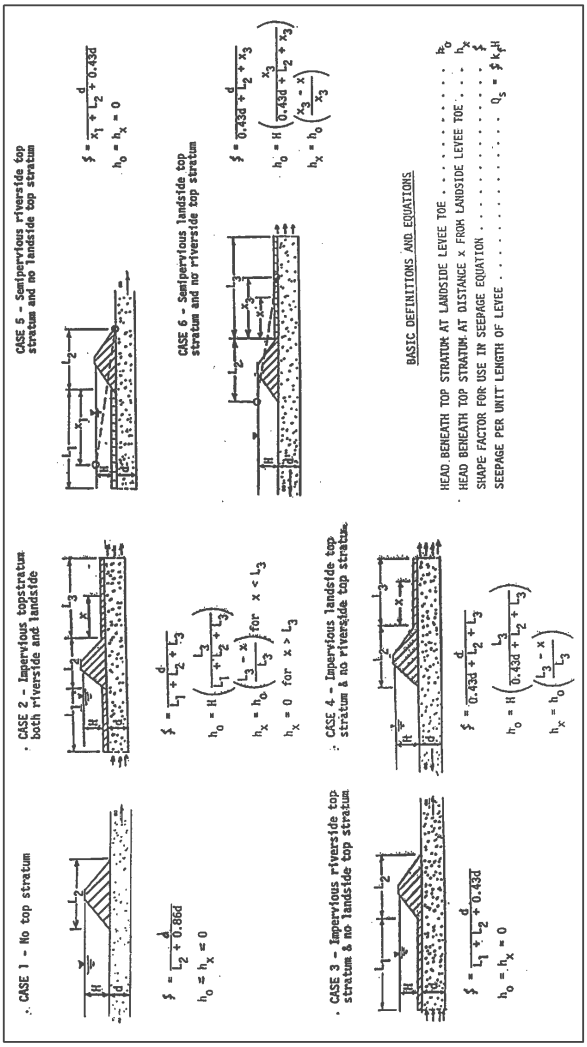

Figure A.2: Blanket theory according to USACE (2000)

B

RELIABILITY ANALYSIS

This appendix recaps the essentials of reliability analysis concepts and techniques for elements and systems as applied throughout the thesis.

B.1. RELIABILITY OF AN ELEMENT

Reliability analysis for elements is concerned with computing the *probability of failure* or unwanted events. Mathematically we define the event of failure F by means of the *limit-state function* $Z = g(\mathbf{X})$ as follows

$$F = \{g(\mathbf{X}) \leq 0\} \tag{B.1}$$

where $\mathbf{X}$ is the vector of random variables. Consequently, the probability of failure is given by

$$P(F) = \int_{g(\mathbf{x})<0} f_{\mathbf{X}}(\mathbf{x})\, d\mathbf{x} \tag{B.2}$$

Alternatively, reliability is often expressed in terms of the *reliability index* β, which is related to the probability of failure by:

$$\beta = -\Phi^{-1}(P(F)) \tag{B.3}$$

where Φ^{-1} is the inverse of the standard normal cumulative distribution function. Computing the probability of failure involves evaluating a multi-dimensional integral of the probability density of the random variables over the failure domain. Since the probabilities in structural reliability problems use to be small, numerous methods have been and are still being developed for this purpose. The ones applied in this thesis are briefly discussed below. For an extensive overview of reliability analysis techniques for structural problems the reader is referred to Ditlevsen (1996) or Lemaire et al. (2009).

B.2. Crude Monte Carlo Simulation (MCS)

In MCS random samples of the entire set of random variables are generated and the limit state function is evaluated for each realization $\mathbf{x}^{(i)}$. The probability of failure is approximated by:

$$P(F) \approx \hat{P}_f = \frac{N_F}{N} = \frac{1}{N}\sum_{i=1}^{N} \mathbf{1}\left[g(\mathbf{x}^{(i)}) < 0\right] \tag{B.4}$$

N_F being the number of LSF-evaluations leading to failure. The generation of failure samples is a Bernoulli process with the (yet unknown) probability of failure $P(F)$ being the "success probability" and number of trials equal to N. For small values of $P(F)$ the variation coefficient of the estimate is approximately:

$$V_{\hat{P}_f} = \frac{\sqrt{Var[\hat{P}_f]}}{E[\hat{P}_f]} = \frac{\sqrt{\frac{1}{N}P(F)(1-P(F))}}{P(F)} \approx \frac{1}{\sqrt{N_F}} \tag{B.5}$$

Consequently, at least 400 failure samples are necessary to achieve a "relative error" of 5% or less. In other words, if we expect the probability of failure to be as small as p, the number of MCS-realizations should be at least: $N \gtrsim 400/p$. Note that the efficiency in independent of the number of random variables, while in methods like numerical integration the required number of calculations increases in the form k^m, k being the number of discretized intervals and m the number of random variables.

The method applied in this thesis is based on the Matlab-code FERUM (Bourinet et al., 2009). Samples are generated in uncorrelated standard Gaussian space (u-space), transformed to correlated standard Gaussian space (z-space) by Nataf-transformation (Nataf, 1962) and, subsequently, to real space (x-space) using inverse CDF, which are usually available in closed form for the distribution types applied here.

B.3. First Order Reliability Method (FORM)

The *First Order Reliability Method* (FORM) is based on the linearization of the limit state ($Z = g(\mathbf{x}) = 0$) in the so-called *Design Point* in standard Gaussian space (u-space). The design point $\mathbf{x}^*$ is the point on the limit state ($Z = 0$) closest to the origin of the u-space. Consequently, it is the point with the highest probability density fulfilling in the failure region (see Fig. B.1).

The reliability index β is the distance from the origin of the u-space to the design point and given by:

$$\beta = \min_{X \in F} = \sqrt{\mathbf{u}^T\mathbf{u}} \tag{B.6}$$

For correlated equivalent Normal variables according to Hasofer and Lind (1974) the definition may be re-written as:

$$\beta = \min_{X \in F} \sqrt{\left(\mathbf{X} - \mu^N\right)^T \mathbf{C}^{-1}\left(\mathbf{X} - \mu^N\right)} \tag{B.7}$$

$$= \min_{X \in F} \sqrt{\left(\frac{X_i - \mu_i^N}{\sigma_i^N}\right)^T \mathbf{R}^{-1}\left(\frac{X_i - \mu_i^N}{\sigma_i^N}\right)} \tag{B.8}$$

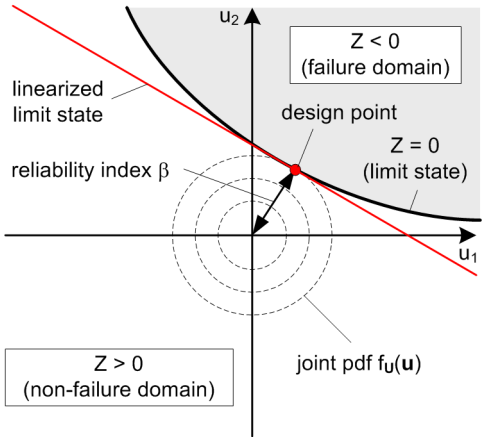

Figure B.1: FORM (geometrical) definitions for two dimensions in u-space

where **C** is the covariance matrix and **R** the correlation matrix, while μ_i^N and σ_i^N are the mean and standard deviation of the equivalent Normal distribution of variable X_i, for which the CDF as well as the PDF assume the same value as for the original variable:

$$\mu_i^N = x_i - \Phi^{-1}\left\{F_{X_i}(x_i)\right\}\sigma_i^N \tag{B.9}$$

$$\sigma_i^N = \frac{\phi\left\{\Phi^{-1}[F_{X_i}(x_i)]\right\}}{f_{X_i}(x_i)} \tag{B.10}$$

The failure probability is then determined by the inverse relation of the definition of the reliability index (Eq. B.3):

$$P(F) = \Phi\left(-\beta\right) \tag{B.11}$$

The same transformations to account for correlations and non-normal distributions as for MCS are applied (see B.2). Besides reliability FORM also gives information on the relative importance of the random variables in form of the *influence coefficients* α_i (also called *importance factors*) which are defined as follows (using alternative expressions):

$$\alpha_i = -u_i^*/\beta \tag{B.12}$$

$$= \frac{\left(\frac{\partial g(\mathbf{u})}{\partial u_i}\right)_{\mathbf{u}=\mathbf{u}^*}}{\sqrt{\sum_{j=1}^{n}\left[\left(\frac{\partial g(\mathbf{u})}{\partial u_j}\right)_{\mathbf{u}=\mathbf{u}^*}\right]^2}} \tag{B.13}$$

$$= \frac{\left(\frac{\partial g(\mathbf{X})}{\partial X_i}\right)_{\mathbf{X}=\mathbf{x}^*}\sigma_i^N}{\sqrt{\sum_{j=1}^{n}\left[\left(\frac{\partial g(\mathbf{X})}{\partial X_j}\right)_{\mathbf{X}=\mathbf{x}^*}\sigma_j^N\right]^2}} \tag{B.14}$$

$$= \left(\frac{\partial g(\mathbf{X})}{\partial X_i}\right)_{\mathbf{X}=\mathbf{x}^*}\frac{\sigma_i^N}{\sigma_Z} \tag{B.15}$$

Especially the last version (Eq. B.15) illustrates that both, sensitivity and relative uncertainty are included in the definition. Since by definition, squared influence coefficients sum up to 1 ($\sum \alpha_i^2 = 1$), α_i^2 is regarded a practical measure of the relative contribution of variable X_i to the probability of failure.

B.4. First Order Second Moment Method (FOSM)

The *First-Order Second Moment Method* (FOSM) is popular in engineering practice due to its simplicity and ease of implementation in, for example, spreadsheet analysis. However, it is well-known that the method has severe deficiencies for non-linear limit states (see Baecher and Christian, 2003). The goal of applying FOSM in this thesis is to appraise its suitability to the envisaged applications, mainly for reliability analysis for heave and piping.

The main difference of FOSM with respect to FORM is that we linearize the limit state in the expected value $\mu_{\mathbf{X}}$ instead of the design point $\mathbf{x}^*$. Hence, the reliability index is approximated by:

$$\beta = \frac{\mu_Z}{\sigma_Z} \approx \frac{g(\mu_{\mathbf{X}})}{\sqrt{\sum_{i=1}^{n}\sum_{j=1}^{n}\left[\left(\frac{\partial g(\mathbf{X})}{\partial X_i}\right)_{\mathbf{X}=\mu_{\mathbf{X}}}\left(\frac{\partial g(\mathbf{X})}{\partial X_j}\right)_{\mathbf{X}=\mu_{\mathbf{X}}}\rho_{i,j}\sigma_i\sigma_j\right]^2}} \tag{B.16}$$

For independent variables and evaluating the partial derivatives of the limit state function with respect to the random variables using finite difference (with a step size of $\delta\sigma_j$) the denominator changes to:

$$\beta \approx \frac{Z(\mu_{\mathbf{X}})}{\sqrt{\sum_{j=1}^{n}\left[\frac{Z(\mu_j+\sigma_j)-Z(\mu_j)}{\delta}\right]^2}} \tag{B.17}$$

Hence, only $n+1$ LSF-evaluations are required. An importance factor similar to FORM can be computed using:

$$\alpha_i = \frac{\left[\frac{g(\mu_i+\sigma_i)-Z(\mu_i)}{\delta}\right]^2}{\sqrt{\sum_{j=1}^{n}\left[\frac{g(\mu_j+\sigma_j)-g(\mu_j)}{\delta}\right]^2}} \tag{B.18}$$

B.5. SUBSET SIMULATION (SUBSIM)

The *Subset Simulation* (SubSim) method proposed by Au and Beck (2001) a based on Markov Chain Monte Carlo Simulation. Let F be the set representing the failure region, F_0 be the total set ($F_0 = \Omega$) and F_i (i=1...k) be subsets satisfying:

$$F_0 \supset F_1 \supset F_2 \supset ... \supset F_k \supset F \tag{B.19}$$

Using these subsets the probability of failure can be computed by:

$$P(F) = P(F|F_k)P(F_k|F_{k-1})...P(F_1|F_0) = P(F|F_k)\prod_{i=1}^{k} P(F_i|F_{i-1}) \tag{B.20}$$

Honjo (2008) gives a comprehensive description of the computational procedure and

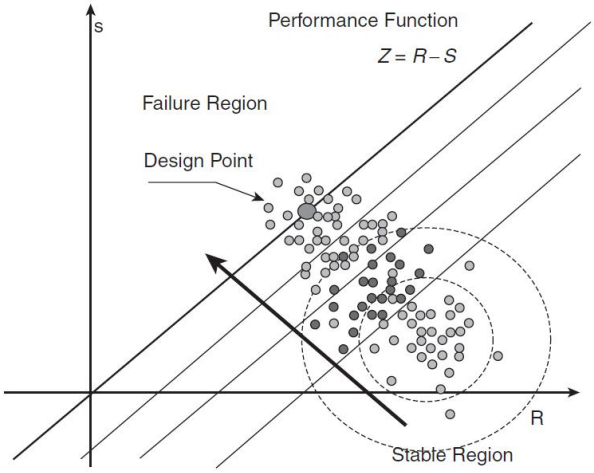

Figure B.2: A conceptual illustration of the SubSim method (Honjo, 2008)

the generation of samples my MCMC.

An importance measure that quite closely resembles the FORM importance factors α_i can be defined as:

$$\tilde{\alpha}_i = \frac{-u_m}{\|u_m\|} \tag{B.21}$$

where u_m is the mean value of the samples leading to failure in u-space. Notice that this importance measure is only meaningful for a single limit state and cannot be used in system reliability problems.

B.6. Error Measures

Except MCS which is near exact and, therefore, used as the benchmark solution, all other presented methods are approximations producing estimates $\hat{P}(F)$ of the "real" probability of failure $P(F)$. A meaningful expression for the relative error in the estimate as compared to the correct (i.e., benchmark) solution is:

$$\varepsilon_{P_f} = \left(\frac{\hat{P}(F) - P(F)}{P(F)} \right) \tag{B.22}$$

This measure will be used throughout this thesis wherever comparisons of reliability analysis methods are made.

B.7. System Reliability

While element reliability addresses the probability of failure of a structural component or a single failure mechanism, system reliability theory is required to determine the probability of sub(systems) and failure modes involving several mechanisms. The two basic types of systems are the *serial system* and the *parallel system*.

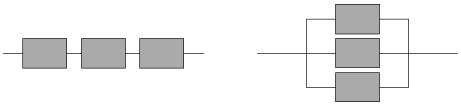

Figure B.3: A conceptual illustration of serial and parallel systems

While failure of any component leads to system failure, a parallel system only fails, if all its components fail at the same time[1]. A polder or dike ring system is an example of a series system. Failure of any dike section or hydraulic structure in the flood protection system would lead to inundation. Examples of parallel system behavior are typically encountered where several (often sequential) mechanisms have to occur in a failure mode. For example, where a blanket layer is present, heave needs to occur for piping to be initiated. Hence, both heave and piping are necessary for piping failure (see chapter 3).

Mathematically, series system failure can be described as the union of the component failure events:

$$P(F) = \bigcup_{i=1}^{n} P(F_i) \tag{B.23}$$

Parallel systems failure, on the other hand, is their intersection:

$$P(F) = \bigcap_{i=1}^{n} P(F_i) \tag{B.24}$$

[1] Notice that only brittle elements are considered here.Parallel systems with ductile failure behaviour of the elements need to be treated differently but are not relevant to the scope of this study.

B.7.1. PROBABILITY BOUNDS

For practical applications we can make use of the exact solutions for the reliability of systems with n components presented in Table B.1, once the component failure probabilities $P(F_i)$ are known. In the absence of information on the correlation between the LSFs, the extreme cases of full dependence, independence or mutual exclusivity may serve as upper or lower bounds. For situations where the correlation is known and there

system	gate	operator	components		
			mutually exclusive	independent	fully dependent
series	OR	$\cup$	$\sum_{i=1}^{n} P_i$ (upper bound)	$1-\prod_{i=1}^{n}(1-P_i)$	$\max\{P_i\}$ (lower bound)
parallel	AND	$\cap$	0 (lower bound)	$\prod_{i=1}^{n} P_i$	$\min\{P_i\}$ (upper bound)

Table B.1: Probability of failure of a system with n components

are approximations to get a better estimate such as the narrower bounds proposed by Ditlevsen (1979):

$$P(F) \leq \sum_{i=1}^{n} P(Z_i<0) - \sum_{i=2}^{n} \max_{j<i} \left[P(Z_i<0 \cap P(Z_j<0)\right] \tag{B.25}$$

$$P(F) \geq P(Z_1<0) + \sum_{i=2}^{n} \max\left[\left(P(Z_i<0) - \sum_{j=1}^{i-1} P(Z_i<0 \cap Z_j<0)\right), 0\right]$$

where

$$\Phi(-\beta_1^*)\cdot\Phi(-\beta_2) < P(Z_i<0 \cap Z_j<0) < \Phi(-\beta_1)\cdot\Phi(-\beta_2^*) + \Phi(-\beta_1^*)\cdot\Phi(-\beta_2)$$

$$\beta_i^* = \frac{\beta_i - \rho_{(Z_i,Z_j)}\beta_j}{\sqrt{1-\rho_{Z_i,Z_j}^2}}$$

B.7.2. FIRST ORDER (LEVEL II) METHODS

First order methods such as FORM can only analyze one limit state (LSF) at a time. Hence, probability of system failure cannot be determined in one FORM analysis. However, the influence coefficients α_i offer possibilities to combine limit states and provide point estimates for the system failure probability.

To begin with, the correlation between two failure modes is given by:

$$\rho_{Z_1,Z_2} = \sum_{i=1}^{n} \alpha_{i,1}\alpha_{i,2} \tag{B.26}$$

Mendell and Elston (1974) proposed the following point estimate:

$$P(F_1 \cap F_2) \approx \Phi\left[\frac{\rho_{Z_1,Z_2}\, a - \beta_2}{\sqrt{1-\rho_{Z_1,Z_2}^2\, a(a-\beta_1)}}\right]\Phi(-\beta_1) \tag{B.27}$$

with

$$a = \frac{1}{\Phi(-\beta_1)\sqrt{2\pi}} \exp\left(-\frac{\beta_2^2}{2}\right) \tag{B.28}$$

As shown by Phoon (2008) the estimate is quite accurate except for cases with large differences between the reliability indices en high correlation at the same time.

Also the point estimate method by Hohenbichler and Rackwitz (1983) has proven to be reasonably accurate. It does not offer a closed form solution, but requires solving the following probability:

$$P(F_2|F_1) = P(\beta_2 - \rho\Phi^{-1}(1-\Phi(\beta_1)\Phi(u)) - w\sqrt{1-\rho^2} < 0) \tag{B.29}$$

where u and w are independent standard Gaussian variables and $\rho = \rho_{Z_1,Z_2}$. Eq. B.29 can be solved by any reliability analysis method (e.g., FORM) and the parallel system failure probability term is found by using the definition of conditional probability:

$$P(F_1 \cap F_2) = P(F_2|F_1)P(F_1) \tag{B.30}$$

B.7.3. Level III Methods

Exact (level III) methods are usually perfectly capable of determining failure probabilities for different limit states simultaneously and also probabilities of failure of (sub)systems, if the system limit states are defined properly by using set theory or fault tree analysis.

Notice that in case of Subset simulation one needs to take care of a proper scaling of the limit state functions in order to define proper intermediate limit states and properly select the realisations that are used as seeds in the subsequent MCMC-steps.

C

LOCAL WATER LEVEL STATISTICS

This appendix describes how the (Gumbel) probability distributions for local water levels were derived in this thesis.

Gumbel Distribution for Maxima The uncertainty in the annual maximum local water level is described by a Gumbel distribution for maxima:

$$F_H(h) = \exp\left[-\exp\left(-\frac{h-\alpha}{\beta}\right)\right] \tag{C.1}$$

Gumbel Distribution based on MHW and decimate height The design water levels (MHW = Maatgevend Hoogwater) correspond with region-specific protection levels expressed in terms of exceedance probabilities (F_{exc}, see Rijkswaterstaat, 2007). Combining this information with the so-called decimate height h_{dec} (water level difference that reduces F_{exc} by a factor 10), the local Gumbel parameters can be derived using the expressions below. In order to obtain the parameters, this set of equations needs to be solved:

$$F_{exc} = \exp\left[-\exp\left(-\frac{MHW-\alpha}{\beta}\right)\right] \tag{C.2}$$

$$\frac{F_{exc}}{10} = \exp\left[-\exp\left(-\frac{(MHW-h_{dec})-\alpha}{\beta}\right)\right] \tag{C.3}$$

This results in the follwing parameters:

$$\beta = \frac{h_{dec}}{z(F_{exc}) - z(F_{exc}/10)} \tag{C.4}$$

$$\alpha = MHW + \beta z(F_{exc}) \tag{C.5}$$

where $z(F) = \ln(-\ln(1-F))$.

D

UPDATING SCENARIO PROBABILITIES

Observations such as the survival of an observed load condition can be used to update the reliability of a structure. Where we deal with continuous and discrete probability distributions, the latter often referring to scenarios of, for example, adverse geological details, it is interesting to investigate the impact of taking the information into account on the scenario probabilities. This appendix shows how scenario probabilities can be updated using survival information.

D.1. BAYES THEOREM

The posterior probability of scenario E_i, given the evidence ε is given by

$$P(E_i|\varepsilon) = \frac{P(\varepsilon|E_i)P(E_i)}{\sum_j P(\varepsilon|E_j)P(E_j)} \tag{D.1}$$

The posterior probability distribution of random variables X is similarly defined by

$$f(x|\varepsilon) = \frac{P(\varepsilon|x)f_X(x)}{\int P(\varepsilon|x)f(x)dx} \sim P(\varepsilon|x)f_X(x) \tag{D.2}$$

Eq. D.2 also holds for the joint PDF of a vector of random variables $\mathbf{X}$. The like likelihood functions $P(\varepsilon|E_i)$ and $P(\varepsilon|x)$ will be denoted as $\mathbb{L}(E_i)$ and $\mathbb{L}(x)$ respectively.

D.2. ONLY SCENARIOS

The simplest case for scenario updating is a situation where there are scenarios (E_i) with a deterministic resistance r_i each. The probability of failure $(F = \bigcup_i r_i < S|E_i)$ is then

$$P(F) = \sum_i P(r_i < S|E_i)P(E_i) \tag{D.3}$$

We want to include the information that the historical load $\acute{s}$ has been survived, which is denoted as the following event or evidence:

$$\varepsilon = \{\bar{F}|S = \acute{s}\} \tag{D.4}$$

The (relative) likelihood of a scenario is then the conditional probability of survival (i.e., non-failure):

$$L(E_i) = P(\bar{F}|E_i) = P(r_i \geq \acute{s}) \tag{D.5}$$

Since the r_i are deterministic, the likelihood function is a Heaviside step function:

$$L(E_i) = \mathbb{H}(r_i - s*) = \begin{cases} 1, & r_i \geq \acute{s}, \\ 0, & r_i < \acute{s}, \end{cases} \tag{D.6}$$

The posterior probabilities are by definition:

$$P(E_i|\varepsilon) \sim L(E_i)P(E_i)\mathbb{H}(r_i - s*) \tag{D.7}$$

Thus, the updating in this simple case implies that scenarios with $r_i < \acute{s}$ are excluded (i.e., the posterior probability is zero) and the remaining scenario probabilities are normalized.

D.3. Conditional Discrete Resistance Distributions

An extension from the previous case is that the resistance per scenario is a discrete random variable R_i with possible realisations r_{ij} and prior PMF $p(r_{ij}|E_i)$, for which the shorthand notation $p(r_{ij})$ will be used where index i already indicates the dependence with respect to scenario E_i. The probability of failure

$$P(F) = \sum_i P(R_i < S|E_i)P(E_i) = \sum_i P(E_i) \sum_j P(r_{ij} < S)\, p(r_{ij}) \tag{D.8}$$

is updated with the same event as in the previous case.

$$\varepsilon = \{\bar{F}|S = \acute{s}\} \tag{D.9}$$

Since the conditional probability distributions of the resistance per scenario are conditionally independent ($R_i \perp R_j \,|\, E_i$), their likelihood function does not depend on the scenario likelihoods.

$$L(r_{ij}) = P(\bar{F}|r_{ij}) = P(r_{ij} \geq \acute{s}) = \mathbb{H}(r_{ij} - s*) = \begin{cases} 1, & r_{ij} \geq \acute{s}, \\ 0, & r_{ij} < \acute{s}, \end{cases} \tag{D.10}$$

The posterior conditional random variables are the normalized remaining variables (i.e., the values for which the structure would have survived):

$$p(r_{ij}|\varepsilon) = \frac{L(r_{ij})p(r_{ij})}{\sum_j L(r_{ij})p(r_{ij})} \tag{D.11}$$

On the other hand, the likelihood function of the scenarios does imply the likelihood function of the conditional resistance variables:

$$L(E_i) = \sum_j P(r_{ij} \geq \acute{s}) p(r_{ij}) = \sum_j \mathbb{H}(r_{ij} - \acute{s}) p(r_{ij}) \tag{D.12}$$

Hence, the relative likelihood of the scenarios is actually their prior conditional probability of survival: $L(E_i) = P(\bar{F}|E_i)$. The posterior probability of the scenarios is obtained by applying Bayes' rule:

$$P(E_i|\varepsilon) = \frac{L(E_i)P(E_i)}{\sum_j L(E_j)P(E_j)} = \frac{P(\bar{F}|E_i)P(E_i)}{\sum_j P(\bar{F}|E_j)P(E_j)} \tag{D.13}$$

D.4. CONDITIONAL CONTINUOUS RESISTANCE DISTRIBUTIONS

In contrast to the previous case, R_i are now continuous random variables with PDF $f_{R_i}(r)$. The probability of failure is then given by:

$$P(F) = \sum_i P(E_i)P(R_i < S|E_i) = \sum_i P(E_i) \int f_{R_i}(r)(1 - F_S(r))\,dr \tag{D.14}$$

The observation is again survival of loading $\acute{s}$:

$$\varepsilon = \{\bar{F}|S = \acute{s}\} \tag{D.15}$$

Analogous to D.10, the likelihood function of the conditional random variable R_i is given by:

$$L(r_i) = P(\bar{F}|r_i) = P(r_i \geq \acute{s}) = \mathbb{H}(r_i - s*) = \begin{cases} 1, & r_i \geq \acute{s}, \\ 0, & r_i < \acute{s}, \end{cases} \tag{D.16}$$

The posterior distribution $f(r_i|\varepsilon)$ is the prior truncated at $\acute{s}$ and normalized with k to obtain a proper PDF:

$$f(r_i|\varepsilon) = k\mathbb{H}(r_i - \acute{s}) f_{R_i}(r_i) \tag{D.17}$$

The likelihood of the scenarios is, just like in the previous case, the prior conditional probability of the evidence (i.e., survival):

$$L(E_i) = P(\varepsilon|E_i) = P(\bar{F}|E_i, \{S = \acute{s}\}) = P(R_i > \acute{s}) = \int_{\acute{s}}^{\infty} f_{R_i}(r)\,dr = 1 - F_{R_i}(\acute{s}) \tag{D.18}$$

The posterior probability of the scenarios is obtained by applying Bayes' rule:

$$P(E_i|\varepsilon) = \frac{P(\bar{F}|E_i, \{S = \acute{s}\})P(E_i)}{\sum_j P(\bar{F}|E_i, \{S = \acute{s}\})P(E_j)} \tag{D.19}$$

Furthermore, the posterior probabilities of failure are determined applying the posterior probability distributions for the scenarios ($P(E_i|\varepsilon)$) and the conditional resistance variable ($f(r_i|\varepsilon)$) in Eq. D.14 instead of the priors.

D.5. Conditional and Unconditional Continuous Resistance Distributions

D.5.1. Case 1: Unconditional Distribution Aleatory

In this case, in addition to R_i which are the conditional resistances in scenario E_i we introduce scenario-independent noise term on the resistance side Δ. The additional term is assumed (fully) aleatory, which implies that it cannot be updated. Different realisations in time are independent. The effect of such a "noise term" is the same as caused by, for example, measurement uncertainties in the observed load, time-variant elements in the resistance (e.g., rainy periods influencing the humidity of relevant ground properties) or spatial variability within the site.

The probability of failure is now given by:

$$P(F) = \sum_i P(E_i)P(R_i + \Delta < S|E_i) = \sum_i P(E_i) \iint f_{R_i}(r) f_\Delta(\delta)(1 - F_S(r+\delta))\, dr\, d\delta \tag{D.20}$$

The observation is again survival of loading $\acute{s}$:

$$\varepsilon = \{\bar{F}|S = \acute{s}\} \tag{D.21}$$

In contrast to the previous cases, the likelihood function is not a heavy-side step function anymore but a non-trivial probability. The updated distribution is not truncated anymore, but re-distributed. That is the effect of introducing a non-observed random element that is assumed to be aleatory (i.e., with independent realisations in each event).

$$L(r_i) = P(\bar{F}|r_i) = P(r_i + \Delta \geq \acute{s}) = P(\Delta \geq \acute{s} - r_i) = 1 - F_\Delta(\acute{s} - r_i) \tag{D.22}$$

Applying Bayes' rule at this point as usual gives:

$$f(r_i|\varepsilon) = k(1 - F_\Delta(\acute{s} - r_i)) f_{R_i}(r_i) \tag{D.23}$$

Similar changes apply to the likelihood of the scenarios, which remains the (prior) conditional probability of the evidence (i.e., survival):

$$L(E_i) = P(\bar{F}|E_i, \{S = \acute{s}\}) = P(R_i + \Delta > \acute{s}) = \iint [1 - F_S(r_i + d)] f(r_i|\varepsilon) f_\Delta(\delta)\, dr_i\, d\delta \tag{D.24}$$

The remaining steps to obtain the updated quantities are analogous to the other case applying the standard formulae.

D.5.2. Case 2: Unconditional Distribution Epistemic

In contrast to case 1, now we consider another scenario-independent term R_u which is epistemic. In other words, it is not a noise term but reducible uncertainty. The probability of failure is now given by:

$$P(F) = \sum_i P(E_i)P(R_i + R_u + \Delta < S|E_i) \tag{D.25}$$

The observation is again survival of loading $\acute{s}$:

$$\varepsilon = \{\bar{F}|S = \acute{s}\} \tag{D.26}$$

The likelihood function is now two-dimensional and the same for both scenarios.

$$L(r_i, r_u) = P(\bar{F}|r_i, r_u) = P(r_i + r_u + \Delta \geq \acute{s}) = P(\Delta \geq \acute{s} - r_i - r_u) = 1 - F_\Delta(\acute{s} - r_i - r_u) \quad \text{(D.27)}$$

Therefore, the joint posterior distribution for each scenario is also two-dimensional. Notice that, even though the prior distributions were independent, the posterior may be correlated and can , thus, not be taken simply as the product of the posterior marginal distributions.

$$f(r_i, r_u|\varepsilon) = k(1 - F_\Delta(\acute{s} - r_i - r_u)) f_{R_i}(r_i) f_{R_u}(r_u) \quad \text{(D.28)}$$

Similar changes apply to the likelihood of the scenarios, which remains the (prior) conditional probability of the evidence (i.e., survival):

$$L(E_i) = P(\bar{F}|E_i, \{S = \acute{s}\}) = P(R_i + R_u + \Delta > \acute{s}) \quad \text{(D.29)}$$

The remaining steps to obtain the updated quantities are analogous to the other case applying the standard formulae.

E

EXAMPLE DECISION TREE

This appendix describes how a fully risk-based decision tree would look like for the example treated in Box 2 on page 60. Suppose we are dealing with the same example as in Box 2 except for the fact that there is no target reliability constraint, but we know that the that failure of the levee section would cause a damage of 10M€. What would we choose to do now: inspect, retrofit or do nothing?

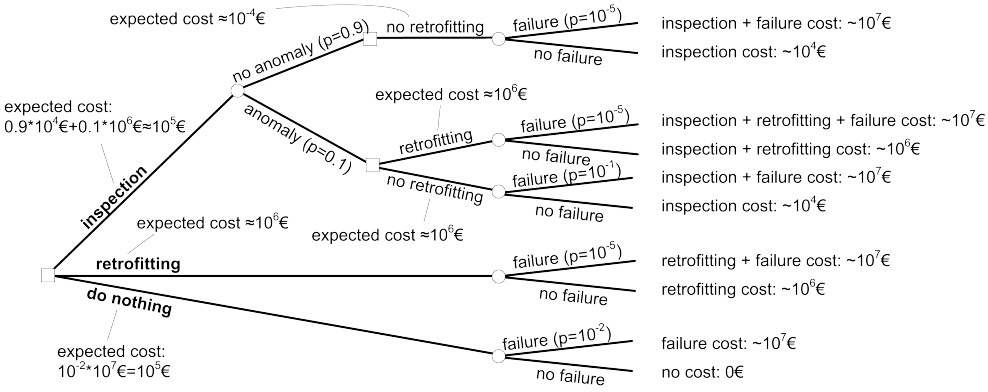

Figure E.1: Simple Example Decision Analysis - Fully Risk-based Decision Tree

The decision tree now includes the cost of failure and the decision whether to do retrofitting after inspection is now also a matter of the lowest expected cost. It is left up to the reader to retrace that investing in inspection or doing nothing would be preferred over retrofitting right-away with virtually no difference in expected cost. Notice that solving a decision tree works from the consequences to the initial decision (here from right to left) and that the nodes represented by squares are decision nodes, while circles represent the state of nature.

F

First-order Survival Updating

Calle (1999, 2005) describes an approach to update the reliability of a structure (i.e., an element or failure mode) based on first-order reliability analysis (FOSM or FORM). It is based on performance functions, which are formulated for the survived conditions as well as for the conditions to be assessed in the future. The correlation between the two functions, which can be derived from the FORM results, is the key for the updating procedure.

The performance function for the survived ("historical") situation is denoted as:

$$Z_H = Z(\mathbf{X_H}) \tag{F.1}$$

where $\mathbf{X_H}$ represents the vector of all random variables involved in the performance function (input variables, model parameters, model uncertainties etc.; here: R and S). In a FOSM framework, the reliability index is given by:

$$\beta_H = \frac{E[\mathbf{X_H}]}{\sigma(\mathbf{X_H})} \tag{F.2}$$

The influence coefficients are defined as:

$$\alpha_{X_i,H} = \frac{\partial Z_H}{\partial X_i} \frac{\sigma(X_i)}{\sigma(Z_H)} \tag{F.3}$$

The probability of failure is calculated as:

$$P(Z_H < 0) = \Phi(-\beta_H) \tag{F.4}$$

So far, the calculated probability corresponds to the a-priori probability of failure in the Bayesian approach. Hence, the reliability index is denoted as β'_H.

The vector of random variables for future assessments is denoted as $\mathbf{X_F}$. the In the same way as for the survived conditions, we can determine the (a-priori) expected value

$E[Z_F]$, the standard deviation $\sigma(Z_F)$, the reliability index β'_F and the influence coefficients $\alpha_{X_i,F}$. The probability of failure is determined by:

$$P(Z_F < 0) = \Phi(-\beta'_F) \tag{F.5}$$

The fact that the historical load situation was survived means that the performance function Z_H must have been greater than zero. The most important assumption made in this approach is now that Z_H and Z_F are normal distributed random variables[1]. The conditional expectation and standard deviation of Z_F can then be expressed as:

$$E[Z_F|Z_H = \xi] = E[Z_F] + \rho(Z_H, Z_F)\ \sigma(Z_F)\ \frac{\xi - E[Z_H]}{\sigma(Z_H)} \tag{F.6}$$

$$\sigma(Z_F|Z_H = \xi) = \sigma(Z_F)\ \sqrt{1 - \rho^2(Z_H, Z_F)} \tag{F.7}$$

where $\rho(Z_H, Z_F)$ is the correlation coefficient between Z_H and Z_F, determined by:

$$\rho(Z_H, Z_F) = \sum_{i=1}^{n} \sum_{j=1}^{n} \alpha_{X_i,H}\ \alpha_{X_j,F}\ \rho(X_{i,H}, X_{j,F}) \tag{F.8}$$

The conditional expectation of Z_F, given $Z_H < 0$, can be determined by:

$$E[Z_F|Z_H > 0] = \int_0^\infty E[Z_F|Z_H = \xi]\ f''_{Z_H}(\xi)\ d\xi \tag{F.9}$$

where $f''_{Z_H}(\xi)$ is a truncated normal distribution, based on the a-priori distribution $f'_{Z_H}(z_H)$, truncated at zero due to the observation of survival, that is:

$$f''_{Z_H}(\xi) = \frac{\varphi\left(\frac{\xi - E[Z_H]}{\sigma(Z_H)}\right)}{\sigma(Z_H)\Phi\left(\frac{E[Z_H]}{\sigma(Z_H)}\right)} = \frac{\varphi\left(\xi/\sigma(Z_H) - \beta'_H\right)}{\sigma(Z_H)\Phi\left(\beta'_H\right)} \tag{F.10}$$

The conditional standard deviation of Z_F, given $Z_H < 0$, is remains the same as in Eq. F.7, since it is independent of ξ. Assuming a normal distribution of the resulting posterior reliability index is given by:

$$\beta''_{F|Z_H>0} \approx \frac{E[Z_F|Z_H > 0]}{\sigma(Z_F|Z_H > 0)} \tag{F.11}$$

Elaboration of the right side gives:

$$\beta''_{F|Z_H>0} \approx \frac{1}{\sqrt{1 - \rho^2(Z_H, Z_F)}} \left(\beta'_F + \rho(Z_H, Z_F)\frac{\varphi(\beta'_H)}{\Phi(\beta'_H)}\right) \tag{F.12}$$

The updated probability of failure becomes:

$$P''(Z_{T|Z_H>0} < 0) \approx \Phi(-\beta''_{F|Z_H>0}) \tag{F.13}$$

[1] For limitations and references refer to Calle (2005).

G

RELIABILITY UPDATING WITH EQUALITY INFORMATION

This appendix contemplates two methods for (Bayesian) reliability updating with equality information, their commonalities and differences. The first, from here on called the "Transformation Method", is described in Ditlevsen (1996), the latter in Straub (2011).

G.1. BASIC DEFINITIONS

The failure event is defined as

$$F \equiv Z(\mathbf{X} \leq 0) \tag{G.1}$$

where $Z(\cdot)$ is the (failure) limit state function and $\mathbf{X}$ the vector of random variables with PDF $f_{\mathbf{X}}(\mathbf{x})$. Consequently, the probability of failure is given by

$$P(F) \equiv \int_{Z(\mathbf{x})\leq 0} \cdots \int f_{\mathbf{X}}(\mathbf{x}) d\mathbf{x} \tag{G.2}$$

If observation can be described in equality form by

$$\varepsilon \equiv \{h(\mathbf{X} = 0)\} \tag{G.3}$$

where $h(\cdot)$ is the observation limit state function, there are different methods to update the probability of failure, i.e. to obtain

$$P(F|\varepsilon) = \frac{P(F \cap \varepsilon)}{P(\varepsilon)} \tag{G.4}$$

Two methods to compute the updated reliability are described and compared below.

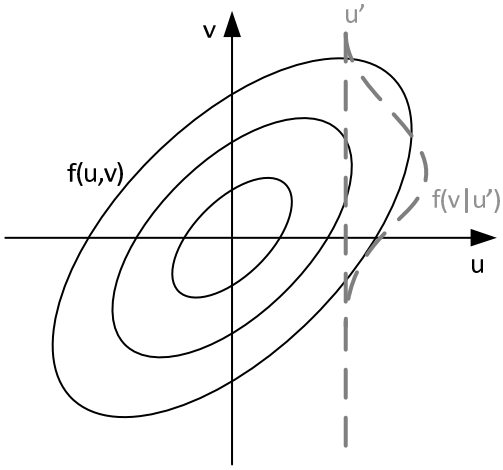

Figure G.1: Probability density of v conditional on observed $\acute{u}$, where v and u are standard normal distributed and correlated with ρ.

G.1.1. TRANSFORMATION METHOD

The "transformation method" is based on transforming the limit state function (i.e., safety margin) g and the observation h into Standard Normal space variables u and v.

If $\acute{u}$ is observed, the conditional probability distribution $f(v|\acute{u})$ is Normal distributed with mean and standard deviation:

$$\mu_{v|\acute{u}} = \rho\acute{u} \tag{G.5}$$

$$\sigma_{v|\acute{u}} = \sqrt{1-\rho^2} \tag{G.6}$$

where ρ is the (linear) correlation coefficient. For extreme cases this signifies:

- $\rho = 0$ (no information): If there is zero correlation, no information is provided and the updated mean and standard deviation are equal to their prior values (i.e., $\mu_{v|\acute{u}} = 0$ and $\sigma_{v|\acute{u}} = 1$).
- $\rho = 1$ (perfect information): If there is perfect correlation, the updated mean equals the observed (transformed) value and the standard deviation is zero (i.e., $\mu_{v|\acute{u}} = \acute{u}$ and $\sigma_{v|\acute{u}} = 0$).

G.1.2. STRAUB (2011)

Straub starts by partitioning the random variables $\mathbf{X}$ in two sets: $\mathbf{X}_g$ and $\mathbf{X}_h$, whereby the latter contain the random variables in $\mathbf{X}$ that only appear in $h(\mathbf{x})$ and the former the remaining ones. If X_h is a scalar variable[1], the likelihood function (in general: $L(\mathbf{x}|\varepsilon) = P(\varepsilon|\mathbf{X}=\mathbf{x})$) can be written as

$$L(\mathbf{x}_g) \propto \sum_{j=1}^{n_h} f_{X_h}[\hat{x}_{h,j}(\mathbf{x}_g)] \tag{G.7}$$

where $\hat{x}_{h,j}$ are the n_h roots of $h(x_h, \mathbf{x}_g)$ for given $\mathbf{x}_g$. In most cases X_h represents a measurement error e_m, in which case the likelihood simplifies to

$$L(\mathbf{x}_g) = f_{e_m}[s_m - s(\mathbf{x}_g)] \tag{G.8}$$

where s_m is the measured value of the system charateristic $s(\mathbf{x})$ and $f_{e_m}(\cdot)$ is the the PDF of the measurement error.

The key element in the the transformation to an inequality problem is rewriting the likelihood function as the following identity

$$L(\mathbf{x}_g) = \frac{1}{c} P\left(U - \Phi^{-1}[cL(\mathbf{x}_g)] \leq 0\right) \tag{G.9}$$

where U is a standard Normal random variable and c is a positive constant[2] chosen to ensure that $0 \leq cL(\mathbf{x}_g) \leq 1$. This enables expressing the likelihood function by the following equivalent (observation) limit state function

$$h_e(\mathbf{x}_g, u) = u - \Phi^{-1}[cL(\mathbf{x}_g)] \tag{G.10}$$

and the corresponding (inequality) domain

$$\varepsilon_e \equiv \{h_e(\mathbf{x}_g, u) \leq 0\} \tag{G.11}$$

The conditional probability of failure is obtained by

$$P(F|\varepsilon) = \frac{P(F \cap \varepsilon)}{P(\varepsilon)} = \frac{\int_{F \cap \varepsilon_e} f_{\mathbf{X}_g}(\mathbf{x}_g)\varphi(u)\, du\, d\mathbf{x}_g}{\int_{\varepsilon_e} f_{\mathbf{X}_g}(\mathbf{x}_g)\varphi(u)\, du\, d\mathbf{x}_g} \tag{G.12}$$

where $\varphi(\cdot)$ is the standard normal PDF and similarly for multiple observations (Straub, 2011). Notice that both, the numerator as well as the denominator can be evaluated straightforwardly using standard (structural) reliability analysis methods, including sampling techniques such as Monte Carlo simulation.

[1] For observations depending on several random variables or several simultaneous observations refer to the original paper (Straub, 2011).

[2] For a Normal distributed measurement error, a proper choice of c is $c = \sigma_{e_m}/\varphi(0) \approx \sigma_{e_m}/0.39$, where σ_{e_m} is the standard deviation of the measurement error e_m.

G.2. Simple Example (Normal-Linear)

The example **limit state function** is

$$Z = R - S \tag{G.13}$$

where $R \sim N(6, \sqrt{2})$ and $S \sim N(2, \sqrt{2})$, which makes Z also Normal distributed with $Z \sim N(4, 2)$.

The **prior reliability index**, hence, is

$$\beta = \frac{\mu_Z}{\sigma_Z} = \frac{4}{2} = 2 \tag{G.14}$$

resulting in a prior probability of failure of $P(F) = 2.3 \cdot 10^{-2}$.

Suppose we have a **measurement** (i.e., observation) of the resistance of $r'_m = 8$ with measurement error $e_m \sim N(0, 1)$.

In the following, this example will be elaborated using both methods. Since all random variables are Normal distributed and the limit states are linear, the "Transformation Method" solution will give the exact answer. We will see that also the method by Straub, here solved using Monte Carlo simulation, gives the exact same answer.

G.2.1. Transformation Method

Since both, resistance R and measurement error e_m are uncertain, the observation is a random variable, too, which is described by

$$R_m = R + e_m \tag{G.15}$$

and Normal distributed: $R_m \sim N(\mu_R, \sqrt{\sigma_R^2 + \sigma_{e_m}^2}) = N(6, \sqrt{3})$. The joint distribution of failure and the observation is thus bivariate Normal with correlation coefficient:

$$\rho_{Z,R_m} = \frac{COV(Z, R_m)}{\sigma_Z \sigma_{R_m}} = \frac{\sigma_R^2}{\sigma_Z \sigma_{R_m}} = \frac{2}{2\sqrt{3}} \tag{G.16}$$

Transforming the observed resistance value r'_m into standard normal gives

$$\acute{u} = \frac{r'_m - \mu_h}{\sigma_{R_m}} = \frac{8-6}{\sqrt{3}} \tag{G.17}$$

Inserting in equations (G.5) and (G.6) provides the conditional moments of v:

$$\mu_{v|\acute{u}} = \frac{1}{\sqrt{3}} \cdot \frac{2}{\sqrt{3}} = 2/3 \tag{G.18}$$

$$\sigma_{v|\acute{u}} = \sqrt{1 - (1/\sqrt{3})^2} = \sqrt{2/3} \tag{G.19}$$

Now we transform into real space again ($v|\acute{u} \rightarrow Z|r'_m$)

$$\mu_{Z|r'_m} = \mu_{v|\acute{u}} \sigma_Z + \mu_Z = 2/3 \cdot 2 + 4 = 16/3 \tag{G.20}$$

$$\sigma_{Z|r'_m} = \sigma_{v|\acute{u}} \sigma_Z = \sqrt{8/3} \tag{G.21}$$

Thus, the conditional (i.e., updated) reliability index becomes

$$\beta'' = \frac{\mu_{Z|r'_m}}{\sigma_{Z|r'_m}} = \frac{16/3}{\sqrt{8/3}} \approx 3.27 \tag{G.22}$$

with a corresponding probability of failure of $P''_f = 5.5 \cdot 10{-}4$. Since all random variables are Normal distributed and the limit states are linear, this solution is exact.

G.2.2. STRAUB (2011)

The equality information can be described by

$$h(R, \varepsilon_m) = R + \varepsilon_m - r'_m \tag{G.23}$$

The corresponding likelihood function is given by

$$L(r) = f_{\varepsilon_m}(r'_m - r) \tag{G.24}$$

Hence, the corresponding equivalent inequality limit state function for the observation can be written as

$$h_e(r, u) = u - cL(r) = u - cf_{\varepsilon_m}(r'_m - r) \tag{G.25}$$

where in this example we can assume $c = 1$ m.
Hence, to determine the posterior probability of failure the following expression can be solved by standard reliability analysis methods:

$$P(F|\varepsilon) = \frac{P(F \cap \varepsilon)}{P(\varepsilon)} = \frac{\iiint\limits_{\{r<s\} \cap \{h_e(r,u) \leq 0\}} f_R(r) f_S(s) \varphi(u) du ds dr}{\iint\limits_{h_e(r,u) \leq 0)} f_R(r) \varphi(u) du dr} \tag{G.26}$$

Monte Carlo simulation with $n = 10^7$ realizations gives exactly the same posterior reliability index as the (for this example exact) "Transformation Method": $\beta'' \approx 3.27$.

G.3. CONCLUDING REMARK

The simple example with Normal random variables and linear limit states showed that the Straub (2011) method gives exactly the same result as the "Transformation Method" method, for which the result is exact because no approximations or errors in the transformation are made. The great advantage of Straub's method is that it can be used in a straightforward fashion with simulation-based reliability analysis methods, for which it is used throughout this thesis.

H

APPLICATION EXAMPLE RESULTS

This appendix contains the detailed results of the application example used throughout this thesis, while the respective chapters only provide summaries and highlights.

H.1. PRIOR ANALYSIS

This section contains the detailed results of the prior analysis from section 3.5.

Table H.1: Application Example - Prior Results Summary

PRIOR ANALYSIS					**P(F) =**	**1.9E − 3**
i	**P(E_i)**	**Uplift P(F_u|E_i)**	**Heave P(F_h|E_i)**	**Piping P(F_p|E_i)**	**Failure P(F|E_i)**	**P(E_i)P(F|E_i)**
1	17.6%	$1.8E-2$	$1.0E-1$	$4.8E-4$	$1.4E-4$	$2.5E-5$
2	62.4%	$2.8E-2$	$1.7E-1$	$5.7E-4$	$2.2E-4$	$1.3E-4$
3	4.4%	$1.0E-0$	$1.0E-0$	$8.7E-3$	$8.9E-3$	$3.9E-4$
4	15.6%	$1.0E-0$	$1.0E-0$	$8.3E-3$	$8.3E-3$	$1.3E-3$

H.2. PRIOR FRAGILITY CURVES

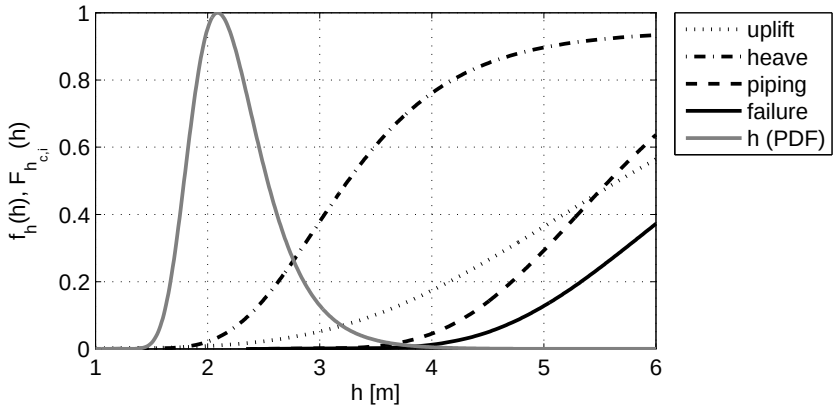

Figure H.1: Prior fragility curves, E_1

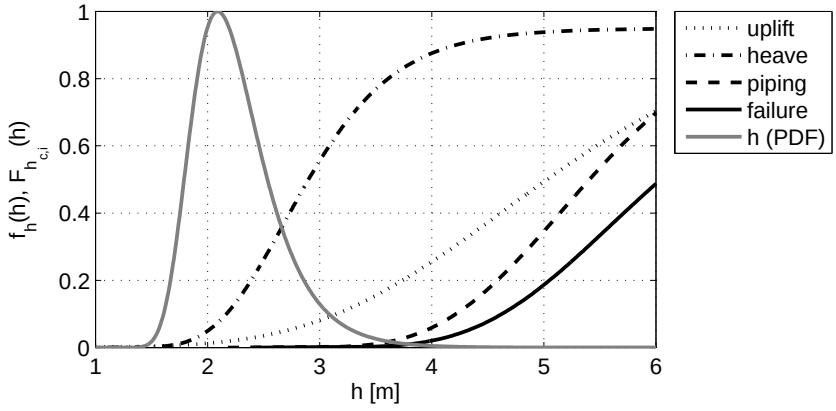

Figure H.2: Prior fragility curves, E_2

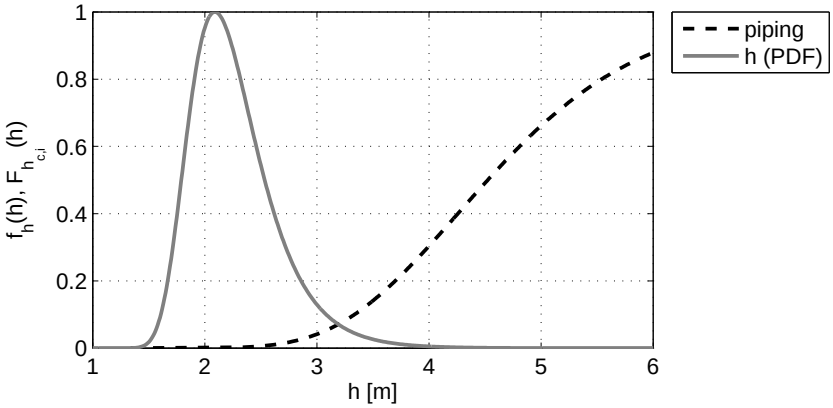

Figure H.3: Prior fragility curves, E_3

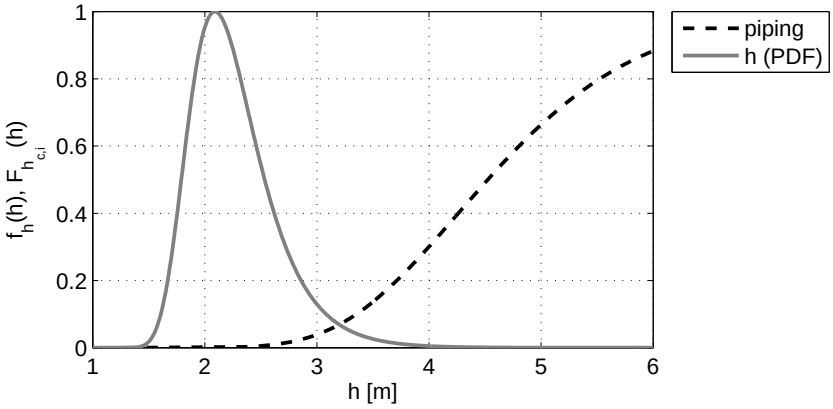

Figure H.4: Prior fragility curves, E_4

H.3. FIELD OBSERVATIONS

This section contains the results of the posterior analysis of the application example for field observations as discussed in section 5.5.

Table H.2: Application example for field observations, dike ring 10 (Mastenbroek) - prior and posterior analysis results summary

PRIOR ANALYSIS					**P(F) =**	**1.9E − 3**
i	**P(E$_i$)**	**Uplift P(F$_u$|E$_i$)**	**Heave P(F$_h$|E$_i$)**	**Piping P(F$_p$|E$_i$)**	**Failure P(F|E$_i$)**	**P(E$_i$)P(F|E$_i$)**
1	17.6%	$1.8E-2$	$1.0E-1$	$4.8E-4$	$1.4E-4$	$2.5E-5$
2	62.4%	$2.8E-2$	$1.7E-1$	$5.7E-4$	$2.2E-4$	$1.3E-4$
3	4.4%	$1.0E-0$	$1.0E-0$	$8.7E-3$	$8.9E-3$	$3.9E-4$
4	15.6%	$1.0E-0$	$1.0E-0$	$8.3E-3$	$8.3E-3$	$1.3E-3$
POSTERIOR - NO SEEPAGE					**P(F) =**	**1.4E − 4**
i	**P(E$_i$|ε)**	**P(F$_u$|E$_i$,ε)**	**P(F$_h$|E$_i$)**	**P(F$_p$|E$_i$,ε)**	**P(F|E$_i$,ε)**	**P(E$_i$|ε)P(F|E$_i$,ε)**
1	22.4%	$6.3E-3$	$1.0E-1$	$4.3E-4$	$1.0E-4$	$9.6E-5$
2	77.6%	$8.7E-3$	$1.7E-1$	$5.2E-4$	$1.5E-4$	$4.0E-4$
3	0.0%	$1.0E-0$	$1.0E-0$	$8.7E-3$	$8.9E-3$	0.0
4	0.0%	$1.0E-0$	$1.0E-0$	$8.3E-3$	$8.4E-3$	0.0
POSTERIOR - SEEPAGE					**P(F) =**	**7.1E − 3**
i	**P(E$_i$|ε)**	**P(F$_u$|E$_i$,ε)**	**P(F$_h$|E$_i$)**	**P(F$_p$|E$_i$,ε)**	**P(F|E$_i$,ε)**	**P(E$_i$|ε)P(F|E$_i$,ε)**
1	2.7%	$3.3E-1$	$1.1E-1$	$1.1E-3$	$6.3E-4$	$3.1E-5$
2	15.2%	$3.4E-1$	$1.9E-1$	$8.8E-4$	$4.9E-4$	$1.3E-4$
3	18.1%	$1.0E-0$	$1.0E-0$	$8.7E-3$	$8.7E-3$	$1.6E-3$
4	64.0%	$1.0E-0$	$1.0E-0$	$8.4E-3$	$8.4E-3$	$5.4E-3$
POSTERIOR - SAND BOILS					**P(F) =**	**7.9E − 3**
i	**P(E$_i$|ε)**	**P(F$_u$|E$_i$,ε)**	**P(F$_h$|E$_i$)**	**P(F$_p$|E$_i$,ε)**	**P(F|E$_i$,ε)**	**P(E$_i$|ε)P(F|E$_i$,ε)**
1	1.1%	$1.2E-1$	$3.1E-1$	$2.0E-3$	$1.7E-3$	$2.1E-5$
2	7.7%	$1.6E-1$	$4.0E-1$	$1.2E-3$	$1.0E-3$	$9.4E-5$
3	20.1%	$1.0E-0$	$1.0E-0$	$8.9E-3$	$8.7E-3$	$1.7E-3$
4	71.2%	$1.0E-0$	$1.0E-0$	$8.4E-3$	$8.4E-3$	$6.0E-3$

H.3.1. POSTERIOR ANALYSIS - NO UPLIFT

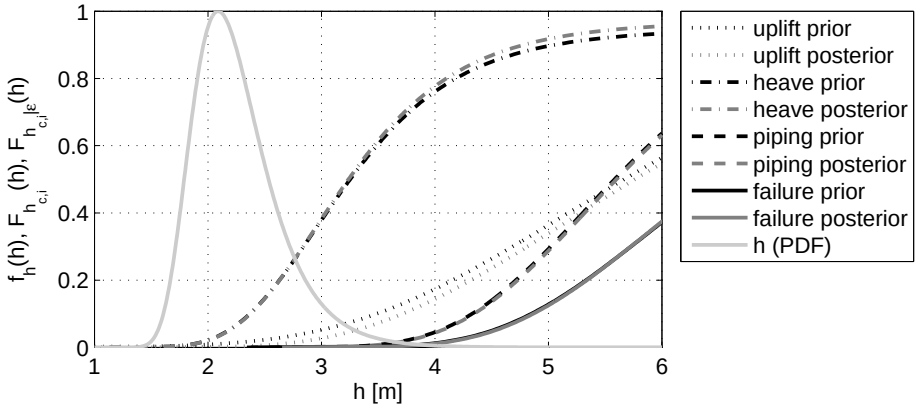

Figure H.5: Posterior fragility curves, no uplift, E_1

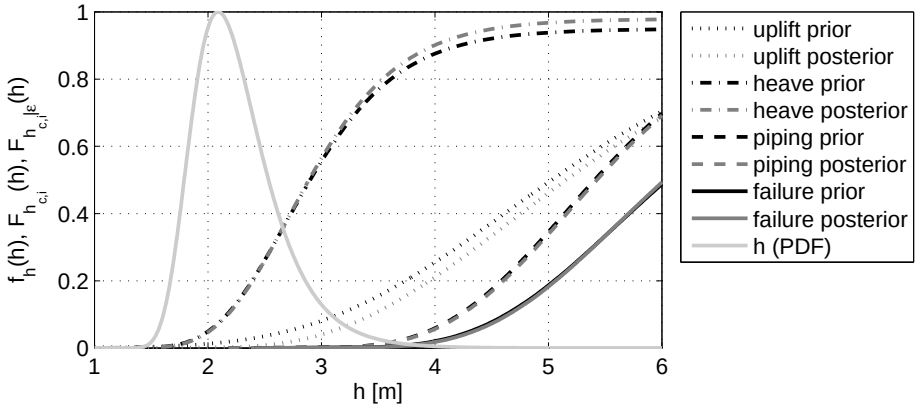

Figure H.6: Posterior fragility curves, no uplift, E_2

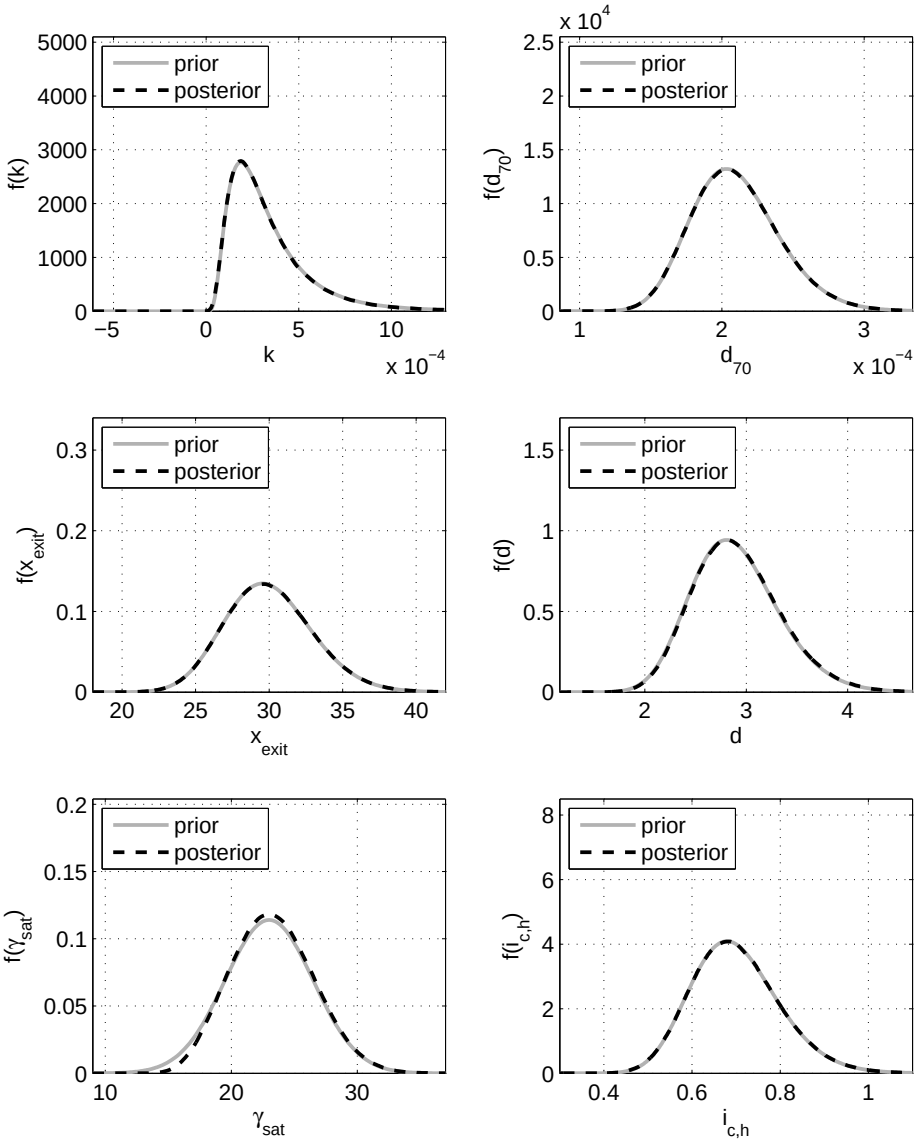

Figure H.7: Posterior distributions, no uplift, E_1

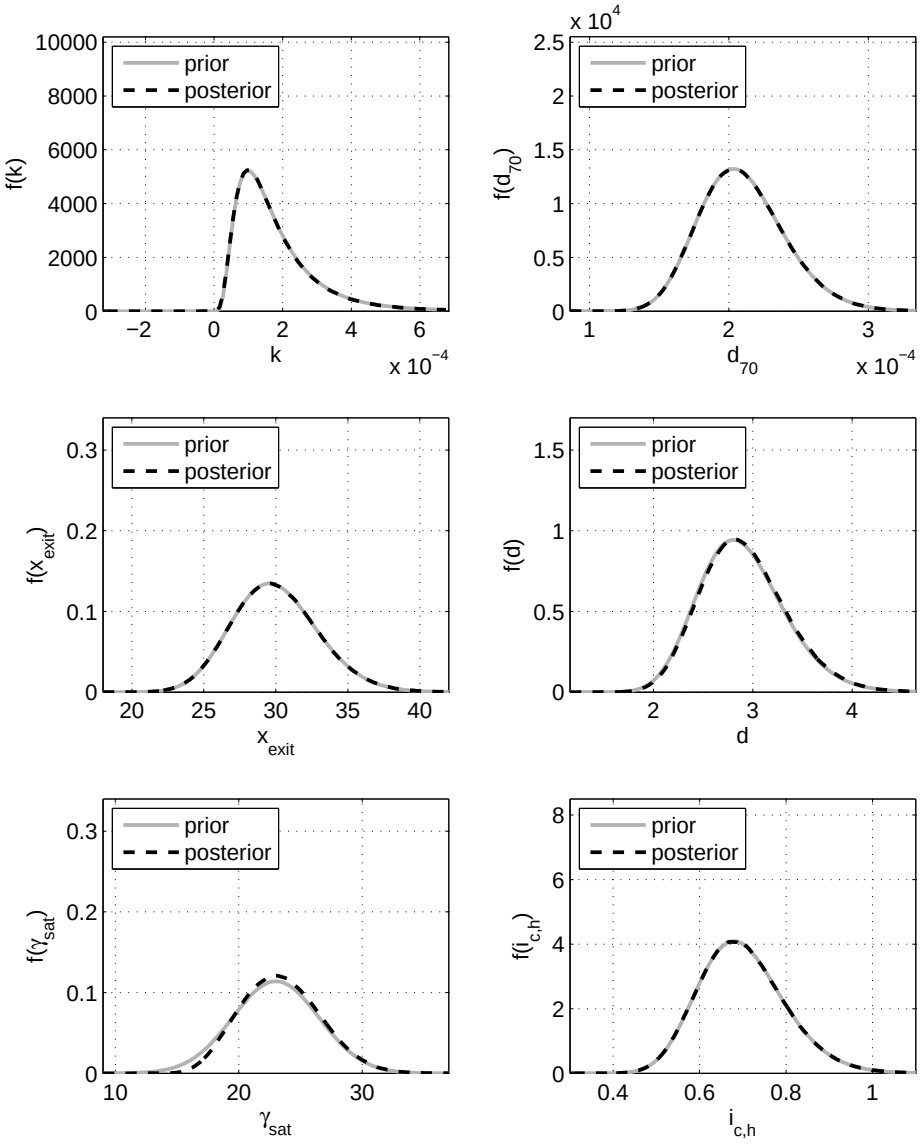

Figure H.8: Posterior distributions, no uplift, E_2

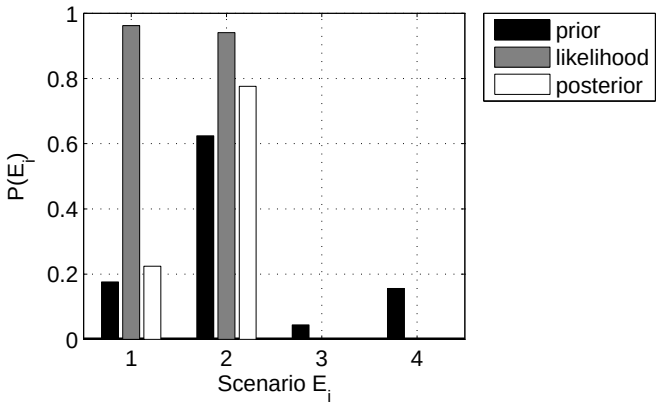

Figure H.9: Prior and posterior scenario probabilities, no uplift

H.3.2. POSTERIOR ANALYSIS - UPLIFT & NO PIPING

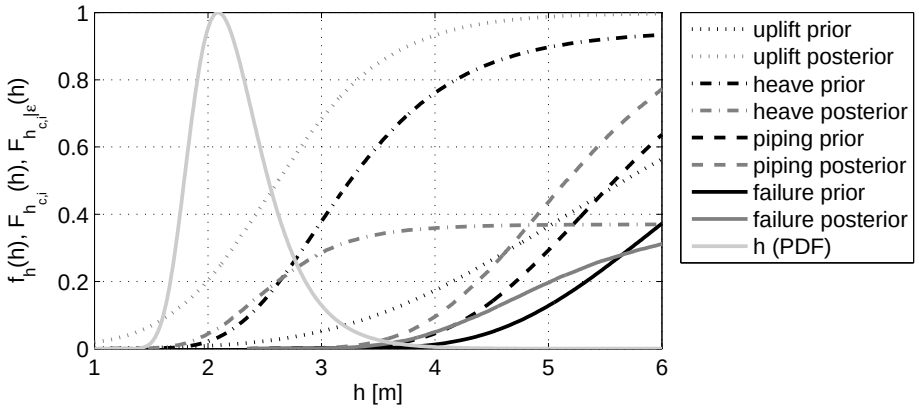

Figure H.10: Posterior fragility curves, uplift, E_1

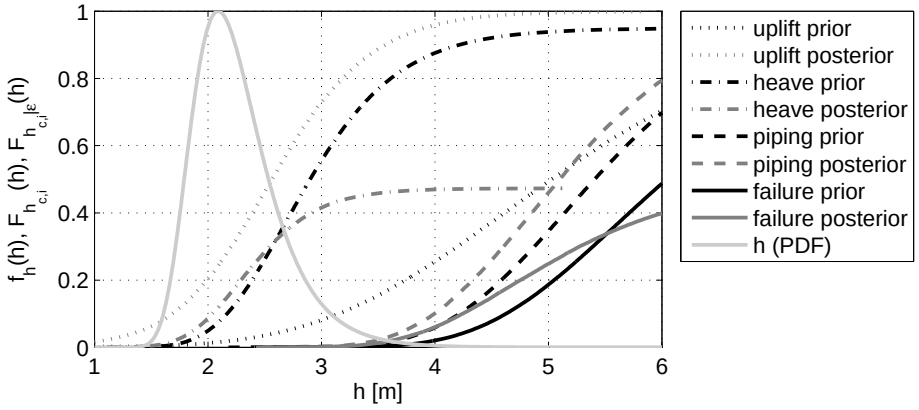

Figure H.11: Posterior fragility curves, uplift, E_2

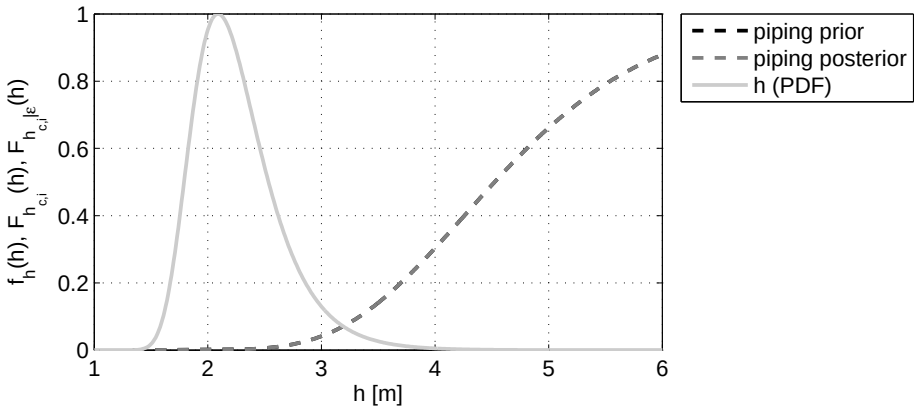

Figure H.12: Posterior fragility curves, uplift, E_3

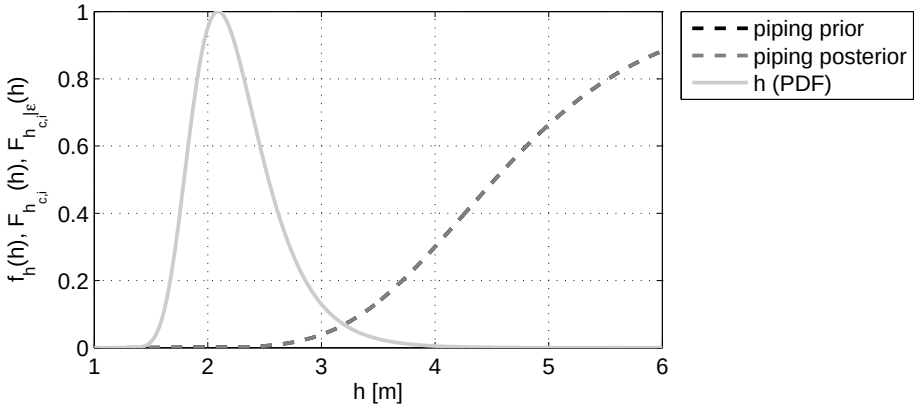

Figure H.13: Posterior fragility curves, uplift, E_4

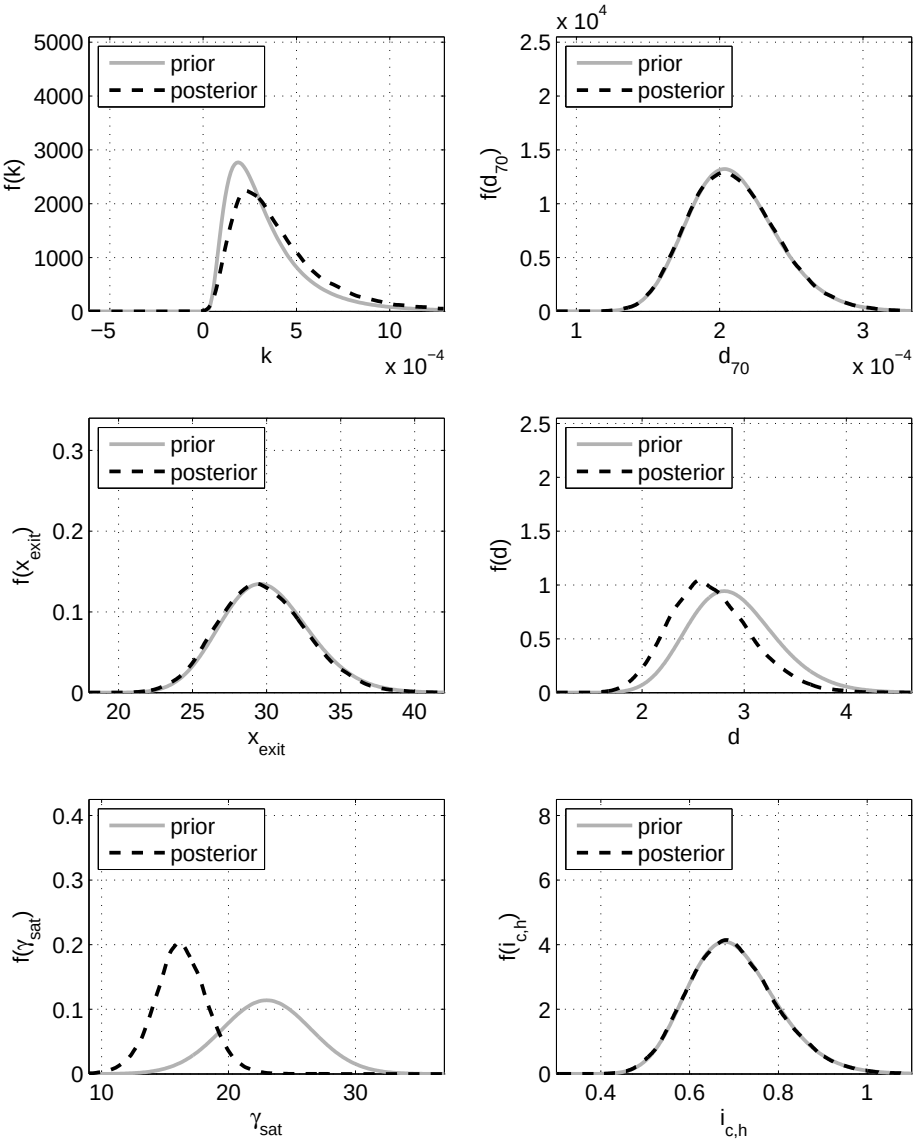

Figure H.14: Posterior distributions, uplift, E_1

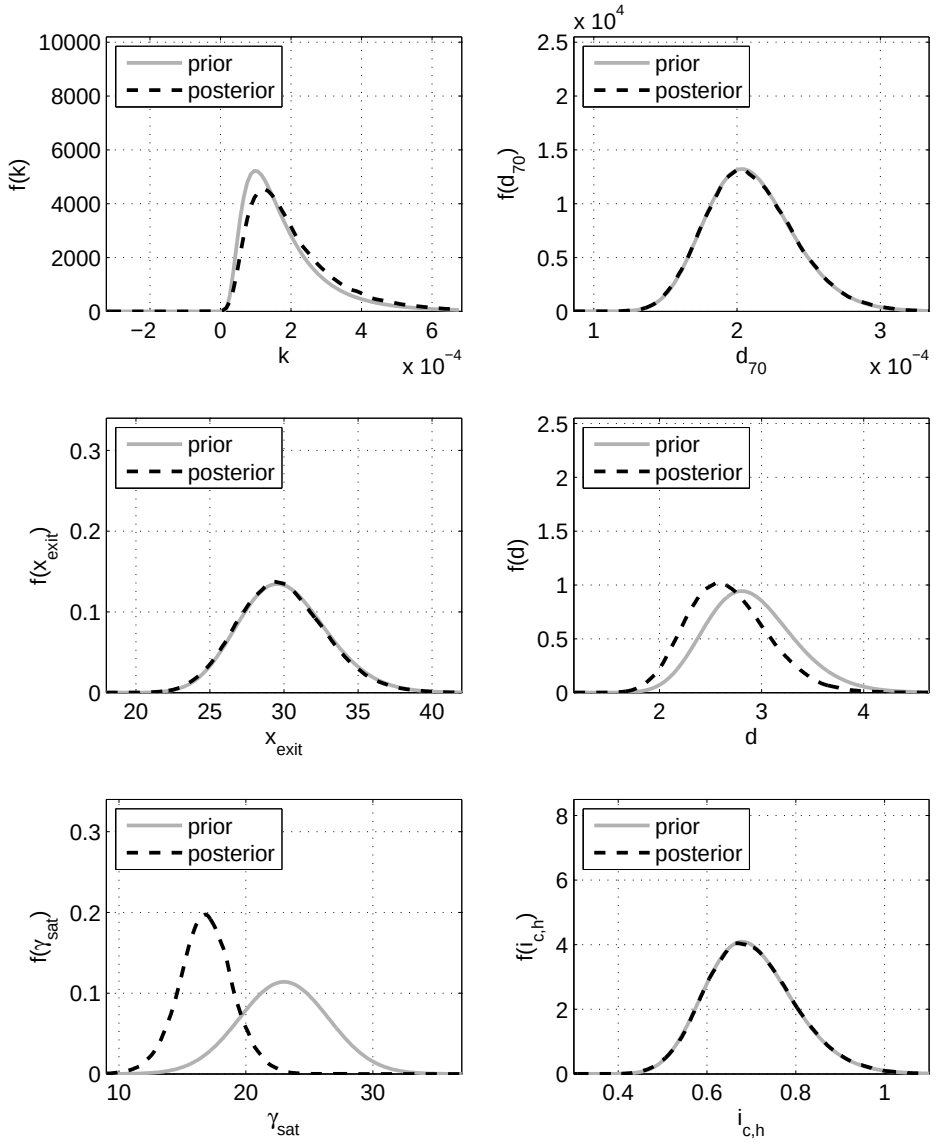

Figure H.15: Posterior distributions, uplift, E_2

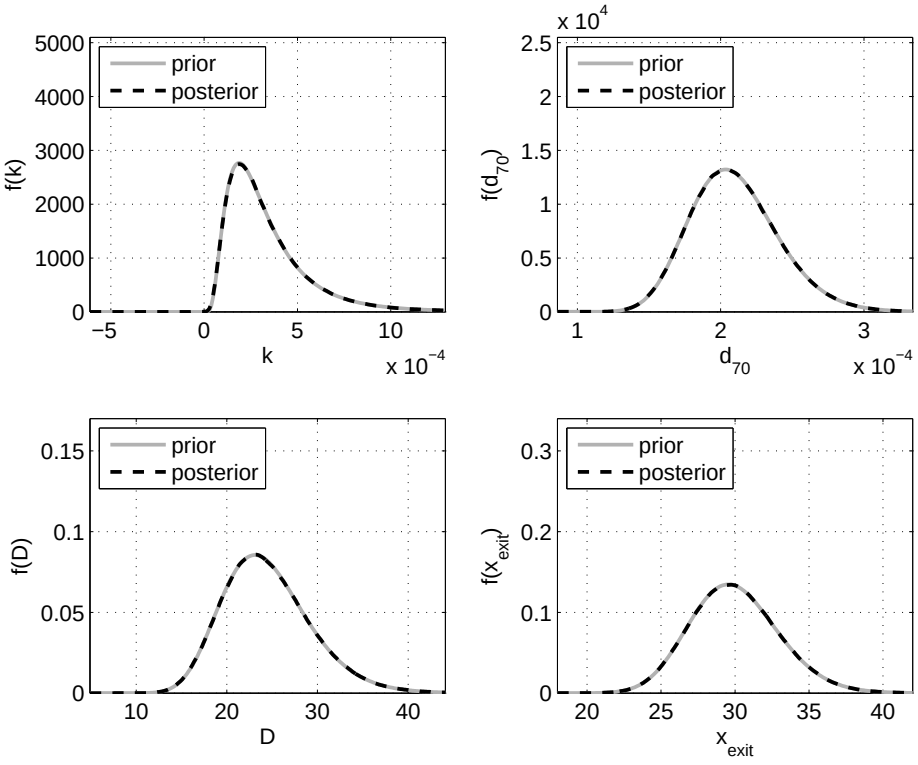

Figure H.16: Posterior distributions, uplift, E_3

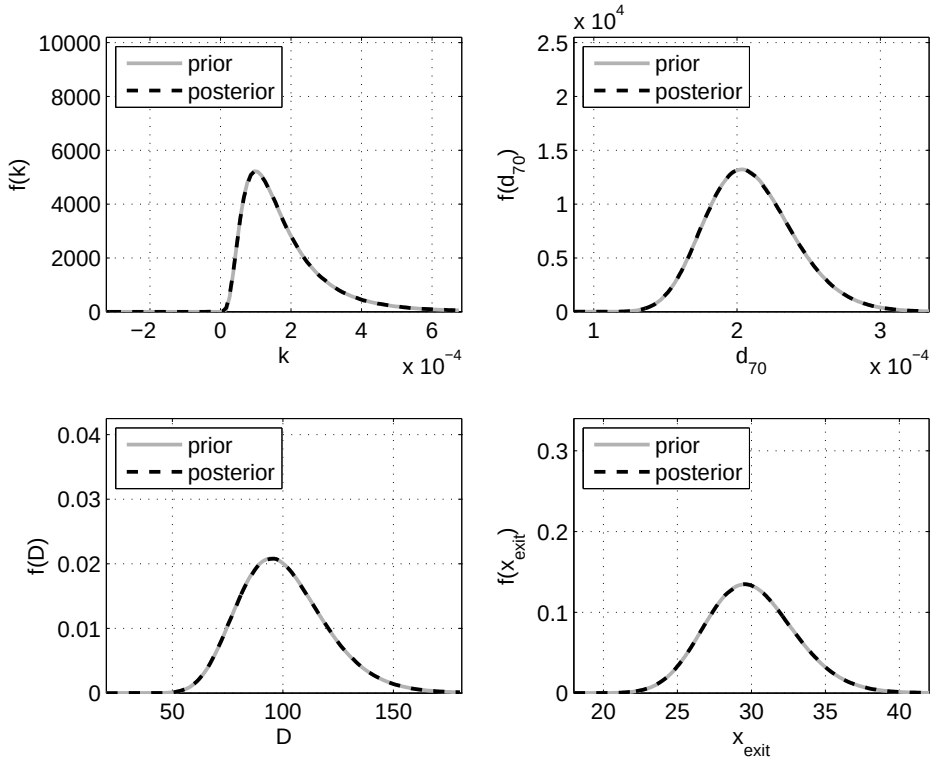

Figure H.17: Posterior distributions, uplift, E_4

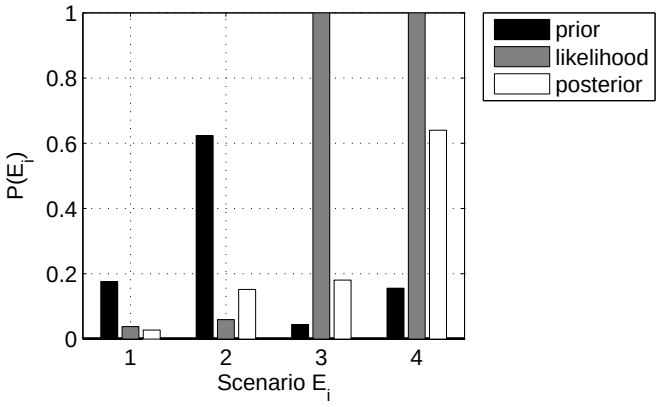

Figure H.18: Prior and posterior scenario probabilities, uplift

H.3.3. POSTERIOR ANALYSIS - UPLIFT & HEAVE

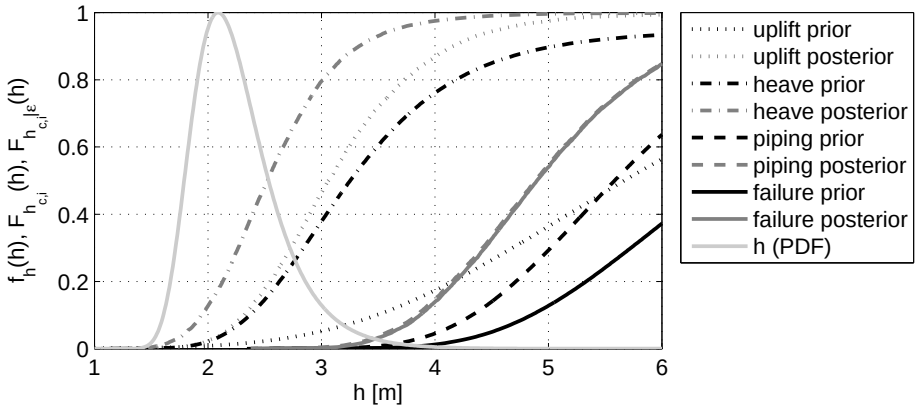

Figure H.19: Posterior fragility curves, uplift & heave, E_1

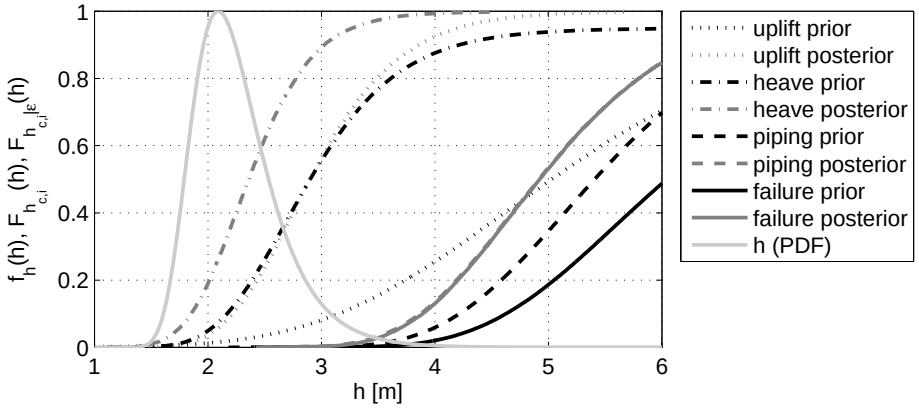

Figure H.20: Posterior fragility curves, uplift & heave, E_2

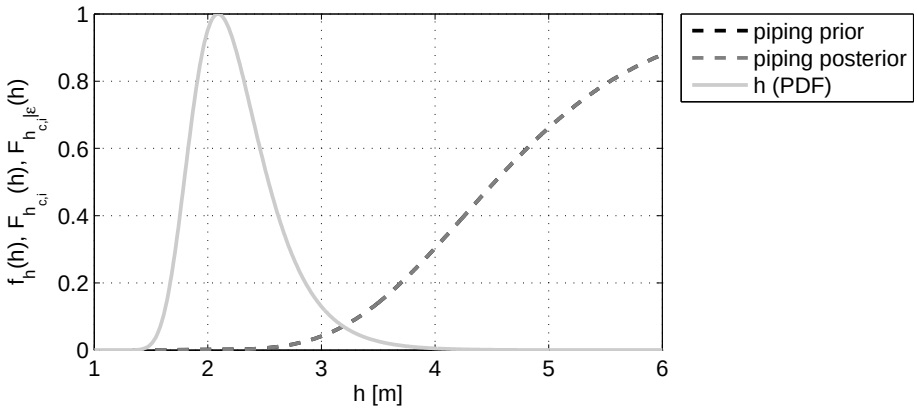

Figure H.21: Posterior fragility curves, uplift & heave, E_3

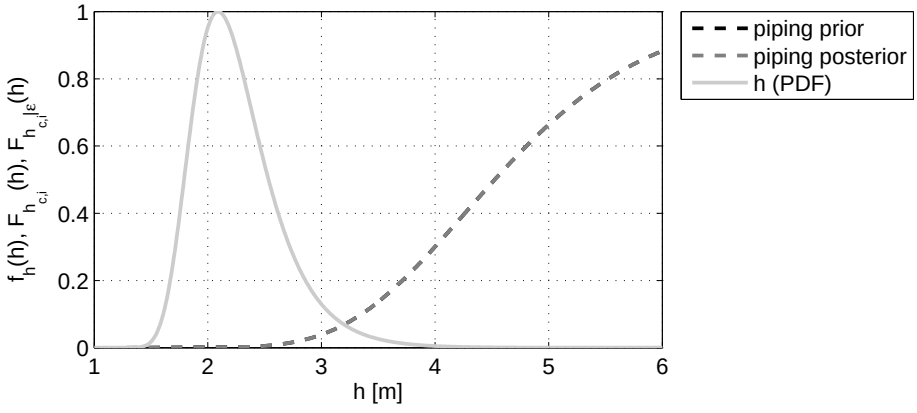

Figure H.22: Posterior fragility curves, uplift & heave, E_4

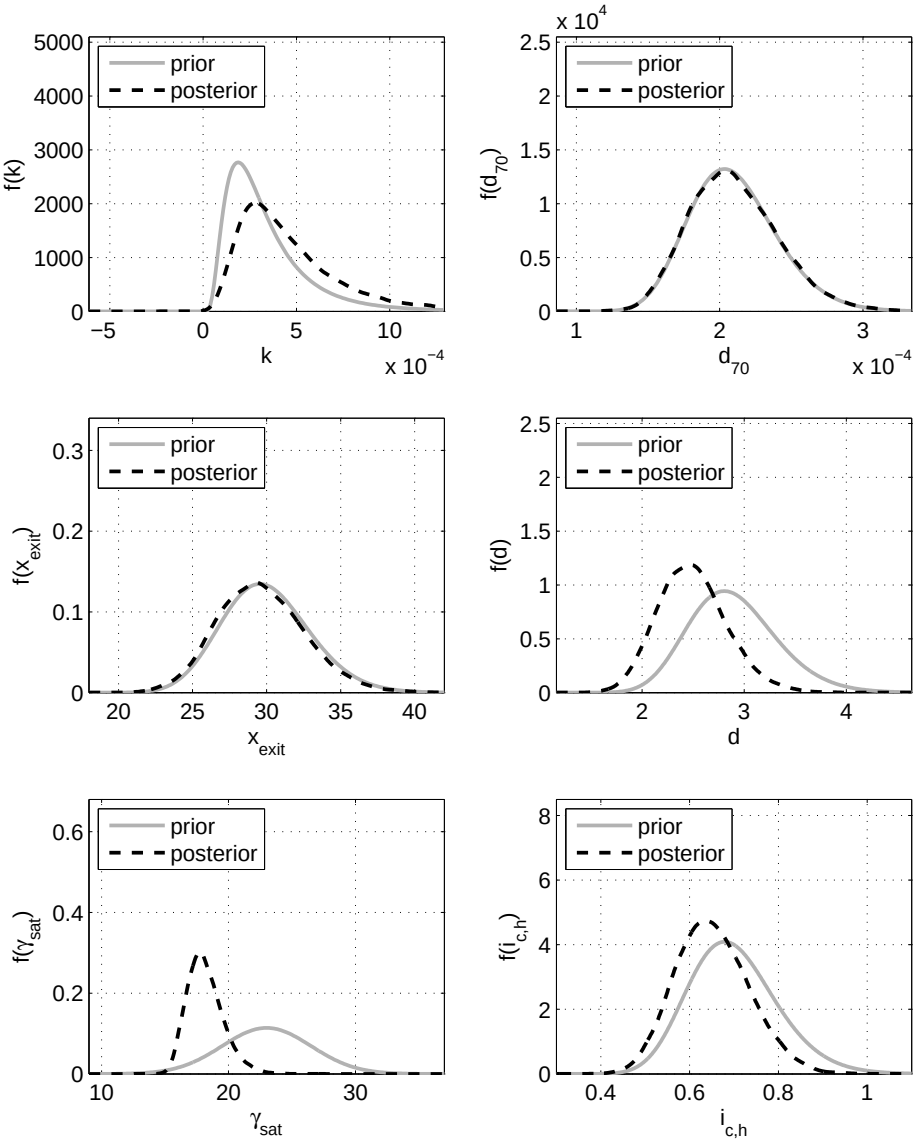

Figure H.23: Posterior distributions, uplift & heave, E_1

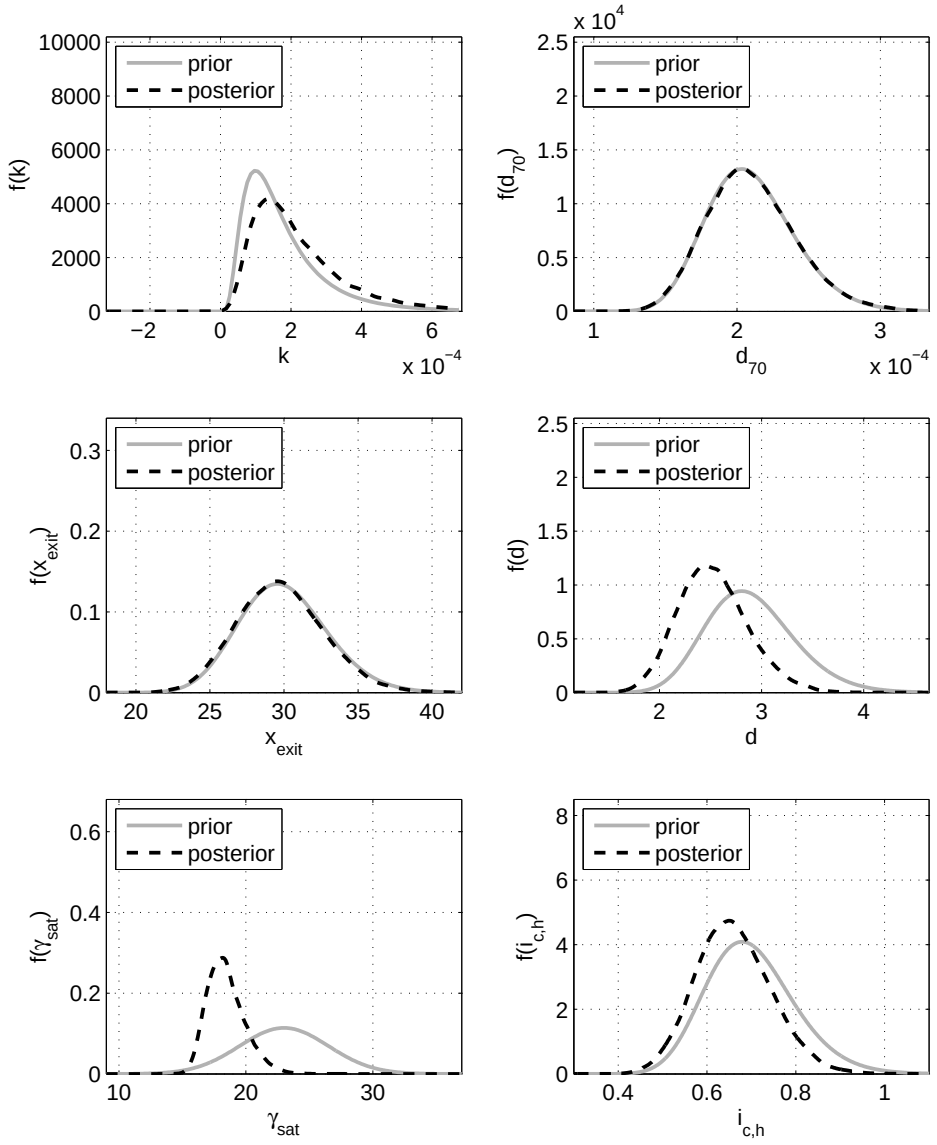

Figure H.24: Posterior distributions, uplift & heave, E_2

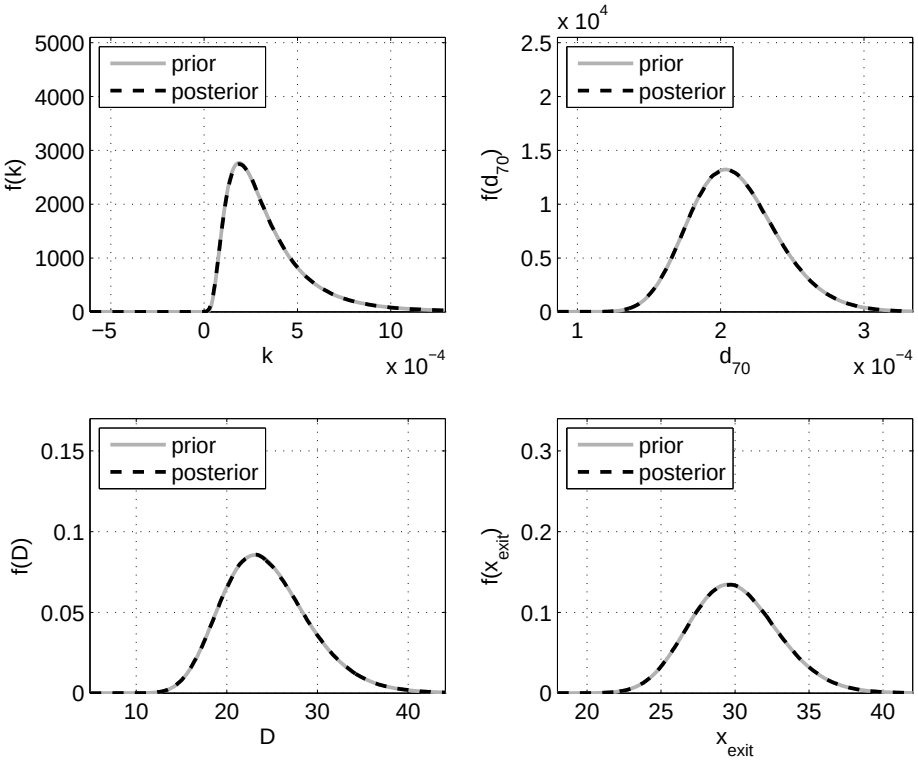

Figure H.25: Posterior distributions, uplift & heave, E_3

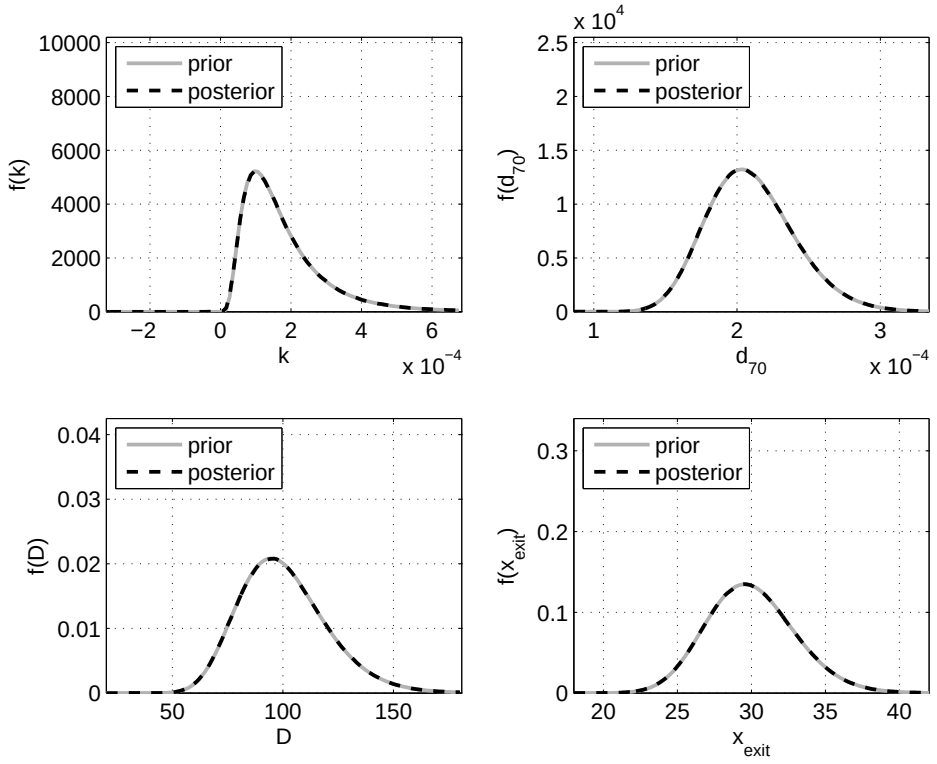

Figure H.26: Posterior distributions, uplift & heave, E_4

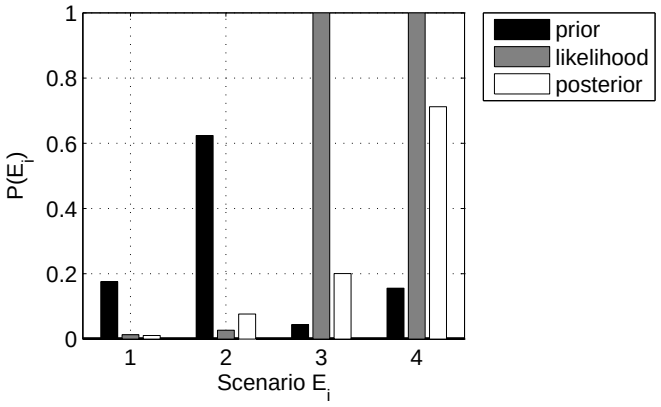

Figure H.27: Prior and posterior scenario probabilities, uplift & heave

H.4. HEAD MONITORING

This section contains the results of the posterior analysis of the application example for head monitoring as discussed in section 6.3.

The fictitious observations in this example can be summarized by the following parameters

- measured value of hydraulic head: ϕ_m = 2.1 m
- measurement error: σ_e = 0.1 m
- observed water level: $\acute{h}$ = 3.5 m

Notice that the underlying assumption is that the measured head is the steady state response to the observed water level. In other words, the water level needs to remain high for a long duration (i.e. several days) to justify such an assumption.

Table H.3: Application example head monitoring, dike ring 10 (Mastenbroek) - prior and posterior analysis results summary

PRIOR ANALYSIS					**P(F) =**	**1.9E−3**
i	**P(E_i)**	**Uplift P(F_u|E_i)**	**Heave P(F_h|E_i)**	**Piping P(F_p|E_i)**	**Failure P(F|E_i)**	**P(E_i)P(F|E_i)**
1	17.6%	$1.8E-2$	$1.0E-1$	$4.8E-4$	$1.4E-4$	$2.5E-5$
2	62.4%	$2.8E-2$	$1.7E-1$	$5.7E-4$	$2.2E-4$	$1.3E-4$
3	4.4%	$1.0E-0$	$1.0E-0$	$8.7E-3$	$8.9E-3$	$3.9E-4$
4	15.6%	$1.0E-0$	$1.0E-0$	$8.3E-3$	$8.3E-3$	$1.3E-3$
POSTERIOR ANALYSIS					**P(F) =**	**1.4E−4**
i	**P(E_i|ε)**	**P(F_u|E_i,ε)**	**P(F_h|E_i)**	**P(F_p|E_i,ε)**	**P(F|E_i,ε)**	**P(E_i|ε)P(F|E_i,ε)**
1	41.3%	$1.6E-2$	$8.8E-2$	$1.5E-4$	$5.0E-5$	$2.1E-5$
2	58.7%	$2.4E-2$	$1.5E-1$	$2.4E-5$	$1.8E-5$	$1.1E-5$
3	0.0%	n/a	n/a	n/a	n/a	0.0
4	0.0%	n/a	n/a	n/a	n/a	0.0

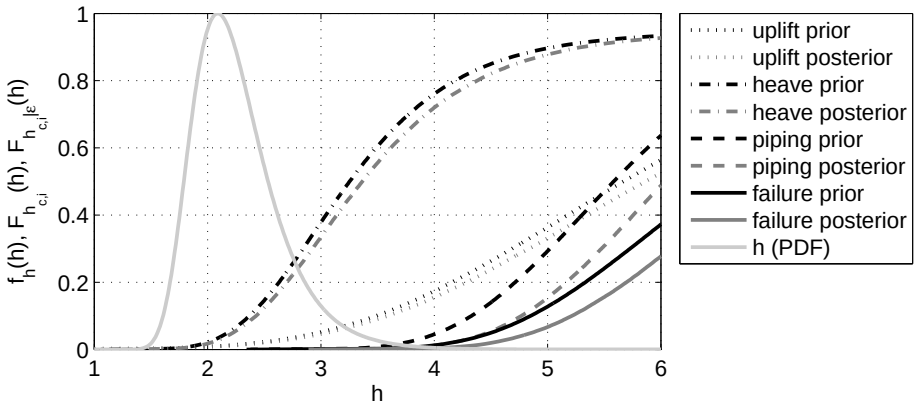

Figure H.28: Posterior fragility curves, E_1

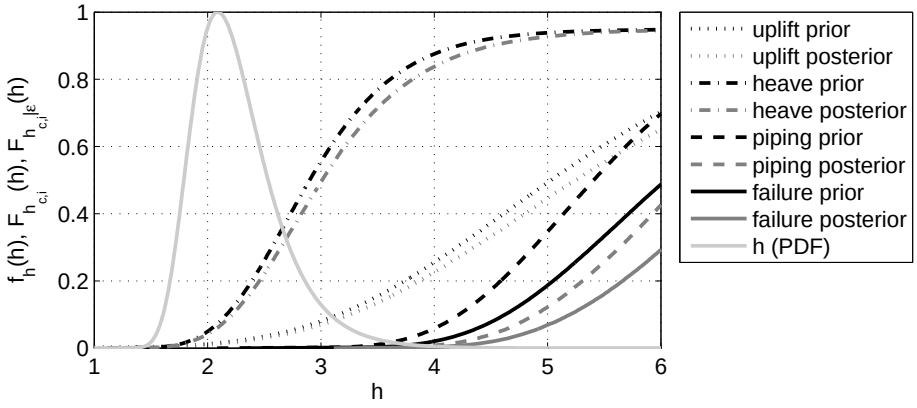

Figure H.29: Posterior fragility curves, E_2

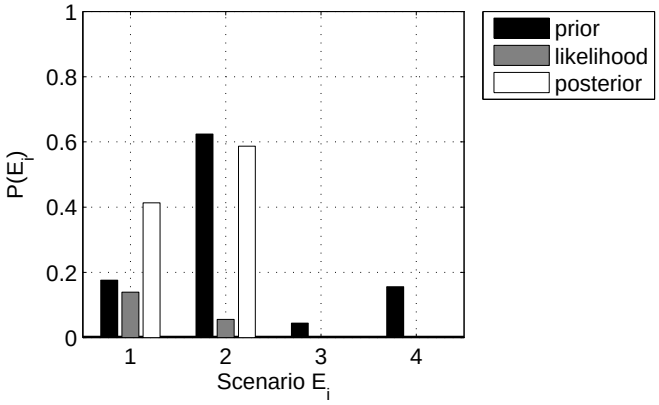

Figure H.30: Prior and posterior scenario probabilities

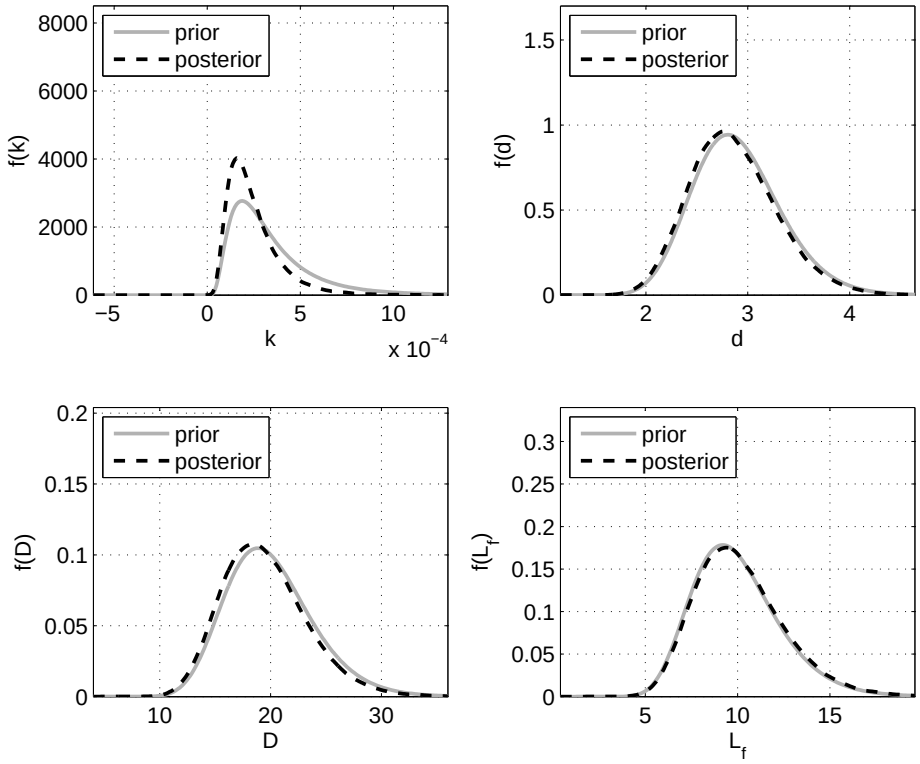

Figure H.31: Posterior distributions, E_1

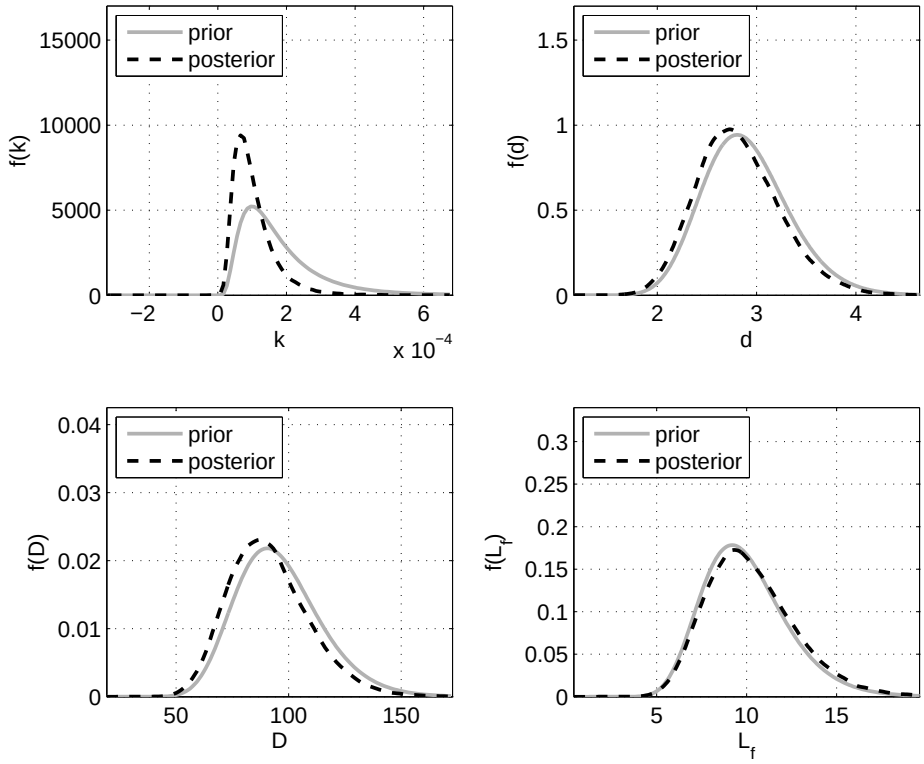

Figure H.32: Posterior distributions, E_2

I

PROBABILITY OF ANOMALY DETECTION

The following sections contain the derivations of the probability of detection (PoD; i.e., the probability of detecting an anomaly, given it is present) for different probability distribution functions of the anomaly width B. For a given (equidistant) inter-CPT distance d, the probability of detecting (i.e., hitting) the anomaly is given by:

$$P(D|A) = \begin{cases} 1 & B > d \\ B/d & B \leq d \end{cases} \tag{I.1}$$

$$= P(B > d) + \int_0^d \frac{\xi}{d} f_B(\xi) d\xi \tag{I.2}$$

$$= 1 - F_B(d) + \int_0^d \frac{\xi}{d} f_B(\xi) d\xi \tag{I.3}$$

Consequently, the probability of not detecting (i.e., missing) it is:

$$P(\bar{D}|A) = 1 - P(D|A) = F_B(d) - \int_0^d \frac{\xi}{d} f_B(\xi) d\xi \tag{I.4}$$

In the following, we will derive $P(\bar{D}|A) = 1 - PoD$, because the expression is shorter and more relevant to the problem than $P(D|A)$ itself.

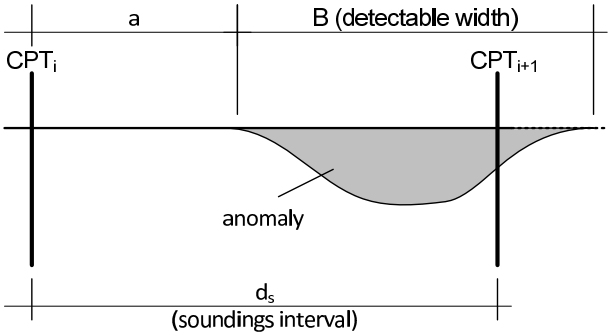

Figure I.1: Definitions for the derivation of the PoD of an anomaly by equi-distant soundings (CPT)

I.1. NORMAL-DISTRIBUTED WIDTH B

The PDF and CDF of a Normal-distributed width B ($B \sim N(\mu_B, \sigma_B)$) are denoted respectively as:

$$f_B(\xi) = \frac{1}{\sqrt{2\pi}\sigma_B} \exp -\frac{1}{2}\left(\frac{\xi-\mu_B}{\sigma_B}\right)^2 = \frac{1}{\sigma_B}\phi\left(\frac{\xi-\mu_B}{\sigma_B}\right) \tag{I.5}$$

$$F_B(\xi) = \int_{-\infty}^{\xi} f_B(\xi)d\xi = \Phi\left(\frac{\xi-\mu_B}{\sigma_B}\right) \tag{I.6}$$

where $\Phi(\cdot)$ and $\Phi(\cdot)$ are the standard Normal CDF and PDF respectively. Inserting the PDF in Eq. I.4 gives:

$$P(\bar{D}|A) = F_B(d) - \frac{1}{d\sqrt{2\pi}\sigma_B}\int_0^d \xi \exp\left(-\frac{1}{2}\left(\frac{\xi-\mu_B}{\sigma_B}\right)^2\right)d\xi \tag{I.7}$$

$$= F_B(d) - \frac{\sigma_B}{d}\int_{-\infty}^{d} \frac{\xi-\mu_B}{\sigma_B}\frac{\exp\left(-\frac{1}{2}\left(\frac{\xi-\mu_B}{\sigma_B}\right)^2\right)}{\sqrt{2\pi}\sigma_B}d\xi \tag{I.8}$$

$$-\frac{1}{d}\int_{-\infty}^{d} \mu_B \frac{\exp\left(-\frac{1}{2}\left(\frac{\xi-\mu_B}{\sigma_B}\right)^2\right)}{\sqrt{2\pi}\sigma_B}d\xi \tag{I.9}$$

$$= F_B(d)(1-\frac{\mu_B}{d}) - \frac{\sigma_B}{d}\int_{-\infty}^{d} \frac{\xi-\mu_B}{\sigma_B}\frac{\exp\left(-\frac{1}{2}\left(\frac{\xi-\mu_B}{\sigma_B}\right)^2\right)}{\sqrt{2\pi}}d\xi \tag{I.10}$$

Substituting with

$$t = \frac{\xi - \mu_B}{\sigma_B} \Rightarrow \xi = \sigma_B t + \mu_B \tag{I.11}$$

$$d\xi = \sigma_B dt \tag{I.12}$$

$$\xi = -\infty \Rightarrow t = -\infty \tag{I.13}$$

$$\xi = d \Rightarrow t = \frac{d - \mu_B}{\sigma_B} \tag{I.14}$$

gives

$$P(\bar{D}|A) = F_B(d)(1 - \frac{\mu_B}{d}) - \frac{\sigma_B}{d} \int_{-\infty}^{\frac{d-\mu_B}{\sigma_B}} t \frac{\exp\left(-\frac{1}{2}t^2\right)}{\sqrt{2\pi}} dt \tag{I.15}$$

$$= F_B(d)(1 - \frac{\mu_B}{d}) \tag{I.16}$$

$$- \frac{\sigma_B}{d} \left(\frac{\exp\left(-\frac{1}{2}\left(\frac{d-\mu_B}{\sigma_B}\right)^2\right)}{\sqrt{2\pi}} \right) \tag{I.17}$$

$$= F_B(d)(1 - \frac{\mu_B}{d}) - \frac{\sigma_B}{d} \phi\left(\frac{d - \mu_B}{\sigma_B}\right) \tag{I.18}$$

$$= F_B(d)(1 - \frac{\mu_B}{d}) - \frac{\sigma_B^2}{d} f_B(d) \tag{I.19}$$

Note that by choosing zero as the lower limit for the integration would probably avoid problems with negative berm width values. For properly accounting for this fact it would be better to choose a distribution type that does not allow negative values, like a Truncated Normal or a Lognormal Distribution. Nevertheless, for small coefficients of variation, say less than 10%, the expression is a very good approximation for results not to close to zero.

I.2. TRUNCATED NORMAL-DISTRIBUTED WIDTH B

The PDF and CDF of a Truncated Normal-distributed width B ($B \sim TN(\mu_B, \sigma_B, a, b)$) with limits a and b ($-\infty \leq a < b \leq \infty$) are denoted respectively as:

$$f_B(\xi) = \frac{\frac{1}{\sigma_B}\phi(\frac{\xi - \mu_B}{\sigma_B})}{\Phi(\frac{b-\mu_B}{\sigma_B}) - \Phi(\frac{a-\mu_B}{\sigma_B})} \tag{I.20}$$

$$F_B(\xi) = \frac{\Phi(\frac{\xi-\mu_B}{\sigma_B}) - \Phi(\frac{a-\mu_B}{\sigma_B})}{\Phi(\frac{b-\mu_B}{\sigma_B}) - \Phi(\frac{a-\mu_B}{\sigma_B})}, \tag{I.21}$$

where $\phi(\cdot)$ is the standard Normal PDF, μ_B and σ_B are the mean and standard deviation of the non-truncated Normal distribution. Since for this specific problem we are only

interested in left-truncating the Normal distribution for avoiding physically impossible negative values of B, with $a = 0$ and $b = \infty$ the expressions simplify to:

$$f_B(\xi) = \frac{\frac{1}{\sigma_B}\phi(\frac{\xi-\mu_B}{\sigma_B})}{1-\Phi(-\frac{\mu_B}{\sigma_B})} = \frac{\frac{1}{\sigma_B}\phi(\frac{\xi-\mu_B}{\sigma_B})}{\Phi(\frac{\mu_B}{\sigma_B})} \tag{I.22}$$

$$F_B(\xi) = \frac{\Phi(\frac{\xi-\mu_B}{\sigma_B})-\Phi(-\frac{\mu_B}{\sigma_B})}{1-\Phi(-\frac{\mu_B}{\sigma_B})} = 1 - \frac{\Phi(\frac{\mu_B-\xi}{\sigma_B})}{\Phi(\frac{\mu_B}{\sigma_B})} \tag{I.23}$$

Inserting the PDF in Eq. I.4 gives:

$$P(\bar{D}|A) = F_B(d) - \frac{1}{d\sqrt{2\pi}\sigma_B\Phi(\frac{\mu_B}{\sigma_B})}\int_0^d \xi \exp\left(-\frac{1}{2}\left(\frac{\xi-\mu_B}{\sigma_B}\right)^2\right)d\xi \tag{I.24}$$

$$= F_B(d) - \frac{\sigma_B}{d\Phi(\frac{\mu_B}{\sigma_B})}\int_0^d \frac{\xi-\mu_B}{\sigma_B}\frac{\exp\left(-\frac{1}{2}\left(\frac{\xi-\mu_B}{\sigma_B}\right)^2\right)}{\sqrt{2\pi}\sigma_B}d\xi \tag{I.25}$$

$$-\frac{1}{d}\int_0^d \mu_B \frac{\exp\left(-\frac{1}{2}\left(\frac{\xi-\mu_B}{\sigma_B}\right)^2\right)}{\sqrt{2\pi}\sigma_B\Phi(\frac{\mu_B}{\sigma_B})}d\xi \tag{I.26}$$

$$= F_B(d)(1-\frac{\mu_B}{d}) - \frac{\sigma_B}{d\Phi(\frac{\mu_B}{\sigma_B})}\int_0^d \frac{\xi-\mu_B}{\sigma_B}\frac{\exp\left(-\frac{1}{2}\left(\frac{\xi-\mu_B}{\sigma_B}\right)^2\right)}{\sqrt{2\pi}}d\xi \tag{I.27}$$

Substituting with

$$t = \frac{\xi-\mu_B}{\sigma_B} \Rightarrow \xi = \sigma_B t + \mu_B \tag{I.28}$$

$$d\xi = \sigma_B dt \tag{I.29}$$

$$\xi = 0 \Rightarrow t = -\frac{\mu_B}{\sigma_B} \tag{I.30}$$

$$\xi = d \Rightarrow t = \frac{d-\mu_B}{\sigma_B} \tag{I.31}$$

gives

$$P(\bar{D}|A) = F_B(d)(1-\frac{\mu_B}{d}) - \frac{\sigma_B}{d\Phi(\frac{\mu_B}{\sigma_B})} \int_{-\frac{\mu_B}{\sigma_B}}^{\frac{d-\mu_B}{\sigma_B}} t\frac{\exp\left(-\frac{1}{2}t^2\right)}{\sqrt{2\pi}}dt \tag{I.32}$$

$$= F_B(d)(1-\frac{\mu_B}{d}) \tag{I.33}$$

$$-\frac{\sigma_B}{d\Phi(\frac{\mu_B}{\sigma_B})}\left(\frac{\exp\left(-\frac{1}{2}\left(\frac{d-\mu_B}{\sigma_B}\right)^2\right)}{\sqrt{2\pi}} - \frac{\exp\left(-\frac{1}{2}\left(-\frac{\mu_B}{\sigma_B}\right)^2\right)}{\sqrt{2\pi}}\right) \tag{I.34}$$

$$= F_B(d)(1-\frac{\mu_B}{d}) - \frac{\sigma_B}{d\Phi(\frac{\mu_B}{\sigma_B})}\left(\phi\left(\frac{d-\mu_B}{\sigma_B}\right) - \phi\left(\frac{\mu_B}{\sigma_B}\right)\right) \tag{I.35}$$

$$= F_B(d)(1-\frac{\mu_B}{d}) - \frac{\sigma_B^2}{d}\left(f_B(d) - f_B(0)\right) \tag{I.36}$$

The main difference between the Normal and the Truncated Normal solution only lies in the normalization constant $1/(1-\Phi(-\mu_B/\sigma_B))$, which is small for small coefficients of variation of the width ($V_B = \sigma_B/\mu_B$).

I.3. LOGNORMAL-DISTRIBUTED WIDTH B

The PDF and CDF of a Lognormal-distributed width B ($B \sim LN(\lambda_B, \zeta_B)$) are denoted respectively as:

$$f_B(\xi) = \frac{1}{\xi\sqrt{2\pi}\zeta_B}\exp -\frac{1}{2}\left(\frac{\ln\xi - \lambda_B}{\zeta_B}\right)^2 \tag{I.37}$$

$$F_B(\xi) = \int_{-\infty}^{\xi} f_B(\xi)d\xi \approx \frac{1}{2} + \frac{1}{2}\,\mathrm{erf}\left[\frac{\ln\xi - \lambda_B}{\sqrt{2\zeta_B^2}}\right] = \Phi\left(\frac{\ln\xi - \lambda_B}{\zeta_B}\right) \tag{I.38}$$

where $\zeta_B = \sqrt{\ln(1+V_B^2)}$ ($V_B = \sigma_B/\mu_B$) and $\lambda_B = \ln\mu_B - \zeta_B^2/2$ are the Lognormal parameters of B. Inserting the PDF in Eq. I.4 gives:

$$P(\bar{D}|A) = F_B(d) - \frac{1}{d\sqrt{2\pi}\zeta_B}\int_0^d \exp\left(-\frac{1}{2}\left(\frac{\ln\xi - \lambda_B}{\zeta_B}\right)^2\right)d\xi \tag{I.39}$$

$$= F_B(d) - \frac{1}{d\sqrt{2\pi}\zeta_B}\int_0^d \exp\left(-\frac{1}{2}\left(\frac{\ln\xi - \lambda_B}{\zeta_B}\right)^2\right)d\xi \tag{I.40}$$

By substitution using the following considerations

$$t = \frac{\ln\xi - \lambda_B}{\zeta_B} \Rightarrow \xi = \exp(\zeta_B t + \lambda_B) \tag{I.41}$$

$$d\xi = \zeta_B \exp(\zeta_B t + \lambda_B)\, dt \tag{I.42}$$

$$\xi = 0 \Rightarrow t = -\infty \tag{I.43}$$

$$\xi = d \Rightarrow t = \frac{\ln d - \lambda_B}{\zeta_B} \tag{I.44}$$

we obtain

$$P(\bar{D}|A) = F_B(d) - \frac{1}{d\sqrt{2\pi}\zeta_B} \int_{-\infty}^{\frac{\ln d-\lambda_B}{\zeta_B}} \exp\left(-\frac{1}{2}t^2\right) \zeta_B \exp(\zeta_B t + \lambda_B)\, dt \tag{I.45}$$

$$= F_B(d) - \frac{\exp(\lambda_B)}{d\sqrt{2\pi}} \int_{-\infty}^{\frac{\ln d-\lambda_B}{\zeta_B}} \exp\left(-\frac{1}{2}t^2 + \zeta_B t\right) dt \tag{I.46}$$

$$= F_B(d) - \frac{\exp(\lambda_B)}{d\sqrt{2\pi}} \int_{-\infty}^{\frac{\ln d-\lambda_B}{\zeta_B}} \exp\left(-\frac{1}{2}(t^2 - 2\zeta_B t)\right) dt \tag{I.47}$$

$$= F_B(d) - \frac{\exp(\lambda_B)}{d\sqrt{2\pi}} \int_{-\infty}^{\frac{\ln d-\lambda_B}{\zeta_B}} \exp\left(-\frac{1}{2}(t^2 - 2\zeta_B t + \zeta_B^2) + \frac{1}{2}\zeta_B^2\right) dt \tag{I.48}$$

$$= F_B(d) - \frac{\exp(\lambda_B + \frac{1}{2}\zeta_B^2)}{d\sqrt{2\pi}} \int_{-\infty}^{\frac{\ln d-\lambda_B}{\zeta_B}} \exp\left(-\frac{1}{2}(t - \zeta_B)^2\right) dt \tag{I.49}$$

We substitute again with

$$u = t - \zeta_B \tag{I.50}$$

$$dt = du \tag{I.51}$$

$$t = -\infty \Rightarrow u = -\infty \tag{I.52}$$

$$t = \frac{\ln d - \lambda_B}{\zeta_B} \Rightarrow u = \frac{\ln d - \lambda_B}{\zeta_B} - \zeta_B \tag{I.53}$$

and obtain

$$P(\bar{D}|A) = F_B(d) - \frac{\exp(\lambda_B + \frac{1}{2}\zeta_B^2)}{d} \int_{-\infty}^{\left(\frac{\ln d-\lambda_B}{\zeta_B} - \zeta_B\right)} \frac{\exp\left(-\frac{1}{2}(u)^2\right)}{\sqrt{2\pi}} du \tag{I.54}$$

$$= F_B(d) - \frac{\exp(\lambda_B + \frac{1}{2}\zeta_B^2)}{d} \Phi\left(\frac{\ln d - \lambda_B}{\zeta_B} - \zeta_B\right) \tag{I.55}$$

$$= \Phi\left(\frac{\ln d - \lambda_B}{\zeta_B}\right) - \frac{\exp(\lambda_B + \frac{1}{2}\zeta_B^2)}{d} \Phi\left(\frac{\ln d - \lambda_B}{\zeta_B} - \zeta_B\right) \tag{I.56}$$

J

CONDITIONAL SIMULATION

This appendix describes a procedure to produce conditional realisations of random fields using LAS and Kriging (adapted from Van den Eijnden, 2010).

Let Z_T be the true but unknown stationary random field with known correlation structure of which we know a limited number of (conditioning) points $Z_{T,i}$ at locations x_i. The following steps lead to conditional realisations for this field:

1. Compute a best estimate of the field by Kriging (Z_K).
2. Simulate a zero-mean unconditional field (Z_0) using the known correlation structure and apply Kriging to the values $Z_{0,i}$ at locations x_i to obtain Z_{0K}. (*The variances of both kriged fields, Z_K and Z_{0K}, are equal because they are both a function of the locations x_i and the correlation structure only.*)
3. Map the difference $Z_0 - Z_{0K}$ on the best estimate of the true field Z_K to generate the conditioned realisation: $Z_C = Z_K + (Z_0 - Z_{0K})$. (*The expected difference between fields Z_T and Z_K is given by the Kriging error and is equal for $Z_0 - Z_{0K}$.*)

The resulting field Z_C is a conditional realisation of the true field Z_T which honors the known conditioning points, the field mean and correlation structure. For an illustration of the steps see Figure J.1.

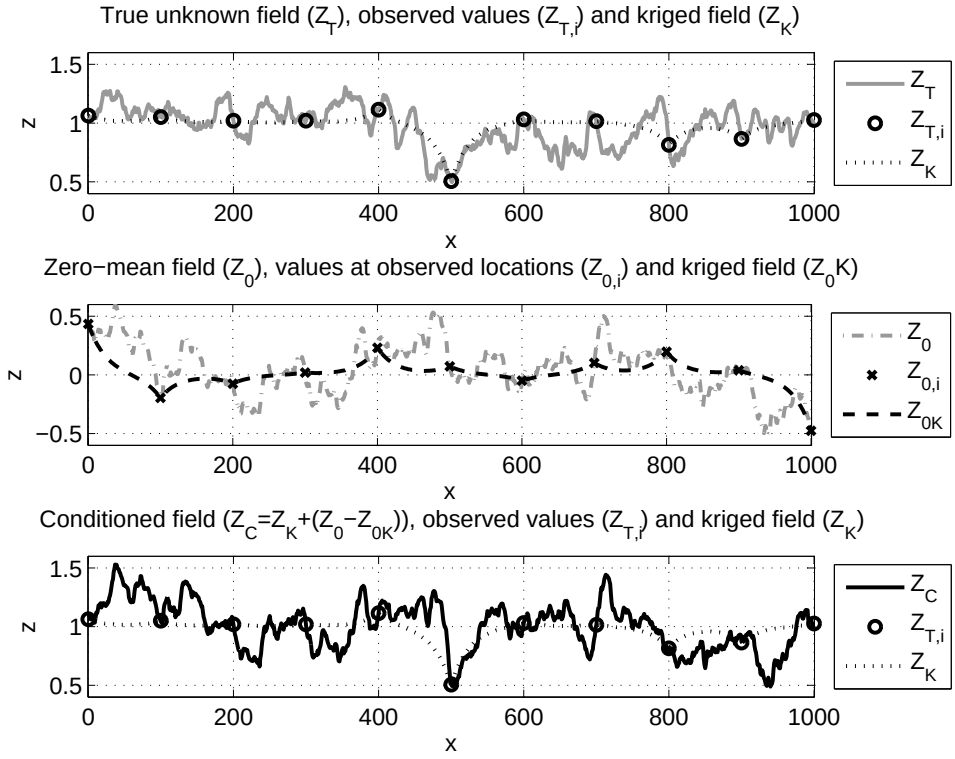

Figure J.1: Illustration of the steps in conditioning random field realisations to observed values in 1D.

LIST OF SYMBOLS

Roman Capital Letters

A	presence of an anomaly (event)	
B	breadth of the dike (footprint) or anomaly	[m]
C	cost (e.g., of a measure)	[€]
C_r	cost of retrofitting	[€]
C_s	cost of site investigation	[€]
C_x	covariance function	
COV	covariance	
D	thickness of the aquifer	[m]
D	detection (event)	
E	event or possible system state (scenario)	
F	failure or system failure (event) or CDF	
$F_{1/2/3}$	resistance/scale/geometry factor in revised Sellmeijer formula	
H	head difference	[m]
H_c	critical head difference (for piping)	[m]
L	seepage length	[m]
L_f	length of the foreshore	[m]
L_h	length of the hinterland	[m]
L_{mode}	length of levee contributing to the system reliability	[m]
N	number of realisations (MCS)	
N_F	number of realisations leading to failure (MCS)	
R	resistance (random variable)	
S	load (random variable), strategy	
V_i	coefficient of variation of X ($=\sigma_i/\mu_i$)	
W	hydraulic resistance	[sm^{-1}]
$\mathbf{X}$	vector of random variables $[X_1 X_2 ... X_n]^T$	
Z	limit state function (random variable)	

For symbols which are used with many subscripts, only the main symbol is stated in the lists below, while the subscripts are listed separately.

Roman Small Letters

a	action (i.e., decision alternative)	
a^*	optimal action or decision alternative	
a_h	Gumbel location parameter for the water level	[m^{-1}]
b_h	Gumbel scale parameter for the water level	[m]
c	percolation factor according to Bligh (1910)	
d	thickness of the blanket layer (at the exit point)	[m]
d_{50}	median grain diameter	[μ m]
d_{70}	70^{th}-percentile of the grain size distribution (aquifer)	[m]
d_{70m}	reference value for d_{70} in revised Sellmeijer model	[m]
d_{CPT}	sounding interval (in longitudinal direction)	[m]
$d_{CPT,x}$	sounding interval (in transversal direction)	[m]
d_s	sounding interval (also denoted as d_{CPT})	[m]
e_m	measurement error	
g	gravitational constant (=9.81)	[ms^{-2}]
$g_i(\cdot)$	performance (limit state) function of failure mode i	
h	water level	[m]
$\acute{h}$	observed water level	[m]
$h(\cdot)$	observation (limit state) function	
$h_e(\cdot)$	equivalent observation (limit state) function	
h_a	top level of the aquifer	[m]
h_c	critical water level	[m]
h_p	phreatic level at exit point (landside)	[m]
h_s	surface level	[m]
i	exit gradient	
i_c	critical gradient	
i_g	limit gradient	
k	specific conductivity (aquifer)	[m/s]
k_f	specific conductivity of the foreshore blanket	[m/s]
k_h	specific conductivity of the hinterland blanket	[m/s]
l_{eq}	equivalent correlation distance of an LSF	
m_B	model factor Bligh's Rule	
m_ϕ	model factor piezometric head / damping model	
m_p	model factor piping	
m_u	model factor uplift	
n	porosity	
p	probability	
p_T	acceptable (target) annual probability of failure	
$_i$	coordinates in a horizontal plane for point i	
u	standard Gaussian random variable	
$u(a)$	utility for action a	
u^*	design point (FORM) in u-space	
$\mathbf{x}^{(i)}$	i^{th} realization of vector of random variables $\mathbf{X}$	
x^*	design point (FORM) in x-space	
x_{exit}	distance of a potential exit point from the dike toe	[m]

Greek Capital Letters

$\Delta\phi_{c,u}$	equilibrium (or limit) potential difference for uplift	[m]
Ω	design parameters for retrofitting measures	
Ψ	design parameters for site investigation measures	
Θ	state of nature	

Greek Small Letters

α_i	importance factor (FORM) of random variable X_i	
β	reliability index	
β_T	target reliability index (annual basis)	
δ	(auto-)correlation distance	[m]
δ_0	scale of fluctuation	[m]
ε	evidence or observation (domain)	
ε_e	equivalent evidence or observation (domain)	
ϵ	relative error	
η	drag coefficient	
γ_d	dry volumetric soil weight	[kN/m^3]
γ_s	volumetric weight of sand grains (=26.5)	[kN/m^3]
γ_{sat}	saturated volumetric weight	[kN/m^3]
γ_w	volumetric weight of water	[kN/m^3]
μ_i	mean value of X_i	
μ_i^N	mean of the equivalent Normal distribution of X_i	
λ	damping factor (piezometric head)	
λ_i	leakage length of aquifer section i	[m]
ν	dynamic viscosity of water at 10^oC (=$1.33 \cdot 10^{-6}$)	[m^2/s]
ω	possible outcomes of experiments	
ϕ	piezometric head or potential	[m]
ρ	coefficient of correlation, correlation function	
σ_i	standard deviation of X_i	
σ_i^N	standard deviation of the equivalent Normal distribution of X_i	
θ	state of nature (parameters)	
θ	bedding angle (in Sellmeijer's rule)	[deg]
τ	distance or lag	[m]
ξ	dummy parameter	

Superscripts

f	future
p	past

Subscripts

a	aquifer
b	landside (in Dutch: *binnenwaarts*)
c	critical
d	design value
e	error
f	foreshore
F	failure
h	heave
k	characteristic value
m	measurement
obs	observation, observed
p	piping (or polder)
r	retrofitting / reinforcement
s	site investigation (or surface)
sys	system (of flood defenses)
u	uplift

Mathematical Operators

$\mathbf{1}[\cdot]$	indicator function
$\bar{A}$	complement of event A (in figures also denoted as $\neg A$)
$E[\cdot]$	expectation operator
$f_X(\cdot)$	probability density function (PDF) of X
$F_X(\cdot)$	cumulative distribution function (CDF) of X
$\mathbb{H}(\cdot)$	Heaviside step function
$\mathbb{L}(\cdot)$	likelihood function
$P(\cdot)$	probability operator
$P(A\|B)$	conditional probability of event A given event B
$\phi(\cdot)$	Standard Gaussian probability density function (PDF)
$\Phi(\cdot)$	Standard Gaussian distribution function (CDF)
$\mathbf{X^T}$	transpose of vector $\mathbf{X}$

Probability Distributions

To indicate that a random variable is Normal or Lognormal distributed, the following notations are used respectively:

$$\begin{aligned} X_i &\sim N(\mu_i, \sigma_i) \\ X_i &\sim LN(\mu_i, \sigma_i) \end{aligned}$$

where μ_i and σ_i are the mean and standard deviation.

Abbreviations

CDF	cumulative distribution function
CoV	coefficient of variation
CPT	Cone Penetration Test
FORM	First Order Reliability Method
GIS	Geographical Information System
JPDF	joint probability density function
LAS	Local Average Subdivision
LSF	limit state function
LSFE	limit state function evaluations
MCMC	Markov chain Monte Carlo (simulation)
MCS	(Crude) Monte Carlo simulation
MSE	mean squared error
n/a	not applicable
NAP	Normaal Amsterdams Peil (reference level)
nom	nominal value
NI	numerical integration
PDF	probability density function
PMF	probability mass function
PoD	probability of detection
QRA	quantitative risk analysis
REF	reference level (e.g., NAP)
RV	random variable
SLS	serviceability limit state
STD	standard deviation
SubSim	Subset Simulation
ULS	ultimate limit state

List of Figures

List of Tables

SAMENVATTING

DIJKEN zijn essentieel voor de hoogwaterbescherming van deltagebieden wereldwijd. Veel dijkdoorbraken worden veroorzaakt door het faalmechanisme piping (interne erosie), piping levert tevens een belangrijke bijdrage aan de faalkans van met name rivierdijken vanwege de aanzienlijke onzekerheden in ondergrondeingeschappen. De voorliggende dissertatie laat zien hoe onzekerheden omtrent piping kunnen worden verkleind en hoe een rationele onderbouwing kan worden gegeven van beslissingen in maatregelen ter reductie van onzekerheden, zoals grondonderzoek of monitoring. In essentie gaat het hierbij om de afweging of investeringen in metingen zich terugbetalen in termen van besparingen op dijkversterkingen die noodzakelijk zijn om het verseiste betrouwbaarheidsniveau te waarborgen.

De kernelementen van de voorgestelde aanpak zijn de Bayesiaanse posterior en beslisanalyse. Posterior analyse stelt ons in staat om de faalkans bij te stellen op basis van nieuwe informatie; met Bayesiaanse beslisanalyse kan een inschatting worden gemaakt van de gevolgen en kosten van de beschouwde beslisopties. Het ultieme doel van de beslisanalyse is de beslisoptie of strategie te bepalen met welke de doelbetrouwbaarheid (norm) met de, naar verwachting, laagste kosten bereikt wordt. De beschouwde strategiën zijn in essentie (a) investeren in het reduceren van onzekerheden zoals grondonderzoek of monitoring of (b) dijkversterking of combinaties van beide. Binnen elke strategie worden ook de ontwerpparameters geoptimaliseerd zoals bijvoorbeeld de afstand tussen sonderingen of de breedte van pipingbermen.

Er worden in deze dissertatie meerdere bronnen van informatie onderzocht. De eerste is veldobservaties tijdens hoogwaters zoals zandmeevoerende wellen of kwel. Tot op heden werd vooral naar het "overleven" van de dijk gekeken door middel van zogenaamde bewezen sterkte analyses. Met de hier voorgestelde aanpak kan worden gedifferentieerd tussen waarnemingen die op meer of juist op minder weerstand tegen piping duiden. De uitkomsten van de beschouwde voorbeelden suggereren dat de piping faalkans grofweg zowel met een factor 10 kan afnemen als met een factor 10 kan toenemen afhankelijk van de a-priori onzekerheden en het type waarneming.

Ook monitoring van de grondwater response in watervoerende lagen tijdens hoogwaters levert belangrijke informatie over de geo-hydrologische gesteldheid in de fundering van de dijk. Het meenemen van deze informatie kan een behoorlijk effect op de faalkans hebben. Hetzelfde geldt voor grondonderzoek bijvoorbeeld door middel van sonderingen, welke met name beter inzicht in de opbouw van de ondergrond geven. Voor piping is hierbij vooral het in kaart brengen van watervoerende en slecht doorlatende lagen van belang. De gekozen beslisanalytische aanpak stelt ons in staat om de optimale monitoring configuratie of sondeerdichtheid te bepalen zodat de totale verwachte kosten bestaande uit meetkosten en versterkingskosten minimaal zijn.

De uitgewerkte voorbeelden en cases doen vermoeden dat het verwerken van veldobservaties, monitoring en grondonderzoek zeer kosteneffectieve maatregelen kun-

nen zijn. Verder laten de resultaten zien dat het gekozen raamwerk suboptimaal is omdat risicoverlaging door verkleinen van onzekerheden niet meer wordt beloond als de norm-faalkans (het vereiste betrouwbaarheidsniveau) eenmaal behaald is. Een volledig risico-gebaseerde aanpak zou tot nog meer efficiëntie leiden, de vraag is echter of dat praktikabel is.

LIST OF PUBLICATIONS

The following publications are related to this thesis:

PEER-REVIEWED JOURNALS / BOOK SECTIONS

Schweckendiek, T., Vrouwenvelder, A.C.W.M., Calle, E.O.F. (2013). *Updating Piping Reliability with Field Performance Observations.* Structural Safety 47, p.13-23.

Schweckendiek, T., Vrouwenvelder, A.C.W.M. (2013). *Reliability Updating and Decision Analysis for Head Monitoring of Levees.* Georisk **7** (2), 110-121.

Schweckendiek, T., Vrouwenvelder, A.C.W.M., Calle, E.O.F., Kanning, W., Jongejan, R.B. (2013). *Target Reliabilities and Partial Factors for Flood Defenses in the Netherlands.* Modern Geotechnical Design Codes of Practice - Implementation, Application and Development, 311-328, Arnold, P., Fenton, G.A. (eds.), IOS Press, ISBN 978-1-61499-162-5.

CONFERENCES

Schweckendiek, T., Calle, E.O.F., Vrouwenvelder, A.C.W.M. (2012). *Updating Levee Reliability with Performance Observations.* Proceedings of FLOODrisk 2012, 359-368, 2^{nd} European Conference on Flood Risk Management, Rotterdam, The Netherlands, November 2012.

Vrijling, J.K., **Schweckendiek, T.**, Kanning, W. (2011). *Safety Standards of Flood Defenses (keynote paper).* Proceedings of ISGSR 2011, 359-368, Third Int. Symp. on Geotechnical Safety and Risk, Munich, Germany, June 2011.

Schweckendiek, T., van Gelder, P.H.A.J.M., Calle, E.O.F. (2011). *On risk-based geotechnical site investigation of flood defenses.* In Faber, Koehler and Nishijima (eds.), Applications of Statistics and Probability in Civil Engineering, 1700-1708, Proceedings of ICASP 11, Zurich, Switzerland.

Lopez de la Cruz, J., **Schweckendiek, T.**, Calle, E.O.F. (2011). *Calibration of Piping Assessment Models in The Netherlands.* Proceedings of ISGSR 2011, 587-595, Third Int. Symp. on Geotechnical Safety and Risk, Munich, Germany, June 2011.

Schweckendiek, T., Calle, E.O.F. (2010). *A Factor of Safety for Geotechnical Characterization.* Proceedings of 17SEAGC, Vol. II: 227-230, Seventeenth Southeast Asian Geotechnical Conference, Taipei, Taiwan, May 2010.

Schweckendiek, T. (2010). *Reassessing Reliability Based on Survived Loads.* Proceedings of ICCE 2010, Int. Conf. on Coastal Engineering, Shanghai, China, July 2010.

OTHER

Klijn, F., **Schweckendiek, T.** (eds.) (2012). *Comprehensive Flood Risk Management: Research for Policy and Practice.* Proceedings of FLOODrisk 2012, 2^{nd} European Conference on Flood Risk Management, Rotterdam, The Netherlands, November 2012. ISBN 978-0-41562-144-1.

Vrijling, J.K., Kok, M., Calle, E.O.F., Epema, W.G., van der Meer, M.T., van den Berg, P., **Schweckendiek, T.** (2010). *Piping - Realiteit of Rekenfout? (in Dutch).* ENW-report (Dutch Expert Network for Flood Defences). www.enwinfo.nl.

CURRICULUM VITÆ

Timo SCHWECKENDIEK

26-05-1978	Born in Cuxhaven, Germany.

EDUCATION

2004–2006	MSc. Civil Engineering (cum laude) Delft University of Technology *Thesis:* Structural reliability applied to deep excavations. *Supervisor:* Prof. drs. ir. J.K. Vrijling
2000–2004	Dipl.-Ing.(FH) European Civil Engineering Management University of Applied Sciences Oldenburg, Germany Universidad Politecnica de Valencia, Spain (2002-2003)
1998–2000	Apprenticeship in carpentry
1997–1998	Military service, Fallschirmjägerbatallion 313, Varel, Germany
1990–1997	Amandus Abendroth Gymnasium, Cuxhaven, Germany

EXPERIENCE

since 2007	Researcher / Consultant, Deltares, Unit Geo-engineering (before 2008: GeoDelft)
2006	Researcher / Consultant (intern), TNO
2004	Cost Estimator (intern), BAUER Spezialtiefbau GmbH
2003–2004	Project Controller, Drees & Sommer
2002	Assistant Site-Manager (intern), Dywidag International GmbH, Panama

AWARDS

2010	Deltares Young Talent Award 2010
2007	Risk Management Study Award (NVRB and GVRM)

PROFESSIONAL AFFILIATIONS

since 2011	ENW (Expertise Network for Flood Protection)
since 2009	ISSMGE-TC304 - Risk Management in Engineering Practice
since 2008	GEOSnet (Geotechnical Safety Network)
since 2008	NVRB (Dutch Association for Risk and Reliability)
2008–2011	ELGIP (European Large Geotechnical Institutes Platform)